Exploring causality in interactions between climate shifts, land degradation and humans: evidence from the Horn of Africa

Sil Lanckriet

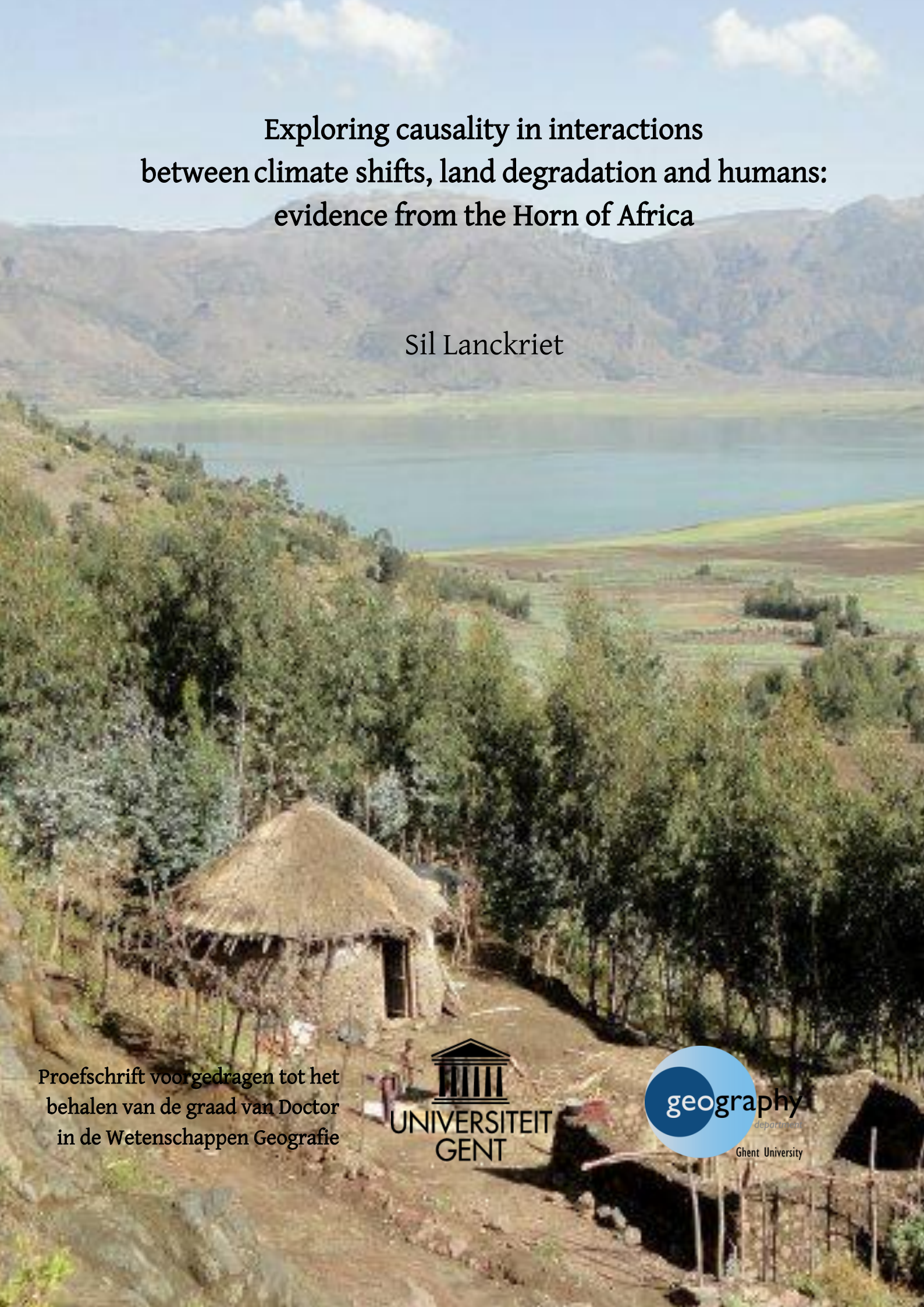

Proefschrift voorgedragen tot het behalen van de graad van Doctor in de Wetenschappen Geografie

UNIVERSITEIT GENT

geography department Ghent University

Faculteit Wetenschappen

Sil Lanckriet

Exploring causality in interactions between climate shifts, land degradation and humans: evidence from the Horn of Africa

Proefschrift voorgelegd tot het behalen van de graad van
Doctor in de Wetenschappen: Geografie

2015-2016

Cover: View of the marginal graben and degraded basalt mountains around Lake Ashenge.

Photograph taken by Mérielle Van de Graaf (April 2012).

Promoters:

Prof. Dr. Jan Nyssen, Department of Geography, Faculty of Sciences, Ghent University, Belgium

Dr. Amaury Frankl, Department of Geography, Faculty of Sciences, Ghent University, Belgium

Members of the Jury:

Prof. Dr. Ben Derudder, Department of Geography, Faculty of Sciences, Ghent University, Belgium (Chair)

Prof. Dr. Veerle Van Eetvelde, Department of Geography, Faculty of Sciences, Ghent University, Belgium (Secretary)

Prof. Dr. Ir. Ann Verdoodt, Department of Soil Management, Faculty of Bioscience Engineering, Ghent University, Belgium

Dr. Jan Moeyersons, Earth Sciences and Natural Hazards, Royal Museum for Central Africa, Belgium

Prof. Dr. Piet Termonia, Department of Physics and Astronomy, Faculty of Sciences, Ghent University, Belgium; Royal Meteorological Institute of Belgium

Prof. Dr. Haripriya Rangan, School of Geography, Faculty of Science, University of Melbourne, Australia

Prof. Dr. Henry Lamb, Department of Geography and Earth Sciences, Aberystwyth University, Wales, UK

Dean: Prof. Dr. Herwig Dejonghe

Rector: Prof. Dr. Anne De Paepe

Αποκλινομένης δὲ μεσαμβρίης παρήκει πρὸς δύνοντα ἥλιον ἡ Αἰθιοπίη χώρη ἐσχάτη τῶνοἰκ εομενέων: αὕτη δὲ χρυσόν τε φέρει πολλὸν καὶ ἐλέφαντας ἀμφιλαφέας καὶ δένδρεαπάντα ἄ γρια καὶ ἔβενον καὶ ἄνδρας μεγίστους καὶ καλλίστους καὶ μακροβιωτάτους.

Where south inclines westwards, the part of the world stretching farthest towards the sunset is Ethiopia; this produces gold in abundance, and huge elephants, and all sorts of wild trees, and ebony, and the tallest and longest-lived and handsomest of all people.

Ἡρόδοτος, *Ἱστορίαι;* Herodotos, The History, Muse 3 114.1 (430 BCE)

Acknowledgements

This study could not have existed without the help of many others. First of all, I thank my promoter Prof. Dr. Jan Nyssen for his support and supervision of my fieldworks in Ethiopia, for his advice in Belgium, for answering my many questions and for his zeal for sustainable development in the Ethiopian Highlands. I equally would like to express my gratitude to my co-promoter Dr. Amaury Frankl, for his strong support, help and advice both in Belgium and in Ethiopia. I thank Prof. Dr. Haripriya Rangan for her hospitality in Australia, our pleasant stay in Ethiopia and for the different opportunities she offered me. I thank Dr. Amanuel Zenebe Abraha and Dr. Tesfay Araya for their support in Mekele, Dr. Jean-Luc Schwenninger for his advice and kindliness in Oxford, Dr. Vanessa Gelorini for her advice on the pollen analysis, and all other co-authors for their valuable inputs. Special thanks go to Dr. Tesfaalem Asfaha, Dr. Cornelis Stal, Dr. Nasem Badreldin, Prof. Dr. Ben Derudder and Dr. Miró Jacob for their auxiliary support.

Furthermore, this study would not have been possible without the enormous support of Seifu, Gebrekidan, Bereket and Yohannes. Their translations and help on the field have been extremely valuable. The kindliness of the many farmers who helped us or let us work on their fields was astonishing. I am very thankful for their hospitality, as well as for the many invitations to *injera* and *sowa*. Their in-depth knowledge of agricultural and environmental management is truly impressive; they taught me so much. To all of them: ክብረት ይሃበለይ!

Additionally, I thank Biadgilgn, Etefa, Hailemariam, Zbelo, Romha, Haileselassie, Teshager, Dereje, Tzega, Mulu, Alemou, Gebregeorgis, Haftu, and many others, for supporting me in Ethiopia. Thanks go to Marlies, Sofie, Wouter and Anthony for our

pleasant trips in the Highlands. I express my gratitude to the people of the Belgo-Ethiopian VLIR-UOS projects at Mekele University for their important logistical support, and to the Special Research Fund (BOF) of Ghent University and the Flanders Research Foundation (FWO) for the project funding. I thank Helga, Hanne, Hanibal, Marijn and Henok for their help in Ghent. Thanks go to Elizabeth, for proofreading the manuscript and to Lys, for our days in Hagere Selam. Special thanks go to Laurens, who has encouraged me since the first day at university.

Last but not least, I cannot forget to thank several other friends, in particular Koen, Feli and all members of De Droge Worsten Groep, KSA Schuiferskapelle, Valuable Tits and Smadders. I owe my deepest thanks to my family; my parents, my brother and my sisters, who are always there for me. Finally, I am deeply grateful to Tasha. In Ghent, Istanbul, Melbourne or Mekele, she has been by my side.

Sil, Gent – 29 October 2015

Table of Contents

List of Tables

List of Figures

List of Acronyms

A	runoff-contributing area
AP/NAP	ratio arboreal/non-arboreal pollen
(B)CE	(Before) Common Era
BT	bed load transport
C_i	catchment-weighted runoff coefficient
CN	Curve Number
d	(channel) depth
D50	median particle diameter
D_e	equivalent dose
DF	debris fan
ENSO	El Niño / La Niña Southern Oscillation
EOT	Empirical Orthogonal Teleconnection
I	rainfall intensity
IOD	Indian Ocean Dipole
LOI	loss-on-ignition
MAM	Minimum Age Model
NTP	number of trapped pebbles
OSL	Optically Stimulated Luminescence
P	rainfall
Q	runoff
Q_p	peak discharge
Q_s	sediment supply
R_{24}	cumulative rainfall over the past 24 hours

SWM	South West Monsoons
(T)W	channel (Top) Width
VEG	total woody vegetation cover

List of Publications

International SCI-ranked journal articles as first author (with SCI impact factor IF)

1. **Lanckriet, S.**, Tesfay Araya Weldeslassie, Cornelis, W., Verfaillie, E., Poesen, J., Govaerts, B., Bauer, H., Deckers, J., Mitiku Haile, Nyssen, J., 2012. Impact of conservation agriculture on catchment runoff and soil loss under changing climate conditions in May Zeg-zeg (Ethiopia). Journal of Hydrology 475, 336-349. (IF = 3.053)
2. **Lanckriet, S.**, Tesfay Araya Weldeslassie, Derudder, B., Govaerts, B., Bauer, H., Deckers, J., Mitiku Haile, Cornelis W., Nyssen, J., 2014. Towards practical implementation of Conservation Agriculture: a case study in the May Zeg-zeg catchment (Ethiopia). Agroecology and Sustainable Food Systems 38 (8), 913-935. (IF = 0.849)
3. **Lanckriet, S.**, Derudder, B., Naudts, J., Bauer, H., Deckers, J., Mitiku Haile, Nyssen, J., 2015. A political ecology perspective of land degradation in the North Ethiopian Highlands. Land Degradation and Development 26 (5): 521-530. (IF = 3.089)
4. **Lanckriet, S.**, Frankl, A., Termonia, P., Nyssen, J., 2015. Droughts related to quasi-global oscillations: a diagnostic teleconnection analysis in North Ethiopia. International Journal of Climatology 35, 1534–1542. (IF = 3.398)
5. **Lanckriet, S.**, Frankl, A., Descheemaeker, K., Gebrekidan Mesfin, Nyssen, J., 2015. Gully cut-and-fill cycles as related to agro-management: a historical curve number simulation in the Tigray Highlands. Earth Surface Processes and Landforms 40 (6), 796-808. (IF = 2.695)
6. **Lanckriet, S.**, Rucina, S., Frankl, A., Ritler, A., Gelorini, V., Nyssen, J., 2015. Nonlinear vegetation cover changes in the North Ethiopian Highlands: evidence from the Lake Ashenge closed basin. Science of the Total Environment 536, 996-1006. (IF = 4.099)
7. **Lanckriet, S.**, Tesfaalem Asfaha, Frankl, A., Amanuel Zenebe, Nyssen, J., 2015. Sediment in alluvial and lacustrine debris fans as an indicator for land degradation around Lake Ashenge (Ethiopia). Land Degradation and Development, in press. (IF = 3.089)
8. **Lanckriet, S.**, Schwenninger, J. L., Frankl, A., Nyssen, J., 2015. The Late-Holocene geomorphic history of the Ethiopian Highlands: supportive evidence from May Tsimble. Catena 135, 290–303. (IF = 2.482)
9. **Lanckriet, S.**, Rangan, H., Nyssen, J., Frankl, A., 2015. The influences of Holocene climatic shifts and cattle migrations on land cover and land use in the Ethiopian Highlands. PLOS ONE, submitted. (IF = 3.534)

International SCI-ranked journal articles as co-author (with impact factor IF)

10. Tesfay Araya, Nyssen, J., Govaerts, B., Baudron, F., Carpentier, L., Bauer, H., **Lanckriet, S.**, Deckers, J., Cornelis, W., 2015. Restoring cropland productivity and profitability in

northern Ethiopian drylands after nine years of resource-conserving agriculture. Experimental Agriculture, in press. (IF = 1.069)

11. Jacob, M., Frankl., A., Hurni, H., **Lanckriet, S.**, De Ridder, M., Etefa Guyassa, Beeckman, H., Nyssen, J., 2015. Vegetation dynamics in the Simen Mountains (Ethiopia), half a century after establishment of the National Park. Regional Environmental Change, submitted. (IF = 2.260)
12. Van Vooren, S., **Lanckriet, S.**, Nyssen, J., 2015. Methods to complete missing values in meteorological and hydrological data series: a review. Physical Geography, submitted. (IF = 0.839).

Book chapters

Nyssen, J., **Lanckriet, S.**, Poesen, J., Jacob, M., Moeyersons, J., Mitiku Haile, Frankl, A., Deckers, J., 2013. Landdegradatie in de Ethiopische hooglanden. Jaarboek De Aardrijkskunde 2013, 77-95.

Nyssen, J., Poesen, J., **Lanckriet, S.**, Jacob, M., Moeyersons, J., Mitiku Haile, Nigussie Haregeweyn, Munro, N., Descheemaeker, K., Enyew Adgo, Frankl, A., Deckers, J., 2015. Land degradation in the Ethiopian Highlands. In: Billi (Ed.) Landscapes and Landforms of Ethiopia, Springer, New York, USA, 369-385 p.

Conference presentations (as first author)

Lanckriet, S., Nyssen, J., Tesfay Araya Weldeslassie, Poesen, J., Govaerts, B., Bauer, H., Deckers, J., Mitiku Haile, Verfaillie, E., Cornelis W., 2013. Water ponding and catchment runoff as influenced by conservation agriculture in May Zeg-zeg (Ethiopia). European Geosciences Union General Assembly. 10 April 2013. Vienna, Austria. Book of Abstracts 15, p. 3479.

Lanckriet, S., Tesfay Araya Weldeslassie, Cornelis, W., Verfaillie, E., Poesen, J., Govaerts, B., Bauer, H., Deckers, J., Mitiku Haile, Nyssen, J., 2013. A holistic evaluation of conservation agriculture as a measure to combat desertification and land degradation in the North Ethiopian Highlands. DesertLand. 17 June 2013. Gent (Belgium). Book of Abstracts, p 108.

Lanckriet, S., Frankl, A., Gebrekidan Mesfin, Descheemaeker, K., Nyssen, J., 2013. Gully incision and infill as influenced by climate, land cover change and agro-management: a case-study in North Ethiopia. Poster presented at the Ghent Africa Platform Meeting, Gent (Belgium). 6 December 2013. Book of Abstracts, p. 56.

Lanckriet, S., Tesfay Araya, Bauer, H., Govaerts, B., Deckers, J., Mitiku Haile, Naudts, J., Derudder, B., Cornelis, W., Nyssen, J., 2013. Pitfalls for large-scale implementation of Conservation Agriculture: a case study in the Tigray Highlands (Ethiopia). Poster presented at the Ghent Africa Platform Meeting, Gent (Belgium). 6 December 2013. Book of Abstracts, p. 57.

Lanckriet, S., Derudder, B., Naudts, J., Bauer, H., Deckers, J., Mitiku Haile, Nyssen, J., 2014. The impact of land tenure on land degradation: a case study in the North Ethiopian Highlands. Day of Young Soil Scientists. 9 February 2014. Brussels (Belgium). Book of Abstracts, p. 34.

Lanckriet, S., Nyssen, J., Derudder, B., Naudts, J., Frankl, A., 2015. A political ecology of land degradation: the case of North Ethiopia. Proceedings of the Institute of Australian Geographers Conference, 1-3 July 2015, Canberra, Australia. Book of Abstracts, p. 145.

Media coverage of research findings

De Morgen (31/07/2014), La Libre Belgique (05/08/2014), RTBF (17/11/2014), AVS (30/07/2014), Le Journal de l'Environnement (30/07/2014), Science X (30/07/2014), Flanders Today (08/08/2014), Science Daily (29/07/2014), Daily News (30/07/2014)

Abstract

Land degradation is traditionally thought to result from human over-population or over-exploitation, and is often considered to accelerate over time. However, here we test the hypothesis that land degradation evolved in a cyclical way that has been in phase with climatic changes. The study presents records of dryland degradation dynamics during the past 4000 years near the strongly dissected Lake Ashenge basin (Ethiopia), a unique natural laboratory for comparing climate, human activity and hydrogeomorphic responses at the northernmost limit of the African monsoons. The datasets are based on luminescence, pollen and short-lived isotope records and are complemented with climate model and hydrological simulation results. The sedimentary evidence provides a paleoenvironmental benchmark demonstrating that distinct Late-Holocene climate shifts indeed matched with phases of increased sediment supply (land degradation) and (upslope) grassland expansions. There are remarkable temporal associations between climatic shifts and cattle migrations that have influenced land cover in the basin. Overall, the data corroborate multi-model projections that climatic shifts can directly and indirectly lead to significant environmental changes in drought-prone regions on the longer term. Supported by calculated management scenarios, it is argued that smallholder agriculture is key to addressing these challenges in a cost-efficient way, and a simulation procedure was presented to effectively model the risk of droughts.

Chapter 1 General introduction

1.1 Problem statement

Climatic variability is recurrently threatening water supplies across the globe and future climate change can put further pressure on water supplies and land resources. This will most likely be the case in the world's drylands, where the magnitude and effects of drought are likely to persist or even increase over the twenty-first century (Sheffield & Wood, 2011). Drylands are areas where the ratio of annual precipitation to annual potential evapotranspiration is smaller than 0.65 (Sheffield & Wood, 2011). Drylands cover over 40% of our planet's land surface and they accommodate about 38% of the global population (Huang et al., 2015).

Following Rossi (2000), we may define drought as a 'recurring natural phenomenon associated with a deficit availability of water resources over a large geographical area and extending along a significant period of time'. Of all natural hazards, droughts may be the most complex and least understood phenomena (Modarres and Ouarda, 2014). Nevertheless, droughts are likely to become more frequent in the future due to regional reductions in precipitation and increased evaporation from higher temperatures under climate change (Sheffield & Wood, 2011). Multi-model multi-scenario simulations (IPCC AR4) project a doubling of the frequency of short-term droughts by the end of the 21st century worldwide, as well as a tripling of the frequency of long-term droughts (Sheffield & Wood, 2011).

Additionally, drylands suffer from processes of desertification, which can be defined as 'the temporary or permanent lowering of the productive capacity of drylands' (UNEP, 1992) and includes deforestation, overgrazing, expansion of cultivation, increasing water runoff and

erosion, and soil degradation. Alternatively, desertification can be defined as 'land degradation in arid, semi-arid and dry sub-humid areas resulting from various factors, including climatic variations and human activities' (UNCCD, 1994). (Dry)land degradation is, together with climate change, named as the biggest global threat to sustainable development (UNEP, 1992). Lal (2001) estimated that yearly between 0.83 and 1.07 billion tonnes CO_2-equivalents are emitted to the atmosphere due to land degradation in drylands. The impact of desertification and land degradation on land and water resources is of key significance for agricultural production (Tubiello & van der Velde, 2015), management of water resources and hydro-energy production (Amanuel Zenebe et al., 2013). Land degradation is, amongst others, such a serious issue because (i) lands and soils are important buffers that regulate the resilience of ecosystems as a whole (Roberts, 2006) and (ii) soil losses have a significant impact on plant and crop productivity (Lal, 1995). For instance, studies from across Africa show that crop yield reductions due to land degradation are considerable over several years of measurement (Eswaran et al., 2001). Land degradation costs at minimum an estimated US$ 40 billion worldwide per year and threatens nearly 1.5 billion people (FAO, 2014).

Most research on land degradation or desertification has centered on explanations based on 19th or 20th century population growth and human factors (Le Houérou, 1996), for instance due to overuse of land under population growth (Meadows et al., 1972; Easdale & Domptail, 2014), non-sustainable agro-industry (Petschel-Held et al., 1999), overexploitation of natural resources (Foley et al., 2005; Tekle Kebrom, 1999), war and military action (Kiernan, 2015); and (neo-)colonial exploitation (Adger et al., 2001). Following Adger et al. (2011), the two dominant discourses on land degradation in drylands are the 'neo-Malthusian perspective' of land cover change due to overpopulation, and the 'populist perspective' of (colonial) overexploitation of natural resources.

Yet, these two explanations do not look at longer term patterns of human activity in relation to climate changes. The responses of drylands to stressors such as climate changes are often distorted and less evident (Le Houérou, 1996). Some climate models project a strongly increased risk of dryland degradation by the end of the 21st century (Huang et al., 2015) but to date there is limited empirical evidence that climate change has impacted surface water quantities, soil erosion and sediment loads across different dry regions of the world (Jiménez Cisneros et al., 2014). Moreover, the impact of (past) climate changes on low-order streams and drainage systems, crucial for the water supply to rural areas in dry

regions worldwide, is understudied and uncertain (de Wit and Stankiewicz, 2006). This is clearly the case in dry Africa, where (paleo)hydrological datasets from smaller rivers are relatively rare (Lespez et al., 2011). Overall, several reasons may exist for this unclarity:

(i) To date, the resolution of climate models does not allow to attribute small-scale hydrological and hydrogeomorphological dynamics to climate change (Jiménez Cisneros et al., 2014). In general, climate models and hydrological models still lack sufficient integration (Jiménez Cisneros et al., 2014) and climate models do not capture feedbacks between environmental changes and human responses (Palmer and Smith, 2014);

(ii) In different low-latitude regions, there is very often a lack of long-term climatic and hydrogeomorphic datasets, including instrumental, tree ring or ice core data (Verschuren et al., 2000); and

(iii) A research focus on the most recent decades only is problematic, since changes in the mean (regional) state of hydroclimatic and hydrogeomorphic processes may evolve rather slowly over time (Batterbury, 1997; Rangan et al., 2012).

Is there a long-term link between climate changes and processes of land degradation? To deal with this question, researchers may turn to sedimentary paleo-records derived from rivers and lakes.

1.2 Regional study

1.2.1 The Ethiopian Highlands as a representative case study

We turn to the highlands of North Ethiopia (region of Tigray) where media attention to famines has created a widespread view of a drought-struck country – especially since the famine of 1984. During the Great Famine of 1984, BBC reporter Michael Burk referred to the plains in the Northern Highlands as ‘the closest thing to hell on earth’. Images of the ‘biblical famine’ infused the perception of Ethiopia as suffering from a drying trend, amplified by the effects of the civil war (Muller, 2013).

Located at the northernmost limit of the Intertropical Convergence Zone, the North Ethiopian Highlands are very vulnerable to climatic changes (Marshall et al., 2009). In the North Ethiopian Highlands, the interplays between climatic vulnerability and land use changes caused declining water availability (Nyssen et al., 2004a; Biazin & Sterk, 2013), as land use changes can induce vulnerability to droughts (Frankl et al., 2011; Frankl et al., 2013). Consequently, water and land productivity in Northern Ethiopia is partly linked to rainfall cycles and drought periods, while crop production is under considerable strain from water deficiencies. Indeed, water and organic matter availability are the key-elements of agricultural productivity in such dry regions, since agriculture is characterized by limited productivity impacts of fertilizers based on N, P and K, that are mainly fixed by soil organic matter (Breman et al., 2001; Pender & Gebremedhin, 2008). Considering the situation of the late 20th century, Nyssen et al. (2004b) wrote in this perspective: 'Soil erosion not only affects soil depth but leads in addition to rapid siltation of reservoirs. Nutrients are lost due to use of cattle dung as fuel, lack of manuring, and soil erosion. Gullying leads to rapid lowering of ground water tables.' According to these authors, land degradation in the Eritrean and Ethiopian Highlands is strongly connected to the geomorphic processes that shape the landscape: sheet and rill erosion throughout the country, wind erosion in the dryer Rift Valley and the peripheral lowlands and gullying in the Highlands. Indeed, gullies are strongly determining actors for land degradation processes in the Highlands. Gullying is a major cause of soil and nutrient losses for the agricultural lands (Frankl et al., 2011). Flashfloods in gully networks have severe negative impacts on both the regional economy and on human health. When overland flows become concentrated, downstream flooding, sediment contamination of the water and severe fluvial erosion can occur. Overall, flash floods can cause up to 600 fatalities with 120,000 affected people per year in Ethiopia (Billi et al., 2015).

An extensive amount of research on environmental degradation has already been conducted in this region. In general this concerns the hydrogeomorphological dynamics of land degradation and desertification in the North Ethiopian (and Eritrean) Highlands, including the human impact affecting the processes occurring. The biophysical environment (climate, soil and water dynamics) in North Ethiopia is very well studied (one could call it one of the best studied regions in Africa). Drought periodicity is among others dependent on the behavior of the meridional branch of the Somali jet (Riddle & Cook, 2008), the behavior of the Madden-Julian Oscillation (Williams & Funk, 2011), the El Nino Southern

Oscillation and the tropical easterly jet (Segele et al., 2009). High rainfall erosivity (Nyssen et al., 2005), economic poverty and a human impact on the natural environment (Bard et al., 2000) impose high pressure on economic production capacity of the agricultural lands. Therefore, soil and water conservation projects are widely implemented, and the effects of integrated catchment management are well studied (Nyssen et al., 2009a). Especially after the large scale degradation phase around the decade of the 1980s (see further), important and successful efforts in soil and water conservation were made, such as the creation of exclosures (Descheemaeker et al., 2006) and the building of dry masonry walls along the contour lines (Nyssen et al., 2004a). Still, an extensive gully network is present both at the mountain slopes and in the Vertisol valleys, enhancing further land degradation (Frankl et al., 2011). By studying old terrestrial and aerial photographs, four major periods of gully dynamics could be detected at regional scale: (i) at least one so far undated incision phase before 1875 CE; (ii) a stable stage (1875-1960 CE) following the prior incision phase; (iii) another cutting stage (1960s-1990s); and (iv) a new stable stage (2000s-present) (Frankl et al., 2011). Yet, the hydrogeomorphic and hydroclimatic situation before 1875 CE remains unclear (Frankl et al., 2011).

1.2.2 Sediment characteristics as research proxies

A strong link exists between region-wide environmental changes and gully formation in the Ethiopian Highlands (Figure 1.1) (Frankl et al., 2011). In many areas, a combination of intensive land degradation and extreme rainfall has been blamed for gully formation, as is the case for Slovakia (Stankoviansky, 2003), France (Vogt, 1953; Auzet et al., 1995) or Australia (Fryirs and Brierley, 1998). In the Ethiopian Highlands, the earliest gully formation (*cut*) processes are observed on historical photographs dating back to 1868, and were tentatively related to the prior occurrence of droughts (Frankl et al., 2011). Later *cut* processes could be related to a combination of drought vulnerability and severe land degradation (Frankl et al., 2011). Consequently, gully characteristics can serve as valuable research 'proxies' for the assessment of land degradation. Vanmaercke et al. (2011) employ sediment yield as a desertification risk indicator. The use of gully research for the assessment of hydrogeomorphological change is also supported by the findings of Avni (2005), that gully incision is a key factor for desertification in the Negev, since desertification is advancing in phase with the gully headcut retreat rates in the region. The

hydrogeomorphological evolution of gullies and streams at longer time scales, and before 1875 CE, can thus shed a light on the temporal evolution of desertification, including its determining factors.

Figure 1.1 Gully system with water flow inside the main channels during the rainy season 2011 (May Zegzeg catchment; photo: Sil Lanckriet). Note that the gully system is not in phase with the current status of vegetation cover in the catchment but is inherited from an earlier situation (before 2000 CE) with a more degraded landscape.

1.3 Objectives and research questions

Our overall aim is to analyze long-term environmental changes (including gully and vegetation cover dynamics) based on alluvial and lacustrine sediments, and compare it with independent lake sediment and instrumental evidence of climatic shifts and drought

variability, as well as with (historical) information on human impacts. The two main research aims are:

1. *Temporal aim*: To extend the existing hydrogeomorphic records of the region, in order to reconstruct hydrogeomorphic changes in the North Ethiopian Highlands over the course of the Late Holocene (millennia-scale, century-scale, decade-scale). Specifically, as the hydrogeomorphic situation before 1875 CE remains unclear, we aim to answer our first research question (RQ1): *Did land degradation occur in a 'nonlinear-cyclic', instead of a 'gradually-accelerating' pattern over time?*

2. *Causal aim*: To use different proxies for identifying the temporal links between the hydrogeomorphological evolution of land degradation, climatic shifts and human amplification. Specifically, we aim to answer the following research questions (RQ2 a, b & c): *Are phases of land degradation largely synchronous with – or slightly preceded by – climate changes? Could there be an additional amplifying effect from human responses to climate change? What are the implications?*

These broad research aims can be further refined to more specific objectives. Objectives for the temporal aim are: 1A. To assess the suitability of luminescence for dating floodplain sediments in order to identify phases of hydrogeomorphic activity over the past four millennia (see Chapter 5); 1B. To study water and sediment dynamics in a representative gully system during one rainy season and link these with decadal-scale gully debris fan dynamics by using short-lived isotope dating (see Chapter 6); 1C. To assess hydroclimatic shifts in the Ethiopian Highlands over the course of the Holocene by synthesizing a large number of paleolacustrine records (see Chapter 7); 1D. To perform an integrated analysis of vegetation cover changes over the past four centuries around a representative endorheic lake in the Highlands (Lake Ashenge) (see Chapter 8).

Objectives for the causal aim are: 2A. To use reanalysis and precipitation datasets to study dry spells and remote atmospheric-oceanic forcing (see Chapter 2); 2B. To assess the interference of land tenure and climate variability with processes of hill-slope runoff over the course of the 20th century (see Chapter 3); 2C. To assess the interference of agro-management and climate variability with gully channel morphologies and peak flows since the late 19th century (see Chapter 4).

As a single proxy alone is inadequate for understanding (paleo)environmental dynamics, multi-proxy methods should be used to capture the complementary advantages of each of the single proxies (Mann, 2002). Therefore, in order to obtain our objectives and answer our research questions, we applied a multi-proxy approach using a variety of different methods (Figure 1.2). This was done in order to compare the dynamics of land degradation with the dynamics of climate change, and human activity (causal aim), on distinct temporal scales: the 'long term' (millennia-scale), the 'medium term' (century-scale), the 'short term' (decade-scale) and the near future (temporal aim). For elucidation of the different methodologies, the reader is referred to the corresponding chapters (see Figure 1.2).

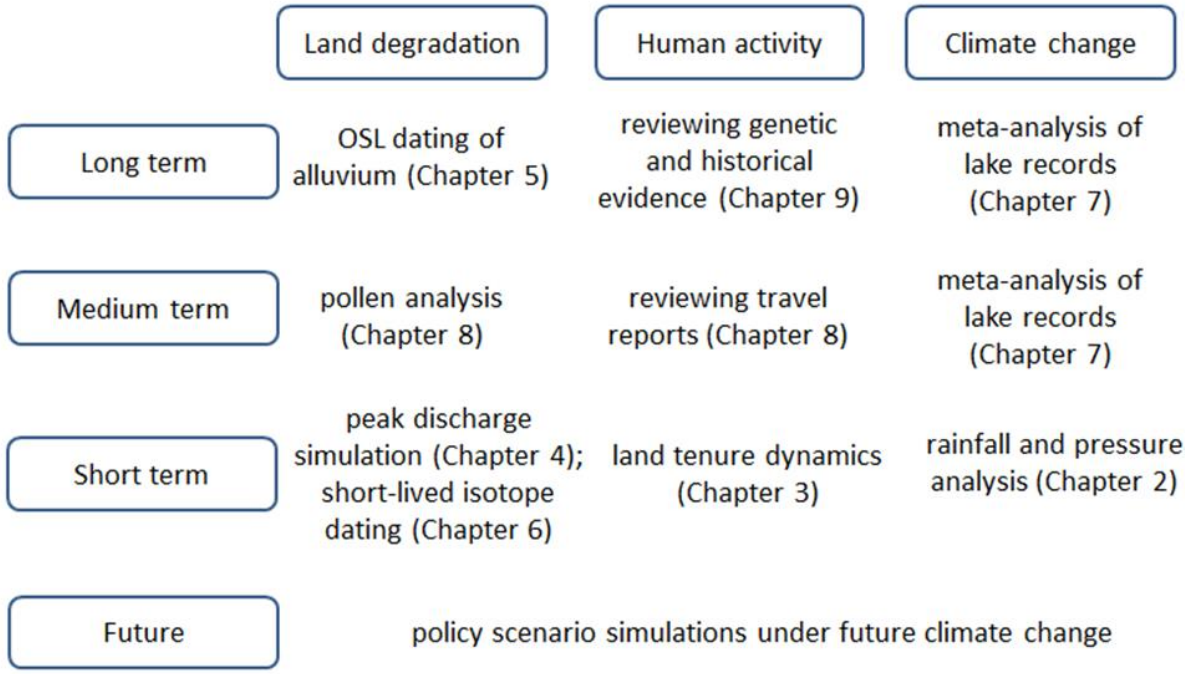

Figure 1.2 Tabular diagram showing the different methods employed in the different chapters. This multi-proxy approach was used to compare the changes in the 'mean state' of land degradation with changes in human activity and climate (causal aim) on different temporal scales: the longer term (millennia-scale), the medium term (centuries-scale) and the short term (decades-scale), as well as the future (Chapter 9) (temporal aim).

1.4 Outline of the thesis

In line with the broad structure of the thesis (Figure 1.3), we will 'follow a raindrop' in its trajectory as part of the hydro(geomorpho)logical cycle.

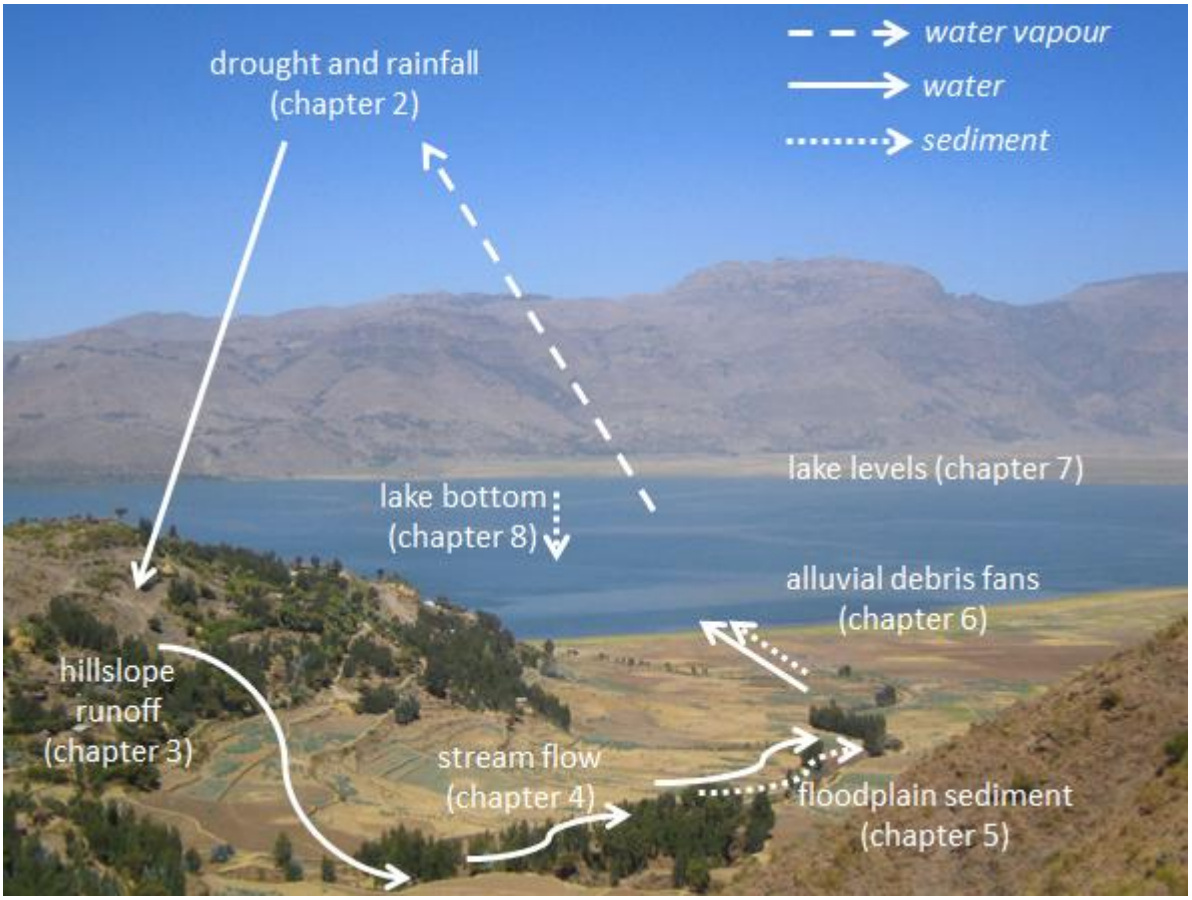

Figure 1.3. The hydrological cycle around Lake Ashenge, with outline of the thesis. See Table 1.1 for the links between processes of the hydrological cycle, human or climatic impacts and the chapters of the thesis. Photo by Olivier Vuigner (12 Februari 2008).

After this first introductory chapter, the first part focuses on the 'upper' part of the hydrological cycle: from ocean to hillslope. In this part, we investigate hydrological changes during the 19th and 20th century, with specific attention to the impact of different driving factors (climatic variability and human interference, including land tenure and agro-management).

The second chapter employs empirical orthogonal teleconnection analysis as an effective way to identify the impact of remote atmospheric-oceanic teleconnections on the occurrence of drought in our study area. The third chapter presents our semi-structured interviews with farmers in eight villages in the Tigray region in order to identify the links between runoff vulnerability at hill-slope scale with regional land tenure policies and periodic drought. The fourth chapter assesses the impact of agro-management and drought on processes of gully cut-and-fill. In order to confront gully channel morphologies with runoff vulnerability of the catchment, we designed a method based on Monte Carlo simulation of catchment-wide curve numbers.

The second part of the thesis focusses on the hydrogeomorphic part of the hydrological cycle: through gullies to (endorheic) lakes. Here, we discuss hydrogeomorphic processes on different temporal scales, by tracing hydrogeomorphic changes as recorded in sediment sequences. By doing so, we analyze and discuss longer-term dynamics of land degradation (millennia-scale, century-scale, decade-scale) in our study area.

As outlined in the fifth chapter, floodplain sediments were dated by means of optically stimulated luminescence (OSL) dating, providing evidence for past gully activity in the Highlands. In order to understand and assess subrecent gully sediment dynamics, the sixth chapter presents our monitoring of a sequence of gully debris fans near Lake Ashenge. Debris fan deposition rates could be obtained from, among others, short-lived isotope counting and remote sensing imagery. The seventh chapter synthesizes different Holocene hydroclimatic shifts in the Highlands, as derived from lake records from across the Horn of Africa. Finally, the eighth chapter presents an integrated land cover/degradation study around Lake Ashenge. From a deep lake core, we derived a radiocarbon-dated pollen reconstruction of land cover changes during the past four centuries.

We end the thesis with a general discussion, where we confront all hydrogeomorphic records, explain how climatic shifts and human agents impacted dryland dynamics over time, and finally discuss a number of future management scenarios under climate change. Below we added a table (Table 1.2) that is summarizing the different hydroclimatic terms used in the thesis, with its explanation and main use.

Table 1.1 Processes of the hydrological cycle as affected by human or climatic impacts, with references to the relevant chapters in the book; and the temporal scales of region-wide changes in the mean state.

Hydrological processes	Strong human impact	Strong climatic impact	Temporal scales of region-wide changes in the mean state[1]
Rainfall; hydroclimate	Chapter 9	Chapter 2	Inter-annual; inter-decadal centuries
Hillslope runoff	Chapter 3	Chapter 9	Years, decades
Gully discharge regime	Chapter 4, Chapter 6	Chapter 6	Years, decades
Floodplain processes	Chapter 5	Chapter 5, Chapter 9	Centuries
Debris fan processes	Chapter 6	Chapter 6	Years, decades
Lake levels	(irrigation)	Chapter 7	Decades, centuries
Lake sedimentation	Chapter 8	Chapter 8	Decades, centuries

[1] Note that we are mainly interested in region-wide changes of the 'mean state' of the processes involved. Rain events or gully discharges can occur on local scales during very short periods of time (e.g. half an hour). However, regime shifts of a region-wide hydrological system – or significant changes in the regional rainfall regime – may develop over years or decades. It can take decades up to centuries to change the regime of river or lake sedimentation, or to change the mean state of the regional hydroclimate.

Table 1.2 Hydroclimatic terminology used in the thesis, with its explanation and main use in the thesis.

Terminology	*Explanation*	*Main use in the thesis*
Climate variability	set of 'variations in the mean state and other statistics (such as standard deviations, the occurrence of extremes, etc.) of the climate on all spatial and temporal scales beyond that of individual weather events' (IPCC, 2007)	Chapter 2
Climate or climatic change(s)	'change in the state of the climate that can be identified (e.g., by using statistical tests) by changes in the mean and/or the variability of its properties, and that persists for an extended period, typically decades or longer' (IPCC, 2007)	Chapter 7, 9
Climate or climatic shift(s)	'an abrupt shift or jump in mean values signaling a change in regime' (IPCC, 2007)	Chapter 7
Drought	'recurring natural phenomenon associated with a deficit availability of water resources over a large geographical area and extending along a significant period of time' (Rossi, 2000)	Chapter 3, 4
Dry year	'dry kiremt season, specifically defined by a negative hydro climatic z-score' (see Chapter 2)	Chapter 2
(Holocene) dry phase	'period of prolonged aridity as identified from paleoclimatic records' (see Chapter 7)	Chapter 7, 9

1.5 The study area

The study focusses on the North Ethiopian Highlands in the Region of Tigray. In this area, several sub-areas with high regional variability in climate, geology, hydrological behavior and land use were selected for detailed study.

The Tigray region is located in the North of the Ethiopian Highlands. Elevations in the Tigray Highlands range between 1500 and 4000 m a.s.l. (Figure 1.4). In this mountainous region, the geology comprises rocks of both Precambrian and Phanerozoic ages. Precambrian metavolcanics and metasediments are situated at the base; with relatively thin Paleozoic formations on top. The Paleozoic rocks include the Enticho Sandstone Formation (of fluvioglacial origin) and the Adaga Arbi glacial deposits (tillites) (Bussert and Schrank, 2007). Later, Mesozoic sandstones (Adigrat sandstone), limestones (Antalo limestone) and shales (Agula shale) were deposited (Merla et al., 1979), followed by the Amba Aradam sandstone (a lateritised sandstone of the Lower Cretaeceous with the upper part containing tuffaceous mudstone). These sedimentary rocks were subsequently covered by Tertiary volcanics, such as the trap basalts of the Ashangi group (black alkali olivine basalts of the Paleocene, Oligocene and Miocene that are often interbedded with lacustrine deposits of silicified limestone and diatomite with gastropods). Drainage is strongly affected by Plio-Pleistocene uplift and occurs mainly towards the Tekeze-Nile river system and partially to the African Rift Valley. After Miocene and Pliocene–Pleistocene tectonic uplift, Early Holocene weathering and soil genesis (Nyssen et al., 2004a) resulted in the occurrence of mainly Vertisols, Vertic Cambisols, Cumulic Regosols, Calcaric Regosols and Phaeozems across the study area (Vanmaercke et al., 2010).

Monsoonal precipitation occurs from June until September in the form of intense rainstorms with large raindrop sizes (Nyssen et al., 2005). Annual precipitation increases from north to south, ranging between 500 and 900 mm yr^{-1} (Jacob et al., 2013). Inter-annual rainfall variability is equally important, as Nyssen et al. (2005) showed average yearly rainfall depths in the study area range between 546 mm in 2002 to 879 mm in 1998 in Hagere

Selam. A specific climatic background of the study area is presented in section 2.2.1 and a paleoclimatic background of the region is given in section 8.2.

The Northern Ethiopian Highland is home to an old agrarian society (Roberts, 1997). In Northern Ethiopia, before the late 19th century, the agro-system was organised in an unequal feudal way (locally named *gult-system,* or later *rist-system*) (Ståhl, 1974). Local noblemen, such as *dedjazmach*, owned most of the lands (Bruce, 1976), and these *rist* lands were often leased in a sharecropping system, locally named *mwufar* (Segers et al., 2010). After the end of the feudal era in 1974, the military regime or DERG (1974-1991) tried to implement a land reform (an overall nationalization of farmlands with strong state control of the farms) which succeeded only partially in the study area (Naudts, 2002). After the end of the military regime in 1991, the Tigray People's Liberation Front (TPLF) initiated another land redistribution, in which all households received about three farm plots. However, lands are still often lent out in the *mwufar* sharecropping system, consisting of a temporary transfer (normally for the duration of one agricultural season) of the use rights of a plot of land in exchange for a share of the grain harvest (Segers et al., 2010). Since the 1990s, important conservation efforts (check dams, stone bunds, exclosures, reforestation) were made and agricultural intensification was enhanced (e.g. improved crop varieties, chemical fertilizers). Still, overgrazing of rangeland is a particular problem in the Highlands, as current stocking rates are well in excess of estimated optimum stocking rates (Bojö and Cassells, 1995; Nyssen et al., 2004). Croplands are commonly cultivated with wheat (*Triticum* spp.), barley (*Hordeum vulgare*), *hanfez*, that is wheat and barley sown together, and the endemic *Eragrostis tef*, and are ploughed with the local ard plough or *mahresha*. For Ethiopia, the total population was estimated at 6.6 million in 1868 while it was about 82 million in 2011 (Nyssen et al., 2014).

Partly due to highly erosive rainfall and the occurrence of steep slopes, soil erosion in the region is widespread (Nyssen et al., 2004a) and active gullies dissect its landscape (Frankl et al., 2013). As stated before, three main phases of gully development in the Northern Ethiopian Highlands were identified over the 20th century: (i) a phase of relatively stable gullies that was evidenced by historical photographs since 1868 and lasted until the 1960s, (ii) a gully incision phase with region-wide activation of the gully channels between the 1960s and ca. 2000, (iii) an initial gully stabilization phase related to reduced flood peaks (after 2000) (Frankl et al., 2011, 2013).

A considerable part of the study is focusing on Lake Ashenge (Figure 1.4), situated in a small marginal graben bounded by NNE-SSW faults, formed parallel to the lower Raya graben. Geology consists of Tertiary volcanics, in particular the trap basalts of the Ashangi group, which are black alkali olivine basalts (Paleocene, Oligocene and Miocene) with frequent intercalations of silicified limestone in-between (Merla et al., 1979). Quaternary basin fill (gravels to clays) is composed of eluvial, colluvial and alluvial material, as well as of paleo lacustrine sediments to the North of the current lake and near Korem (Kurkura Kabeto et al., 2012). Later, a number of gullies incised the valley bottom around the graben lake; and several of them bear debris fans downstream at the lake shore (Frankl et al., 2011). Upper catchments have overall steep slopes gradients (0.5 to 1.0 m m^{-1}) while near to the lake gentle gradients occur (< 0.1 m m^{-1}). Average yearly rainfall is ~900 mm yr^{-1} (station of Maychew) (Frankl et al., 2011) but precipitation is concentrated in the months between June and September when very high rainfall intensities occur. Most catchments have forested upper parts but are in general dominated by croplands, while grazing occurs on grasslands that occur close to the lake.

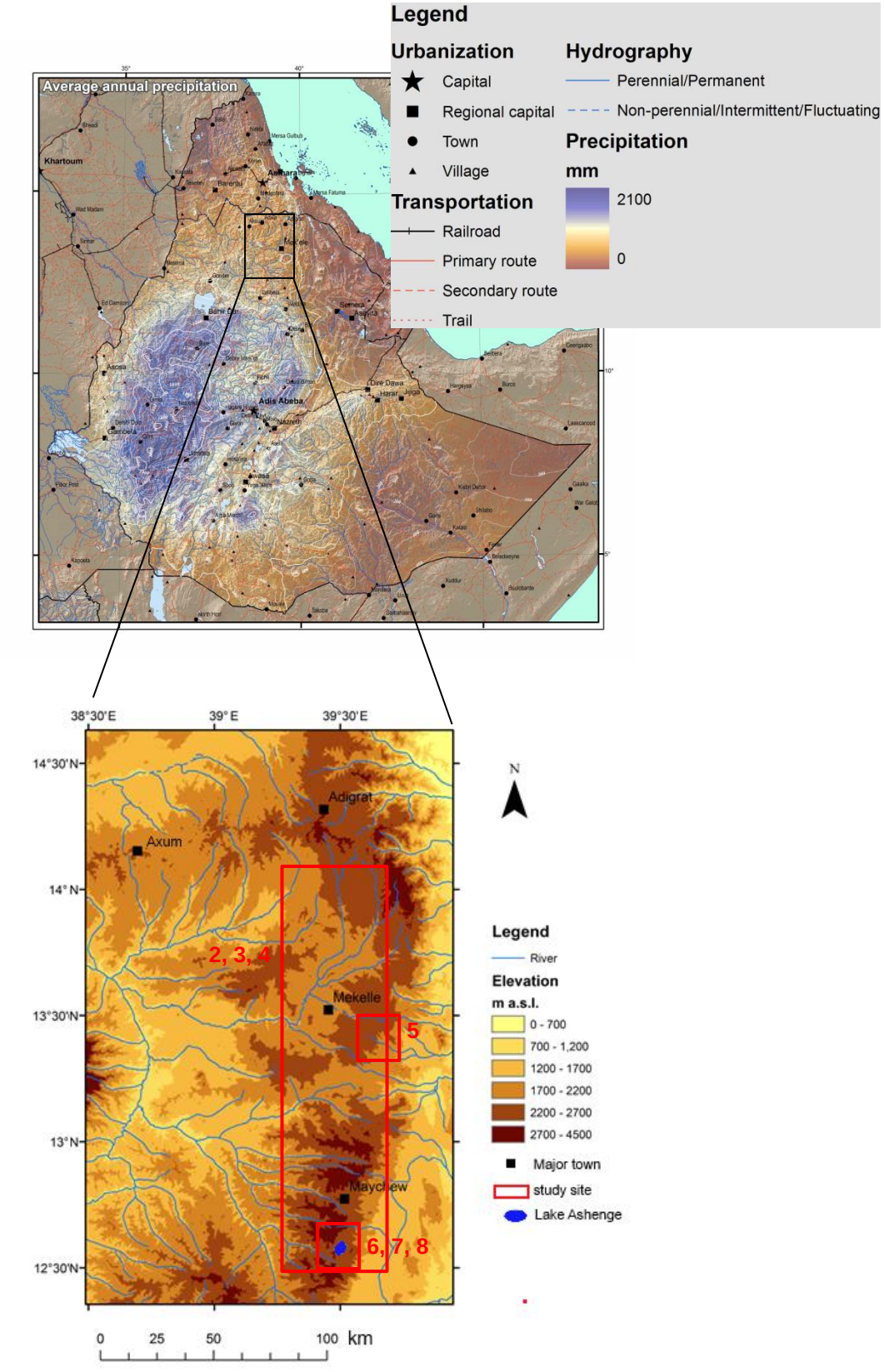

Figure 1.4 General physiographic setting of Ethiopia with topographical shading and depiction of the average annual rainfall (upper figure, derived from Fazzini et al., 2015); and setting of the research area in the Northern Ethiopian Highlands (lower figure) with indication of the study areas for the different chapters.

1.6 References

Adger, N., Benjaminsen, T., Brown, K., Svarstad, H., 2001. Advancing a Political Ecology of global environmental discourses. Development and Change 32, 681-715.

Amanuel Zenebe, Vanmaercke, M., Poesen, J., Verstraeten, G., Nigussie Haregeweyn, Mitiku Haile, Kassa Amare, Deckers, J., Nyssen, J., 2013. Spatial and temporal variability of river flows in the degraded semi-arid tropical mountains of northern Ethiopia. Zeitschrift für Geomorphologie 57(2), 143-169.

Auzet, V., Boiffin, J., Ludwig, B., 1995. Concentrated flow erosion in cultivated catchments: Influence of soil surface state. Earth Surface Processes and Landforms 20 (8), 759–767.

Avni, Y., 2005. Gully incision as a key factor in desertification in an arid environment the Negev highlands, Israel. Catena 63 (2-3), 185-220.

Bard K., Coltorti, M., Di Blasi, M., Dramis F., Fattovich, R., 2000. The environmental history of Tigray (Northern Ethiopia) in the Middle and Late Holocene: a preliminary outline. African Archaeological Review 17 (2), 65-86.

Batterbury, S., Forsyth, T., Thomson, K., 1997. Environmental transformations in developing countries: hybrid research and democratic policy. Geographical Journal 163 (2), 126-132.

Biazin, B., Sterk, G., 2013. Drought vulnerability drives land-use and land cover changes in the Rift Valley dry lands of Ethiopia. Agriculture Ecosystems & Environment 164, 100-113.

Billi, P., Yonas Tadesse Alemu, Ciampalini, R., 2015. Increased frequency of flash floods in Dire Dawa, Ethiopia: Change in rainfall intensity or human impact? Natural Hazards 76 (2), 1373-1394.

Bojö, J., Cassells, D., 1995. Land degradation and rehabilitation in Ethiopia: a reassessment. World Bank, Environmentally Sustainable Development Division, AFTES Working Paper 17, 48 p.

Breman, H., Groot, R., van Keulen, H., 2001. Resource limitations in Sahelian agriculture. Global Environmental Change 11 (1), 59–68.

Bruce, J., 1976. Land reform planning and indigenous communal tenures: a case study of the tenure 'chiguraf-gwoses' in Tigray, Ethiopia. PhD thesis, University of Wisconsin, Madison, USA.

Bussert, R., Schrank, E., 2007. Palynological evidences for a latest Carboniferous-Early Permian glaciation in Northern Ethiopia. Journal of African Earth Science 49, 201-210.

Descheemaeker, K., Nyssen, J., Poesen, J., Raes, D., Haile, M., Muys, B., Deckers, J., 2006. Runoff on slopes with restoring vegetation: A case study from the Tigray highlands, Ethiopia. Journal of Hydrology 331 (1-2), 219-241.

de Wit, M., Stankiewicz, J., 2006. Changes in Surface Water Supply Across Africa with Predicted Climate Change. Science 311 (5769), 1917-1921.

Easdale, M., Domptail, S., 2014. Fate can be changed! Arid rangelands in a globalizing world – A complementary co-evolutionary perspective on the current 'desert syndrome'. Journal of Arid Environments 101, 52–62.

Eswaran, H., Lal, R., Reich, P., 2001. Land degradation: an overview. In: Bridges, E., Hannam, I., Oldeman, L., Pening, F., de Vries, S., Scherr, S., Sompatpanit, S. (eds.). Responses to Land Degradation. Proc. 2nd. International Conference on Land Degradation and Desertification, Khon Kaen, Thailand. Oxford Press, New Delhi, India.

FAO, 2014. Water Scarcity. http://www.fao.org/nr/water/topics_scarcity.html (accessed on 05/05/2014)

Fazzini, M., Bisci, C., Billi, P., 2015. The Climate of Ethiopia. In: Billi (Ed.) Landscapes and Landforms of Ethiopia, Springer, New York, USA, 65-88 p.

Frankl, A., Nyssen, J., De Dapper, M., Haile, M., Billi, P., Munro, N., Deckers, J., Poesen, J., 2011. Linking long-term gully and river channel dynamics to environmental change using repeat photography (Northern Ethiopia). Geomorphology 129, 238-251.

Frankl, A., Poesen, J., Scholiers, N., Jacob, M., Mitiku Haile, Deckers, J., Nyssen, J., 2013. Factors controlling the morphology and volume (V) – length (L) relations of permanent gullies in the Northern Ethiopian Highlands. Earth Surf Process Landforms 38 (14), 1672–1684.

Fryirs, K., Brierley, G., 1998. The character and age structure of valley fills in Upper Wolumla Creek catchment, South Coast, New South Wales, Australia. Earth Surface Processes and Landforms 23, 271-287.

Fujita, K., 2010. The Green Revolution and Its Significance for Economic Development: The Indian Experience and Its Implications for Sub-Saharan Africa. JICA Research 17, 1-27.

GACGC, 1994. World in transition: the threat to soils. Annual Report of the German Advisory Council on Global Change. Bonn, Economica Verlag GmbH.

Huang, J., Yu, H., Guan, X., Wang, G., Guo, R., 2015. Accelerated dryland expansion under climate change. Nature Climate Change, in press. DOI: doi:10.1038/nclimate2837.

IPCC, 2007. Climate Change 2007: Working Group I: The Physical Science Basis – Glossary. Available from:
https://www.ipcc.ch/publications_and_data/publications_and_data_glossary.htm
(accessed on 11/01/2016).

Jacob, M., Frankl, A., Mitiku Haile, Zwertvaegher, A., Nyssen, J., 2013. Assessing spatio-temporal rainfall variability in a tropical mountain area (Ethiopia) using NOAAs Rainfall Estimates. International Journal of Remote Sensing 34 (23), 8319-8335.

Jiménez Cisneros, B., Oki, N.W., Arnell, G., Benito, J.G., Cogley, P., Döll, T., Jiang, T., Mwakalila, S., 2014. Freshwater resources. In: Climate Change 2014: Impacts,Adaptation, and Vulnerability. Part A: Global and Sectoral Aspects. Contribution of Working Group II to the Fifth Assessment Report of the Intergovernmental Panel on Climate Change [Field, C.B., V.R.

Barros, D.J. Dokken, K.J. Mach, M.D. Mastrandrea, T.E. Bilir, M. Chatterjee, K.L. Ebi, Y.O. Estrada, R.C. Genova, B. Girma, E.S. Kissel, A.N. Levy, S. MacCracken, P.R. Mastrandrea, and L.L.White (eds.)]. Cambridge University Press, Cambridge, United Kingdom and New York, NY, USA, pp. 229-269.

Kiernan, K., 2015. Nature, severity and persistence of geomorphological damage caused by armed conflict. Land Degradation and Development 26 (4), 380–396.

Kurkura Kabeto, Aynalem Zenebe, Bheemalingeswara, K., Kinfe Atshbeha, Solomon Gebresilassie, Kassa Amare, 2012. Mineralogical and Geochemical Characterization of Clay and Lacustrine Deposits of Lake Ashenge Basin, Northern Ethiopia: Implication for Industrial Applications. Momona Ethiopian Journal of Science (MEJS) 4 (2), 111-129.

Lal, R., 1995. Erosion-Crop Productivity Relationships for Soils of Africa. Soil Science Society of America Journal 59 (3), 661-667.

Lal, R., 2001. Potential of Desertification Control to Sequester Carbon and Mitigate the Greenhouse Effect. Climatic Change 51 (1), 35-72.

Le Houérou, H., 1996. Climate change, drought and desertification. Journal of Arid Environments 34, 133–185.

Lespez, L., Le Drezen, Y., Garniera, A., Rassec, M., Eichhorn, B., Ozainnee, A., Ballouchef, K., Neumann, K., Huysecom, E., 2011. High-resolution fluvial records of Holocene environmental changes in the Sahel: the Yamé River at Ounjougou (Mali, West Africa). Quaternary Science Reviews 30 (5–6), 737–756.

Mann, M., 2002. The Value of Multiple Proxies. Science 297 (5586), 1481-1482.

Marshall, M., Lamb, H., Davies, S., Leng, M., Zelalem Kubsa, Umer, M., Bryant, C., 2009. Climatic change in northern Ethiopia during the past 17,000 years: A diatom and stable isotope record from Lake Ashenge. Palaeogeography, Palaeoclimatology, Palaeoecology 279, 114–127.

Meadows, D., Meadows, D., Randers, J., Behrens, W., 1972. Limits to growth. Universe Books: New York.

Merla, G., Abbate, E., Azzaroli, A., Bruni, P., Canuti, P., Fazzuoli, M., Sagri, M., Tacconi, P., 1979. A Geological Map of Ethiopia and Somalia (1973). 1:2000.000; and Comment. University of Florence, Firenze.

Modarres R, Ouarda T., 2014. Modeling the relationship between climate oscillations and drought by a multivariate GARCH model. Water Resources Research 50, 1-18.

Muller, T., 2013. The Ethiopian famine revisited: Band Aid and the antipolitics of celebrity humanitarian action. Disasters 37 (1), 61-79.

Naudts, J., 2002. Les Hautes Terres de Tembien, Tigré, Ethiopie; Résistance et limites d'une ancienne civilisation agraire; Conséquences sur la dégradation des terres. Mémoire présenté en vue de l'obtention du Diplôme d'Agronomie Tropicale CNEARC, Montpellier.

Nyssen, J., Poesen, J., Moeyersons, J., Deckers, J., Mitiku Haile, Lang, A., 2004a. Human impact on the environment in the Ethiopian and Eritrean highlands – a state of the art. Earth Sci Rev 64, 273–320.

Nyssen, J., Mitiku Haile, Moeyersons, J., Poesen, J., Deckers, J., 2004b. Environmental policy in Ethiopia: a rejoinder to Keeley and Scoones. Journal of Modern African Studies 42 (1), 137-147.

Nyssen, J., Vandenreyken, H., Poesen, J., Moeyersons, J., Deckers, J., Mitiku Haile, Salles, C., Govers, G., 2005. Rainfall erosivity and variability in the Northern Ethiopian Highlands. J. Hydrol. 311, 172–187.

Nyssen, J., Clymans, W., Poesen, J., Vandecasteele, I., De Baets, S., Nigussie Haregeweyn, Naudts, J., Amanuel Hadera, Moeyersons, J., Mitiku Haile, Deckers, J., 2009. How soil conservation affects the catchment sediment budget – a comprehensive study in the north Ethiopian highlands. Earth Surf. Process. Landforms 34, 1216–1233.

Palmer, P., Smith, M., 2014. Earth systems: Model human adaptation to climate change. Nature 512, 365–366.

Pender, J., Gebremedhin, B., 2008. Determinants of agricultural and land management practices and impacts on crop production and household income in the highlands of Tigray, Ethiopia. Journal of African Economies 17, 395-450.

Petschel-Held, G., Block, A., Cassel-Gintz, M., Kropp, J., Ludeke, M., Moldenhauer, O., Reusswig, F., Schellnhuber, H., 1999. Syndromes of Global Change: a qualitative modelling approach to assist global environmental management. Environmental Modeling and Assessment 4, 295–314.

Rangan, H., Carney, J., Denham, T., 2012. Environmental history of botanical exchanges in the Indian Ocean world. Environment and History 18 (3), 311-342.

Riddle, E., Cook, K., 2008. Abrupt rainfall transitions over the Greater Horn of Africa: observations and regional model simulations. J. Geophys. Res. 113, D15109.

Roberts, N., 2006. The Holocene: an environmental history (second edition). Blackwell Publishing, Oxford, UK.

Segele, Z., Lamb, P., Leslie, L., 2009. Large-scale atmospheric circulation and global sea surface temperature associations with Horn of Africa June – September rainfall. Int. J. Climatol. 29, 1075–1100.

Segers, K., Dessein, J., Develtere, P., Hagberg, S., Haylemariam Girmay, Mitiku Haile, Deckers, J., 2010. The Role of Farmers and Informal Institutions in Microcredit Programs in Tigray, Northern Ethiopia. Perspectives on Global Development and Technology 9 (3-4), 520-544.

Sheffield, J., Wood, E., 2011. Drought: Past Problems and Future Scenarios. Routledge, London, UK, 224 p.

Ståhl, M., 1974. Ethiopia: political contradictions in agricultural development. Rabén & Sjögren, Stockholm, 186 p.

Stankoviansky, M., 2003. Historical evolution of permanent gullies in the Myjava Hill Land, Slovakia. Catena 51, 223-239.

Tekle Kebrom, 1999. Land degradation problems and their implications for food shortage in south Welo, Ethiopia. Environmental Management 23(4), 419–427.

Tubiello, F., van der Velde, M., 2015. Land and water use options for climate change adaptation and mitigation in agriculture. Food and Agriculture Organization of the United Nations (FAO), SOLAW Background Thematic Report - TR04AUN, 38 p.

UNCCD, 1994. United Nations Convention to Combat Desertification. Available from: http://www.unccd.int/en/about-the-convention/Pages/Text-Part-I.aspx (accessed on 11/01/2016).

UNEP, 1992. World Atlas of Desertification. Edward Arnold, London, UK.

Vanmaercke, M., Zenebe, A., Poesen, J., Nyssen, J., Verstraeten, G., Deckers, J., 2010. Sediment dynamics and the role of flash floods in sediment export from medium-sized catchments: a case study from the semi-arid tropical highlands in northern Ethiopia. J. Soils Sediments 10, 611–627.

Vanmaercke, M., Poesen, J., Verstraeten, G., Maetens, W., de Vente, J., 2011. Sediment yield as a desertification risk indicator. Science of the Total Environment 409, 1715-1725.

Verschuren, D., Laird, K., Cumming, B., 2000. Rainfall and drought in equatorial east Africa during the past 1,100 years. Nature 403, 410-414.

Vogt, J., 1953. Erosion des sols et techniques de culture en climat tempéré maritime de transition (France et Allemagne). Revue de Géomorphologie Dynamique 4, 157-183.

Williams, A., Funk, C., 2011. A westward extension of the warm pool leads to a westward extension of the Walker circulation, drying eastern Africa. Clim. Dyn. 37, 2417–2435.

Part I

Chapter 2 Rainfall and drought: modelling the impact of global atmospheric-oceanic teleconnections

This chapter is modified from:

Lanckriet, S., Frankl, A., Termonia, P., Nyssen, J., 2015. Droughts related to quasi-global oscillations: a diagnostic teleconnection analysis in North Ethiopia. International Journal of Climatology 35 (7), 1534–1542.

Abstract

This chapter presents a method to elaborate atmospheric teleconnections and applies it on the drought-prone region of North Ethiopia. By doing so, the relatively new procedure known as empirical orthogonal teleconnection analysis (EOT) was validated as an effective way for identifying the impact of atmospheric patterns in remote oceanic basins on rainfall trends at a particular location. Rainfall trends were investigated, and trend analysis on (optimally interpolated) rain gauge data shows a significant decrease for *kiremt* rainfall (June-September) in North Ethiopia before 1985. EOT analysis of assimilated mean sea level pressure data reveals that not only El Niño/La Niña (ENSO), but also the Indian Ocean Dipole (IOD) has a significant impact in North Ethiopia. Including the variability of the South West Monsoons (SWM), subsequent multivariate regression could model North Ethiopian *kiremt* rainfall from these three teleconnections (R^2 = 0.64), representing 89% of all dry years. In particular, the interaction between these three teleconnections was a major contributor to the 1983–85 droughts and famine. The study hence finds a significant impact of three quasi-global atmospheric teleconnections (ENSO, IOD, SWM) on North Ethiopian rainfall variability. Moreover, it is pointed out that empirical orthogonal teleconnection analysis is a useful tool to identify the relations between drought risk and remote atmospheric systems.

2.1 Introduction

Teleconnections are recurring and persistent, large-scale patterns of pressure and circulation anomalies that span vast geographical areas (Climate Prediction Center, 2015). They are preferred modes of low-frequency (long time scale) variability, such as quasi-global oscillations (the El Niño Southern Oscillation, North Atlantic Oscillation, etc.). Commonly, teleconnections are identified and analyzed using Principal Component Analysis (PCA) or Empirical Orthogonal Functions (EOF); see amongst others Halldor and Venegas (1997). Recently however, the Empirical Orthogonal Teleconnection (EOT) analysis was introduced by van den Dool et al. (2000), as an alternative method to find large-scale atmospheric patterns (Simonti and Eastman, 2010). In earth observation time series data, EOTs examine each pixel over time to find which pixel can explain the greatest amount of variability of all other pixels combined (Clark Labs, 2009). As shown by van den Dool et al. (2000), EOT patterns are very similar to corresponding rotated EOFs, but computation is far more efficient.

Quasi-global teleconnections are important for explaining drought occurrence. Of all natural hazards, droughts may be the most complex and least understood phenomena (Modarres and Ouarda, 2014), partly because of strong associations with quasi-global oscillations (Behera et al., 2005; Hoerling and Kumar, 2003). For example, the El Niño Southern Oscillation (ENSO) is known to influence drought occurrence in amongst others Brazil (Liu and Juarez, 2001), Indonesia, the Philippines (Harger, 1995) and Ethiopia (Abtew et al., 2009).
North Ethiopia was chosen as a case-study region for testing the effectiveness of the EOT method to identify the impact of quasi-global oscillations on drought risk (Figure 2.1a).

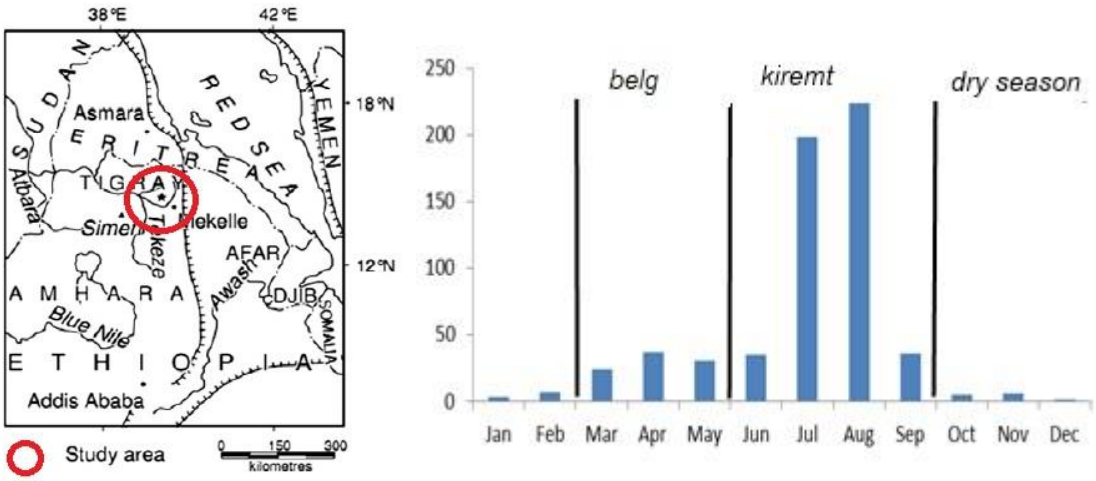

Figure 2.1 (a) Location of the focus area (radius of 125 km around Mekelle) and (b) mean monthly rainfall at Mekelle-Quiha Airport (1960-2004; with 1986 and 1989-1991 missing; data obtained from the Ethiopian Meteorological Agency).

Earlier studies have linked (North-) Ethiopian rainfall with atmospheric teleconnections. Amongst the most relevant reported teleconnections is the El Niño Southern Oscillation (Nicholson and Kim, 1997; Korecha and Barnston, 2007), whereby most authors found dryer conditions in an El Niño year (Abtew et al., 2009; Sileshi and Zanke, 2004; Segele et al., 2009a and b). Indeed, famines and droughts reported in historical sources (Spinage, 2012) show a small frequency peak at 5-10 year variability (Figure 2.2). The impact of El Niño is also found to the south of the Horn of Africa. For example, Wolff et al. (2011) find that equatorial East Africa has more rain and flooding during El Niño and droughts during La Niña years. Nicholson and Selato (2000) obtain similar results (reduced rainfall during La Niña) for southern Africa.

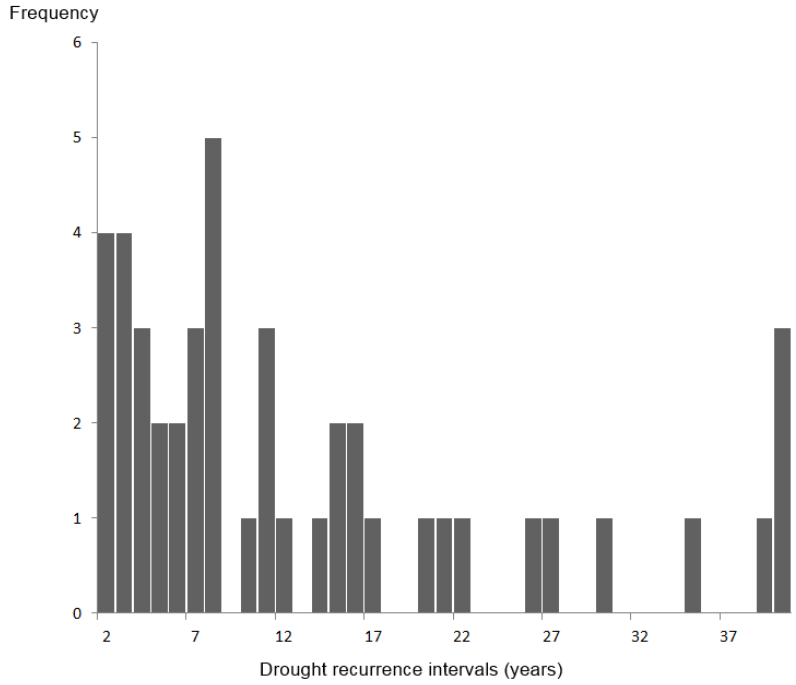

Figure 2.2 Frequency of reported droughts as a function of recurrence intervals of droughts and famines mentioned in historical sources since the 12th century; calculated from Spinage (2012).

As a result of agricultural stagnation, Williams and Funk (2011) estimated that due to low food production, more than 15 million people were food insecure in Kenya, Ethiopia and Somalia in 2009. Food insecurity is however a long-term problem, since famines are reported in Ethiopia since the 12th century (Pankhurst, 1985; Spinage, 2012; summarized in Table 2.1).

Table 2.1 A summary of historical droughts and famines (derived from Spinage, 2012).

1258-1259	1261-1262	1272-1273	1314-1344	1508-1540	1543-1544	1560	1562
1567	1569-1571	1611	1634-1635	1650	1653	1668	1700
1702	1706	1747	1752	1772-1773	1788-1789	1800	1826-1827
1828-1829	1835	1865	1888-1889	1888-1892	1899-1900	1913-1914	1921
1932-1934	1953	1957	1964-1965	1970-1973	1975	1983-1985	

By using rainfall data, the objectives of this study are therefore: (i) to apply an EOT based method to detect teleconnections; and (ii) to understand drought occurrence in North Ethiopia from these teleconnections.

2.2 Materials and methods

2.2.1 Climatic background of the study area

The rainfall regime in North Ethiopia is characterized by three distinct seasons. Most rainfall occurs in the period June–September (*kiremt* rain) during localized but intense convective storm events (Nyssen et al., 2005). *Kiremt* rains are provoked when the intertropical convergence zone is situated at its most northerly position (16–20 °N) (Segele et al., 2009a, 2009b). Yet, yearly rainfall is quite variable, since it is amongst others depending on the variability of the Somali low-level jet and the Tropical Easterly Jet (Segele et al., 2009a, 2009b). Moreover, in the Tigray Highlands, spatial variation of rain is influenced by topography (Nyssen et al., 2005). June-September *kiremt* rains are responsible for the bulk of all yearly precipitation in the region, as shown by the mean monthly rainfall of Mekelle, which is the capital of the northern Tigray region (Ethiopian Meteorological Agency; Figure 2.1b).

Second, from October onwards, a *dry season* prevails, which is equally influenced by the seasonal movement of the intertropical convergence zone (Segele et al., 2009a). Moreover, the North-East Trade Winds, dry winds coming from the Arabian deserts, are blowing during the southern summer and are bringing aridity in Ethiopia (Spinage, 2012). Third, between February and May, on the East-African coast the South-East Trade Winds bring a wet air mass across the Indian Ocean (Spinage, 2012). These rains are named *belg* rains (Jacob et al., 2013), defined between mid-February to mid-May (e.g. Gissila et al. 2004; Diro et al. 2008). *Belg* is amongst others influenced by the early formation of the meridional branch of the Somali jet along the East African coast (Riddle and Cook, 2008), and by a high-amplitude Madden- Julian Oscillation (Williams and Funk, 2011). However, this study focusses on *kiremt* rainfall (June-July-August-September; JJAS), since *kiremt* represents the main moisture source for the regional subsistence agriculture.

Mean annual rainfall for the investigated period is 611 mm for Mekelle-Quiha Airport, with a standard deviation of 148 mm and an average rainfall of the wettest month of 254 mm. For the same period, JJAS rainfall represents on average 81.2 % of the yearly total. In general, caution should be taken, since the years 1986 and 1989-1991 are missing (due to the civil war).

2.2.2 Pressure and rainfall data

In order to compute EOTs, atmospheric pressure time series data were required. Monthly mean sea level pressure data at global scale were obtained as NetCDF files from the ERA-40 reanalysis. ERA-40 is the ECMWF (European Centre for Medium-Range Weather Forecasts) reanalysis of the global atmosphere and surface conditions, over the period from September 1957 to August 2002 with a resolution of 2.5° (Uppala et al., 2005).

The occurrence of droughts was defined from the (daily) rainfall record of Mekelle-Quiha Airport (1960-2009; with 1986 and 1989-1991 missing), as obtained from the Ethiopian National Meteorology Agency (NMA). Missing data were excluded for analysis. For additional verification of the rainfall trend, we also used the optimally interpolated rainfall data from NOAA's PRECipitation REConstruction over Land (PREC/L), since rainfall representation of the ERA40 reanalysis is known to be problematic (Fernandes et al., 2008). This monthly global data set is constructed with interpolation of gauge observations over land (PREC/L) (1948-2011), with a spatial resolution of 0.5°x0.5°. Gauge observations are from over 17,000 stations collected in the Global Historical Climatology Network (GHCN) version 2, including those from the Ethiopian Meteorological Agency and the Climate Anomaly Monitoring System (CAMS) datasets. According to Chen et al. (2002), the optimal interpolation technique of Gandin was used to assimilate the observations. The mean distribution and annual cyclicity of precipitation observed in the PREC/L showed good agreement with those in several published gauge-based datasets and the anomaly patterns associated with ENSO resemble those found in other studies worldwide (Chen et al., 2002). *Kiremt* rainfall was considered as the rainfall for June-September (JJAS). Correlation analysis and Theil-Sen trend analysis were applied to the rainfall time series. Note that the nonparametric Theil-Sen trend approach was chosen since it provides a more robust slope estimate than the least-squares method (Sen, 1968). The rainfall data were, following Hong et al. (2001), standardized to hydro climatic z-scores. Following Amemiya (1985), the hydro climatic variable gets value 1 if the standardized hydro climatic z-score is positive; the variable gets value 0 if the standardized z-score is negative. The probability of having a wet or dry *kiremt* season can then be modeled using a logit regression.

2.2.3 Empirical Orthogonal Teleconnection computations

In order to identify large-scale patterns of pressure anomalies, EOTs were computed with the mean sea level pressure data, using IDRISI software, in a normal setup instead of space-time reversal. EOT analysis provides solutions that are orthogonal in one direction, either space or time, and can be compared to obliquely rotated Principal Components (van den Dool et al., 2000). Because EOTs are constrained to be orthogonal in just one direction rather than in both space and time directions, the computation is more efficient than is the case with EOFs (Smith, 2004). Contrary to EOF methods, EOT allows some freedom to target the analysis towards specific geographic locations. Moreover, there is no need to determine the degree of EOF truncation before rotation (Simonti and Eastman, 2010). Hence, EOTs were calculated on JJAS mean sea level pressure data, and the EOTs that were significantly correlated with JJAS rainfall in Mekelle were used for analysis. Significance of all correlations was tested with a two-sided t-test as described in Snedecor and Cochran (1989):

$$t = r.\sqrt{\frac{n-2}{1-r^2}} \qquad (2.1)$$

Under the null hypothesis that there is no correlation between the two variables, n is the number of observations, r the Pearson product moment correlation coefficient and n-2 the degrees of freedom.

Let $f(s_l, t_k)$ be the spatiotemporal pressure dataset at locations s_l and at time t_k, and $f_\mu(s_l, t_k)$ the mean and trend component; then the EOTs are obtained by computing the pressure anomaly $f'(s_l, t_k)$:

$$f'(s_l, t_k) = f(s_l, t_k) - f_\mu(s_l, t_k) \qquad (2.2)$$

or:

$$f'(s_l, t_k) = \sum_{p=1}^{p} c_p(t_k) e_p(s_l) \qquad (2.3)$$

with:

$$e_p(s_l) = corr(s_l, sb_p)\frac{\sigma(s_l)}{\sigma(sb_l)} \qquad \text{and } c_p(t_k) = f'(sb_p, t_k) \qquad (2.4 \text{ and } 2.5)$$

Here is $e_p(s_l)$ a regression coefficient, *corr* is the correlation function, σ is the standard deviation, sb_p is the point in space with the most spatial variance at a given time, and $c_p(t_k)$ is the p^{th} temporal eigenfunction (Magar et al., 2012). As an *a posteriori* validation of the results, existing indices of atmospheric teleconnections were taken into account. This included the JJAS Multivariate ENSO Index (MEI; Rasmusson and Carpenter, 1982; Wolter, 1987), while a JJAS South West Monsoon Index was used as standardized difference between standardized wind modulus at 925 hPa and standardized zonal wind at 200 hPa, within the West African monsoon domain (5°-17.5°N, 20°W-40°E) (Li and Zeng, 2005). A JJAS Western Tropical Indian Ocean Sea Surface Temperature Index was taken in the region (50-70E; 10S-10N). Hence, *kiremt* rainfall could be linked with teleconnection variables in a multivariate regression.

2.3 Results

2.3.1 Identification of the EOTs

From the first 10 EOTs performed on JJAS mean sea level pressure data, three EOTs were significantly correlated with JJAS rainfall at Mekelle-Quiha Airport: EOT-1, EOT-2 and EOT-5. EOT-1 represents an Atlantic Ocean signal; EOT-2 represents a Pacific Ocean signal and EOT-5 an Indian Ocean signal. These EOTs were also well correlated with JJAS rainfall averaged in an area of 125 km around Mekelle (correlation > 0.30), and its spatial patterns (pixels with the most spatial variance) indicate mean sea level pressure focuses on the Gulf of Guinea, the Southern Pacific and the Western Indian Ocean respectively (Figure 2.3). Other EOTs (e.g. EOT-3 or EOT-4, etc.) were not significantly correlated with *kiremt* rainfall in the study area and were, following Simonti and Eastman (2010), not withheld for further analysis.

EOT-2 is strongly negatively correlated with the MEI (correlation = - 0.67; $p < 0.001$) and positively with the Southern Oscillation Index (correlation = + 0.66; $p < 0.001$), and is therefore closely related to a La Niña signal. As the EOT-5 would relate to a (negative) Indian

Ocean Dipole signal, the variable could be compared to the Dipole Mode Index (DMI). However, while EOT-5 is hardly correlated with the JJAS MEI (correlation = 0.09), and weakly with the JJAS DMI (correlation = - 0.35), it is better correlated with the residuals of the regression JJAS MEI-DMI (correlation = -0.43; p = 0.003). Since EOT-5 does not linearly correlate with MEI, it hence reflects only non-ENSO modes of variability. The Atlantic EOT is weakly correlated with the JJAS Atlantic Meridional Mode (correlation = 0.22), but better with the JJAS mean sea level pressure over Saint Helena (correlation = 0.38; p = 0.008). EOT-1 hence should represent some "Guinea Anticyclone" signal; controlling the South West Monsoons (see Segele et al., 2009b).

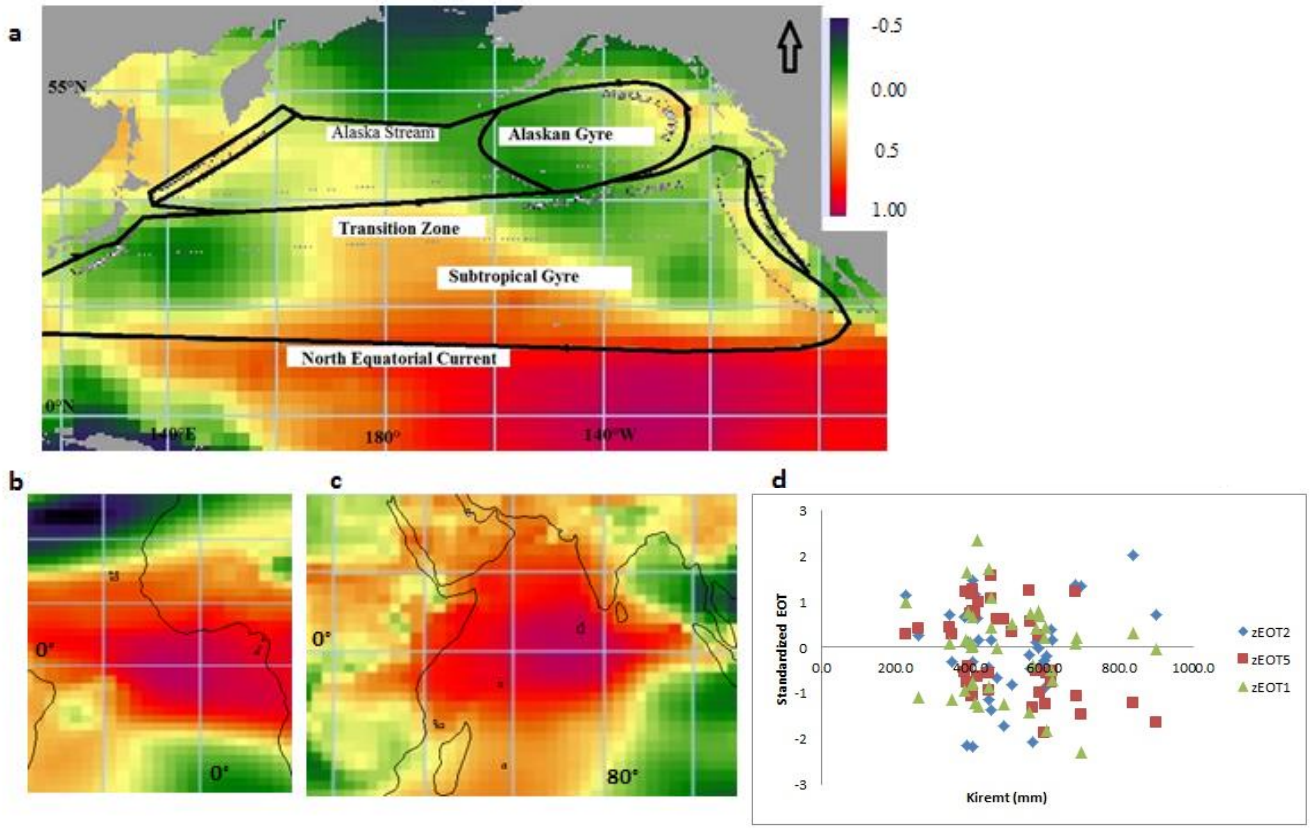

Figure 2.3 (a) EOT-2, the second mean sea level pressure teleconnection, centered on the Southern Pacific; with indication of some other surface oceanic currents (derived from http://geosci.sfsu.edu/); (b) EOT-1, centered on the equatorial Atlantic; (c) EOT-5, centered on the western Indian Ocean; and (d) scatterplots showing the standardized EOT values (zEOT) versus kiremt rainfall as measured at Mekelle-Quiha Airport.

2.3.2 Identification of the inter annual rainfall variability

The *kiremt* time series derived from both NMA as PREC/L do not show any overall trends, although it is clear that *kiremt* precipitation underwent some serious dips during the 1970s and 1980s (Figure 2.4). During the years 1983–85, North Ethiopia was struck by severe droughts – these are the years of the 'Great Famine'. For mean JJAS precipitation, linear and Theil-Sen trends were tentatively calculated as 'declining' (Figure 2.4), but were not significant for the study area ($p > 0.1$). Given this overall stable rainfall regime, the rainfall gauge data imply that there is no gradual drying trend over the second half of the 20th century. Moreover, the data confirm other studies based on Ethiopian meteorological stations contesting a presumed gradual 20th century drying trend (e.g. Conway, 2000; Cheung et al., 2008). Yet, the Theil-Sen trend over the first half of the NMA dataset (before 1985) was declining and significant on the 0.1 level ($p = 0.09$); the Theil-Sen trend over the second half was increasing but not significant ($p = 0.86$). Additionally, a Theil-Sen trend over the PREC/L dataset during the same first period was declining and significant ($p = 0.03$); the Theil-Sen trend over the same second period was increasing but not significant ($p = 0.35$).

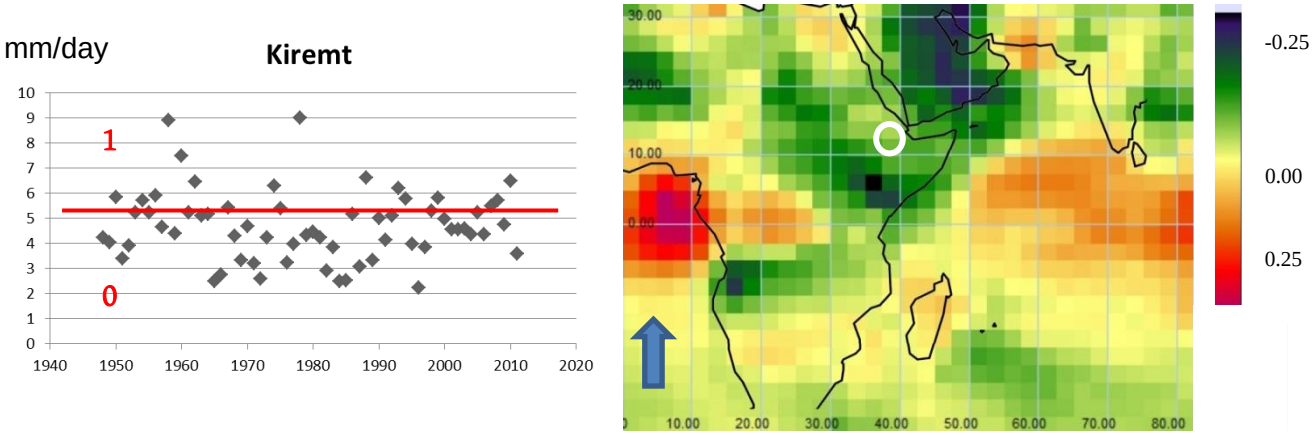

Figure 2.4 (a) Temporal evolution of average daily kiremt rainfall (average daily rainfall between June and September in a given year) (JJAS; in mm per day) spatially averaged over a circle with radius of 125 km around Mekelle. The horizontal red line represents the average of all kiremt seasons, with indication of the wet (value of 1) and dry (value of 0) kiremt seasons. (b) Theil-Sen trend map. The focus area is indicated with a white circle.

2.3.3 Linking EOTs with inter annual rainfall variability

2.3.3.1 Single *kiremt* EOT-logit models

Firstly, logistical regression was performed in order to investigate the impact of the identified teleconnections (see section 3.1) on the probability of having a wet (value of 1) or dry (value of 0) *kiremt* season. All links between the EOTs and the North Ethiopian precipitation data were significant (Table 2.2). Such logistic teleconnection-drought models are simple and significant models, yielding for instance the following equation for EOT2:

$$P(\pi = wet) = \frac{1}{1+e^{-(0.010EOT-2)}} \qquad (2.6)$$

Table 2.2 Significance and regression coefficients of all factors in the EOT-1,2,5 logit models.

	B	Wald	Sig.	Exp(B)
EOT-1	-0.016	7.337	0.007	0.984
Constant	1606.385	7.334	0.007	
EOT-2	0.010	4.738	0.029	5.010
Constant	-0.269	0.695	0.404	0.764
EOT-5	-0.019	8.001	0.005	0.981
Constant	-0.516	2.058	0.151	0.597

As illustrated by Eq. 6, the more negative the EOT-2 signal (occurrence of a strong El Niño), the higher is the risk of a dry year in North Ethiopia. Further, the logit models showed significantly negative relations with EOT-1 and EOT-5.

2.3.3.2 A multivariate kiremt model

In order to formalize the combined interaction of the teleconnections, JJAS rainfall measured in Mekelle-Quiha Airport was linked to the teleconnections through a multivariate regression model. As EOT-1 could not significantly be linked in any linear model but is still significantly correlated with JJAS rainfall, it was replaced by the South

West Monsoon index, which provided a significant result. Finally, a model with 4 variables provided significant results (Table 2.3), and could explain about two third of North Ethiopian rainfall variability. The variables included are the WTIO (West Tropical Indian Ocean SST index), EOT-5, the SWM (South West Monsoon index), the MEI (Multivariate El Niño Index) or EOT-2. These interactions with the study area are shown schematically in Figure 2.5. The WTIO is well correlated with the MEI (0.48) and with the DMI (0.40). The regression replicates the rainfall measurements fairly well (Figure 2.6 a and b), in particular the droughts during the 1980s. A similar procedure based on multivariate logit regression (Table 2.3) allowed to correctly model 83.7 % of the drought risks (Table 2.4).

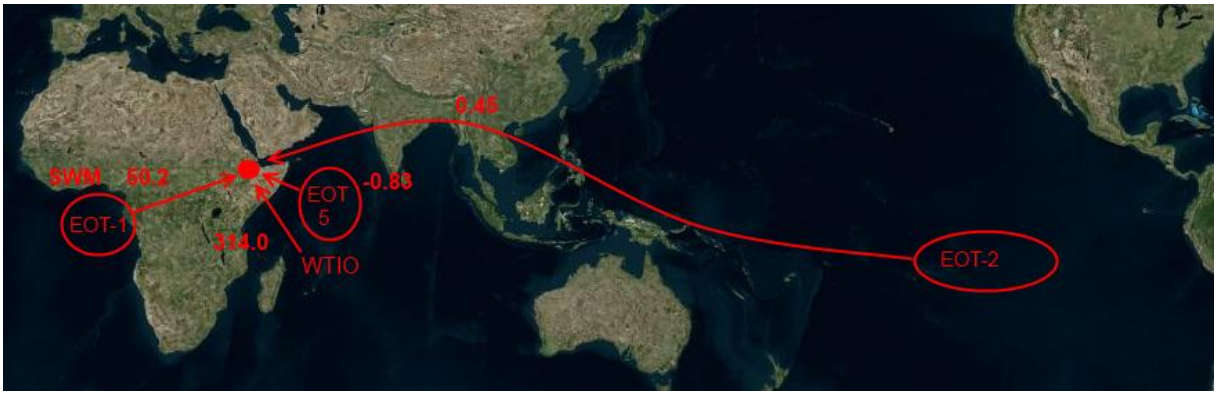

Figure 2.5 Focus areas of the teleconnections spatially overlapping North Ethiopia; and regression coefficients of the multivariate regression for kiremt reconstruction.

Table 2.3 Significance and regression coefficients of all factors in the multivariate models.

Model with EOTs (R^2 = 0.62)			Model with Indices (R^2 = 0.64)			Logit model with Indices (Nagelkerke R^2 = 0.63)		
	B	Sig.		B	Sig.		B	Sig.
Constant	419.16	0.000	Constant	407.59	0.000	Constant	-2.97	0.009
WTIO	313.96	0.000	WTIO	362.63	0.000	WTIO	9.59	0.008
SWM	50.24	0.000	SWM	43.844	0.000	SWM	0.95	0.038
EOT 5	-0.83	0.005	EOT 5	-0.85	0.003	EOT5	-0.025	0.020
EOT 2	0.45	0.018	MEI	-52.89	0.004	MEI	-1.50	0.025

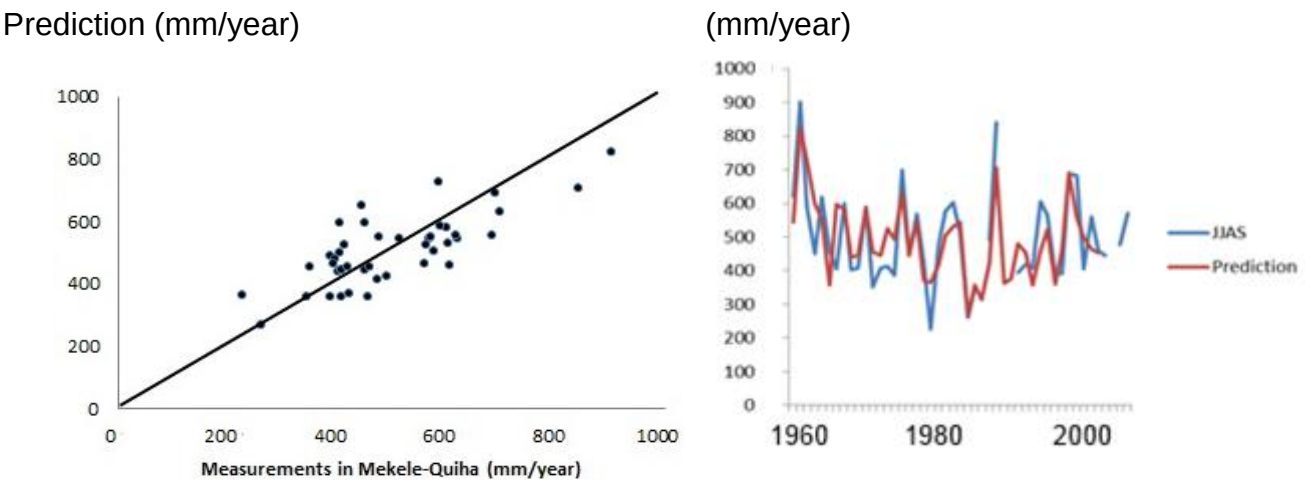

Figure 2.6 (a) JJAS rainfall (mm) based on the regression model versus meteorological measurements in Mekele-Quiha (mm) with R2 = 0.64; (b) Predicted versus measured rainfall (in mm) for Mekele-Quiha (in years after 1960). Independent variables are EOT-2, EOT-5, SWM and WTIO.

Table 2.4 Classification matrix of the multivariate logit model.

		Modeled		
		0	1	% correct
Observed	0	23	3	88.5
	1	4	13	76.5
	%			83.7

2.4 Discussion

2.4.1 Physical mechanisms

The oscillation-controlled rainfall pattern observed in this study can be partly explained using the conceptual regional climate model of Segele et al. (2009 a and b). Through wavelet, regression, correlation, and composite analysis, they concluded that enhanced *kiremt* rainfall in North Ethiopia is dependent on La Niña conditions, in particular since Ethiopian rainfall is associated with monsoon low deepening over the Arabian Peninsula. During La Niñas, pressure lowering in the Arabian Monsoon Through (see Figure 2.7a)

coincides with pressure strengthening in the Mascarene High, which enhances the Somali Low Level Jet and the Tropical Easterly Jet (at 200 hPa). This combination brings more moisture to Ethiopia (Segele et al., 2009b) (Figure 2.7b). Similarly, way to the Northeast of the Horn of Africa, the Asian Monsoons are weakened during El Niño events (Ju and Slingo, 1995). In India, the majority of the warm ENSO (El Niño) episodes are accompanied by dry summers, coincident with low-level anticyclone anomalies (Lau and Nath, 2000).

Our findings are in good agreement with the results of several previous studies (Abtew et al., 2009; Seleshi and Zanke, 2004; Segele et al., 2009 a and b), who find that North Ethiopian rainfall is suppressed during El Niños and enhanced during La Niñas. The ability of EOT analysis to identify ENSO conditions is further supported by performing a logistical regression (p = 0.026) with the MEI, providing results similar to the EOT-2 logit model:

$$P(\pi = wet) = \frac{1}{1+e^{-(-1.008MEI)}} \qquad (2.7)$$

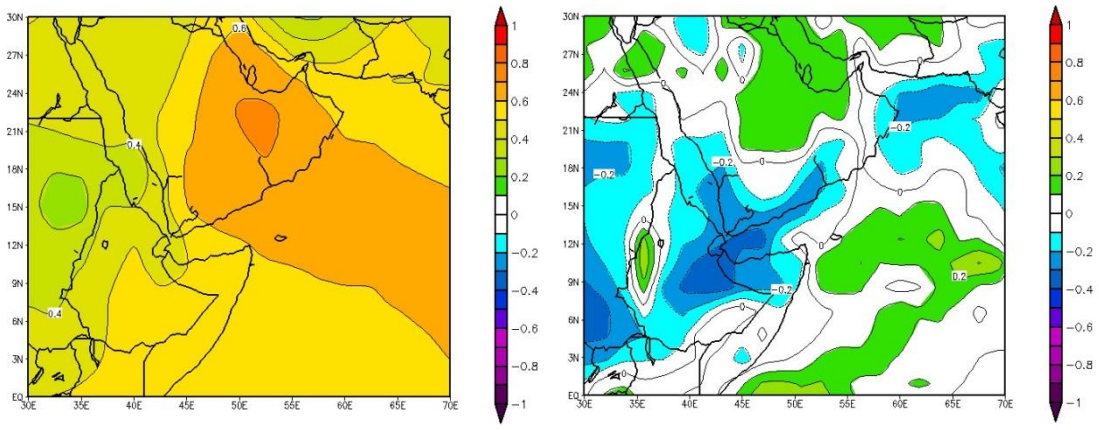

a b

Figure 2.7 (a) Correlation map of JJAS MEI and sea-surface pressure; and (b) correlation map of JJAS MEI and precipitation rate, both based on the NCEP/NCAR reanalysis 1948-2005.

Contrasting with North Ethiopia, equatorial East Africa is wetter during El Niño conditions, because the ITCZ is intensified by a warmer west equatorial Indian Ocean sea surface

temperature (Wolff et al., 2011). There, rainfall occurs from mid-March to the end of May (the so-called Long Rains), and from mid-October to mid-December (the Short Rains).

Further, Saji et al. (199) and Abram et al. (2008) report an impact of the Indian Ocean Dipole on East African rainfall. During positive Indian Ocean Dipole events, equatorial winds switch direction and bring warm waters toward the West (Indian Ocean), which enhance a more powerful monsoon (Woods Hole Oceanographic Institution, 2013). However, this relationship was never formalized for the Northern Horn of Africa, and North Ethiopia in particular. In addition, Segele et al. (2009 a and b) highlight the importance of the South West Monsoons for bringing moisture from the Atlantic Ocean towards the Ethiopian Highlands. As the Congo Air Boundary is situated above Central Ethiopia during July (Bergner and Trauth, 2004), the strength of the Guinea Anticyclone is instrumental in having intensive moisture-bearing South West Monsoons (Segele et al., 2009b). Viste and Sorteberg (2013) confirm the existence of moisture transport from the Gulf of Guinea and the Congo Basin towards the North Ethiopian Highlands, but find that the amount of delivered moisture from these regions is very small as compared to other source regions (i.e. about 12 % of the deliverd moisture from the Indian Ocean). Squared semipartial correlations for each oceanic predictor of our multivariate kiremt model indicate that the Pacific Ocean predictor explains 14.1 %, the Atlantic Ocean predictor explains 29.0 % and the combined Indian Ocean predictors explain 57.0 % of the model's variance. The squared semipartial correlations, informing us on the percentage of rainfall variability uniquely explained by each oceanic predictor, thus suggest a dominant impact of Indian Ocean variabilities on rainfall in Northern Ethiopia.

2.4.2 Implications for land degradation and climate change

In addition to the physical mechanisms that regulate the regional rainfall pattern over North Ethiopia, it is clear that oscillation-induced droughts can have several detrimental effects, as some authors attribute spikes of famine and land degradation to El Niño events. For example, Abtew et al. (2009) conclude that the great Ethiopian famine of 1888-1892 corresponds to a very strong El Nino year (1888). Related to this, Frankl et al. (2011) suggested that before the late 19th century, gullies in Tigray were activated because of similar increased aridity. Equally, the low amplitude interaction between our three teleconnections (EOT-2, EOT-5 and SWM) during the years 1982-1983 (Figure 2.6) is

coinciding with the years of Great Famine and severe land degradation in the Ethiopian Highlands. In line with hydrogeomorphological studies, this chapter formalizes the contribution of oceanic teleconnections to the probability of having a dry year, with consequences for land degradation processes in North Ethiopia. As shown in Figure 2.6b, the 1980s droughts can be well explained in terms of the three identified teleconnections.

Identifying interactions with quasi-global teleconnections is important for projections of future climate change. For East Africa, Williams and Funk (2011) conclude that a warm pool over the Indian Ocean, and the associated movement of diabatically heated air by Walker north-eastern trade winds towards eastern Africa, will suppress *belg* precipitation. However, concerning *kiremt* rains, most climate models predict a wetter Horn-of-Africa climate under conditions of global warming (Williams and Funk, 2011), partially due to a strengthening of the Hadley Circulation. In addition, based on Table 2.3, an enhanced South West Monsoon and increasing Indian Ocean temperatures can further strengthen North Ethiopian rainfall. However, the study illustrated the disruptive character of the El Niño Oscillation which could counter such effects. Hence, future water-soil-crop interactions may depend especially on the impacts of global warming on the El Niño Southern Oscillation, an effect that will need further consideration in Horn of Africa climate projections. At the same time, the temporal pattern of EOT-5 (significantly negatively related with rainfall in North Ethiopia; Table 2.3) reveals a significantly rising trend. Taking into account the exceptional heating of the Indian Ocean over the second half of the 20th century (see Williams and Funk, 2011), this might be a signal of 'Indian Ocean Basin Mode' intensification.

2.5 Conclusions

Focusing on North Ethiopia, this study (i) applied an EOT based method to detect teleconnections; to (ii) understand drought occurrence in North Ethiopia from these teleconnections. Theil-Sen trend analysis on rain gauge data showed a declining precipitation trend before 1985 and a stable trend thereafter. However, inter annual variability was found in the datasets. Regression confirmed the impact of La Niña/El Niño conditions, as the second EOT (based on assimilated mean sea level pressures) had a

significant impact on *kiremt* rainfall. Further, the Indian Ocean Dipole and the South West Monsoons are influencing *kiremt* rainfall variability in North Ethiopia. The interaction between these three teleconnections was found to be a major contributor to the 1983–85 droughts. As the mutual impacts of the Indian Ocean Warming – Indian Ocean Dipole on East African rainfall are still less investigated than the impact of ENSO, we argue that East-African meteorological services must take care to incorporate IOD interactions into their prediction models.

2.6 References

Abtew, W., Melesse, A., Dessalegne, T., 2009. El Niño Southern Oscillation link to the Blue Nile River Basin hydrology. Hydrological Processes 23 (26), 3653-3660.

Amemiya, T., 1985. Advanced Econometrics. Harvard University Press, London.

Behera Swadhin, K., Jing-Jia, L., Masson, S., Delecluse, P., Gualdi, S., Navarra, A., Yamagata, T., 2005. Paramount Impact of the Indian Ocean Dipole on the East African Short Rains: A CGCM Study. J. Climate 18, 4514–4530.

Bergner, A., Trauth, M., 2004. Comparison of the hydrological and hydrochemical evolution of Lake Naivasha (Kenya) during three highstands between 175 and 60 kyr BP. Palaeogeography, Palaeoclimatology, Palaeoecology 215, 17-36.

Camberlin, P., 1994. Les précipitations dans la Corne orientale de l'Afrique: climatologie, variabilité et connexions avec quelques indicateurs océano-atmosphériques. PhD dissertation, Université de Bourgogne, 379 p.

Chen, M., Xie, P., Janowiak, J., Arkin, P., 2002. Global Land Precipitation: A 50-yr Monthly Analysis Based on Gauge Observations. J. of Hydrometeorology 3, 249-266.

Cheung, W., Senay, G., Singh, A., 2008. Trends and spatial distribution of annual and seasonal rainfall in Ethiopia. Int. J. Climatol. 28, 1723–1734.

Clark Labs (2009) Exploring Image Time Series With Earth Trends Modeler: http://www.clarklabs.org/resources/upload/Focus_Paper_ETM.pdf

Climate Prediction Center, 2015. Northern Hemisphere Teleconnection Patterns: Teleconnection Introduction. http://www.cpc.ncep.noaa.gov/data/teledoc/teleintro.shtml (accessed 27/10/2015)

Conway, D., 2000. Some aspects of climate variability in the Northeast Ethiopian Highlands – Wollo and Tigray. SINET – Ethiopian Journal of Science 23, 139–161.

Diro, G., Black, E., Grimes, D., 2008. Seasonal forecasting of Ethiopian spring rains. Meteorological Applications 15, 73–83.

Fernandes, K., Rong, F., Betts, A., 2008. How well does the ERA40 surface water budget compare to observations in the Amazon River basin? J. Geophys. Res. 113, D11117.

Frankl, A., Nyssen, J., De Dapper, M., Haile, M., Billi, P., Munro, N., Deckers, J., Poesen, J., 2011. Linking long-term gully and river channel dynamics to environmental change using repeat photography (Northern Ethiopia). Geomorphology 129, 238-251.

Gissila, T., Black, E., Grimes, D., Slingo, J., 2004. Seasonal forecasting of the Ethiopian summer rains. International Journal of Climatology 24, 1345–1358.

Halldor, B., Venegas, S., 1997. A manual for EOF and SVD analyses of climate data", McGill University, CCGCR Report No. 97-1, Montréal, Québec, 52p.

Harger, A., 1995. ENSO variations and drought occurrence in Indonesia and the Philippines. Atmospheric Environment 29 (16), 1943–1955.

Hoerling, M., Kumar, A., 2003. The perfect ocean for drought. Science 299 (5607), 691-694.

Hong, W., Hayes, M., Weiss, A., Qi, H., 2001. An evaluation of the Standardized Precipitation Index, the China-Z Index and the statistical Z-Score. International Journal of Climatology 21 (6), 745–758.

Jacob, M., Frankl, A., Mitiku Haile, Zwertvaegher, A., Nyssen, J., 2013. Assessing spatio-temporal rainfall variability in a tropical mountain area (Ethiopia) using NOAAs Rainfall Estimates. International Journal of Remote Sensing 34 (23), 8319-8335.

Ju, J., Slingo, J., 1995. The Asian Summer Monsoon and ENSO. Q. J. R. Meteorol. Soc. 121, 1133-1168.

Korecha, D., Barnston, A., 2007. Predictability of June-September rainfall in Ethiopia. Mon. Wea. Rev. 135, 628-650.

Lau, N., Nath, M., 2000. Impact of ENSO on the variability of the Asian-Australian monsoons as simulated in GCM experiments, J. Clim. 13, 4287 – 4309.

Li, J., Zeng, Q., 2005. A new monsoon index, its interannual variability and relation with monsoon precipitation. Climatic and Environmental Research 10, 351-365.

Liu, W., Juarez, R., 2001. ENSO drought onset prediction in northeast Brazil using NDVI. International Journal of Remote Sensing 22 (17), 3483-3501.

Magar, V., Gross, M., Proberts, G., Reeve, D., Cai, Y., 2012. Statistical prediction of coastal and estuarine evolution. Coastal Engineering Proceedings 1 (33), DOI: 10.9753.

Modarres, R., Ouarda, T., 2014. Modeling the relationship between climate oscillations and drought by a multivariate GARCH model. Water Resources Research 50 (1), 601–618.

Nicholson, S., Kim, J., 1997. The relationship of the El Niño Southern Oscillation to African rainfall. Int. J. Climatol. 17, 117–135.

Nicholson, S., Selato, J., 2000. The influence of La Niña on African rainfall. Int J Climatol 20, 1761–1776.

Nyssen, J., Poesen, J., Moeyersons, J., Deckers, J., Mitiku Haile, Lang, A., 2004. Human impact on the environment in the Ethiopian and Eritrean highlands - a state of the art. Earth-Science Reviews 64 (3-4), 273-320.

Nyssen, J., Vandenreyken, H., Poesen, J., Moeyersons, J., Deckers, J., Mitiku Haile, Salles, C., Govers, G., 2005. Rainfall erosivity and variability in the Northern Ethiopian Highlands. J. Hydrol. 311, 172–187.

Pankhurst, R., 1985. The History of Famine and Epidemics in Ethiopia. RRC, Addis Ababa, Ethiopia.

Rasmusson, E., Carpenter, T., 1982. Variations in tropical sea surface temperature and surface wind fields associated with the Southern Oscillation/El Niño. Mon. Wea. Rev. 110, 354-384.

Riddle, E., Cook, K., 2008. Abrupt rainfall transitions over the Greater Horn of Africa: observations and regional model simulations. J. Geophys. Res. 113, D15109.

Rossi, G., 2000. Drought Mitigation Measures: A Comprehensive Framework. Advances in Natural and Technological Hazards Research 14, 233-246.

Saji, N., Goswami, B., Vinayachandran, P., Yamagata, T., 1999. A dipole mode in the tropical Indian Ocean. Nature 401, 360–363.

Segele, Z., Lamb, P., Leslie, L., 2009a. Large-scale atmospheric circulation and global sea surface temperature associations with Horn of Africa June– September rainfall. Int. J. Climatol. 29, 1075–1100.

Segele, Z., Lamb, P., Leslie, L., 2009b. Seasonal-to-Interannual Variability of Ethiopia/Horn of Africa Monsoon. Part I: Associations of Wavelet-Filtered Large-Scale Atmospheric Circulation and Global Sea Surface Temperature. J. Climate 22, 3396–3421.

Sen, P., 1968. Estimates of the regression coefficient based on Kendall's tau. Journal of the American Statistical Association 63, 1379–1389.

Sileshi, Y., Zanke, U., 2004. Recent Change in Rainfall and Rainy Days in Ethiopia. International Journal of Climatology 24, 973-983.

Simonti, A., Eastman, R., 2010. 2005 Caribbean mass coral bleaching event: A sea surface temperature empirical orthogonal teleconnection analysis. Journal of Geophysical Research: Oceans (1978–2012) 115, C11.

Smith, I., 2004. An assessment of recent trends in Australian rainfall. Aust. Met. Mag. 53, 163-173.

Snedecor, G., Cochran, W., 1989. Statistical methods. Iowa State University Press, Iowa, USA, 803 p.

Spinage, P., 2012. African Ecology; Benchmarks and Historical Perspectives. Springer Geography, New York, 1562 p.

Uppala, S., Kållberg, P., Simmons, A., Andrae, U., da Costa Bechtold, V., Fiorino, M., Gibson, J., Haseler, J., Hernandez, A., Kelly, G., Li, X., Onogi, K., Saarinen, S., Sokka, N., Allan, R., Andersson, E., Arpe, K., Balmaseda, M., Beljaars, A., van de Berg, L., Bidlot, J., Bormann, N., Caires, S., Chevallier, F., Dethof, A., Dragosavac, M., Fisher, M., Fuentes, M., Hagemann, S., Hólm, E., Hoskins, B., Isaksen, L., Janssen, P., Jenne, R., McNally, A., Mahfouf, J., Morcrette, J., Rayner, N., Saunders, R., Simon, P., Sterl, A., Trenberth, K., Untch, A., Vasiljevic, D., Viterbo, P., Woollen, J., 2005. The ERA-40 re-analysis. Quart. J. R. Meteorol. Soc. 131, 2961-3012.

van den Dool, H., Saha, S., Johansson, A., 2000. Empirical Orthogonal Teleconnections. Journal of Climate 13, 1421–1435.

Van den Hurk, B., Viterbo, P., Beljaars, A., Betts, A., 2000. Offline validation of the ERA40 surface scheme. ECMWF Tech. Memo 295, ECMWF, 43 p.

Viste, E., Sorteberg, A., 2013. Moisture transport into the Ethiopian highlands. International Journal of Climatology 33, 249-263.

Williams, A., Funk, C., 2011. A westward extension of the warm pool leads to a westward extension of the Walker circulation, drying eastern Africa. Clim. Dyn. 37, 2417–2435.

Wolff, C., Haug, C., Timmermann, A., Sinninghe Damsté, J., Brauer, A., Sigman, D., Cane, M., Verschuren, D., 2011. Reduced inter-annual rainfall variability in East Africa during the last ice age, Science 333, 743-747.

Wolter, K., 1987. The Southern Oscillation in surface circulation and climate over the tropical Atlantic, Eastern Pacific, and Indian Oceans as captured by cluster analysis. J. Climate Appl. Meteor. 26, 540-558.

Yilma, S., Demarée, G., 1995. Rainfall variability in the Ethiopian and Eritrean highlands and its links with the Southern Oscillation Index. Journal of Biogeography 22, 945–952.

Woods Hole Oceanographic Institution, 2015. A tale of two oceans, and the monsoons. http://www.whoi.edu/oceanus/viewArticle.do?id=53506 (accessed on 27/10/2015).

Chapter 3 Hillslope runoff: the impacts of land tenure and drought during the 20th century

This chapter is modified from:

Lanckriet, S., Derudder, B., Naudts, J., Bauer, H., Deckers, J., Mitiku Haile, Nyssen, J., 2015. A political ecology perspective of land degradation in the North Ethiopian Highlands. Land Degradation and Development 26 (5): 521-530.

Abstract

Severe environmental degradation in the north Ethiopian Highlands is often thought to result from mismanagement or overpopulation. However, in this chapter we investigate the impact of the dynamics of the political-ecological system in relation to dry spells. We performed semi-structured interviews with 93 farmers in eight villages in the Tigray region (North Ethiopia), and conceptualized a political-ecological model of land tenure and degradation changes for the region. Results show that different land policies caused and still cause land degradation in several ways. Interviews reveal that the unequal character of land rights during feudal times played an important role in 19th and 20th century land degradation. In particular, poor farmers were forced to construct their farms on marginal terrains, such as steep slopes in dry areas and marshes in cold and humid areas, increasing the catchment water runoff and degradation. The findings further suggest that after the arid phases of the 1970s and 1980s and the end of the Derg regime (1974-1991), environmental conservation strategies were successfully implemented at larger scales. Overall, feudal, Derg, and contemporary land tenure and agricultural investment policies have all had impacts on environmental degradation and have left their fingerprints on the physical landscape of Northern Ethiopia.

3.1 Introduction

Land degradation is the temporary or permanent lowering of the productive capacity of land (UNEP, 1992), and includes deforestation, overgrazing, expansion of cultivation, increasing water runoff and erosion, and soil degradation. In North Ethiopia, the interplays between climatic vulnerability and land use changes caused severe land degradation (Nyssen et al., 2004; Biazin & Sterk, 2013), as land use changes can induce vulnerability to droughts (Frankl et al., 2011; Frankl et al., 2013; Mekuria et al., 2012). Consequently, land degradation in Northern Ethiopia is partly linked to the rainfall cycles and drought periods, while crop production comes under high pressure from water deficiencies. Attention in the media to famines in Ethiopia has created a popular view of a drought-stricken country, with a gradual tendency towards decreasing annual rain ('aridification'). Yilma & Demarée (1995) and Camberlin (1994), in turn, found that the temporary decline of the rainfall in the Sahel observed after about 1965 was also seen to a lesser extent in the north central Ethiopian Highlands. However, analyses of time series of annual precipitation, reaching up to 2000 CE, both for Addis Ababa and the northern Highlands, show that there is no evidence for a long-term trend or change in the region's annual rainfall regime, even though the succession of dry years between the late 1970s and late 1980s produced the driest decade of the last century in the Ethiopian Highlands (Conway, 2000). As discussed in chapter 2, such 20th century climate variability is linked with several quasi-global teleconnections, such as the El Niño Southern Oscillation and African Monsoon variability (Segele et al., 2009a; 2009b). In addition, Cheung et al. (2008) found no significant yearly and seasonal changes in rainfall for the period 1960-2002 in the region comprising the investigated watersheds in northern Ethiopia (Chapter 2).

In absence of a long-term drying trend, land degradation is presumably linked with periodic drought vulnerability of lands suffering from a heavy human impact. From this perspective, Girma Kebbede & Jacob (1988) claim that internal political contradictions and other political factors have a commanding impact on environmental degradation and famine in the Highlands. According to Ståhl (1974) and Ståhl (1990), the problem of land degradation in northern Ethiopia is eventually a *political* one. However, while political ecology has emerged as a top level research field for explaining land degradation (Blaikie, 1985; Andersson et al., 2011; Krings, 2002; Benjaminsen et al., 2010), no comprehensive framework for explaining land degradation from political-ecological perspectives exists for

the Tigray Highlands. Hence, in this chapter we hypothesize that degradation in the Tigray Highlands can be explained by changes in the political-ecological system in relation to dry spells. Using semi-structured interviews with local farmers, the chapter examines i) the impact of feudal political-ecological systems and land policies, and ii) the impact of contemporary political-ecological systems and land policies on land degradation processes (including vegetation cover, gullying, conservation measures).

3.2 Materials and methods

3.2.1 Semi-structured interviews

During two fieldwork campaigns, 93 semi-structured interviews (below coded with one or two letters) were performed in several villages. A first campaign was carried out in April-August 2002 (Naudts, 2002), and included 14 (semi-)structured interviews with key-informants (KI) in the villages of Adi Kolkual, Adi Hantatzo, Guwa, Dingilet, T'ashi and the town of Hagere Selam. The interviews focussed on older farmers, priests, and administrative staff; and additionally on 39 farmers in Hechi and Agerba. During a second campaign in December 2012, forty farmers were interviewed in seven villages, May Bati (MB; 8 interviews), Adi Shuho (AS; 5 interviews), May Mekden (MM; 7 interviews), Nebelet (N; 5 interviews), Sinkata (S; 6 interviews), Ashenge (A; 2 interviews) and Lahama (L;7 interviews); (Figure 3.1). Some additional interviews were performed with the chairman of the Bureau of Agriculture (Hagere Selam), and several village leaders.

All informants were interviewed independently and individually. During two-day walks through the village and its surrounding fields, the farmers were asked targeted questions, and they were invited to show and locate the phenomena they were talking about. Only if all interviewed farmers in one village came independently and individually to the same insights, these insights were used in the study. Care was taken to ensure that if one or more of the interviewed farmers were giving statements that were inconsistent with statements by other farmers in the village, no answers and insights of the farmers in this village were used. The results of this study are therefore only mentioning consistent insights of individually interviewed farmers in a certain village. The method forms thus an adaptation of the AGERTIM technique introduced in the study area by Nyssen et al. (2006) and relates to

the Participatory Rural Appraisal techniques (Bryceson et al., 1981; Young & Hinton, 1996). This method is however based on independent individual interviews instead of group interviews and cannot be labelled 'participatory' since there is no two-way reciprocity.

Key persons and farmers were asked open questions concerning the key characteristics of the rural society, and historical relations between the environment (biophysical, political and socio-economical) and the state of the agricultural practices (starting from 1950). As such, questions were asked concerning:

(i) The land distribution during feudal times – and the evolution towards today; e.g. *Where were the croplands located? Where were the larger parcels located? etc.*

(ii) The land tenancy system during feudal times – and the evolution towards today; e.g. *Who owned which parcels? Who rented parcels? Who were the noblemen?etc.*

(iii) The land degradation during feudal times – and the evolution towards today; e.g. *Were the gullies more active than today? Were there conservation measures? etc.*

Given the ages of the interviewed people, such method can produce reliable results up to the 1940s – none of the interviewees could inform about the period before the Italian occupation (1936-1941). More information on the interview methodology can be found in Appendix A5.

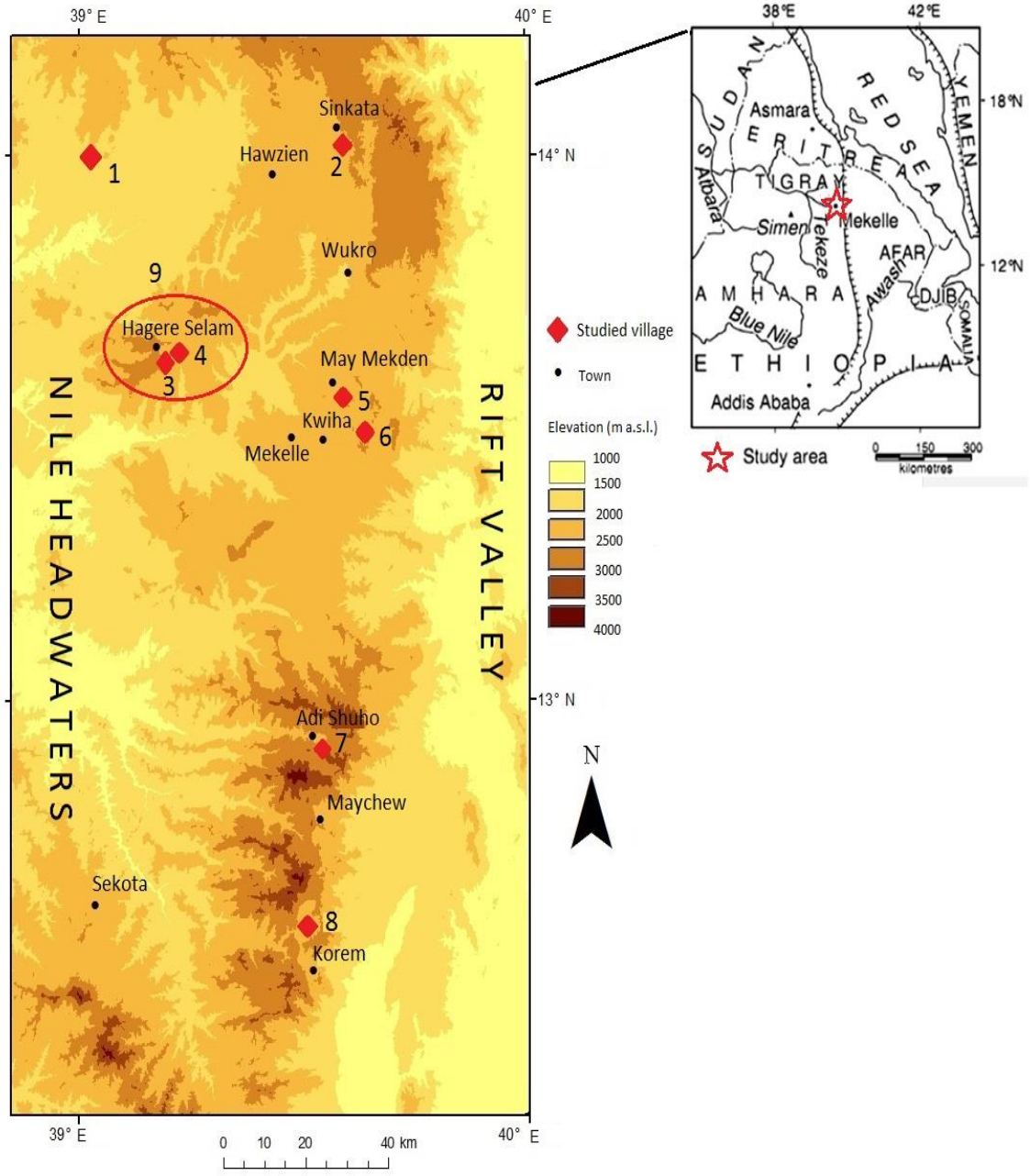

Figure 3.1 Study area (based on an SRTM image) in the North Ethiopian Highlands (Tigray); and location of the villages for the 2012 interviews: 1 = Nebelet (N); 2 = Sinkata (S); 3 = Hechi (H); 4 = May Ba'ati (MB); 5 = May Mekden (MM); 6 = Lahama (L); 7 = Adi Shuho (AS); 8 = Ashenge (A). 9 = the region (red ellipse) where key informants (KI) were interviewed in 2002.

3.2.2 The study area at micro-scale: the example of Hechi

As an example of a 'typical' rural village, the village of Hechi is discussed below. Hechi is located at an altitude of approximately 2200 m, and is only accessible on foot. The village is located in the district of Dogua Tembien, approximately 4 km east of the district town Hagere Selam. Here, villages are situated in two main agro-ecological zones in the valley: a low-lying calcareous zone and an upper-lying basalt zone. Hechi is representative for the catchment, since the village lands are situated both at the lower calcareous agro-ecological zone and at the upper basalt agro-ecological zone. The evolution of the village since the 1950s has been studied intensely by Naudts (2002). It has an area of 500-600 ha and has around 200 houses with approximately 1000 inhabitants. Most farmers own some cattle (notably oxen), grazing freely over most lands during the dry season (October till March). Cattle provide traction while ploughing, but produce also milk, meat and manure. Furthermore, cattle function as a saving buffer for times of extreme drought; and can be considered as a status symbol (Naudts, 2002).

An average rural household in the village owns approximately 5 goats and 1 donkey. They own or rent on average 0.75-1.2 ha cropland, with 60% of the households having less than 1 ha. All cropland (commonly cultivated with wheat, barley, *hanfez*, which is wheat and barley sown together, and *Eragrostis tef*) is ploughed with the local ard plough or *mahresha*. In Hechi, about half of all farmers own only one ox. Since one ox is not sufficient to use the *mahresha*, two neighbours have to share their oxen, although traction can come from a cow or donkey too (Naudts, 2002).

3.2.3 Conceptual political-ecological model

In order to conceptualize the different degradation periods since the 1940s, each period will be considered as a 'political-ecological layer', superimposing previous layers, an approach similar to 'the geological metaphor theory', developed by Doreen Massey. According to Massey (1984), the structure of local economies can be seen as a product of the combination of 'layers' of the successive deposition of new waves of investment. Hence, the contemporary Tigrayan physical landscape can be read as a historical product of the combination of successive layers of economic activity and conservation policies. Each 'layer' has its own political power groups, its own way of producing agricultural goods, its own

social relations, and its own inherited environment, all resulting in different kinds of environmental degradation and environmental conservation. Three-dimensional block diagrams will be used to conceptually model the landscape in each of the periods.

3.3 Results

Based on the interview results and Massey's (1984) 'geological metaphor', a conceptual political-ecological model for landscape evolution was constructed using three block diagrams (Figure 3.2). Notably, three main 'political-ecological layers' would be i) the feudal era (before the start of the civil war in 1974); ii) the Derg and civil war period, coinciding with a major dry phase; and iii) the post-war period (after 1991). These three eras correspond well with the successive hydrogeomorphic phases in North Ethiopian gully systems, identified by Frankl et al. (2011).

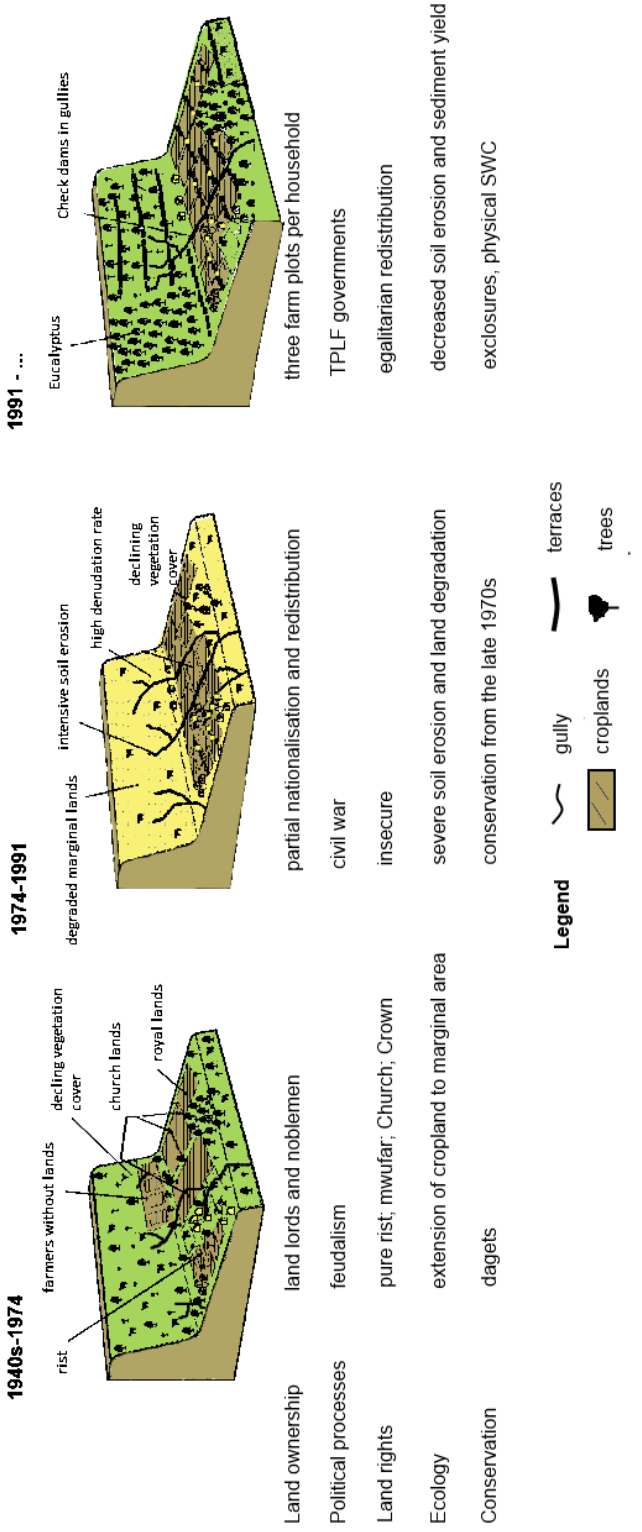

Figure 3.2 A political-ecologic model of land degradation in the North-Ethiopian Highlands.

3.3.1 Droughts under feudal land tenure before and during the 1970s

In this period (1950-1974), several severe droughts occurred (1953, 1957, 1964-1965, 1970-1973) (Spinage, 2012). Then, the croplands were mainly situated at the flatter low-lying areas (MB, L; 2012). Between the parcels, some vegetation and trees were present (KI, 2002; L, MB; 2012). As from 1930, the eucalyptus tree was introduced in the landscape (KI, 2002). All lands were principally owned by the emperor (KI, 2002). According to the interviews (N, MB, MM, L, A; 2012), noblemen (*dejazmach*, meaning 'commanders', a title granted for life) had superior power in the villages; with notably strong power for the 'king' of a village, locally named *tikashum*. Basically, the nobility had private ownership over the croplands (*rist* lands) by the approval of the Crown and these *rist* lands were attributed to 'the first occupiers', and then transferred to their heirs. These *rist* lands were often lent out in a sharecropping system (Thomas et al., 1991), locally named *mwufar* or *tefurti* (KI, 2002; MB, N, L, 2012). Other rist lands were not lent out, and can be considered as '*pure rist*' lands (MB, N, L, 2012). Hence, several interviewees (KI, 2002; Table 3.1) indicate that there were four main types of land rights: i) about one third of the lands were used in *pure rist*; ii) about one third of the lands were *rist* lands lent out in *tefurti*; and iii) the rest of the lands were owned by the orthodox church; or iv) direct property of local noblemen ('lands of the Crown'). However, lands of the Church and the Crown could also be rented out in *mwufar* or laboured by paid day labourers.

Table 3.1 Abundance of three feudal land tenancy types in the studied villages, as estimated by the interviewees in 2012.

Land tenancy	May Mekden	All other villages
'Pure' Rist	20-40%	20-40%
Rist in mwufar (tefurti)	> 40%	20-40%
Church or Crown	< 20%	20-40%

Simultaneously, there was an important power synergy between the Orthodox Church and the village *tikashums*, as *tikashums* were chosen by the orthodox priests of the village (MB, MM, L, N; 2012). In all examined villages, one *tikashum* ruled the village, except for the village of Adi Shuho, where four *tikashums* rotated every 1-3 years (AS, 2012). The latter might be a system that originates from the Oromo culture more to the south (Melbaa Gadaa, 1988).

The land inequity is a clear reflection of the social inequity during the feudal era. According to most of the interviewed farmers (N, A, L, MB, MM, AS, 2012), social inequity was very high during the feudal time. Twenty farmers stated that the poor had to rent from the rich, and they had to give up to one third of their yield (KI, 2002; N, A, L, MB, MM, AS, 2012). The poorest of all farmers could only survive as day laborers (MB, N; 2012). When asked to describe the economic equity during the feudal era, several farmers replied that 60% of the farmers were very poor, 30% were medium poor, and 10% were very rich. Lahama seems an exception, as five farmers there stated that 95% of the farmers were very poor, while 5% were very rich. The impact of the unequal economic power is well reflected in the estimates of land tenancy during feudal times (Table 3.1).

According to the interviews, this unequal character of land rights during feudal times must have played an important role in 19th and early 20th century land degradation. Two mechanisms were identified that mediated such a relationship between land tenancy and degradation. Firstly, farmers stated that most lands, notably the larger, low-lying and level parcels, were owned by noblemen (ristholders) assumed to be descendants of the founders of the village or by the orthodox church (L, N, S, MM; 2012). Wealthier aristocrats generally took advantage of their superior political and market power to ensure initial access to better quality resources, as conceptualized by Barbier (1997). These large lands are the *rist* lands that were lent out in the sharecropping system *mwufar* (MB, MM, N, L, 2012). Possibly, tenure insecurity was discouraging long-term investments, increasing the degradation (Clay et al., 1994; KI, 2002). This insecure land tenure could have reinforced the tendency towards short-term time horizons in production decisions, and may have biased land use decisions against long-term land management strategies (Barbier, 1997; KI, 2002).

Secondly, interviewees state that inhabitants without genealogical relations to the founding families, and without resources to enter into sharecropping contracts, had no land rights (KI, 2002). They were increasingly forced to farm land on steep sloping and marginal terrains (KI, 2002; N, L, MM; 2012). Hence, not only population pressure, but also social inequality, would have induced an upslope extension of farming activities, inducing degradation at these highly erodible (steep) locations. This was notably observed in the village of Nebelet, where the interviewed farmers state that during the Haile Selassie era (before 1974), there were farmlands above at the cliff, cultivated by very poor farmers. More downslope, there was bareland, and even more downslope, there were flatter farmlands of the Church, and the rist lands (N, 2012). This land structure can also be seen on the oldest

aerial photograph available for the study area (Figure 3.3; 1935), acquired by the 7a Sezione Topocartografica during the Italian occupation of Ethiopia (Nyssen et al., 2015).

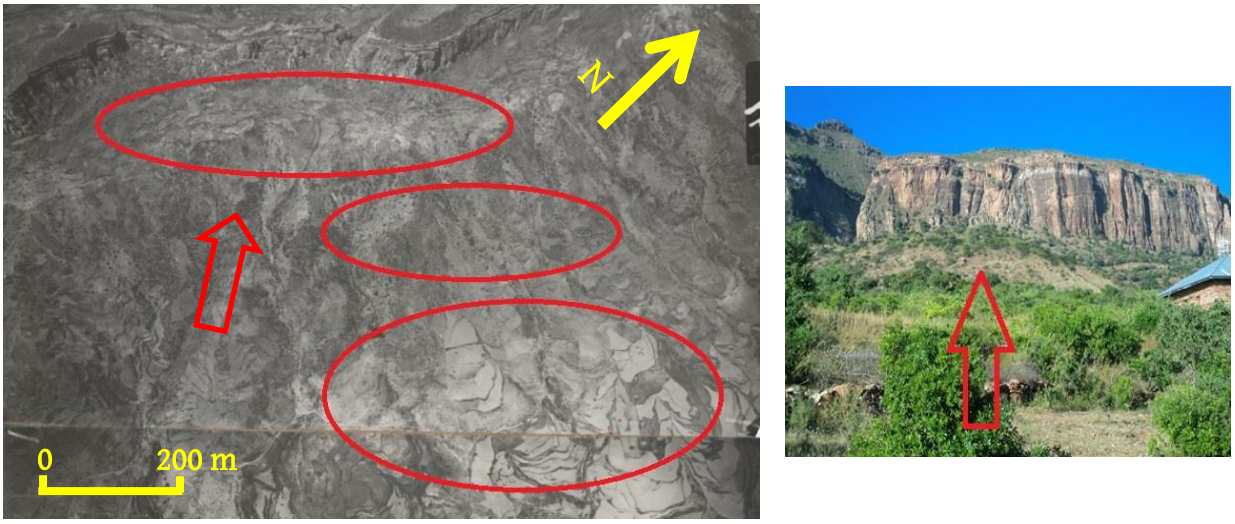

Figure 3.3 Low-oblique aerial photograph 11-3-74 (taken on 5 October 1935; on the left) shows the marginal farmlands of the poor farmers (upper ellipse), intermediate bare land on steep slopes and the cropland owned by the Church and the rist lands (lower ellipse). The right photograph shows, at the upper (northwestern) part, that the lands of the poor farmers have been abandoned as they have received their share in the lands at the valley bottom (photo taken by S. Lanckriet, 14 December 2012). The red arrow on both photographs indicates identical viewpoint. As the aerial photograph has not been geometrically corrected, the scale bar is only indicative.

Interviewees pointed at two main mechanisms for an upslope extension of croplands during the feudal era (an extension by 'poor' farmers, and an extension by 'rich' farmers), depending on agro-climatological conditions. In both cases, due to inferior economic power, the poorer farmers had only access to the more marginal lands. Firstly, farmers in Lahama and May Mekden state that the downslope plots were perceived as 'the most fertile', with more moisture and closer to the houses of the village. Consequently, interviewees state that richer farmers acquired access to these lands (L, MM, 2012). For example in Lahama, the interviewees state that the lowlying irrigated lands were owned by the Church during feudal times (Figure 3.4). Simultaneously, they state that the more upslope lands were managed in rist and by poor farmers, and these lands extended more upslope over time (L, 2012). These villages are located at relatively low altitudes (Figure 3.1), with hotter and dryer conditions. In contrast, a second extension mechanism was identified in Adi Shuho,

which is located at much higher altitudes (Figure 3.1), with colder and wetter conditions. Here, farmers stated that notably the downslope lands were cultivated by poorer farmers, because it was a marshy area (Figure 3.4). The upslope lands were perceived as more fertile, because they were not marshy, less ploughed and less grazed since they are located further from the village. In Adi Shuho the richer farmers probably occupied the lower slopes (being warmer than the valley bottoms; Figure 3.5). These lands equally extended more upslope over time, and were owned by the Church (AS, 2012).

Figure 3.4 (left) In warm semi-arid Lahama (N13.4993; E39.6122), the low-lying irrigated lands (greenish on the photograph) were owned by the Church during feudal times. However (right) in Adishu (N12.9315; E39.5245), the cold rainy highland marshy lands (greenish on the photograph) were cultivated by poorer farmers during feudal times.

Figure 3.5 (left) Historical photograph of the Adi Shuho "marsh" during feudal times (1961; A.T. (Dick) Grove); (right) Repeated photograph taken from the same location (2008; Amaury Frankl).

Consequently, land degradation occurred, since most of the trees and shrubs between the fields and on steep slopes were cleared, thereby increasing runoff and soil erosion (French et al., 2009). Land cover studies that span the past 8 decades show that the areal extent of 'private' croplands was at their maximal extent during the late feudal times (~1960s), while the 'communal lands' (bushlands, shrublands, lands with woody vegetation cover) had their minimal areal extent (De Meyere, 2014). Some small gullies existed (L, AS; 2012) and periodically, the northern part of the Highlands knew drought periods and famines (1910 - 1913, 1958 - 1959, 1966, 1973 - 1975) (Pageau, 1989; Pankhurst, 1986). However, during feudal times, traditional conservation practices did exist, as the *daget* system (lynchets) provided some geomorphic protection (Nyssen et al., 2000). At the same time, farmers traditionally had strategies of survival during difficult periods (eg. seasonal migration, church assistance and help from local noblemen; MB, 2012). However, there was no centrally coordinated implementation of conservation policies (KI, 2002). Hence, the political-ecological system of 1950-1974 was of a feudal origin, in a society with different social classes (farmers without lands, ristholders, descendants of the village founder, ...). A lack of centralized conservation policies together with an increased vulnerability to droughts (expansion of croplands) then led to extreme land degradation in the 1970s (Munro et al., 2008), exhausting the agricultural system and amongst others contributing to the collapse of the imperial government (KI, 2012).

3.3.2 Drought and social upheaval (1974-1991)

After the fall of the Haile Selassie regime in 1974, a military junta (DERG) was installed with Soviet support, but their land reforms (nationalisation of all farms and land redistribution to all households) were only partially implemented in Tigray (KI, 2002). From 1979 onwards, the Tigray People Liberation Front started a civil war against the DERG government. The Dogua Tembien district was located in the front zone of the war, with detrimental consequences for the agricultural economy (KI, 2002). For example, the market at Hagere Selam was not accessible for months, production stagnated, and land rights became insecure (KI, 2002). Furthermore, a phase of severe droughts (1979-1984) struck the country (Mattsson & Rapp, 1991). Together with the degraded environmental situation inherited from the imperial period, this led to a new and even worse famine (1984) that harassed the region (KI, 2002). Such results are in line with the findings of Kiernan (2015), who showed that proxy conflicts during the Cold War were bringing substantial damage to the physical landscape.

This resulted in a second historical degradation period, after the 1960s, when farmers were confronted with severe soil erosion (Frankl et al., 2011). Yet, already from the late 1970s onwards, some soil and water conservation efforts were undertaken in those areas under control of the TPLF (Munro et al., 2008). However, Munro et al. (2008) conclude from their historical photo monitoring study that the Highlands of Ethiopia had become progressively exhausted. There were "high rates of soil erosion; widespread destruction of the natural vegetation; little thought given to any rehabilitation of land or its cover; runoff was rapid and destructive; and the diminishing returns on agricultural production were leading the country on a downward spiral of degradation" (Munro et al., 2008). For instance the famine of 1984 resulted from the consequences of the civil war, combined with failed yields and severe land degradation during a drought period (KI, 2002; Chapter 2). During 1982 and 1983, many farmers in the Highlands didn't even plant crops on their croplands due to military activity and a lack of proper seed material (KI, 2002). As the interviews proved, this land degradation can amongst others be attributed to the economic stagnation during the civil war (KI, 2002), and the land degradation inherited from the feudal period (N, 2012).

3.3.3 Wetter conditions and conservation investments (after 1991)

After the fall of the DERG regime in 1991, rainfall recovered (Chapter 2) and the focus of the new government was put on 'development' thinking (Milas & Latif, 2000). However, we observed that subsistence farming persists in the study area. This is in line with the 65% of all Tigray household poverty that is chronic, while 35% is transitory (Fredu Nega et al., 2010). Also, we observed that in the study area more than 90% of the population lives from agriculture, and farmers' crop yields range from 500 to 1500 kg ha^{-1} (KI, 2002). Farmers who have only one ox generally rely on the food relief programme and particularly on food for work (KI, 2012).

In the post-war political-ecological system, land policies were substantially reorganised. After the victory by TPLF, the new regime organized a new land reform in 1991. Under the new constitution, all land in Ethiopia became owned by the state, while farmers only received usufruct rights (Crewett et al., 2008). Economic equity improved significantly, since agriculture was intensified (amongst others through the introduction of irrigation and fertilizers) and all farmers received a similar amount of land (generally three farm plots); (S, MB, N, A; 2012). Land cover studies show that the areal extent of croplands started to decrease after the late feudal times, while simultaneously the extent of the 'communal lands' (bushlands, shrublands, lands with woody vegetation cover) started to increase again (De Meyere, 2014). A massive public investment policy named 'Conservation-based Agricultural Development Led Industrialization' was introduced by the government. Soil and water conservation became implemented at large scales, leading to reduced soil erosion rates (Munro et al., 2008; Adimassu et al., 2014). The reforms were predominantly led by the district offices of the Ethiopian Ministry of Agriculture and influenced by guidelines of the World Bank, the United Nations System and the International Union for the Conservation of Nature (Tadesse Kidane-Mariam, 2003). Also NGOs were involved in the on-the-ground implementation of the conservation policies (Kumasi & Asenso-Okyere, 2011). Tasesse Kidane-Mariam (2003) describes these reforms as a 'technocratic, state-centered management strategy framework based on population control, poverty reduction, sustainable development, and capacity-building'. For instance, the massive implementation of food for work programmes allows farmers to work in infrastructure projects during the dry season in exchange for food distribution (Fredu Nega et al., 2010). Hence, the combination of egalitarian land rights with effective implementation of soil and water policies resulted in decreased land degradation (MB, MM, N, S; 2012), which is registered by

remote sensing (de Mûelenaere et al., 2014; Kassa Teka Belay et al., 2014), repeat photography (Nyssen et al., 2009) and by changing gully activities (Frankl et al., 2011).

3.4 Discussion

3.4.1 Land degradation driven by mismanagement?

No attempt for explaining land degradation from a political-ecological viewpoint existed for the Tigray Highlands. Commonly, land degradation has been viewed as the result of overexploitation of natural resources or overpopulation. Some argued that land degradation in the Highlands is generally resulting from the abuse of natural resources by the land users and farmers (Tekle Kebrom, 1999). However, our interviews showed that knowledge on (*ex situ*) soil and water conservation among farmers is in fact quite impressive. Currently, huge conservation efforts (such as exclosures and stone bunds) are made, and even during the feudal time, the *daget* system provided soil erosion control. This *daget* system was quite effective (Nyssen et al., 2000). Partly as a result of this effectiveness, soil degradation before the 1970s was not as severe as during the 1970-1980s. For example, Frankl et al. (2011) show that ephemeral river systems were quite stable during the pre-1970 period. In contrast, the interviews indicate that the feudal land tenure plays an important role, rather than mismanagement by the farmers. According to Stocking (1995), the main features of the mismanagement hypothesis are i) the identification of an environmental problem through selective use of measurements; ii) conceptualising the blame for the problems in terms of ignorance and lack of education; iii) and determination of technical solutions of soil and water conservation or changes in land management practices. However, according to Berg (1992), this view completely denies the huge indigenous knowledge in the study area on environmental resource management in the Ethiopian Highlands.

3.4.2 Land degradation driven by population growth?

Since the 1970s, some research focussed on the harmful consequences of rapid population growth (Meadows et al, 1972). Modern population growth is assumed to result in accelerated soil erosion due to progressive change in land cover (Wøien, 1995, Tekle Kebrom & Hedlund, 2000). Notably in developing countries, the overpopulation hypothesis is a popular degradation explanation (Stocking, 1995). Hence, under comparable biophysical conditions, more degraded areas should be found in highly populated regions (Grepperud, 1996). However, there is convincing evidence that areas with high population pressure and market access can be centres of innovations and land care practices (Tiffen et al., 1994). High population density is not necessarily related to land degradation; it is what a population does to the land and the regulatory frameworks installed that determine the extent of degradation (Mitiku Haile et al., 2006; Lemenih et al., 2014). Clearly, our interviews show that current conservation efforts are resulting in reduced soil erosion rates, although population increased over that time. People can be a major asset in reversing a trend towards degradation. Keyzer et al. (2001) attempted a detailed national assessment of soil degradation in Ethiopia. Their study showed that soil degradation has an impact on soils of lower fertility and where population density is low. Hence, the overpopulation hypothesis can hardly be validated as overall low population densities existed through the whole historical period of 19th and early 20th century, when land degradation occurred (Nyssen et al., 2009).

Such degradation explanations are often presented in a sensational way. For example, Tekle Kebrom stated in 1999 for a region in North Ethiopia that 'unbalanced utilization of forest resources for any use may lead to total degradation of the land in the year 2010' (Tekle Kebrom, 1999), while instead an increase of woody biomass is observed during this period (Nyssen et al., 2009). The interview results presented here consider land degradation as a complex web of political-ecological interactions, rather than a simple or sensational depletion of resources. Moreover, the identified political-ecological eras correspond remarkably well with the main periods of environmental degradation in the region (Frankl et al., 2011): a stable but exhausting pre-1970 environment (with stable gullies); a degrading environment 1970-1990 (with enhanced gully activity); and an improving environmental situation post-1990 (with stabilizing gullies).

The political-ecological complexity can be further illustrated by the environmental impact of the exceptional feudal land tenure of *chigurafgwoses* or *shehena*, observed in some parts of Tigray and Eritrea before the DERG came to power. In *chigurafgwoses*, the lands were equally distributed to all farmers in the village. Contrary to the insecure and unequal *rist* system, *chigurafgwoses* created incentives for environmental management since "one loses his land if it is neglected, to the contrary of what happens in the case of rist property where rights are not lost in case of land abandonment or neglect" (Nadel, 1946). Finally, for places all over Africa, a growing number of studies are focusing on the effects of land tenure, land ownership and land policies on land degradation (Mastewal Yami et al., 2013; Lestrelin & Giordano, 2007; Bennett et al., 2012; Glover & Elsiddig, 2012). In these studies, ineffective land policies are considered as a substantial cause of land degradation, covering a range of tenure systems from neoliberal (Klepeis & Vance, 2003), communist (Shmelev, 1991; Stringer & Harris, 2014) to feudal (Moore, 2002) or insecure (Tenge et al., 2004) systems. *Political ecology* provides an appropriate analytical framework, as it analyses land degradation "from an actor-oriented perspective in the context of unequal power relations, resulting from political decisions, actions and omissions on different levels of action" (Krings, 2002). On a broader level, such a framework is equally valuable for the analysis of land degradation worldwide (Warren, 2002; Robbins, 2012; Zhao et al., 2013; Fleskens & Stringer, 2014), or for analyzing global environmental problems in general, including deforestation, the loss of biodiversity, desertification and climate change (Adger et al., 2001; Peet el al., 2010).

3.5 Conclusions

Land degradation in the North-Ethiopian Highlands should not only, or even mainly, be thought of as the result of mismanagement or overpopulation; but is structurally inherent to the political-ecological system and its related conservation policies. Cycles of land degradation seem to correlate well with changes in the land policies, as three main historical political eras were identified: i) the late feudal era, ii) the dry wartime era, and iii) the post-war era. Indeed, traditional feudal, civil war, and post-war conservation policies follow each other successively. Firstly, the feudal land system could cause land degradation

in several ways. The interviews showed that the unequal character of land rights during feudal times played a role in 20th century land degradation. In particular, farmers 'without lands' were forced to farm at steeper slopes; and rich farmers (or the Church) cultivated their lands away from marshy areas. The existence of some widely implemented conservation structures (such as *dagets*) indicates that knowledge on soil management existed. Overall, land degradation has been more severe during the feudal times, when there were less communal lands, less public investments, and a highly unequal distribution of extensive croplands that were in private hands of the nobility or the Church. Secondly, severe land degradation during the eighties coincided with severe drought and with the civil war, resulting in economic decline and a lack of conservation efforts. Thirdly, the recently observed reduction of soil erosion and sediment yields shows that, despite the increased population pressure, the new conservation efforts and equal land rights succeeded in slowing down the land degradation processes. Finally, while adding a political-ecological framework to the Ethiopian land degradation debate, this chapter emphasises the key role of environmental policies and land ownership in contemporary environmental change.

Acknowledgements

This study would not have been possible without the enormous support, friendship and help of our translators Seifu Kebede and Yohannes Gebregziabher, the support and kindliness of the many farmers who were willing to participate in the interviews, the friendship and help of Lys Moulaert, the support and material assistance of the Belgo-Ethiopian VLIR MU-IUC programme, and a travel scholarship of Ghent University (BOF).

3.6 References

Adger, N., Benjaminsen, T., Brown, K., Svarstad, H., 2001. Advancing a Political Ecology of global environmental discourses. Development and Change 32, 681-715.

Adimassu, Z., Mekonnen, K., Yirga, C., Kessler, A., 2014. Effect of soil bunds on runoff, soil and nutrient losses, and crop yield in the Central Highlands of Ethiopia. Land Degradation and Development 25 (6), 554–564.

Andersson, E., Brogaard, S., Obsson, L., 2011. The Political Ecology of Land Degradation. Annual Review of Environment and Resources 36, 295-319.

Barbier, E., 1997. The economic determinants of land degradation in developing countries. Philosophical Transactions of the Royal Society of London Series B: Biological Sciences 352 (1356), 891-899.

Benjaminsen, T., Aune, J., Sidibe, D., 2010. A critical political ecology of cotton and soil fertility in Mali. Geoforum 41 (4), 647-656.

Bennett, J., Palmer, A., Blackett, M., 2012. Range degradation and land tenure change: insights from a released communal area of Eastern Cape Province, South Africa. Land Degradation and Development 23 (6), 557-568.

Berg, T., 1992. Indigenous Knowlegde and Plant Breeding in Tigray, Ethiopia. Forum for Development Studies 19 (1), 13-22.

Biazin, B., Sterk, G., 2013. Drought vulnerability drives land-use and land cover changes in the Rift Valley dry lands of Ethiopia. Agriculture Ecosystems & Environment 164, 100-113.

Blaikie, P., 1985. The Political Economy of Soil Erosion in Developing Countries. Longman, London, UK.

Bruce, J., 1976. Land reform planning and indigenous communal tenures: a case study of the tenure 'chiguraf-gwoses' in Tigray, Ethiopia. PhD thesis University of Wisconsin, Madison, USA.

Bryceson, D., Manicom, L., Kassam, Y., 1981. The methodology of the participatory research approach. In Research for the People, Research by the People: Selected Papers from the International Forum on Participatory Research in Ljubljana, Yugoslavia, 1980, Erasmie T, de Vries J, Dubell F (eds) Linköping University, 94–109.

Camberlin, P., 1994. Les précipitations dans la Corne orientale de l'Afrique: climatologie, variabilité et connexions avec quelques indicateurs océano-atmosphériques. PhD dissertation, Université de Bourgogne 379 pp.

Cheung, W., Senay, G., Singh, A., 2008. Trends and spatial distribution of annual and seasonal rainfall in Ethiopia. Int J Climatol 28, 1723–1734.

Clay, D., Guizlo, M., Wallace, S., 1994. Population and land degradation. The Environmental and Natural Resources Policy and Training Project, Michigan State University Press, East Lansing, USA.

Conway, D., 2000. Some aspects of climate variability in the North East Ethiopian highlands—Wollo and Tigray Sinet. Ethiopian Journal of Science 23 (2), 139– 161.

Crewett, W., Bogale, A., & Korf, B., 2008. Land Tenure in Ethiopia. Continuity and Change, Shifting Rulers, and the Quest for State Control. CAPRI Working Paper 91.

De Meyere, M., 2014. Runoff variability as impacted by physiographical factors and spatio-temporal changes in land use and cover - A case on the Rift Valley escarpment of Northern Ethiopia. Unpublished Msc. Thesis, Ghent University, Ghent, Belgium.

de Mûelenaere, S., Frankl, A., Haile, M., Poesen, J., Deckers, J., Munro, N., Veraverbeke, S., Nyssen, J., 2014. Historical landscape photographs for calibration of Landsat land use/cover in the Northern Ethiopian Highlands. Land Degradation and Development 25 (4), 319–335.

Fleskens, L., Stringer, L., 2014. Land management and policy responses to mitigate desertification and land degradation. Land Degradation and Development 25 (1), 1–4.

Frankl, A., Nyssen, J., De Dapper, M., Mitiku Haile, Billi, P., Munro, N., Deckers, J., Poesen, J., 2011. Linking long-term gully and river channel dynamics to environmental change using repeat photography (North Ethiopia). Geomorphology 129 (3-4), 238-251.

Frankl, A., Poesen, J., Scholiers, N., Jacob, M., Mitiku Haile, Deckers, J., Nyssen, J., 2013. Factors controlling the morphology and volume (V) – length (L) relations of permanent gullies in the Northern Ethiopian Highlands. Earth Surf. Process. Landforms 38, 1672-1684.

Fredu Nega, Mathijs, E., Deckers, J., Mitiku Haile, Nyssen, J., Tollens, E., 2010. Rural poverty dynamics and impact of intervention programs upon chronic and transitory poverty in northern Ethiopia. African Development Review 22 (1), 92-114.

French, C., Sulas, F., Madella, M., 2009. New geoarchaeological investigations of the valley systems in the Aksum area of northern Ethiopia. Catena 78 (3), 218-233.

Girma Kebbede, Jacob, M., 1988. Drought, famine and the political economy of environmental degradation in Ethiopia. Geography 318, 65-70.

Glover, E., Elsiddig, E., 2012. The causes and consequences of environmental changes in Gedaraf, Sudan. Land Degradation and Development 23 (4), 339-349.

Grepperud, S., 1996. Population pressure and land degradation: the case of Ethiopia. Journal of Environmental Economics and Management 30, 18-33.

Kassa Teka Belay, Van Rompaey, A., Poesen, J., Van Bruyssel, S., Deckers, J., Kassa Amare, 2014. Spatial analysis of land cover changes in Eastern Tigray (Ethiopia) from 1965–2007: are there signs of a forest transition? Land Degradation and Development 26 (7), 680-689.

Keyzer, M., Sonneveld, B., Zod, J., 2001. The Effect of Soil Degradation on Agricultural Productivity in Ethiopia: a Non-Parametric Regional Analysis in Economic Policy Reform and Sustainable Land Use in LDC's. In: Heerink, H Van Kenken and Kurpious M (eds) Physica Verlag: pp 269-292.

Kiernan, K., 2015. Nature, severity and persistence of geomorphological damage caused by armed conflict. Land Degradation and Development 26 (4), 380–396.

Klepeis, P., Vance, C., 2003. Neoliberal Policy and Deforestation in Southeastern Mexico: An Assessment of the PROCAMPO Program. Economic Geography 79 (3), 221–240.

Krings, T., 2002. A critical review of the Sahel Syndrome Concept from the viewpoint of Political Ecoloy. Geographische Zeitschrift 90 (3-4), 129-141.

Kumasi, T., Asenso-Okyere, K., 2011. Responding to Land Degradation in the Highlands of Tigray, Northern Ethiopia. IFPRI Discussion Paper 01142, International Food Policy Research Institute.

Lemenih, M., Kassa, H., Kassie, G., Abebaw, D., Teka, W., 2014. Resettlement and woodland management problems and options: a case study from North-West Ethiopia. Land Degradation and Development 25 (4), 305–318.

Lestrelin, G., Giordano, M., 2007. Upland development policy, livelihood change and land degradation: interactions from a Laotian village. Land Degradation and Development 18 (1), 55-76.

Machado, M., Perez-Gonzalez, A., Benito, G., 1998. Paleoenvironmental changes during the last 4000 yr in Tigray, Northern Ethiopia. Quaternary Research 49, 312– 321.

Massey, D., 1984. Spatial Divisions of Labour: Social Structures and the Structure of production. London: MacMillan.

Mastewal Yami, Wolde Mekuria, Hauser, M., 2013. The effectiveness of village bylaws in sustainable management of community-managed exclosures in Northern Ethiopia. Sustainability Science 8 (1), 73-86.

Mattsson, J., Rapp, A., 1991. The recent droughts in Western Ethiopia and Sudan in a climatic context. AMBIO 20 (5), 172-175.

Meadows, D., Meadows, D., Randers, J., Behrens, W., 1972. Limits to growth. Universe Books: New York.

Mekuria, A., Vlek, P., Denich, M., 2012. Application of the caesium-137 technique to soil degradation studies in the Southwestern Highlands of Ethiopia. Land Degradation and Development 23 (5), 456-464.

Melbaa Gadaa, 1988. Oromia: an introduction to the history of the Oromo People. Khartoum, Sudan.

Milas, S., Latif, J., 2000. The Political Economy of Complex Emergency and Recovery in Northern Ethiopia. Disasters 24 (4), 363-379.

Mitiku Haile, Herweg, K., Stillhardt, B., 2006. Sustainable Land Management – A New Approach to Soil and Water Conservation in Ethiopia. Mekelle, Ethiopia: Land Resources Management and Environmental Protection Department, Mekelle University; Bern,

Switzerland: Centre for Development and Environment (CDE), University of Bern, and Swiss National Centre of Competence in Research (NCCR) North-South, 269 p.

Moore J., 2002. The crisis of feudalism - An environmental history. Organization & Environment 15 (3), 301-322.

Munro, R., Deckers, J., Mitiku Haile, Grove, A., Poesen, J., Nyssen, J., 2008. Soil landscapes, land cover change and erosion features of the Central Plateau region of Tigrai, Ethiopia: Photo-monitoring with an interval of 30 years. Catena 75 (1), 55-64.

Nadel, S., 1946. Land tenure on the Eritrean plateau. Africa 16 (1-2), 99-109.

Naudts, J., 2002. Les Hautes Terres de Tembien, Tigré, Ethiopie; Résistance et limites d'une ancienne civilisation agraire; Conséquences sur la dégradation des terres. Mémoire présenté en vue de l'obtention du Diplôme d'Agronomie Tropicale CNEARC, Montpellier.

Nyssen, J., Mitiku Haile, Moeyersons, J., Poesen, J., Deckers, J., 2000. Soil and water conservation in Tigray (Northern Ethiopia): the traditional daget technique and its integration with introduced techniques. Land Degradation and Development 11, 199-208.

Nyssen, J., Poesen, J., Moeyersons, J., Deckers, J., Mitiku Haile, Lang, A., 2004. Human impact on the environment in the Ethiopian and Eritrean highlands - a state of the art. Earth-Science Reviews 64 (3-4), 273-320.

Nyssen, J., Poesen, J., Veyret-Picot, M., Moeyersons, J., Mitiku Haile, Deckers, J., Dewit, J., Naudts, J., Kassa Teka, Govers, G., 2006. Assessment of gully erosion rates through interviews and measurements: a case study from northern Ethiopia. Earth Surface Processes and Landforms 31 (2), 167–185.

Nyssen, J., Mitiku Haile, Naudts, J., Munro, N., Poesen, J., Moeyersons, J., Frankl, A., Deckers, J., Pankhurst, R., 2009. Desertification? Northern Ethiopia re-photographed after 140 years. Science of the Total Environment 407 (8), 2749-2755.

Nyssen, J., Petrie, G., Sultan Mohamed, Gezahegne Gebremeskel, Frankl, A., Stal, C., Seghers, V., Debever, M., Demaeyer, Ph., Kiros Meles Hadgu, Billi, P., Mitiku Haile, 2015. Historical aerial photographs of Ethiopia in the 1930s and their fusion with current remotely sensed imagery for retrospective geographical analysis. Journal of Cultural Heritage, submitted.

Pageau, D., 1989. Sécheresses, désertification et famines : la zone sahélienne et l'Ethiopie. Série notes et travaux - Centre Sahel 13; Université Laval, Québec, Canada 29 p.

Pankhurst, R., 1986. The History of Famine and Epidemics in Ethiopia prior to the Twentieth Century. Addis Ababa: Relief and Rehabilitation Commission, 120 p.

Peet, R., Robbins, P., Watts, M., 2011. Global Political Ecology. Routledge, Oxford.

Robbins, P., 2012. Political Ecology: A Critical Introduction. John Wiley & Sons, Chichester.

Roberts, N., 1997. The Holocene, an environmental history. Blackwell Publ, Oxford, UK.

Segele, Z., Lamb, P., Leslie, M., 2009a. Large-scale atmospheric circulation and global sea surface temperature associations with Horn of Africa June– September rainfall. Int. J. Climatol. 29, 1075–1100.

Segele, Z., Lamb, P., Leslie, M., 2009b. Seasonal-to-Interannual Variability of Ethiopia/Horn of Africa Monsoon. Part I: Associations of Wavelet-Filtered Large-Scale Atmospheric Circulation and Global Sea Surface Temperature. J. Climate 22, 3396–3421.

Segers, K., Dessein, J., Develtere, P., Hagberg, S., Haylemariam Girmay, Mitiku Haile, Deckers, J., 2010. The Role of Farmers and Informal Institutions in Microcredit Programs in Tigray, Northern Ethiopia. Perspectives on Global Development and Technology 9 (3-4), 520-544.

Shmelev, G., 1991. Soviet agrarian policy past and present. Food Policy 16 (4), 273-276.

Spinage, P., 2012. African Ecology; Benchmarks and Historical Perspectives. Springer Geography, New York, 1562 p.

Ståhl, M., 1974. Ethiopia: political contradictions in agricultural development. Rabén & Sjögren, Stockholm, 186 p.

Ståhl, M., 1990. Environmental degradation and political constraints in Ethiopia Disasters. The journal of disaster studies and management 14, 140-150.

Stocking, M., 1995. Soil erosion in developing countries: where geomorphology fears to tread! Catena 25 (1–4), 253-267.

Stringer, L., Harris, A., 2014. Land degradation in Dolj County, Southern Romania: Environmental changes, impacts and responses. Land Degradation and Development 25 (1), 17–28.

Tadesse Kidane-Mariam, 2003. Environmental and Habitat Management: The Case of Ethiopia and Ghana. Environmental Management 31 (3), 313–327.

Tekle Kebrom, 1999. Land degradation problems and their implications for food shortage in south Welo, Ethiopia. Environmental Management 23 (4), 419–427.

Tekle Kebrom, Hedlund, L., 2000. Land cover changes between 1958 and 1986 in Kalu district, Southern Wello, Ethiopia. Mountain Research and Development 2, 42-51.

Tenge, A., De Graaff, J., Hella, J., 2004. Social and economic factors affecting the adoption of soil and water conservation in West Usambara Highlands, Tanzania. Land Degradation and Development 15 (2), 99-114.

Terwilliger, V., Zewdu Eshetu, Huang, Y., Alexandre, M., Umer, M., Tsige Gebru. 2011. Local variation in climate and land use during the time of the major kingdoms of the Tigray Plateau in Ethiopia and Eritrea. Catena 85 (2), 130-143.

Thomas, P., Ofcansky, B., LaVerle, B., 1991. Ethiopia: A Country Study. GPO for the Library of Congress, Washington.

Tiffen, M., Mortimore, M., Gichuki, F., 1994. More people less erosion: Environmental recovery in Kenya. London: John Wiley.

UNEP, 1992. World Atlas of Desertification. London: Edward Arnold.

Wøien, H., 1995. Deforestation, information and citations: a comment on environmental degradation in Highland Ethiopia. Geojournal 37 (4), 501-512.

Yilma, S., Demarée, G., 1995. Rainfall variability in the Ethiopian and Eritrean highlands and its links with the Southern Oscillation Index. Journal of Biogeography 22, 945– 952.

Young, D., Hinton, R., 1996. An introduction to participatory appraisal techniques: sharing experience from China and Nepal. VSO, London, UK.

Warren, A., 2002. Land degradation is contextual. Land Degradation and Development 13 (6), 449-459.

Zhao, G., Mu, X., Wen, Z., Wang, F., Gao, P., 2013. Soil erosion, conservation, and eco-environment changes in the loess plateau of China. Land Degradation and Development 24 (5), 499-510.

Chapter 4 Gully dynamics: gully cut-and-fill cycles driven by drought and agro-management

This chapter is modified from:

Lanckriet, S., Frankl, A., Descheemaeker, K., Gebrekidan Mesfin, Nyssen, J., 2014. Gully cut-and-fill cycles as related to agro-management: a historical curve number simulation in the Tigray Highlands. Earth Surface Processes and Landforms 40 (6), 796-808.

Abstract

Gully cut-and-fill dynamics are often thought to be caused by extreme rainfall and/or deforestation related to population pressure. However, in this case-study of nine representative catchments in the North Ethiopian Highlands, we find that large-scale deforestation cannot explain gully morphology changes over the 20th century. Firstly, by using a Monte Carlo simulation to estimate historical catchment-wide curve numbers, we show that the landscape was already heavily degraded in the 19th and early 20th century – a period with low population density. The mean catchment-wide curve number (>80) one century ago was, under the regional climatic conditions, already resulting in considerable simulated historical runoff responses. Secondly, 20th century land cover and runoff coefficient changes were confronted with 20th century changing gully morphologies. As the results show, large-scale land cover changes and deforestation alone cannot explain the observed processes. The study therefore invokes interactions between *authigenic* factors, periodic droughts, cattle grazing, small-scale plot boundary changes, cropland management and land policies to explain the gully cut processes. Finally, semi-structured interviews and sedistratigraphic analysis of three filled gullies confirm the dominant impact of (crop)land management (tillage, check dams in gullies and channel diversions) on gully cut-and-fill processes. Overall, periodic drought and agricultural land management – including land tenure, increased cattle grazing and land distribution – can be very strong drivers of 20th century gully morphodynamics.

4.1 Introduction

Gully incision (*cut*) and subsequent aggradation (*fill*) occur in successive cycles (Vanwalleghem et al., 2005a). At the first stage of gully initiation, mechanic actions of water on the soil are predominant at the gully bottom and rapid mass movement occurs on the gully sides (Sidorchuk, 1999). Gully channel formation is very intense during this early period of gully initiation, when the morphological characteristics of the gully (length, depth, width, cross-sectional area, and volume) are far from stable. Kosov et al. (1978), quoted in Sidorchuk (1999), showed that the first gully incision stage is relatively short and lasts for about 5% of the gully's lifetime, but 90% of the gully's length, 60% of the gullied area and 35% of the gully's volume are formed during this period. Hence, at first gully length development is an important geomorphic process, followed by subsequent width development (Schumm, 2005). After the first 'dynamic' incision phase, a long period of geomorphic 'maturity' occurs (Sidorchuk, 1999). In particular, the growth of gully volume is exponentially decaying in rate with time (Thomas et al. 2004), while in the North Ethiopian Highlands gully volume follows a sigmoidal trend (Nyssen et al., 2006). Maturity is then followed by gully infill, which was measured by Vanwalleghem et al. (2005a) in Belgium, showing very rapid infill rates (*in casu* 6.4 cm a^{-1}). Fuller and Marden (2010) showed that gully incision and aggradation can even be yearly processes. Vanwalleghem et al. (2005a) therefore concluded that gully incision and infilling under cropland can be relatively rapid processes, as they found five cycles of cut-and-fill in 350 years.

Worldwide often a combination of intensive land use change and extreme rainfall is blamed for gully formation (e.g. Stankoviansky, 2003; Vogt, 1953; Fryirs & Brierley, 1998; Carnicelli et al., 2009). A literature review regarding the drivers of Holocene terrestrial gully cut-and-fill processes all over the world (Table 4.1) shows influences of (neo)tectonics, road building, climate changes, land cover change and deforestation, overgrazing, cropland management and sea-level change. As expected, land cover and climate changes are mentionned as the main gully cut-and-fill drivers in most of the studies. Meanwhile, the impact of cropland management (with 4 relevant studies) is not often investigated and therefore highly underrepresented in such geomorphic studies (Table 4.1). However, cropland management could have a very significant influence on gully cut and fill processes, even under stable land cover. Stolz (2011) showed for example from a case study in Germany that the

historical introduction of the improved three-field crop rotation system intensified agriculture and led to increased soil erosion and gully formation. Nagasaka et al. (2005) discussed the same phenomenon under mechanization of agriculture in modern Japan. The study of Zaimes & Schultz (2012) focused on the effect of riparian land management on gullying; while Casali et al. (1999) showed the impact of tillage practices, stubble maintenance, and gully refill by local farmers.

Table 4.1 Drivers of Holocene terrestrial gully cut-and-fill cycles.

Continent	Country	Location	Elevation (m a.s.l.)	Period considered	Number of cycles	Main contributing factors							Reference
						Sea-level change	Tectonics	Road building	Climate change	Land use chage	Cropland management	Overgrazing	
EU	UK	Isle of Wight	0	12 ka	1	X			X				Leyland & Darby (2009)
	Germany	Wolfsgraben – Bavaria	200-300	1200 BC - now	7				X	X			Dotterweich et al. (2003)
		Taunus	200-600	Early Medieval	1						X		Stolz et al. (2011)
	Poland	Silesia	200-300	1949-now	1				X				Malik (2008)
	Slovakia	Myjava	200-1000	1300s-1500s-now	2 - 3				X	X			Stankoviansky et al. (2003)
	Hungary	Balaton Lake (Tetves)	100-300	1968-2004	> 4					X			Kertesz & Gergely (2011)
		Rakaca	100-300	1800-2003	1					X			Gabris et al. (2003)
	Belgium	Meerdaal	30-110	1743 BC – 364 AD	2			X					Vanwalleghem et al. (2003)
		Meerdaal & Tesaart	30-110		1					X			Vanwalleghem et al. (2006)
		Meerdaal	30-110		1					X			Vanwalleghem et al. (2008)
	Spain	Rambla Salada	100-400	1997	1					X			Wijdenes et al. (2000)
		Carcavo	200-900	2004-2007	1					X			Lesschen et al. (2007)
		Guadalentin & Sierra de Gata	120-1100	1996-1998	1					X			Vandekerkhove et al. (2000)
		El Cautivo	200-400	Pleisto/ Holocene	6				X	X			Alexander et al. (2008)
		Navarra	200-600	1994-1996	> 2						X		Casali et al. (1999)
	Portugal	Alentejo & Serra de Negueira	150-900	1996-1998	1					X			Vandekerkhove et al. (2000)

	Italy	Basilicata	50-400	Neolithic - now	4				X				Boenzi et al. (2008)
		Sicily	200-400	1995-2000s	1				X				Capra et al. (2009)
		Basilicata	50-400	4500 BP	4				X				Piccarreta et al. (2012)
		Sardinia	0-400	1955-1999	1					X			Zucca et al. (2006)
	Greece	Lesvos	0-260	1996-1998	1					X			Vandekerkhove et al. (2000)
AF	Ethiopia	Ziway-Shala	1600-1900	5 ka	> 5		X		X				Carnicelli et al. (2009)
		Debre-Mawi	1900-2400	1980-2008	1					X			Tebebu et al. (2010)
		Umbulo	1500-3000	1965-2000	1					X			Moges & Holden (2009)
	Madagascar	Antananarivo Region	1000-2000	1985-1990	1			X	X	X			Wells & Andriamihaja (1993)
	RD Congo	Kinshasa	272	1957-2010	1			X					Makanzu et al. (2014)
	Nigeria	Anambra	0-500	Quaternary	> 2		X						Egboka (1990)
	Kenya	Chesegan	1000-1400	2000s	1			X					Jungerius et al. (2002)
	South Africa	Sneeuberg (Great Karoo)	500-2000	19th century-now	1							X	Boardman et al. (2003)
		Keiskamma	600-900	1990s	1							X	Mhangara et al. (2012)
		Umtata	150-2800	2008	1							X	Le Roux & Sumner (2012)
AS	Israel	Yehezkel	100	2000s	1			X					Svoray & Markovitch (2009)
		Negev	0-1000	1400 BP – 2000s	1				X		X		Avni (2005)
	Iran	Hableh Rood	1000-2000	1957-2005	1				X	X			Samani et al. (2010)
	China	Gansu	1500-2500	Holocene	1				X	X			Schutt et al. (2011)
	Japan	Hokkaido	0-300	1960-now	1						X		Nagasaka et al. (2005)
	Mongolia	Karakorum	1000-3000	6 ka	2				X			X	Lehmkuhl et al. (2011)
AM	USA	Providence Canyon	100-140	1840-now	1			X		X			Hyatt & Gilbert (1999)
		South Carolina	300-800	1939-1999	1					X			Galang et al. (2007)
		Iowa	200-500	1990	1						X		Zaimes & Schultz (2012)
		Santa Cruz (California)	0-2000	19th century	1 - 2							X	Perroy et al. (2012)
OC	New Zealand	Waiapu	200-1200	1939-2003	1 - 3					X			Parkner et al. (2006)
	Australia	Naas River	600	14 ka	> 3				X	X			Eriksson et al. (2006)
	Australia	Queensland	50-600	1800s-now	1				X	X			Saxton et al. (2012)

In the Ethiopian Highlands, Frankl et al. (2011, 2013) pointed to the re-activation of a dense gully network in the 1960s, which results in relatively wide gullies at present (Figure 4.1).

The gully channels are already visible on historical photographs of the 19th and early 20th century as a dormant system inherited from a pre-20th century activation. During the re-activation of the system, there were high denudation rates, a high sediment supply and activation of first-order streams (Frankl et al., 2011). Related 20th century land degradation in Northern Ethiopia is amongst others linked to interplays of drought and land cover changes (de Mûelenaere et al., 2014; Biazin and Sterk, 2013). Land cover changes induce vulnerability for climatic shocks, resulting in environmental degradation in the Highlands (Frankl et al., 2011; 2013). Based on repeating historical landscape photographs, it can be seen that the Northern Ethiopian landscape was already largely deforested in the 19th century (Nyssen et al., 2009; Meire et al., 2013). However, if deforestation was mainly a pre-20th century process, it would be less responsible as a direct driver of 20th century land degradation processes. This would then lead to the need to investigate other driving factors of 20th century land degradation, which are more related to agricultural management (*agro-management*; e.g. including land tenure changes, environmental management programs, agricultural intensification and land distribution). Yet, the historical evolution of agricultural management is difficult to assess. For instance, the spatial distribution of the historical dynamics of overgrazing, land ownership and cropland management (e.g. fertilization, plowing frequency) are poorly known as they are invisible on historical aerial and terrestrial photographs.

Figure 4.1 Example of a gully, in the Northern Ethiopian Highlands (13.65126°N – 39.21895°E; looking upslope from the study site in May Ba'ati); for illustration purpose. Livestock for scale.

Taking these elements into account, two research issues arise. First, the direct impact of land cover changes on 20th century gully cut-and-fill processes was never quantified and estimated for the Highlands. Second, as stated before, the impact of agro-management on gully cut-and-fill dynamics is not well understood worldwide and in particular in North Ethiopia. Therefore, this chapter presents a simple method for estimating historical curve numbers. This Monte Carlo based method will be illustrated using case studies of 19th century and early-20th century gully activity in six catchments in North Ethiopia. Then, we will estimate the contribution of land-cover changes on changing gully peak discharges over the 20th century in these catchments. Finally, the impact of cropland management on gully infill will be studied in three additional catchments.

4.2 Materials and methods

4.2.1 Case-study sites in North Ethiopia

4.2.1.1 Repeat photography sites with one century interval

Historical gully top widths (W) were identified based on the quantification of historical changes in gully cross-sections using repeat photography (Frankl et al., 2011) (Figure 4.3) (Table 4.2). Frankl et al. (2011) measured the observable top width, maximum depth and bottom width of the gully cross-sections for the 19th and early 20th century by comparing it to the early 21st century situations. This was done by calibrating gully top widths on digitized terrestrial photographs with field measurements. For a full description of this methodology, the reader is referred to Frankl et al. (2011). Frankl et al. (2011) showed that the accuracy of these top width measurements is 10%, as assessed by five replicates of the measurement procedure by experienced geomorphologists. In order to compare the early 20th century situation with the early 21st century for relatively 'stabilized' gullies, only the photographs taken before 1943 and after 2000 could be used in this study. This included six repeated photograph couples in six catchments on basalt near Bolago (1 couple), Atsela (2 couples) and Ashenge (3 couples); (Figure 4.2). The reader must consider the fact that the gully widths identified on the photographs are reflecting the environment 'at its most

degraded state'. The channel widths from the early 21st century are therefore probably the result of flashfloods occurred during the 1980s-1990s; while the channel widths of the early 20th century are the results of flashfloods occurred during the 19th or early 20th century.

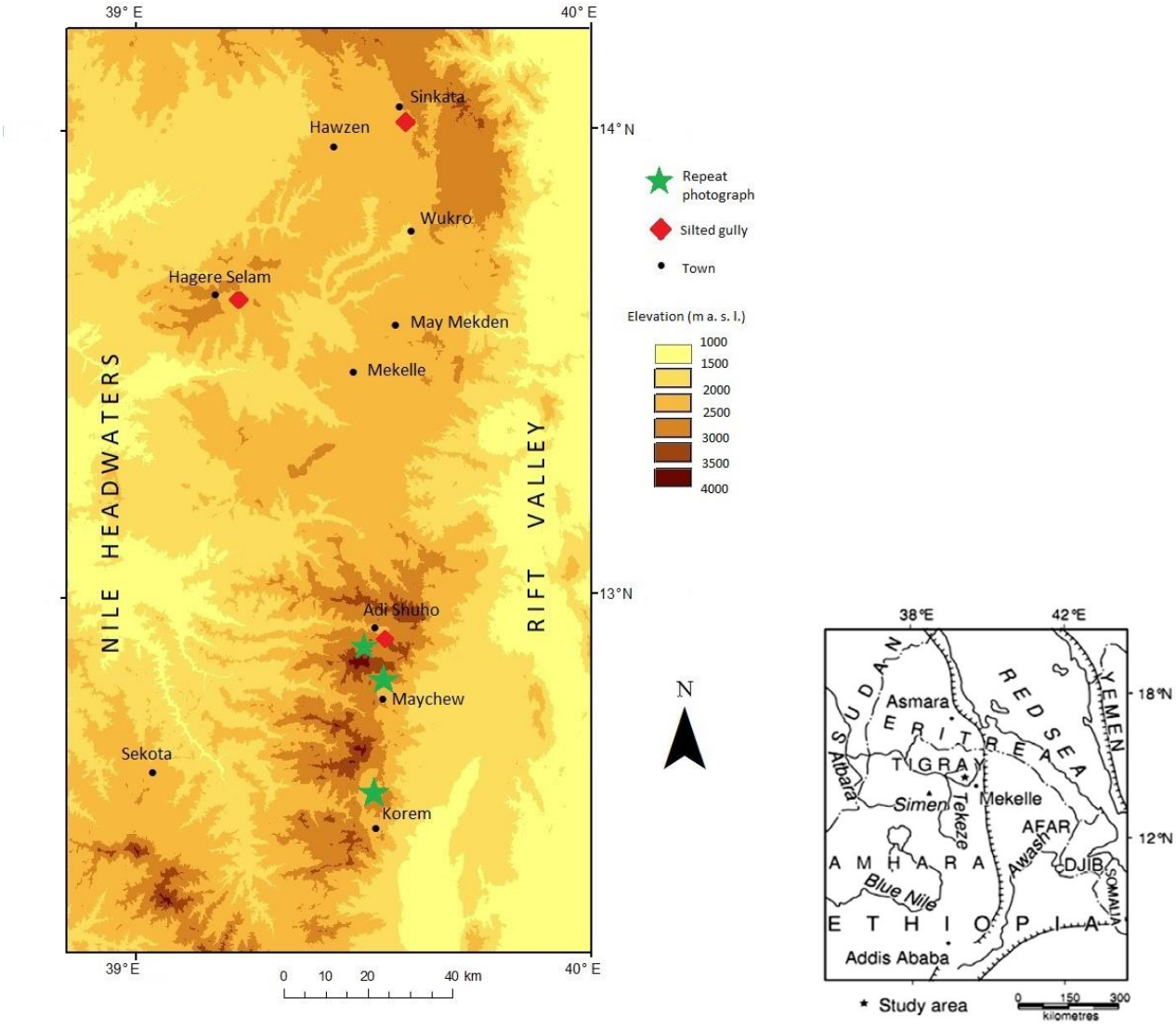

Figure 4.2 Study area with the location of the three investigated silted gullies (May Ba'ati is located next to Hagere Selam; the other gullies near Sinkata and Atsela (Adi Shuho)); and the location of the repeated photographs of gully cross-sections (2 sites near Atsela; 1 to the North of Maychew (Bolago); and 3 sites near Korem (Ashenge)).

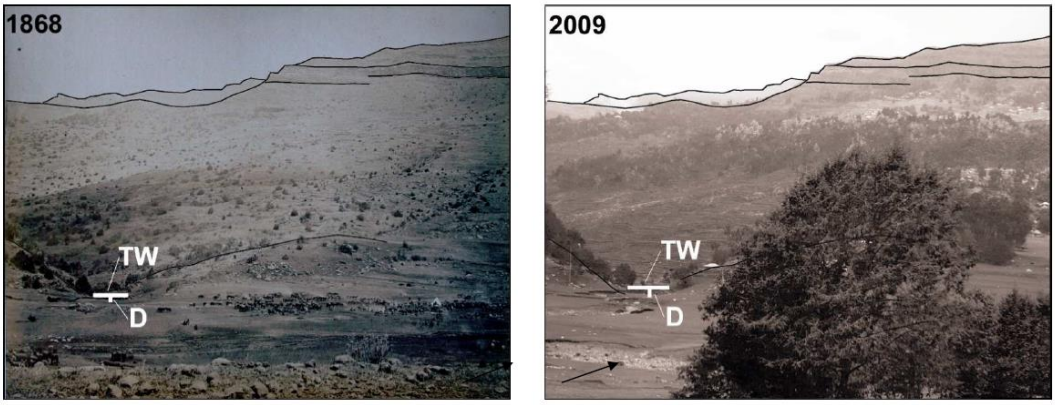

Figure 4.3 Example of a historical photograph (Royal Engineers, 1868) with modern analog (Amaury Frankl, 2009) in the Bolago catchment (Viewpoint: 12.82722° N, 39.51777° E), with indication of the calibrated gully top widths (W) and depths (D); (after Frankl et al., 2011); accuracy of the top width measurements is 10%, and accuracy of the depth measurement is 16% (Frankl et al., 2011).

Table 4.2 Historical and recent top widths of the cross-sections analyzed by Frankl et al. (2011), with an accuracy of 10%.

Code	date	$TW_{historical}$ (m)	date	TW_{recent} (m)	ΔTW (m)	Coordinates (WGS84)
M	1942	10.94	2009	14.82	3.88	12°54'44" N, 39°31'16" E
M	1942	8.81	2009	11.90	3.09	12°54'44" N, 39°31'16" E
P	1868	13.3	2009	16.00	2.70	12°49'37" N, 39°31'04" E
Q	1936	14.42	2009	19.00	4.58	12°33'45" N, 39°31'22" E
R	1936	0	2009	11.60	11.60	12°33'55" N, 39°31'27" E
S	1936	0	2009	12.50	12.50	12°33'55" N, 39°31'27" E
Average		7.9		14.3	6.4	

The codes are derived from Frankl et al. (2011); $TW_{historical}$ and TW_{recent} correspond to the gully top widths derived from the historical and recent photographs respectively; ΔTW corresponds to the difference between the two situations.

4.2.1.2 Filled gullies

Additionally, three partially silted channels were chosen in distinct environments in the Highlands of Northern Ethiopia (Figure 4.4), depending on the occurrence of different lithologies and based on short interviews with local farmers that focused on changes in local gully morphodynamics (Figure 4.2). The partially filled channel in Ma'ay Bati (13.65126°N – 39.21895°E) is located downslope of the Amba Aradam sandstone cliff. The channel itself has been incised in colluvium overlying oolitic limestones and marls of the Antalo formation (Merla et al., 1979). The filled channel in Sinkata (14.04785°N – 39.58263°E) is located downslope of a cliff of Paleozoic Enticho Sandstone. The channel itself has been incised in colluvium overlying Precambrian metavolcanics (Bussert and Schrank, 2007). The paleochannel in Atsela (12.93180°N – 39.52446°E) is incised in colluvium overlying trap basalts of the Ashangi group (Merla et al., 1979). The paleochannels are located in or near low-lying croplands on relatively gentle slopes (< 0.1 m m^{-1}); on soils with vertic properties.

Figure 4.4 Infilled gully channels, for illustration purpose. From left to right, the upslope part of the May Bati gully (13.65126°N – 39.21895°E); the downslope part of the channel in Sinkata (14.04785°N – 39.58263°E) and the channel in Atsela (12.93180°N – 39.52446°E). The red arrow indicates the historical stream direction.

4.2.2 Monte Carlo simulation of curve numbers using land cover data

Based on existing historical land cover data obtained using warped repeat photography (see Meire et al., 2013) with a particular areal extent A_x for a particular land cover type x, and with runoff coefficients C_x calibrated for these land cover types (Descheemaeker et al., 2006; Lanckriet et al., 2012), catchment-weighted runoff coefficients C_i could be calculated as:

$$C_i = \frac{\sum C_x . A_x}{\sum A_x} \qquad (4.1)$$

The areal extent of the land cover types was calculated by warping land cover units from terrestrial photographs to the horizontal plane of the map, including a meticulous quality check of the warping results (Meire et al., 2013). These catchment-weighted runoff coefficients C_i could be converted to catchment-weighted curve numbers CN_i, by combining the following equations based on the calibrations by Descheemaeker et al. (2006) and Descheemaeker et al. (2008) for the Tigray Highlands (on basalt and limestone):

$$\begin{cases} C_i = \kappa - \lambda * \ln(VEG_i) & (4.2) \\ CN_i = 100 - \xi * e^{(\mu * VEG_i)} & (4.3) \end{cases}$$

where calibration parameters κ = 165.4 and λ = 37.6 (Descheemaeker et al., 2006); VEG_i the total woody vegetation cover (VEG; in %) and calibration parameters μ = 0.021 and ξ = 8.99

(Descheemaeker et al., 2008). Because the VEG term disappears while combining Equation 4.2 and 4.3, there is no need to determine woody vegetation cover. CN represents the catchment-wide average curve number defined as:

$$Q = \frac{(P - 0.2s)^2}{P + 0.8s} \text{ with } s = \frac{25400}{CN} - 254 \qquad (4.4)$$

where Q is the runoff (mm), P is the daily rainfall (mm) and s is the storage parameter (SCS, 2004). The curve number (CN) method is an empirical way to predict direct runoff from rainfall excess. According to Boughton (1989), curve numbers are widely used to predict runoff under varying land cover conditions in catchments from 0.25 ha up to 1000 km^2. For relevant land cover types, one can empirically calibrate the curve number and derive S, which is the maximum storage of the catchment. It is assumed that rainfall less than 20% of the maximum storage will not contribute to runoff (SCS, 2004). Despite their empirical nature, curve numbers are useful runoff prediction tools in semi-arid areas (see El-Hames, 2012; Teka et al., 2013). Here, hydrological models are not always directly applicable. When rigorously calibrated under local conditions, the method can provide accurate predictions of runoff, which is the case in Tigray (Descheemaeker et al., 2008). Hence, we preferred to use this method, since it is a very well calibrated runoff model in the Tigray Highlands and because of the possibility of integrating the curve numbers with runoff coefficients.

However, since the runoff coefficients C_x calculated by Descheemaeker et al. (2006) and Lanckriet et al. (2012) have considerable standard deviations, the curve numbers had to be estimated using a Monte Carlo simulation, in order to account for error propagation. The simulation was based on 10 000 runs, following the rule of thumb that such simulations yield errors less than 1% (Koop et al., 2007). As shown by the runoff plot data of Descheemaeker et al. (2006) and Lanckriet et al. (2012), we can apply a normal distribution of the runoff coefficients (variance taken as 0.1Cx). Given a standard deviation of 0.09 on the runoff coefficients (Lanckriet et al., 2012), allowing such a large variance ensures us that all errors are surely incorporated. Monte Carlo sensitivity analysis allowed assessing the impact of the different land cover types on the catchments' runoff vulnerability. Using the curve number method, runoff responses to a given daily rainfall sequence could be simulated with the obtained catchment-wide curve numbers. This daily rainfall sequence was taken for a random year (2006), measured at the Mekele-Quiha Airport meteorological

station, which represents a high-quality record for the region. The year 2006 can be considered as a 'normal' year with a total June-September rainfall of 570 mm.

4.2.3 Estimations of peak discharge changes from land cover changes

Based on the same existing historical land cover change data (Meire et al., 2013), and with the runoff coefficients calibrated for these land cover types (Descheemaeker et al., 2006; Lanckriet et al., 2012), peak discharge changes ΔQ_p induced by those changes ΔC could be calculated following the rational formula (Dunne and Leopold, 1978):

$$Q_p = \gamma CIA \Rightarrow Q_p \propto C \Rightarrow \Delta Q_p = \Delta C \qquad (4.5)$$

where γ is a calibration parameter; C is the runoff coefficient; ΔC is the change in runoff coefficient; A is the runoff-contributing area (ha); Q_p is peak flow discharge (m^3/s); and I is the rainfall intensity (mm/h). The rational method is still widely used because it is a simple model that requires few input parameters (Vanwalleghem et al., 2005), and gives satisfactory results (Viessman et al., 1989; Titmarsh et al., 1995), even for dryland areas (Graf, 2002). The equation can however induce errors (Graf, 2002) and was therefore calibrated in our study area by Tesfaalem et al. (2015), who show that the model yields satisfactory results. Moreover, we use here only the proportionality between Q_p and C.

4.2.4 Peak flow discharges from gully top widths on photographs

Gully peak flow discharges Q_p can also be estimated from the gully channel top widths W. Nachtergaele et al. (2002) showed from field measurements, field experiments and laboratory experiments, that in general a good W-Q_p relation is valid for ephemeral gullies, but also for permanent stabilized gullies such relationships can be applied (Sidorchuk, 1999). Derivation of peak flow discharge (Q_p) can thus be done using the following equation (Nachtergaele et al., 2002):

$$W = \alpha . Q_p^{\ \beta} \Leftrightarrow Q_p = \sqrt[\beta]{\frac{1}{\alpha} W} \qquad (4.6)$$

In general, the exponent β takes values of ca. 0.3 for rills (Nachtergaele et al., 2002); and approaches 0.5 for flashfloods in semi-arid areas (Graf, 2002). Torri et al. (2006) show that differences in climate, air temperature, channel gradient, land cover, texture and presence of a dry season are negligible for the value of β, which is in general 0.51 for channels wider than 0.5 m. Reported values for α are 1.13 for rills (Gilley et al., 1990), and range between 2.51 (Nachtergaele et al., 2002), 3.0 and 3.17 (Sidorchuk, 1999; Nachtergaele et al., 2002) for gullies. In our study area, Frankl et al. (2013) found that channel widths are indeed strongly and positively related to a discharge proxy (catchment area), following a power relation. For our wide and permanent gullies, the overall β coefficient was chosen (0.51; Torri et al., 2006) and α was set at its most extreme values 2.51 and 3.17 (Sidorchuk, 1999).

4.2.5 Interviews, profile pits and literature review

In order to investigate the sedistratigraphy of the silted channels, eight profile pits of approximately 2 x 1 m² and 2 m depth were dug into the channels of the three gullies (December 2012). More pits were dug in the largest channels, in order to 'capture' the entire gully width signal. One pit was dug in the May Bati gully, two pits in the Sinkata gully (both in the middle of the channel, with 50 m separation) and five pits in the Atsela gully (all in the middle of the channel, with 10 m separation from each other). Stratigraphy (color, boundaries, fabric, and stoniness) was recorded for all four sides of all eight pits. At the middle of the downslope side of the pits, samples for laboratory analysis were taken at depth intervals of approximately 15 cm. Wet sieving was performed at 64 µm, and dry sieving of the largest fractions (at 2 mm, 1 mm, 500 µm, 250 µm, 106 µm and 75 µm). Mineralogy was determined with microscopy for the 250 µm - 106 µm fraction of the samples at 50 cm depth. Some 2.5-3 g of the remaining silt and clay fraction was mixed with a 40 ml 0.2% sodium hexametaphosphate solution, shaken by sonication, and analyzed with X-ray sedigraphy (Micromeritics, 2014). Texture was determined using the USDA classification. Finally, in the surroundings of the infilled gullies, 16 open interviews with key informants (elder farmers who had lived and worked in the area since their childhood) were conducted (4 around the May Bati gully, 6 around the Sinkata gully and 6 around the Atsela gully). Farmers were asked to describe the gully evolution and the timing and processes of the gully infill.

Further, in line with earlier research in the study area (e.g. Naudts, 2000; Smit & Tefera, 2011) and using experience with interviewing gained in earlier research (Chapter 3), the likely relation between a changing agro-management (including property rights, the size of land holdings, conservation activities and cropland management) and gully cut-and-fill could be identified.

4.3 Results

4.3.1 Estimation of catchment-wide Curve Numbers

Based on the existing land cover data and runoff coefficients, catchment-scale runoff coefficients were calculated for the early 20th and 21st century using Eq. 1 (Table 4.3). It is clear that land cover changes and deforestation resulted *ceteris paribus* hardly in overall higher runoff responses over the 20th century (runoff coefficients +2.7, +3.3 and -32.8 % for the catchments); (Table 4.3).

Table 4.3 Twentieth century land cover (A_x) changes in our study catchments (reported in Meire et al., 2013), runoff coefficients (C_x) calibrated by Descheemaeker et al. (2006) and Lanckriet et al. (2012) with normal distributions N (C_x, 0.1C_x) chosen for the Monte Carlo simulation; and predicted catchment runoff coefficients C (Eq. 4.1), with their corresponding Curve Numbers CN (Eq. 4.2 and 4.3). We also depict estimated peak discharge changes ΔQ_p.

Catchment	Ashenge		Atsela (1944-2008)		Bolago (1868-2008)		
A_x (%)	1936	2008	1944	2008	1868	2008	C_x (%)
Cropland	64.8	64.8	61.6	55.0	5.0	14.2	30.4
Bush land	29.6	25.4	36.7	23.1	83.7	4.0	34.8
Village	0.0	5.6	0.0	13.0	0.0	16.0	60.0
Bare ground	5.6	4.2	0.0	0.0	0.0	0.0	70.7
Grassland	0.0	0.0	1.4	1.4	5.2	26.0	23.5
Forest	0.0	0.0	0.3	7.4	6.1	39.7	0.03
Weighted C (%)	34.0	34.9	31.8	32.9	31.9	21.4	
$\Delta C = \Delta Q_p$	+2.7 %		+3.3 %		-32.8 %		
ΔQ_p from ΔW (Eq. 4.1)	+71.2 %		+80.2 %		+43.3 %		
$CN_{historical}$	82.0		81.3		81.3		

Curve numbers were then calculated under the 19th and early 20th century land cover situation using Eq. 4.2 & 4.3 (Table 4.3). The resulting average curve number based on the Monte Carlo simulation (Figure 4.5a) is $CN_{average}$ = 81.5; with st. dev. = 2.3 (Figure 4.5a). Since these simulated catchment-wide curve numbers are relatively high (on average >80), it is clear that the Highlands were already heavily degraded and deforested during the 19th and early 20th century. This can be illustrated by simulating the runoff response with the average early 20th century curve numbers as compared to curve numbers of contemporary croplands using Eq. 4.4 (Nyssen et al., 2010; Figure 4.6). For the same daily rainfall sequence, the early 20th century runoff response is simulated higher than the contemporary (hypothetical) cropland runoff response. In general, and contrary to the common perception, the simulation shows that the impact of land cover on surface water runoff in the Highlands was one century ago about the same as today. Finally, Monte Carlo sensitivity analysis (effect of the land cover type on the curve number) showed that the curve numbers were very sensitive to the areal extent of bushland during the early 20th century (Figure 4.5b) – whereas runoff sensitivity shifted towards the areal extent of cropland during the early 21st century (Figure 4.5c).

It is worth mentioning that the recent photograph of the relatively wide gully in Bolago may not show a situation in equilibrium with the current environmental conditions, but instead may show a situation inherited from the 1970s or 1980s, before recent reforestation took place. As stated before, the largest peak discharges must indeed be a result of a situation when the catchments were in their most degraded state.

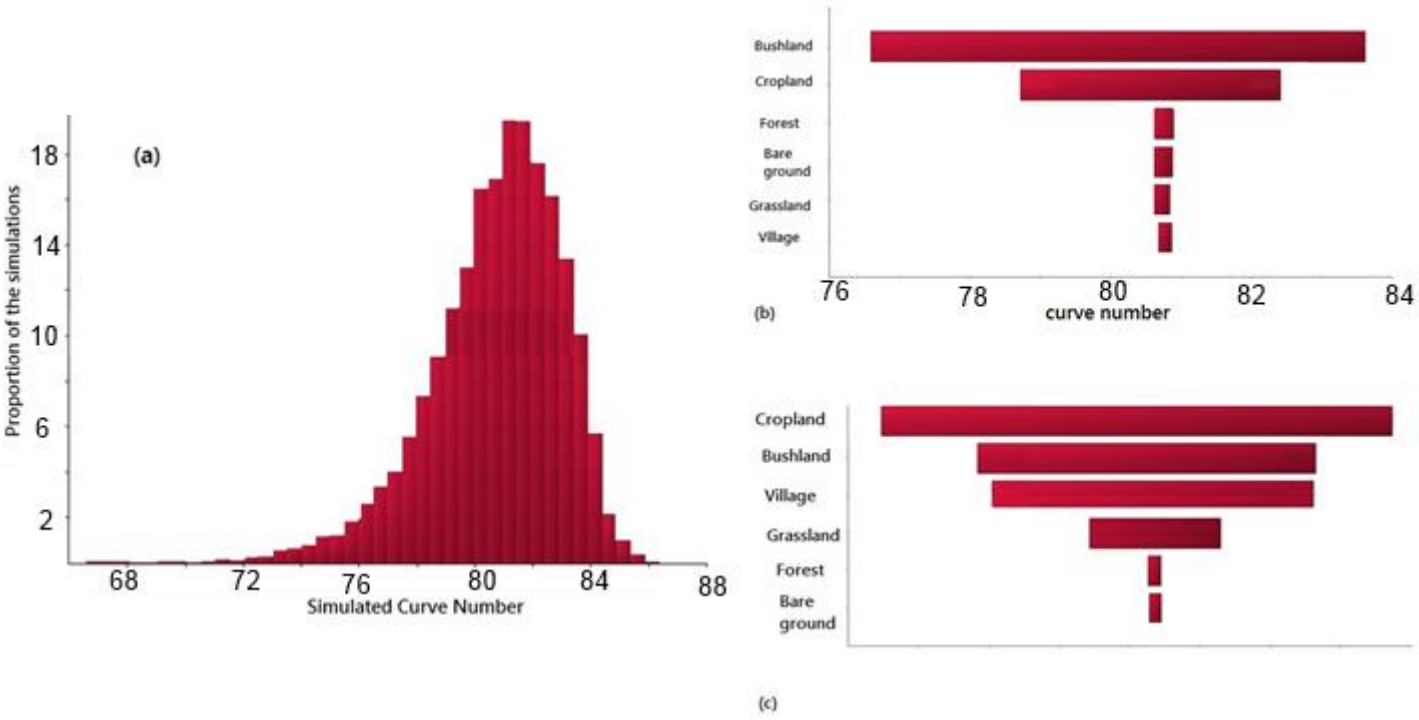

Figure 4.5 (a) Monte Carlo simulation (10 000 runs) of the curve numbers calculated with the data from Table 4.3; proportions in %; (b) results of the sensitivity analysis of the early 20th century landscape vulnerability to runoff; and (c) resulting sensitivity analysis of the early 21th century landscape vulnerability to runoff.

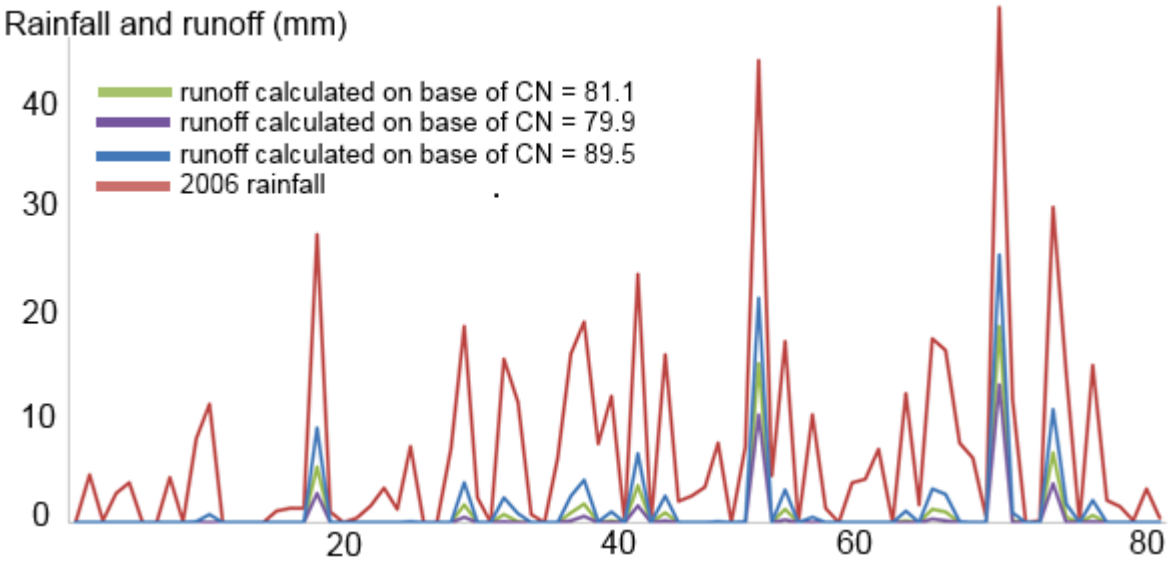

Figure 4.6 2006 rainfall (in red - Mekelle Airport; days after 1 June) was used to simulate catchment-scale runoff (Curve Number method) during the early 20th century (CN = 81.1; weighted average; in green), under cropland (free grazing, no stone bunds; in purple; CN = 79.9; Nyssen et al., 2010) and for fallow lands (CN = 89.5; in blue; after Nyssen et al., 2010).

4.3.2 Reconstruction of peak discharge changes over the 20th century

Historical peak flow discharges simulated for the different gully widths (Eq. 4.6) ranged between 7 and 53 m^3/s (Table 4.4).

Table 4.4 Estimated peak flow discharges Qp, with a minimum and a maximum estimation, as calculated with Eq. (4.6), required to cause the gully morphology (Δ corresponds to the difference between the two situations).

Locations	$Q_{p,\ historical\ MIN}$ (m^3/s)	$Q_{p,\ historical\ MAX}$ (m^3/s)	$Q_{p,\ recent\ MIN}$ (m^3/s)	$Q_{p,\ recent\ MAX}$ (m^3/s)	$\Delta\ Q_{p\ MIN}$ (m^3/s)	$\Delta\ Q_{p\ MAX}$ (m^3/s)	Coordinates (WGS84)
Atsela A	11.34	17.93	20.49	32.52	9.15	14.59	12.91911° N, 39.52189° E
Atsela B	7.42	11.73	13.33	21.15	5.91	9.42	12.91931° N, 39.52156° E
Bolago	16.62	26.30	23.81	37.79	7.19	11.49	12.82953° N, 39.51419° E
Ashenge A	19.48	30.82	33.35	52.93	13.87	22.11	12.56397° N, 39.52031° E
Ashenge B	x	x	12.68	20.11	12.68	20.11	12.56528° N, 39.52417° E
Ashenge C	x	x	14.68	23.29	14.68	23.29	12.56250° N, 39.52278° E
Average	9.14	21.69	19.72	31.30	10.58	16.8	

Average gully width increase over the 20th century was 6.4 m, with a significant t-test for the difference of means of the two periods ($p < 0.05$). Even under the extreme scenario of a 10% underestimation in historical top width measurements and a 10% overestimation in recent top width measurements, the average gully width increase over the 20th century was still 4.2 m. This corresponds to a minimum 20th century average peak discharge increase of 10.6 ± 3.7 m^3/s (Table 4.4), equal to a discharge increase of 71.2 % in Ashenge, 80.2 % in Atsela and 43.3 % in Bolago. Moreover, two downstream gully channels around Ashenge (AB and AC) did not exist in the early 20th century, but incised in the course of the late 20th century. However, over the 20th century, it is unlikely that rainfall intensities (I) changed, as from

1900 no long term changes in annual rainfall have been observed for the nearby Blue Nile basin (Nyssen et al., 2007): 'on average it rains as much around the year 2000 as around 1900' (see Chapter 2). Moreover, based on available station data of rainfall intensity during the past four decades, Billi et al. (2015) showed that there were no significant changes in rainfall intensity for Ethiopia. Possibly, due to road building, some catchment areas (A) might have increased in the Highlands (Nyssen et al., 2002), but this was not the case for our study catchments. Therefore, the huge average increase in stabilized gully width (6.4 m), the important minimum increase in estimated gully peak discharges (10.6 ± 3.7 m^3/s) and the incision of the two downstream gully channels at Lake Ashenge during the second half of the 20th century must be related to changes in the runoff coefficient C.

4.3.3 Reconstruction of the gully infill

The influence of cropland management on gully cut-and-fill was clearly visible in the filled gully channels. The profile of the May Bati pit (Figure 4.7) suggests an unlayered antropogenic colluvial infill, given the fact that the texture of the black layer vertic material is the same (median grain size < 2 μm) as textures of the surrounding Vertisols (Lanckriet et al., 2012). The possibility of an alluvial aggradation was discarded, since the sediments were not layered and showed no sedigraphic variability. As confirmed by farmers and as suggested by the texture analysis, the process of infill here is probably caused by a combination of tillage erosion and sheetwash that occurred in the last ten years.

Six open interviews with local farmers around the gully of Atsela reveal that this channel flow had been diverted by farmers some decennia ago (Figure 4.8). Six interviews with farmers around the Sinkata gully reveal that the gully filled in due to the construction of large gabion dams, around ten years ago (Figure 4.8). The stratigraphic descriptions of the profile pits (Figure 4.7) confirm these hypotheses (colluvial unlayered vertic infill of the May Bati gully; and an alluvial layered infill with rounded gravel and boulders of the Atsela and Sinkata infill). As illustrated by the Atsela case, gullying is dependent on flow diversions by farmers around plot boundaries. Indeed, observations in the study area show that several gullies are not always situated in the lowest parts of the landscape. This social-qualitative information yields independent evidence, strengthening our main argument: gully systems are very sensitive to agro-management.

<table>
<tr><td colspan="2">May Bati (13.65126°N; 39.21895°E)</td><td colspan="2">Sinkata A (14.04785°N; 39.58263°E)</td></tr>
<tr><td> 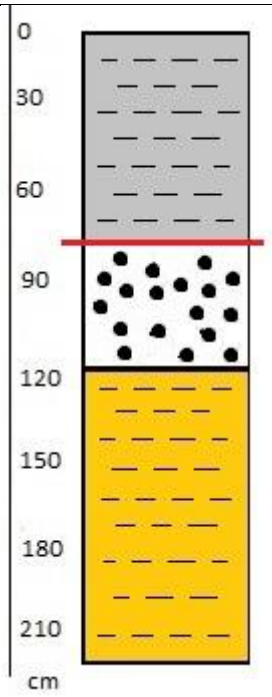
</td><td>Black clayey layer of vertic colluvium, containing mainly open 2:1 phyllosilicates (smectites) and feldspars (Moulaert, 2012) – transported by tillage erosion & sheetwash.

White calcareous rounded gravel indicating the paleo-bed

Yellowish clayey weathered parent material, containing lime and some quartz, kaolinite, and micas; (Moulaert, 2012)</td><td> 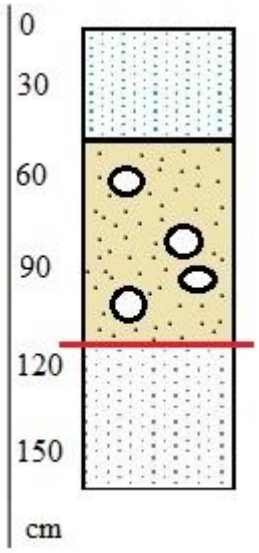
</td><td>Alluvial white sand

Alluvium of randomly distributed sandstone pebbles in a sandy layered matrix, containing some micritic limestone fragments, sparitic calcite, quartz, biotite and zircon

Pale white sand, supposedly weathered Enticho sandstone</td></tr>
<tr><td colspan="2">Sinkata B (14.04786°N; 39.58262°E)</td><td colspan="2">Atsela (12.93180°N; 39.52446°E)</td></tr>
<tr><td> 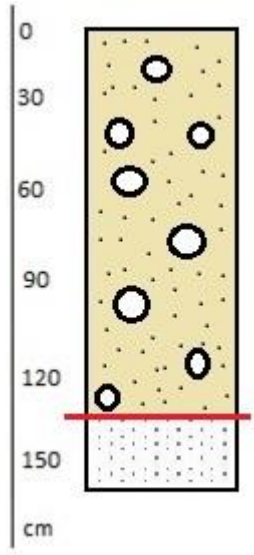
</td><td>Alluvium of randomly distributed sandstone pebbles in a sandy layered matrix, containing some micritic limestone fragments, sparitic calcite, quartz, biotite and zircon

Pale white sand; weathered Enticho sandstone</td><td> 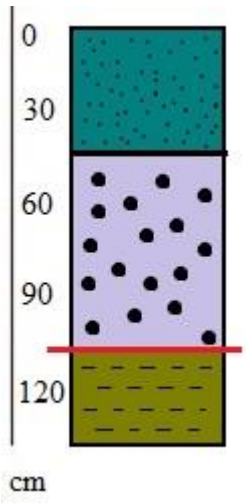
</td><td>Alluvium of dark layered sands, containing hornblende, some plagioclase, quartz, zircon, biotite and muscovite

Alluvial rounded gravel (diameter 5 cm)

Heavy black (vertic) clay</td></tr>
</table>

Figure 4.7 Schematized stratigraphy of the downslope sides of all eight profile pits. Depths are given in centimeters (cm). For Atsela, only one profile is shown, since all six profile pits showed similar layered alluvial sands and gravel. The red lines indicate the interface between infill and original bed.

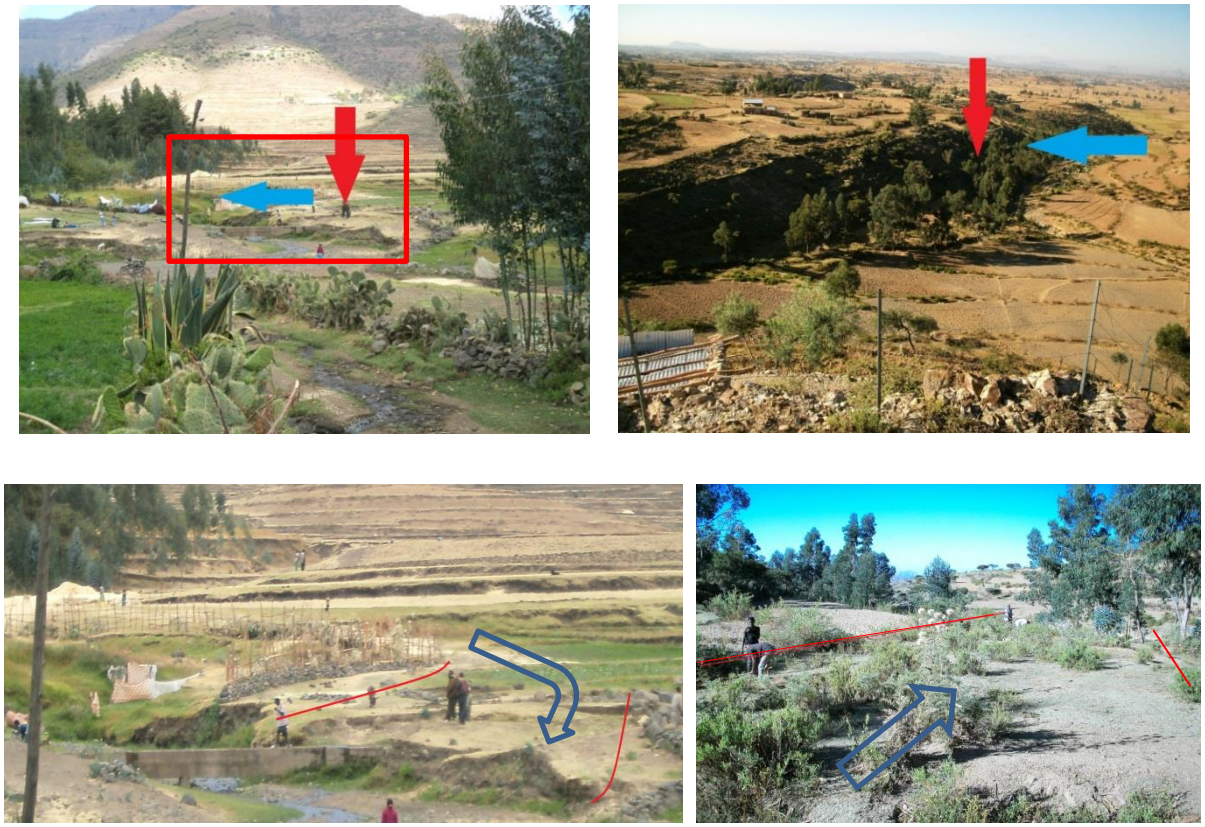

Figure 4.8 Location with red arrow of the silted gullies in Atsela (left; 12.93180°N – 39.52446°E) and Sinkata (right; 14.04785°N – 39.58263°E). The filled blue arrows show the direction of channel diversion for Atsela, and the location of the large gabions for Sinkata. Closer view of the channels in Atsela (lower left) and Sinkata (lower right). The red lines indicate the channel boundaries and the blue open arrow indicates the historical stream direction.

4.4 Discussion

4.4.1 Explanatory factors for peak discharge increase

Over the second half of the 20th century, we observed a huge increase in stabilized gully width and an increase in estimated gully peak discharges. However, as shown in section 4.3.1, the impact of land cover on surface water runoff in the Highlands was one century ago about the same as today. In particular, instead of the expected peak discharge increases of 71.2 %, 80.2 % and 43.3% (on average 64.9%), peak discharge increases due to land cover

changes are calculated (using Eq. 4.5) at only 2.7%, 3.3 % and -32.8 % respectively (Table 4.3). Therefore, neither road building, deforestation nor large-scale land cover changes can explain the changing gully morphology and peak discharges (average ΔW = 6.4 m; average minimum ΔQ_p = 10.6 m^3/s; $p < 0.05$). Apart from *authigenic* factors (e.g. natural channel widening), we therefore invoke interactions between periodic drought, the management of the croplands and land boundary changes that can explain the observed gully widening. In general, sociopolitical factors and drought lead to land management decisions which have impact on gully widening.

Firstly, an upslope extension of croplands during the 20th century, as reported by Naudts (2002), probably further decreased the vegetation cover and increased the runoff coefficient (C), due to the removal of remnant vegetation on the slopes. This trend has to be considered in its complex sociopolitical context. For example, the upslope extension of cropland during the 19th and 20th century may reflect the unequal character of land rights during late-feudal times. This extension was strongly related to an unequal division of land holding sizes, property rights and political power within the peasant community. The analysis of chapter 3 showed that during this period, farmers who were unable to claim genealogical relations with the founding families of the villages had no land rights and were forced to construct their farms and cultivate land on steep sloping and marginal terrains. This conversion of (woody) vegetation by croplands was leading to higher area-weighted runoff coefficients and thus gully peak discharges. In the same political context, it is also important to note the huge impact of the civil war on land degradation processes (Chapter 3), and the land reorganizations that often follow periods of war.

Secondly, changes in the land boundaries (removal of vegetation strips and traditional *daget* conservation structures), equally increased the runoff coefficient of the catchment. According to Nyssen et al. (2007), traditional conservation structures (*dagets* and grass strips on plot boundaries) have been narrowed, from 2 m around 50 years ago, to even less than 0.5 m at present. Thirdly, there has been a steady intensification of the agricultural production during the second half of the 20th century in Northern Ethiopia. Fallowing (*mistigao*) was a common practice, especially till the 1970s, with fallow lands simultaneously being grazing land for the village herds (Corbeels et al., 2000). Grabham & Black stated in 1925 on the regional agricultural system that "it seems to involve an area remaining fallow nearly twice as large as that under crop. The consequence is that only about one-third of

the land around villages is cultivated." Runoff responses on fields with fallowing (CN = 89.5; Nyssen et al., 2010) were simulated using Eq. 4.4, confirming that the high runoff production on such fields could have contributed to the high historical runoff in our case-catchments (Figure 4.6). Possibly, the plowing frequency of croplands increased over the 20th century, which would result in more concentrated flows and lead to soil compaction, resulting in a higher runoff coefficient and offsetting the hydrological effect of reduced fallowing (Smit & Tefera, 2011). Tesmesgen et al. (2008) show that the high yearly tillage frequency in the Highlands (4-5 times for teff and 3-4 times for maize) stems from the need to plow before the soil is wetted by rainfall. Periodic dry spells during the rainy season (the large droughts during the 1980s) can impact vegetation cover and can force farmers to plow frequently in order to avoid soil moisture losses. The more the farmer is educated and experienced, and the bigger his land and family, the higher is the tillage frequency on his fields (Tesmesgen et al., 2008). As shown by Lanckriet et al. (2012), average runoff coefficients under reduced tillage experiments are about half of the values under the current high tillage frequency (18.8% compared to 30.4%). Under a scenario of reduced tillage on all croplands in the early 20th century, area-weighted runoff coefficients would have been considerably smaller (for instance 24.7% for Atsela 1944, 31.3% for Bolago 1868). Overall, the scenario indicates that these gully systems are very sensitive to increased tillage frequency.

Finally, increased cattle grazing can have an important impact on catchments' runoff coefficients. According to Nyssen et al. (2004), the contemporary stocking rates are well in excess of estimated optimum stocking rates, resulting in decreased surface roughness, soil compaction and decreased hydraulic conductivity. As a consequence, infiltration becomes difficult and runoff coefficients increase (Nyssen et al., 2004). Cattle numbers in Ethiopia (and Eritrea) have more than doubled from 24.9 million in 1961, to 31.1 million in 1995 and 56.1 million in 2013 (FAO, 2015).

4.4.2 Comparison with other studies

Given the environmental data scarcity in the Ethiopian Highlands, the methods presented here will reflect general environmental patterns. Since the equations employed are empirical, this study does not pretend to simulate gully peak discharges exactly. However, we presented a case-study in a limited number of catchments, with a simple methodology to estimate long-term trends in catchment-wide curve numbers. We showed that neither

aridification nor deforestation could explain the observed gully morphodynamics, which is in sharp contrast with most geomorphic gully studies (Table 4.1). The average historical curve number ($CN_{average}$ = 81.5) was leading to considerable historical runoff responses. This contradicts several studies which claim that deforestation in North Ethiopia was mainly a 20th century process, although the origin of the data in these studies seems rather perfunctory. Parry (2003) states for example that "Ethiopia lost 98% of its forest cover during the last 50 years". Gore (1992) even claimed that Ethiopia's forested land had decreased from 40 to 1 percent from 1950 to 1992. Additionally, there is a common narrative that Ethiopia and Eritrea had "44 % forest cover in 1885" (McCann, 1997), or "40 % in 1900" (Allen-Rowlandson, 1989; Robinson et al., 1995). The situation may be different in the South of the country, but this study confirms the findings by Nyssen et al. (2009) who conclude that the Northern Ethiopian Highlands were already highly degraded before the 20th century.

As population density in that period was rather low (Nyssen et al. (2009) estimated the population of Ethiopia in 1868 at about 9% of today's population), this historical land degradation could not be of Malthusian origin. Indeed, gully cut processes prior to 1868 were observed from historical photographs, and are possibly related to the occurrence of droughts (Frankl et al., 2011). However, little information is available on the pre-19th century Northern Ethiopian climate (Little Ice Age; impact of El Niño) and pre-19th century land cover, so additional information should be gathered in this respect.

In line with observations in the filled gullies, a case study in the Amhara region (Smit and Tefera, 2011) shows that gullying in the Ethiopian Highlands is sometimes impacted by interactions between farmers who use their political power positions to avoid and divert harmful flows from the neighbors' farmlands. In general, cropland management and sociopolitical aspects of rural societies deserves more attention in geomorphological studies.

4.5 Conclusions

This study incorporated different driving factors (land cover changes and changes in cropland management) that influence the shape and dimensions of gullies in the Northern

Ethiopian Highlands. Gully incision was reconstructed by estimating historical peak flow discharges using values for historical gully width, as derived from recent photographs (2008-2009) and historical photographs (1868-1942). Average gully width increase over the 20th century was significant ($p < 0.05$) and was estimated at 6.4 m. Minimum peak discharges increased significantly (ΔQ_p: $p < 0.05$) during the 20th century and were calculated on average at 10.6 ± 3.7 m^3/s. Monte Carlo simulation allowed to reconstruct curve numbers one century ago (on average 81.1). This shows that the North Ethiopian Highlands were already severely deforested during in the 19th century. If deforestation is mainly a pre-20th century process, it is a less direct driver of 20th century land degradation processes. Hence, interactions between periodic drought (e.g. during the 1970s and 1980s), agricultural management (e.g. including environmental management, agricultural intensification and land distribution), small-scale land boundary changes (e.g. removal of *dagets* and grass strips) and sociopolitical factors (e.g. land tenure change, civil war) could be strong contributing factors. The historical evolution of those drivers is not directly visible on historical photographs. The estimated catchments' runoff response resulting from 20th century land cover changes shows however that catchment-scale runoff changes and processes of gully widening can be partly linked to small-scale land-cover changes, but also to changes in the cropland management. Finally, sedistratigraphic analysis of recently filled gullies suggests a strong agronomic interference (tillage operations, conservation structures, channel diversions). Hence, a combination of simulations and historical evidence suggests that periodic drought and agro-management are important drivers of gullying and related land degradation processes.

Acknowledgements

This study would not have been possible without the enormous support, friendship and help of our translator Seifu Kebede, the important input on mineralogy of Florias Mees, the support and kindliness of the many farmers who helped us, the discussions at the Physical Geography Research Group of the UGent, the funding of UGent Special Research Fund (BOF), as well as the logistical support through Belgian VLIR projects at Mekelle University (IUC and Graben TEAM).

4.6 References

Alexander, R., Calvo-Cases, A., Arnau-Rosalén, E., Mather, E., Lázaro-Suau, R., 2008. Erosion and Stabilisation Sequences in Relation to Base Level Changes in the El Cautivo Badlands SE Spain. Geomorphology 100 (1-2), 83–90.

Avni, Y., 2005. Gully incision as a key factor in desertification in an arid environment the Negev highlands, Israel. Catena 63 (2-3), 185-220.

Biazin, B., Sterk, G., 2013. Drought vulnerability drives land-use and land cover changes in the Rift Valley dry lands of Ethiopia. Agriculture Ecosystems & Environment 164, 100-113.

Billi, P., Yonas Tadesse Alemu, Ciampalini, R., 2015. Increased frequency of flash floods in Dire Dawa, Ethiopia: Change in rainfall intensity or human impact? Natural Hazards 76 (2), 1373-1394.

Boardman, J., Parsons, J., Holland, R., Holmes, P., Washington, R., 2003. Development of Badlands and Gullies in the Sneeuberg Great Karoo, South Africa. Catena 50 (2-4), 165–184.

Boenzi, F., Caldara, M., Capolongo, D., Dellino, P., Piccarreta, M., Simone, O., 2008. Late Pleistocene–Holocene landscape evolution in Fossa Bradanica Basilicata (southern Italy). Geomorphology 102 (3-4), 297–306.

Boughton, W. C., 1989. A review of the USDA SCS curve number method, Australian Journal of Soil Research 27, 511-523.

Bruce, J., 1976. Land reform planning and indigenous communal tenures: a case study of the tenure 'chiguraf-gwoses' in Tigray, Ethiopia. PhD thesis, University of Wisconsin, Madison, USA.

Bussert, R., Schrank, E., 2007. Palynological evidences for a latest Carboniferous-Early Permian glaciation in Northern Ethiopia. Journal of African Earth Science 49, 201-210.

Camberlin, P., 1994. Les précipitations dans la Corne orientale de l'Afrique: climatologie variabilité et connexions avec quelques indicateurs océano-atmosphériques. PhD dissertation, Université de Bourgogne, Dijon, France, 379 p.

Capra a Porto, P., Scicolone, B., 2009. Relationships between rainfall characteristics and ephemeral gully erosion in a cultivated catchment in Sicily (Italy). Soil and Tillage Research 105 (1), 77–87.

Carnicelli, S., Benvenuti, M., Ferrari, G., Sagri, M., 2009. Dynamics and driving factors of late Holocene gullying in the Main Ethiopian Rift (MER). Geomorphology 103 (4), 541-554.

Casali, J., Giraldez, J., 1999. Ephemeral Gully Erosion in Southern Navarra (Spain). Catena 36 (1–2), 65–84.

Chow, V., David, R., Larry, W., 1988. Applied Hydrology. McGraw-Hill, New York, USA, 572 p.

Conway, D., 2000. Some aspects of climate variability in the North East Ethiopian highlands - Wollo and Tigray Sinet. Ethiopian Journal of Science 23 (2), 139– 161.

Corbeels, M., Shiferaw, A., Mitiku Haile, 2000. Farmers' knowledge of soil fertility and local management strategies in Tigray, Ethiopia. Managing Africa's Soils 10, 1-24.

de Mûelenaere, S., Frankl, A., Mitiku Haile, Poesen, J., Deckers, J., Munro, N., Veraverbeke, S., Nyssen, J., 2014. Historical landscape photographs for calibration of landsat landuse/cover in the Northern Ethiopian Highlands. Land Degradation & Development 25 (4), 319–335.

Descheemaeker, K., Nyssen, J., Poesen, J., Raes, D., Haile, M., Muys, B., Deckers, J., 2006. Runoff on slopes with restoring vegetation: A case study from the Tigray highlands, Ethiopia. Journal of Hydrology 331 (1-2), 219-241.

Descheemaeker, K., Poesen, J., Borselli, J., Nyssen, J., Raes, D., Haile, M., Muys, B., Deckers, J., 2008. Runoff curve numbers for steep hillslopes with natural vegetation in semi-arid tropical highlands, northern Ethiopia. Hydrological Processes 22 (20), 4097-4105.

Dotterweich, M., Schmitt, A., Schmidtchen, G., Bork, H., 2003. Quantifying Historical Gully Erosion in Northern Bavaria. Catena 50 (2-4), 135–150.

Dotterweich, M., Rodzik, J., Zgłobicki, W., Schmitt, A., Schmidtchen, G., Bork, H., 2012. High Resolution Gully Erosion and Sedimentation Processes and Land Use Changes Since the Bronze Age and Future Trajectories in the Kazimierz Dolny Area (Nałęczów Plateau SE-Poland). Catena 95, 50–62.

Egboka, B., 1989. Implications of palaeo- and neotectonics in gully erosion-prone areas of southeastern Nigeria. Natural Hazards 3 (3), 219-231.

El-Hames, A., Al-Wagdany, A., 2012. Reconstruction of flood characteristics in urbanized arid regions: case study of the flood of 25 November 2009 in Jeddah, Saudi Arabia. Hydrological Sciences Journal 57 (3), 507–516.

Eriksson, M., Olley, J., Kilham, D., Pietsch, T., Wasson, R., 2006. Aggradation and Incision Since the Very Late Pleistocene in the Naas River, South-Eastern Australia. Geomorphology 81 (1-2), 66–88.

FAO (Food and Agriculture Organization of the United Nations, Statistical division), 2015. Available on: http://faostat.fao.org/site/573/DesktopDefault.aspx?PageID=573#ancor (Accessed on 27/11/2015).

Frankl, A., Nyssen, J., De Dapper, M., Haile, M., Billi, P., Munro, N., Deckers, J., Poesen, J., 2011. Linking long-term gully and river channel dynamics to environmental change using repeat photography (Northern Ethiopia). Geomorphology 129, 238-251.

Frankl, A., Poesen, J., Scholiers, N., Jacob, M., Mitiku Haile, Deckers, J., Nyssen, J., 2013. Factors controlling the morphology and volume (V) – length (L) relations of permanent gullies in the Northern Ethiopian Highlands. Earth Surf. Process. Landforms 38, 1672-1684.

Fryirs, K., Brierley, G., 1998. The character and age structure of valley fills in Upper Wolumla Creek catchment, South Coast, New South Wales, Australia. Earth Surface Processes and Landforms 23, 271-287.

Fuller, I., Marden, M., 2010. Rapid channel response to variability in sediment supply: Cutting and filling of the Tarndale Fan, Waipaoa catchment, New Zealand. Marine Geology 270, 45-54.

Gabris, G., Kertesz, A., Zambo, L., 2003. Land use change and gully formation over the last 200 years in a hilly catchment. Catena 50, 151–164.

Galang, M., Markewitz, D., Morris, L., Bussell, P., 2007. Land use change and gully erosion in the Piedmont region of South Carolina. Journal of Soil and Water Conservation 62 (3), 122 - 129.

Gilley, J., Kottwitz, E., Simanton, J., 1990. Hydraulic characteristics of rills. Trans ASAE 33, 1900-1906.

Gore, A., 1992. The Earth in Balance: Ecology and the Human Spirit. Houghton Mifflin, Boston, 416 p.

Grabham, G., Black R., 1925. Report of the Mission to Lake Tana 1920-1921. Government Press, Cairo, Egypt.

Graf, W., 2002. Fluvial Processes in Dryland Rivers. The Blackburn Press, Caldwell, USA.

Hyatt, J., Gilbert, R., 2000. Lacustrine sedimentary record of human-induced gully erosion and land-use change at Providence Canyon, southwest Georgia, USA. Journal of Paleolimnology 23 (4), 421–438.

Jacob, M., Frankl, A., Mitiku Haile, Zwertvaegher, A., Nyssen, J., 2013. Assessing spatio-temporal rainfall variability in a tropical mountain area (Ethiopia) using NOAAs Rainfall Estimates. International Journal of Remote Sensing 34 (23), 8319-8335.

Jungerius, P., Matundura, J., van de Ancker, J., 2002. Road construction and gully erosion in West Pokot, Kenya. Earth Surface Processes and Landforms 27 (11), 1237–1247.

Kertész, Á., Gergely, J., 2011. Gully erosion in Hungary: review and case study. Procedia - Social and Behavioral Sciences 19, 693–701.

Koop, G., Poirier, D., Justin, L., 2007. Bayesian Econometric Methods. Cambridge University Press, USA.

Kosov, B., Nikolskaya, I., Zorina, Y., 1978. Experimental research on gully formation. In: Experimental Geomorphology 3, Makkaveev N (ed). Moscow University Press: Moscow, 113–140 (in Russian).

Lanckriet, S., Tesfay Araya, Cornelis, W., Verfaillie, E., Poesen, J., Govaerts, B., Bauer, H., Deckers, J., Mitiku Haile, Nyssen, J., 2012. Impact of conservation agriculture on catchment runoff and soil loss under changing climate conditions in May Zeg-zeg (Ethiopia). Journal of Hydrology 475, 336-349.

Lehmkuhl, F., Hilgers, A., Fries, S., Hülle, D., Schlütz, F., Shumilovskikh, L., Felauer, T., Protze, J., 2011. Holocene Geomorphological Processes and Soil Development as Indicator for Environmental Change Around Karakorum, Upper Orkhon Valley (Central Mongolia). Catena 87 (1), 31–44.

Le Roux, J., Sumner, P., 2012. Factors controlling gully development: comparing continuous and discontinuous gullies. Land Degradation and Development 23 (5), 440-449.

Lesschen, J., Kok, K., Verburg, P., Cammeraat, L., 2007. Identification of vulnerable areas for gully erosion under different scenarios of land abandonment in Southeast Spain. Catena 71 (1), 110–121.

Leyland, J., Darby, S., 2009. Effects of Holocene climate and sea-level changes on coastal gully evolution : insights from numerical modeling. Earth Surface Processes and Landforms 34, 1878-1893.

Machado, M., Perez-Gonzalez, A., Benito, G., 1998. Paleoenvironmental changes during the last 4000 yr in Tigray, Northern Ethiopia. Quaternary Research 49, 312– 321.

Makanzu, F., Dewitte, O., Ntombi, M., Moeyersons, J., 2014. Topographic and road control of mega-gullies in Kinshasa (DR Congo). Geomorphology 217, 131–139.

Malik, I., 2008. Dating of small gully formation and establishing erosion rates in old gullies under forest by means of anatomical changes in exposed tree roots (Southern Poland). Geomorphology 93 (3-4), 421–436.

McCann, J., 1997. The Plow and the Forest: Narratives of Deforestation in Ethiopia 1840-1992. Environmental History 2 (2), 138-159.

McCuen, R., 2005. Hydrologic Analysis and Design, 3rd Ed. Pearson Prentice Hall, Upper Saddle River, NJ, USA.

Meire, E., Frankl, A., De Wulf, A., Mitiku Haile, Deckers, J., Nyssen, J., 2012. Land use and cover dynamics in Africa since the nineteenth century: warped terrestrial photographs of North Ethiopia. Reg Environ Change 13, 717–737.

Merla, G., Abbate, E., Azzaroli, A., Bruni, P., Canuti, P., Fazzuoli, M., Sagri, M., Tacconi, P., 1979. A Geological Map of Ethiopia and Somalia. 1:2000.000; and Comment. University of Florence, Firenze, Italy.

Mhangara, P., Kakembo, V., Kyoung Jae, L., 2011. Soil Erosion Risk Assessment of the Keiskamma Catchment, South Africa, Using GIS and Remote Sensing. Environmental Earth Sciences 65 (7), 2087–2102.

Moges, A., Holden, N., 2009. Land Cover Change and Gully Development Between 1965 and 2000 in Umbulo Catchment, Ethiopia. Mountain Research and Development 29 (3), 265-276.

Moulaert, L., 2012. The use of subsurface plastic dams (geomembrane) for stabilizing gullies in Vertisol areas – May Bati (Ethiopia). Msc Thesis, Ghent University.

Nachtergaele, J., Poesen, J., Sidorchuk, A., Torri, D., 2002. Prediction of concentrated flow width in ephemeral gully channels. Hydrological Processes 16, 1935-1953.

Nagasaka, A., Yanai, H., Sato, S., Hasegawa, S., 2005. Soil Erosion and Gully Growth Associated with Cultivation in Southwestern Hokkaido, Japan. Ecological Engineering 24 (5), 503–508.

Naudts, J., 2002. Les Hautes Terres de Tembien, Tigré, Ethiopie; Résistance et limites d'une ancienne civilization agraire; Conséquences sur la degradation des terres. Mémoire présenté en vue de l'obtention du Diplôme d'Agronomie Tropicale; CNEARC Montpellier.

Nyssen, J., Poesen, J., Moeyersons, J., Luyten, E., Veyret-Picot, M., Deckers, J., Haile, M., Govers, G., 2002. Impact of road building on gully erosion risk: a case study from the Northern Ethiopian Highlands. Earth Surf Process Landforms 27, 1267–1283.

Nyssen, J., Poesen, J., Moeyersons, J., Deckers, J., Haile, M., Lang, A., 2004. Human impact on the environment in the Ethiopian and Eritrean highlands – a state of the art. Earth Sci Rev 64, 273–320.

Nyssen, J., Poesen, J., Veyret-Picot, M., Moeyersons, J., Haile, M., Deckers, J., Dewit, J., Naudts, J., Teka, K., Govers, G., 2006. Assessment of gully erosion rates through interviews and measurements: a case study from northern Ethiopia. Earth Surf Process Landforms 31, 167–185.

Nyssen, J., Descheemaeker, K., Nigussie Haregeweyn, Mitiku Haile, Deckers, J., Poesen, J., 2007. Lessons learnt from 10 years research on soil erosion and soil and water conservation in Tigray. Tigray Livelihood Papers 7, 53 p.

Nyssen, J., Haile, M., Naudts, J., Munro, N., Poesen, J., Moeyersons, J., Frankl, A., Deckers, J., Pankhurst, R., 2009. Desertification? Northern Ethiopia re-photographed after 140 years. Sci Total Environ 407, 2749–2755.

Nyssen, J., Clymans, W., Descheemaeker, K., Poesen, J., Vandecasteele, I., Vanmaercke, M., Mitiku Haile, Haregeweyn Nigussie, Moeyersons, J., Martens, K., Amanuel Zenebe, Van Camp, M., Gebreyohannes Tesfamichael, Deckers, J., Walraevens, K., 2010. Impact of soil and water conservation on catchment hydrological response – a case in northern Ethiopia. Hydrol Process 24, 1880–1895.

Nyssen, J., Frankl, A., Mitiku Haile, Hurni, H., Descheemaeker, K., Crummey, D., Ritler, A., Portner, B., Nievergelt, B., Moeyersons, J., Munro, R., Deckers, J., Billi, P., Poesen, J., 2014. Environmental conditions and human drivers for changes to north Ethiopian mountain landscapes over 145 years. Science of the Total Environment 485-486 (1), 164-179.

Parkner, T., Page, M., Marutani, T., Trustrum, N., 2006. Development and controlling factors of gullies and gully complexes (East Coast New Zealand). Earth Surface Processes and Landforms 31 (2), 187–199.

Parry, J., 2003. Tree choppers become tree planters. Appropriate Technology 30 (4), 38-39.

Perroy, R., Bookhagen, B., Chadwick, O., Howarth, J., 2012. Holocene and Anthropocene Landscape Change: Arroyo Formation on Santa Cruz Island, California. Annals of the Association of American Geographers 102 (6), 1229-1250.

Piccarreta, M., Capolongo, D., Miccoli, M., 2012. Deep gullies entrenchment in valley fills during the Late Holocene in the Basento basin, Basilicata (southern Italy). Geomorphologie – Relief Processus Environment 2, 239-248.

Robinson, I., MacKay, R., Afwerki Solomon, Yragelem Afwerki, 1995. A Review of the Agricultural Rehabilitation Programmes of Eritrea Bangor: Centre for Arid Zone Studies. University of Wales, Bangor, Wales, UK.

Samani, N., Aliakbar Hassan, Ahmadi Aliasghar, Mohammadi Jamal, Ghoddousi Salajegheh, Boggs, G., Razieh, P., 2009. Factors Controlling Gully Advancement and Models Evaluation (Hableh Rood Basin Iran). Water Resources Management 24 (8), 1531–1549.

Saxton, N., Olley, J., Smith, S., Ward, D., Rose, C., 2012. Gully Erosion in Sub-Tropical South-East Queensland, Australia. Geomorphology 173, 80–87.

Schumm, S., 2005. River variability & complexity. Cambridge University Press, Cambridge, UK.

Schütt, B., Frechen, M., Hoelzmann, P., Fritzenwenger, G., 2011. Late Quaternary Landscape Evolution in a Small Catchment on the Chinese Loess Plateau. Quaternary International 234 (1-2), 159–166.

SCS, 2004. Hydrology National Engineering Handbook, Supplement A, Section 4. Soil Conservation Service, USDA, Washington DC, USA, 79 p.

Segers, K., Dessein, J., Develtere, P., Hagberg, S., Haylemariam Girmay, Mitiku Haile, Deckers, J., 2010. The Role of Farmers and Informal Institutions in Microcredit Programs in Tigray, Northern Ethiopia. Perspectives on Global Development and Technology 9 (3-4), 520-544.

Sidorchuk, A., 1999. Dynamic and static models of gully erosion. Catena 37 (3), 401-414.

Smit, H., Tefera, G., 2011. Understanding land degradation on a hill slope of the Choke Mountains in Ethiopia. Building resilience to Climate Change in the Blue Nile highlands, Addis Ababa, Ethiopia, 18 p.

Solleiro-Rebolledo, E., Sycheva, S., Sedov, S., McClung de Tapia, E., Rivera-Uria, Y., Salcido-Berkovich, C., Kuznetsova, A., 2011. Fluvial processes and paleopedogenesis in the Teotihuacan Valley México: Responses to late Quaternary environmental changes. Quaternary International 233 (1), 40–52.

Ståhl, M., 1974. Ethiopia: political contradictions in agricultural development. Rabén & Sjögren, Stockholm, 186 p.

Stankoviansky, M., 2003. Historical evolution of permanent gullies in the Myjava Hill Land, Slovakia. Catena 51, 223-239.

Stolz, C., 2011. Spatiotemporal budgeting of soil erosion in the abandoned fields area of the Rahnstatter Hof, near Michelbach (Taunus Mts Western Germany). Erdkunde 65 (4), 355-370.

Svoray, T., Markovitch, H., 2009. Catchment scale analysis of the effect of topography tillage direction and unpaved roads on ephemeral gully incision. Earth Surface Processes and Landforms 34 (14), 1970–1984.

Tebebu, T., Abiy, Z., Zegeye, D., Dahlke, H., Easton, Z., Tilahun, S., Steenhuis, T., 2010. Surface and subsurface flow effect on permanent gully formation and upland erosion near Lake Tana, in the northern highlands of Ethiopia. Hydrology and Earth System Sciences 14 (11), 2207–2217.

Teka, D., Van Wesemael, B., Vanacker, V., Hallet, V., 2013. Hydrological Response of Semi-arid Degraded Catchments in Tigray, Northern Ethiopia. EGU General Assembly 2013, 7-12 April, 2013, Vienna, Austria, 7187-1.

Tesfaalem A, Frankl A, Mitiku Haile, Nyssen J., 2015. Catchment rehabilitation and hydro-geomorphic characteristics of mountain streams in the western Rift Valley escarpment of Northern Ethiopia. Land Degradation and Development, online early view. DOI: 10.1002/ldr.2267.

Thomas, J., Iverson, N., Burkest, M., Kramer, L., 2004. Long Term Growth of a valley bottom gully - Western Iowa. Earth Surface Processes and Landforms 2, 995 – 1009.

Titmarsh, G., Cordery, I., Pilgrim, D., 1995. Calibration procedures for the rational and USSCS design flood methods. Journal of Hydraulic Engineering 121, 61-70.

Torri, D., Poesen, J., Borselli, L., Knapen, A., 2006. Channel width–flow discharge relationships for rills and gullies. Geomorphology 76, 273–279.

Vandekerckhove, L., Poesen, J., Wijdenes, D., Nachtergaele, J., Kosmas, C., Roxo, M., De Lisboa, N., Superior, E., De Bragana, A., 2000. Thresholds for gully initiation and sedimentation in Mediterranean Europe. Earth Surface Processes and Landforms 25, 1201-1220.

Van de Wauw, J., Baert, G., Moeyersons, J., Nyssen, J., De Geyndt, K., Nurhussein Taha, Amanuel Zenebe, Poesen, J., Deckers, J., 2008. Soil–landscape relationships in the basalt-dominated highlands of Tigray, Ethiopia. Catena 75 (1), 117-127.

Vanmaercke, M., Poesen, J., Verstraeten, G., Maetens, W., de Vente, J., 2011. Sediment yield as a desertification risk indicator. Science of the Total Environment 409, 1715-1725.

Vanwalleghem, T., Van Den Eeckhaut, M., Poesen, J., Deckers, J., Nachtergaele, J., Van Oost, K., Slenters, C., 2003. Characteristics and controlling factors of old gullies under forest in a temperate humid climate: a case study from the Meerdaal Forest (Central Belgium). Geomorphology 56 (1-2), 15–29.

Vanwalleghem, T., Bork, H., Poesen, J., Schmidtchen, G., Dotterweich, M., Nachtergaele, J., Bork, H., Deckers, J., Brüsch, B., Bungeneers, J., De Bie, M., 2005a. Rapid development and infilling of a buried gully under cropland, central Belgium. Catena 63 (2–3), 221-243.

Vanwalleghem, T., Poesen, J., Van Den Eeckhaut, M., Nachtergaele, J., Deckers, J., 2005b. Reconstructing rainfall and land-use conditions leading to the development of old gullies. The Holocene 15, 378-386.

Vanwalleghem, T., Bork, H., Poesen, J., Dotterweich, M., Schmidtchen, G., Deckers, J., Scheers, S., Martens, M., 2006. Prehistoric and Roman gullying in the European loess belt: a case study from central Belgium. The Holocene 16 (3), 393-401.

Vanwalleghem, T., Poesen, J., Vitse, I., Bork, H., Dotterweich, M., Schmidtchen, G., Deckers, J., Lang, A., Mauz, B., 2007. Origin and evolution of closed depressions in central Belgium, European loess belt. Earth Surface Processes and Landforms 32, 574-586.

Vanwalleghem, T., Van Den Eeckhaut, M., Poesen, J., Govers, G., Deckers, J., 2008. Spatial analysis of factors controlling the presence of closed depressions and gullies under forest: Application of rare event logistic regression. Geomorphology 95 (3-4), 504–517.

Viessman, W., Knapp, J., Lewis, G., 1989. Introduction to hydrology. Harper and Row, New York, USA.

Virgo, K., Munro R., 1978. Soil and erosion features of the Central Plateau region of Tigrai, Ethiopia. Geoderma 20, 131–157.

Vogt, J., 1953. Erosion des sols et techniques de culture en climat tempéré maritime de transition (France et Allemagne). Revue de Geomorphologie Dynamique 4, 157-183.

Wanielista, M., Kersten, R., Eaglin, R., 1997. Hydrology: Water Quantity and Quality Control. John Wiley & Sons, NJ, USA.

Wells, N., Andriamihaja, B., 1993. The initiation and growth of gullies in Madagascar: are humans to blame? Geomorphology 8 (1), 1-46.

Wijdenes, D., Poesen, J., Vandekerckhove, L., Ghesquiere, M., 2000. Spatial distribution of gully head activity and sediment supply along an ephemeral channel in a Mediterranean environment. Catena 39 (3), 147–167.

Zaimes, G., Schultz, R., 2012. Assessing Riparian Conservation Land Management Practice Impacts on Gully Erosion in Iowa. Environmental Management 49 (5), 1009–1021.

Zucca, C., Canu, A., Della Peruta, R., 2006. Effects of land use and landscape on spatial distribution and morphological features of gullies in an agropastoral area in Sardinia (Italy). Catena 68 (2-3), 87–95.

Micromeritics, 2014. Overview SediGraph III Plus. http://www.micromeritics.com/ (accessed on 14/05/2014)

Part II

Chapter 5 Floodplain dynamics on a Late-Holocene timescale: supportive luminescence evidence from May Tsimble

This chapter is modified from:

Lanckriet, S., Schwenninger, J. L., Frankl, A., Nyssen, J., 2015. The Late-Holocene geomorphic history of the Ethiopian Highlands: supportive evidence from May Tsimble. Catena 135, 290-303.

Abstract

Alluvial sedimentary archives contain important geochronological and paleo-environmental information on past geomorphic processes in semi-arid regions. For North Ethiopia in particular, flashflood sediments transported by ephemeral streams can provide interesting chronological information on Late-Holocene land degradation, whether or not impacted by climate or land cover changes upstream. Here we compare geomorphic records with independent regional records of rainfall regime changes, land use/cover changes and macrohistory, supported by optically stimulated luminescence (OSL) dates for fluvial activity at a sediment sequence in the May Tsimble catchment, in the Northeastern Highlands. Based on all datasets, we identified different degradation phases over the past 4000 years, broadly between 1550 and 600 BCE, and after 400 CE. At least one prior incision phase is responsible for the stabilized gullies that can be seen on photographs around 1900 and another incision phase is dated to the late 20th century.

5.1 Introduction

In drylands worldwide, land degradation and desertification put severe pressure on food production and food security (Goudie, 2013). Deciphering the Late-Holocene history of land degradation forms an important aspect of a full understanding of the relative impacts of its (long-term) driving factors, including climate, land cover changes and sociopolitical impacts. River sediment yield and cycles of stream incision and deposition can provide suitable proxies for the intensity of land degradation (Avni, 2006; Vanmaercke et al., 2011, 2014), since erosion by ephemeral streams in drylands constitutes between 50 to 80% of all sediment production (Poesen et al., 2002). These sediments get accumulated or aggraded in alluvial floodplains, stored as valuable archives on Late-Holocene land degradation (Broothaerts et al., 2013).

We turn to the North Ethiopian Highlands, where severe gullying is indeed a major cause of land degradation (Frankl et al., 2013; Nyssen et al., 2004). Nyssen et al. (2009) showed that intense degradation occurred at least since the late 19th century. As explained before, the oldest gully activity phase identifiable using repeat photography was a phase of relatively stable gullies that was evidenced on historical photographs of 1868-1936, lasting until the 1960s (Frankl et al., 2011, 2013). Hence, at a regional scale, Frankl et al. (2011) have identified one cut-and-fill cycle since the second half of the 19th century, and identified an earlier one based on the interpretation of historical photographs. Although at least one cycle had existed before 1868, the status of the gully networks that developed (and stabilized) before 1868 is unclear, since other hydrogeomorphic information on gullies before this period is lacking and no reliable direct sediment dating is available yet. A thorough chronological study on older cycles was never performed. It is hitherto not known if there is a continuous acceleration of geomorphic processes at longer time scales in the North Ethiopian Highlands. However, it is likely that the current cycle is the last of a series of cut-and-fill cycles, since driving factors were equally active during the previous centuries (Chapter 4).

The sediments deposited by flashfloods in aggraded paleo-channels or preserved in terraces can also provide information on the driving factors of ephemeral stream systems. A literature review (Chapter 4) shows that vegetation cover change is a dominant driving

factor of gullying named in most of the studies worldwide. Indeed, in the Ethiopian Highlands a decreasing vegetation cover upstream leads to intensified stream erosion and increased sediment supply downstream (aggradation) (Frankl et al., 2011). Simultaneously, Carnicelli et al. (2009) discuss the possibility that in the Ethiopian Highlands increased runoff under a wetter climate leads to overall gully incision; while decreased runoff and sediment transport capacity under a dryer climate would increase the sediment supply downstream (aggradation). This is in line with the findings by Pelletier et al. (2011), who indicate that because of decreased runoff volumes, a drier climate is less capable of facilitating stream incision.

Obtaining reliable chronologies of stream activity is a key element for the acquisition of accurate environmental information on early land degradation intensities. This can be a particularly difficult task in drylands such as North Ethiopia, partly because ephemeral stream sediments are often not containing convenient organic matter to use for radiocarbon dating. Exceptionally, Machado et al. (1998) obtained an alluvial chronology for three sites in North Ethiopia using radiocarbon dating on buried paleosols. Optically stimulated luminescence (OSL) dating of flash flood sediments can be a valuable alternative, although it can suffer from insufficient or heterogeneous bleaching (Bourke et al., 2003; Arnold et al., 2007). OSL dating of relatively young sediments is also difficult given a low signal-to-noise ratio and processes such as thermic transfer (Costas et al., 2012; Eipert, 2004). A literature review regarding luminescence dating of ephemeral stream deposits all over the world (Table 5.1) shows that it is often possible to extract OSL ages from these flashflood sediments, although bleaching properties can strongly impact the level of accuracy. The review shows that most studies focusing on ephemeral stream sediments are dealing with heterogeneous bleaching properties (13 out of 20 studies). Solutions to this problem are given by residual age calculation, analysis of single grains or small aliquots and/or by applying the Minimum Age Model (MAM) of Galbraith et al. (1999) (7 out of the 13 studies). In this model, the (log) equivalent doses D_e form a random sample from a mixed truncated normal distribution. For (young) fluvial sediment samples, (un)logged MAM-3 or MAM-4 models are often preferred over other equivalent dose decision models, such as the Central Age Model, the L-5% model or the Finite Mixture Model (Bailey and Arnold, 2006). Some studies report bleaching properties dependent on grain size, with the coarsest quartz grains (e.g. 212-250 µm) yielding the lowest values of D_e (Wallinga, 2002; Alexanderson,

2007). Others employ a residual age calculation from a modern sample to empirically determine the age-overestimation due to poor bleaching (Table 5.1), as it is a very simple and straightforward method.

Table 5.1 Luminescence dating of ephemeral stream deposits all over the world. Only relevant papers (empirical research on Late Pleistocene or Holocene stream deposits) were incorporated in the review. Note that OD = Over Dispersion; IRSL = Infra-Red Stimulated Luminescence; and MAM = Minimum Age Model.

Cont	Country	Location	Sediments	Clim.	Is OSL suitable?	Solution	Age	OSL lab	Source
AM	Mexico	Oaxaca	Gully fluvial sands	Aw	No: paucity of quartz grains; incomplete bleaching	x	3.5 ka	Athens, USA	Leigh et al. (2013)
	USA	Southern Colorado	Arroyo	BSk	Partly: hetero-geneously bleaching	Single-grain model, single aliquot model	20 ka – 0 ka	Oxford, UK	Arnold et al. (2007)
		Kanab Creek (Utah)	Arroyo sediments	Dsa	Incomplete bleaching if OD > 15 % for small aliquots or OD > 25 % for single-grains. Note that best OSL properties come from downstream reaches, ripple crossbeds or thin plane beds)	MAM-3 for small aliquots and MAM-4 for single-grain	6.7 – 3.5 ka	Utah State University Laboratory	Summa-Nelson & Rittenour (2012)
		Buckskin Wash (Utah)	Arroyo sediments and canyon paleofloods	Dsa	Incomplete bleaching	Single-grain analysis and MAM model	1.1 – 2.8 ka	Utah State University Laboratory	Harvey et al. (2011)
		California and Arizona	Arroyo channel sediments, infill and terrace	Csb and BSh	Incomplete bleaching	Non-logarithmic (unlogged) versions of CAM and MAM-3 or MAM-4 models	Modern and young samples (<350 years)	N/A	Arnold et al. (2009)
AF	Zambia	Chipata	Gully section	Aw, Cfa, Cwa	Yes	x	60ka - Holocene	Roskilde, Denmark	Thomas et al. (2001)
	Ethiopia	May Tsimble	Gully terraces	BSh	Yes	Residual age of modern sample	4 ka - now	Oxford (UK)	This study
	Tanzania	Irangi Hills	Gully fan	BSh	Heterogeneous bleaching	Minimum age model	900 and 600-300 BP	N/A	Eriksson et al. (2000)
	South Africa	Cape Point	Alluvial/colluvial fan	Csb	Yes	x	83 - 32 ka	Sheffield, UK	Shaw et al. (2001)
		Modder River	Alluvial gully (donga) infill	BSk	Incomplete bleaching	Minimum age model	0.39 ka	N/A	Tooth et al. (2013)
		Schoons pruit, Mooi, Klip	Floodplain deposits	Cwb	Incomplete bleaching (scatter in D_e or overdispersion OD > 20 %)	Finite Mixture Model (or Central Age Model if OD < 20%	0.06 – 21.7 ka	Aberystwyth Laboratory	Keen-Zebert et al. (2013)
		KwaZulu-Natal (N)	Colluvial gully (donga) infill	Cwb	IRSL (K-feldspar)	No	Late Pleistocene	N/A	Botha et al. (1994)
AS	Israel	Negev Highland	Fluvio-loess (Pleistocene loess mobilized during flashfloods)	BW	Large errors due to residual OSL signal (incomplete bleaching)	x	45 ka – 0.7 ka	N/A	Avni et al. (2012)
			Fluvio-loess / alluvium in ephemeral streams	BW	Yes for older deposits	Residual age of modern sample	70 ka to 0 ka	N/A	Avni et al. (2006)
	Mongolia	Upper Orkhon	Gully sediments	Dwb	Anomalous fading for K-feldspar dating; poor bleaching	Fading correction with g-value; Finite Mixture Model	0.7 – 15 ka	N/A	Lehmkuhl et al. (2011)
	Tibet	Tsangpo Valley	Gully terrace sediments	BSk	Partial bleaching if skew > $2\sigma_e$	Minimum Age Model	8.8 – 0.6 ka	N/A	Pelletier et al. (2011)
	China	Chifeng (Inner Mongolia)	Gully fan sediments	Dwa	Partial bleaching; coarse-grains are better bleached than fine-grains	Only using well-bleached samples	MIS 4-2	N/A	Avni et al. (2010)
		Gansu	Fluvially reworked loess in accumulation terraces	BWk	Yes (low scatter in D_e)	x	22.5 – 17.7 ka	N/A	Schütt et al. (2011)
		Jinsha River	Debris-flow	Cwa, Cwb	Yes	x	11 ka-4 ka	Bejing, China	Chen et al. (2008)
	Borneo	Western Kalimantan	Gully fill	Af	Scatter between aliquots (due to measuring procedure or incomplete bleaching	No	6-4 ka and 480 BP	UK	Teeuw et al. (1999)
EU	Germany	Franken	Gully sediments	Dfb	Partly: heterogeneous bleaching	Using (i) large quartz grains, (ii) Minimum Age Model, and (iii) single-grain analysis	Late Holocene	Liverpool, UK	Lang & Mauz (2006)

The aim of this study is to assess the Late-Holocene environmental evolution of the North Ethiopian Highlands using alluvial sedimentary archives. This can be done (i) by comparing geomorphic chronologies with other paleo environmental records from the region; and (ii) by bringing supportive evidence from dating of aggradation in a suitable catchment.

5.2 Methods

5.2.1 Description of the study area and reconnaissance survey

The North Ethiopian Highlands drain towards the African Rift and the Tekeze-Nile rivers. The region is composed of Precambrian metavolcanics and Mesozoic sedimentary rocks, which include (from lower to upper) Adigrat sandstone, Antalo limestone, Agula shales, and Amba Aradam sandstone. These sedimentary rocks were intruded by younger (Cenozoic) dolerite dykes and sills and on top Tertiary basalts are found (Merla et al., 1979). Except for Enticho sandstone and the Adaga Arbi tillites, Paleozoic rocks are rare (Bussert and Schrank, 2007).

As it is wise to start with a mineralogical reconnaissance survey before turning to the luminescence procedures (Duller, 2008), several sites where observations had been done on the presence of old debris cones or (filled) paleo channels (Frankl et al., 2013) were visited during December 2012. Samples were taken at approximately 0.5 m depth in profile pits at interesting sediment accumulations in the main gullies, identified during walks around their catchments. Mineralogy of the sandy fraction (250-106 μm) was studied by microscope (Table 5.2). In the catchments of Nebelet and May Tsimble, in the uplands of the Rift Valley escarpment, sufficient quartz was present in the sediment samples (Table 5.2). As the stream system of May Tsimble is much more extensive compared to that of Nebelet, another fieldwork focused on the May Tsimble catchment. Downstream of the large upper stream network in May Tsimble (Figure 5.1), an interesting sequence of terraces was identified in September 2013.

Table 5.2 Geology and mineralogy of the four catchments investigated during the reconnaissance survey.

Location	Sampled location (WGS84)	Geology of the catchment	Mineralogy of the sandy fraction (250-106µm) in the sampled fill sediments
May Mekden	13.57834 °N, 39.57178 °E	Agula shales and Antalo limestone	90 % micritic limestone fragments; 10 % quartz; some zircon, sparitic calcite grains
Nebelet	14.12790 °N, 39.26888 °E	Enticho sandstone cliffs with underlying Precambrian metavolcanics	Nearly exclusively quartz; some opaque grains; mudstone fragments; possible plagioclase and microcline
May Tsimble	13.40372 °N, 39.67131°E	Antalo limestone with dolerite and sandstone near the water divide	Nearly exclusively quartz; some plagioclase and microcline; opaque grains
Ashenge	12.56571 °N, 39.51157 °E	Tertiary basalts (Ashangi group) and consolidated volcanic ashes	70 % hornblende; 25 % opaque grains; 5 % plagioclase; some quartz, zircon, biotite, muscovite

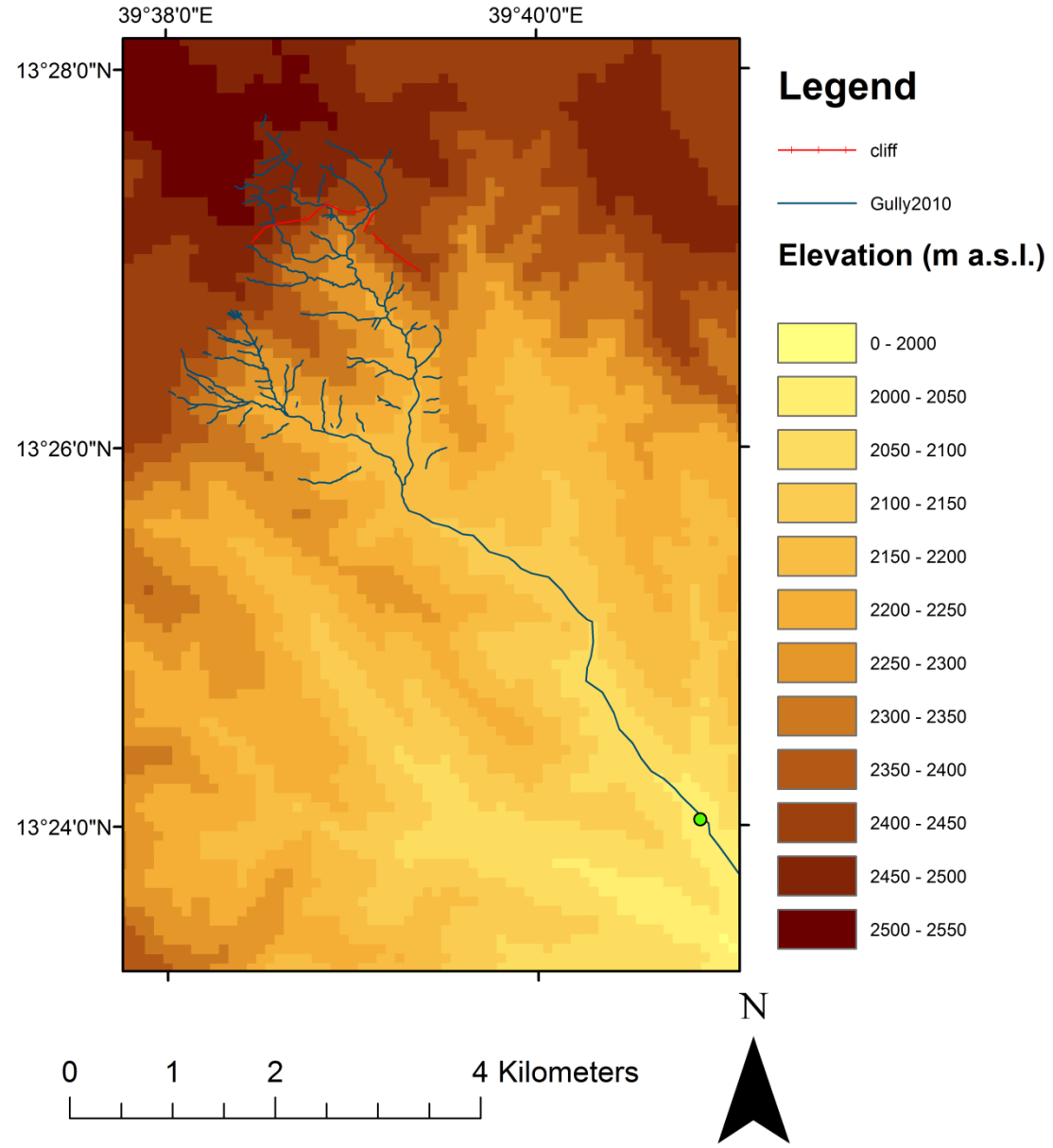

Figure 5.1 Upper stream network in the May Tsimble catchment, upstream of our sampling site (indicated with green dot). For general localization of the catchment, see Figure 5.5 (location C).

5.2.2 Paleo-environmental datasets

Available alluvial records were compared with independent paleo-environmental datasets from the nearby region. Two high-quality records of rainfall regime changes have been derived from stable oxygen isotope and diatom analysis from Lake Ashenge (focus on BCE) (Marshall et al., 2009) and from Lake Hayk (focus on CE) (Lamb et al., 2007) (see Figure 5.5 for location of Lake Hayk). High-quality information of land cover changes was derived from pollen analysis of cores from Lake Hayk (Darbyshire et al., 2003) and Lake Ashenge (Marshall et al., 2009). Macrohistory – the long-term patterns of political, economic and social change (Collins, 1999) – was derived from groundwork studies on the pre-Axumite period (Phillipson, 2009), on the Axumite period (Phillipson, 2012) and on the post-Axumite dynasties (Pankhurst, 1990; Marcus, 2002). All reported dates are expressed in (B)CE, including the calibrated radiocarbon dates derived from literature.

5.2.3 Complementary OSL evidence from May Tsimble

The May Tsimble catchment comprises a large ephemeral stream system about 20 km to the southeast of Mekelle, the capital city of the Tigray region in northern Ethiopia. Rainfall in the catchment likely ranges between 400-800 mm because of regional rainfall gradients and high relief. The sampling site (at around 2000 m a.s.l.) is located 6-8 km from the source of the stream, which is located in mountains rising to 2550 m a.s.l. Very recent flood deposits were observed at a height of 1.70 m above the channel floor, indicating the occurrence of individual flashflood events. The main stream is confined to a single ~3-m deep channel, with pool-riffle sequences cut into the alluvium until it reaches the underlying Antalo limestone bedrock. The channel width is about 9 m near the village of Lahama. The identified sequence of terraces is located at the left bank of the May Tsimble stream, along an abandoned palaeochannel next to the active channel (Figure 5.2). Topographic heights and positions of all terraces were recorded (Figure 5.2, Table 5.3). In line with the method developed by Nyssen et al. (2006), we performed semi-structured interviews with 6 farmers, focusing on the stream evolution and the timing and processes of the changes in morphology. Samples for OSL dating were extracted from the terrace walls and in two profile pits (Figure 5.2), in line with the recommendations of Duller (2008). For instance, we sampled at sandy lenses, used opaque tubes and wrapped them in thick black plastic. The sampled alluvial terraces are, similar to the contemporary bedload, mainly consisting of

large sandy lenses with pebbles of dolerite, sandstone and limestone in-between. The sampling locations were chosen to include all alluvial terraces, in order to investigate the possibility of a complex terrace genesis instead of floodplain aggradation.

In order to estimate residual ages, one subrecent sample was collected from a sandy alluvium recently deposited just upstream of a new check dam built in 2010, 0.5 km upstream of the studied cross-section (Figure 5.3).

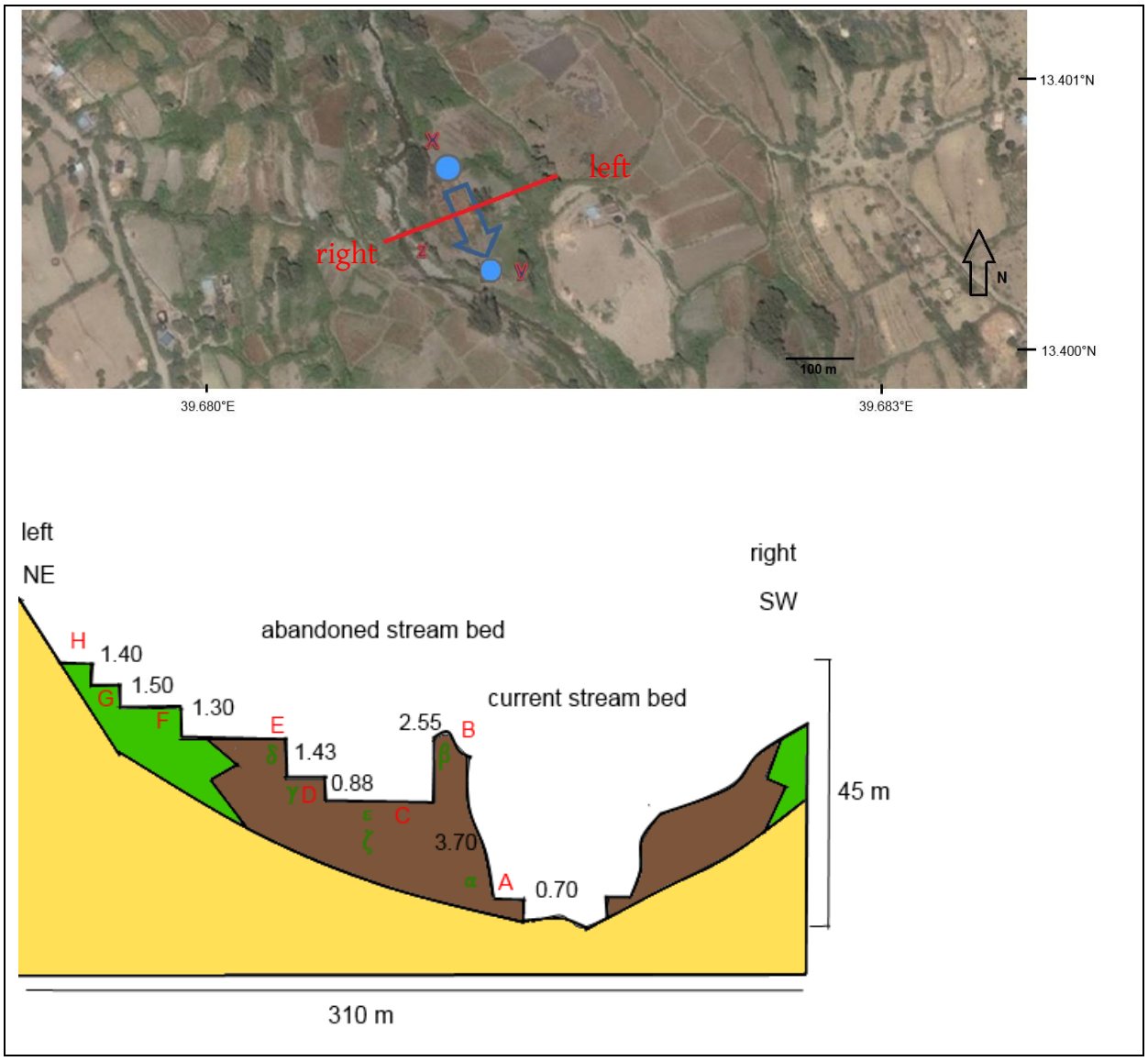

Figure 5.2 Location of the study site from a BingMaps® satellite image with blue dots indicating the start and end of the paleo channel and the blue arrow indicating the paleo stream direction (up); and schematic profile of the study site with sequence of terraces (below) as indicated on the satellite image by red line, including relative heights (in m), coded terraces or locations (in red Latin letters) and OSL sample field codes (in green Greek letters). The Antalo limestone bedrock is indicated in yellow, colluvium in green and alluvium is indicated in brown. See Table 5.3 for the coordinates.

Table 5.3 Coordinates (WGS 84) and codes of all locations and terraces. Error of the GPS measurements is 3 to 5 m. See Figure 5.2 for localization in the schematic profile.

Location	Code	Latitude (°N)	Longitude (°E)
Modern sample	M	13.40650°	39.67477°
Inlet of the paleochannel	X	13.40114°	39.68072°
Outlet of the paleochannel	Y	13.40050°	39.68125°
Waterfall	Z	13.40020°	39.68089°
Lowest terrace	A	13.40081°	39.68080°
Terrace	B	13.40069°	39.68092°
Profile pit	C	13.40107°	39.68092°
Subterrace pit	D	13.40051°	39.68107°
Terrace	E	13.40111°	39.68096°
Terrace (daget)	F	13.40116°	39.68175°
Terrace (daget)	G	13.40122°	39.68183°
Terrace (daget)	H	13.40100°	39.68242°

Figure 5.3 Sampling site (indicated with red arrow) and sampling of the modern sample (M), just upstream of a newly built check dam in the May Tsimble channel.

Measurements were performed at the Oxford University Luminescence Dating Laboratory on sand-sized quartz (180-255µm) extracted from the seven samples (X6431-X6437) using standard preparation techniques including wet sieving, HCl (10%) treatment to remove

carbonates, HF treatment (48%) to dissolve feldspathic minerals and heavy mineral separation with sodium polytungstate. All samples were measured in automated Risø luminescence readers (Bøtter-Jensen, 1988, 1997, 2000) using a SAR post-IR blue OSL measurement protocol (Murray and Wintle, 2000; Banerjee et al., 2001; Wintle and Murray, 2006). Dose rate calculations are based on the concentration of radioactive elements (potassium, thorium and uranium) within the samples and were derived from elemental analysis by Induced Coupled Plasma Mass Spectroscopy / Atomic Emission Spectroscopy using a fusion sample preparation technique. The final OSL age estimates include an additional 2% systematic error to account for uncertainties in source calibration. Dose rate calculations are based on Aitken (1985). These incorporated beta attenuation factors (Mejdahl, 1979), dose rate conversion factors (Adamiec and Aitken, 1998) and an absorption coefficient for the water content (Zimmerman, 1971). The contribution of cosmic radiation to the total dose rate was calculated as a function of latitude, altitude, burial depth and average over-burden density based on data by Prescott and Hutton (1994). The OSL dates were then corrected with the average residual age of the modern samples and confronted with the vertical floodplain aggradation, based on the relative vertical position of the samples above the Antalo limestone bedrock (in cm).

5.3 Results

5.3.1 May Tsimble alluvial record

OSL age estimates (Table 5.4) for burial by other sediments are based on the concentration of radioisotopes within the sample and include corrections for cosmic radiation and moisture content (Appendix A1; Section 5.7). Both the recent sample and the sample from the upper right terrace correspond to modern ages, which is consistent with the statements made by the interviewees. The other deposition dates range from 1846 ± 950 BCE to 1504 ± 290 CE. Despite the considerable errors due to the low sensitivity of the quartz, the dated sequence is consistent with the relative vertical position above the Antalo limestone bedrock. The dates point to a relatively simple genesis by floodplain aggradation instead of a more complex terrace genesis. One deposition date, sampled from the bottom of a profile pit, yielded a date of 22,976 ± 4760 BCE but this age estimate was strongly dependent upon

the influence on the mean D_e estimate by a single outlier measurement. According to Wallinga (2002), the accuracy of OSL ages older than about 13 ka for such fluvial deposits can be dubious given the strong possibility of insufficient resetting at deposition and/or the inclusion of reworked older mineral grains having retained a residual signal (Duller, 2008). Because of this inconsistency this Pleistocene date was not considered.

Table 5.4 OSL data and aggradation depths (above the Antalo limestone base).

Description	Lab Code	Burial Depth (cm)	Water Content (%)	Paleodose (Gy)	±	Dose Rate (Gy/ka)	±	OSL age (years before 2014)	Age after correction	±	Aggradation depth (above Antalo limestone base) (cm)
Residual age	X6431 (M)	34	13.3	0.48	0.2	1.22	0.07	<400	2010 CE		
Right upper terrace	X6432 (β)	150	13.6	0.27	0.24	1.45	0.07	<200	~ 1960 CE		474
Left upper terrace	X6433 (δ)	99	15.4	0.62	0.35	1.22	0.06	510	1804 CE	290	502
Top of the profile pit	X6435 (ε)	28	17.8	2.34	0.2	1.22	0.07	1920	394 CE	210	342
Left lower subterrace pit	X6434 (γ)	132	11.0	3.63	0.26	1.22	0.06	2970	656 BCE	270	326
Bottom of the aggradation	X6437 (α)	370	19.4	3.21	0.78	0.83	0.04	3860	1546 BCE	950	21
Bottom of the profile pit	X6436 (ζ)	120	14.5	27.27	4.98	1.09	0.05	24990	22676 BCE	4760	250

We corrected the luminescence ages for an average residual age of 300 years (200-400 years for samples X6432 and X6431), an order of magnitude that is in line with findings by Porat et al. (2001). By confronting the dates with their vertical position above the bedrock, we calculated average floodplain aggradation rates. We identify two broad periods of aggradation (Figure 5.4). Aggradation is dated around ~1550 BCE and ~650 BCE, followed by a period of low aggradation rates from ~ 650 BCE till 400 CE. Another phase of high aggradation rates starts around ~ 400 CE.

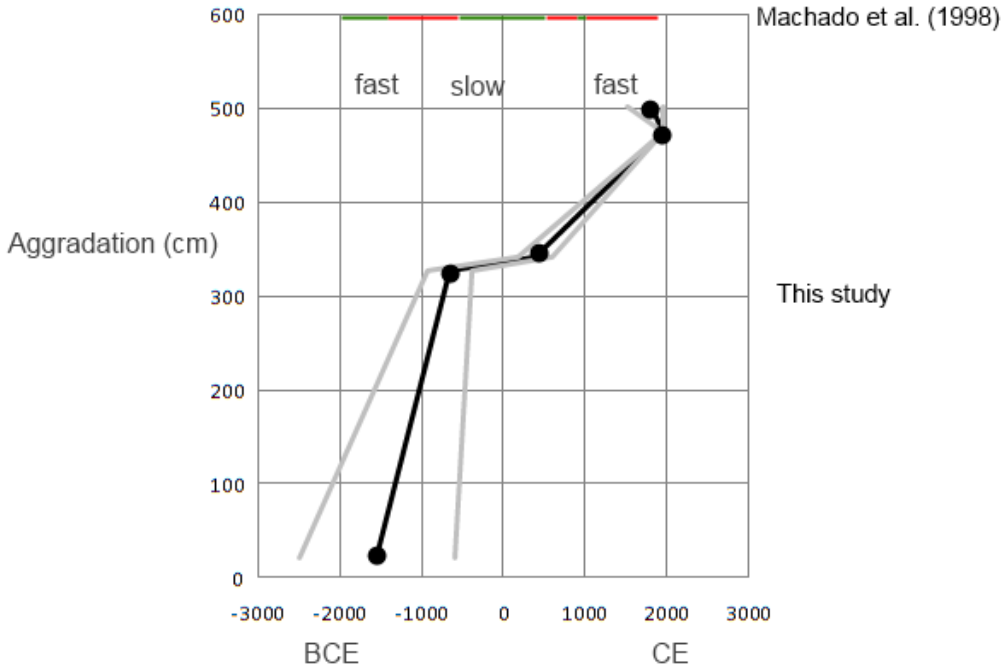

Figure 5.4 Measured deposition ages (black dots) of sediment (BCE and CE) with errors (grey lines) as corrected for the residual age, and average floodplain aggradation above the Antalo limestone base (cm) with indication of fast and slow aggradation rates. The broad degradation periods identified by Machado et al. (1998) are indicated with red bars, the Vertisol stabilization periods are indicated with green bars.

5.3.2 Wechi, Adwa and May Kinetal alluvial records

Based on three records of infilled valley deposits (the Wechi record, the Adwa record and the May Kinetal record; dated with 6 radiometric, 22 accelerator mass spectrometry and 3 thermoluminescence dates) (Figure 5.5), Machado et al. (1998) identified three main stabilization periods over the past 4000 years (ca. 2000–1500 BCE, 500 BCE-500 CE and 950-1000 CE) with Vertisol formation and three degradation episodes (ca. 1500–500 BCE, 500-950 CE, after 1000 CE) with increased sediment supply in Tigray. Because of the broad similarities with our record and the three records of Machado et al. (1998), we believe that the four records reflect a regional signal of altering geomorphic stability and degradation in the North Ethiopian Highlands. All the datasets confirm the occurrence of degradation phases between ~1500 and 600 BCE, and from ~500 CE onwards. However, Machado et al. (1998) interpret these geomorphic degradation periods directly as phases of aridity, which should not necessarily be the case (Nyssen et al., 2004).

5.4 Discussion

The paleoenvironmental records are localized on Figure 5.5. Diatom-inferred conductivity from Lake Ashenge (Marshall et al., 2009) as a proxy for dry climatic conditions shows association with the luminescence dates for aggradation at May Tsimble and the radiocarbon dates for colluvial and fluvial activation of Machado et al. (1998) (Figure 5.6). Links between climate shifts and land degradation will be further discussed in chapter 9; in what follows we will present a geomorphic overview of the later Holocene in the study region.

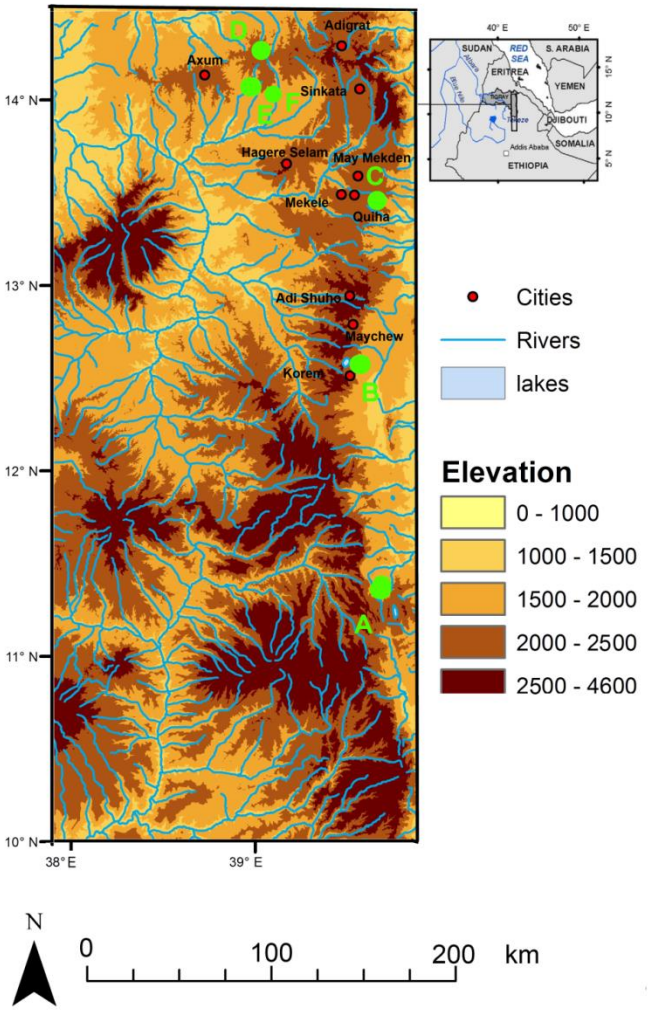

Figure 5.5 Map of all mentioned paleo environmental records in the Northern Highlands, with A = Lake Hayk (Darbyshire et al., 2003; Lamb et al., 2007), B = Lake Ashenge (Marshall et al., 2009), C = May Tsimble (this study), D = Yeha (Pietsch & Machado, 2012), E = Adwa (Machado et al., 1998), F = Wechi and May Kinetal (Machado et al., 1998).

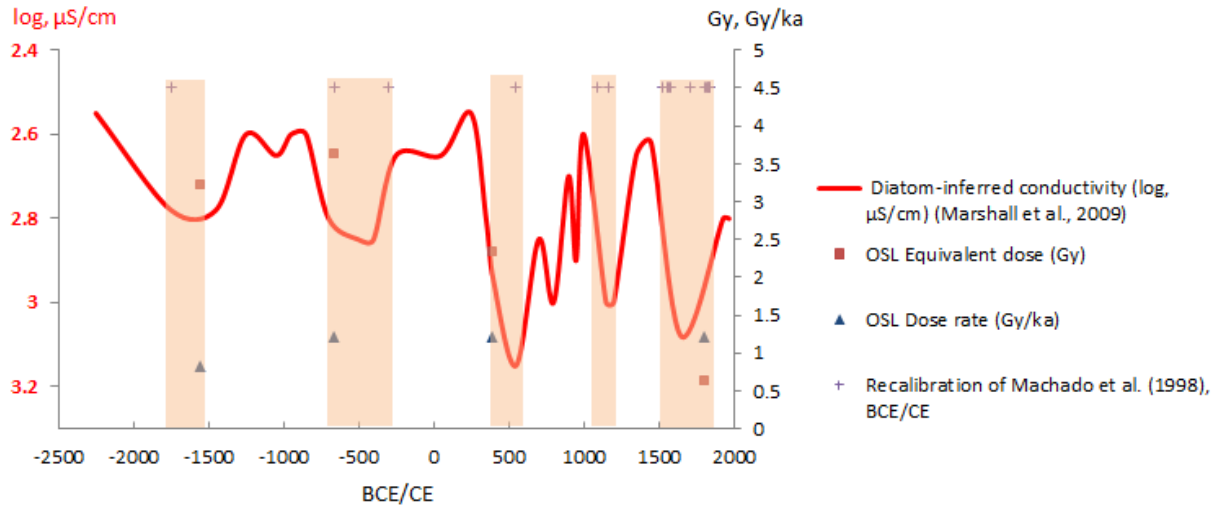

Figure 5.6 Conductivity record of Lake Ashenge as a proxy for aridity indicated as a red line (visual estimation from Marshall et al., 2009); with luminescence dates at the May Tsimble sequence presented with values of equivalent doses and dose rates; and radiocarbon dates of all alluvial and colluvial deposits identified by Machado et al. (1998), as calibrated with the CalPal-2007-Hulu calibration curve (see section 7.2.1). Orange bars indicate probable spikes of land degradation.

5.4.1 Geomorphic stability before ~1600 BCE

After the dry Last Glacial Maximum (see Chapter 7), precession-driven insolation changes initiated the African Humid Period (Marshall et al., 2009). We identified tufa deposits in the main May Tsimble channel on a waterfall next to our study site (Figure 5.7b), illustrative of the stable geomorphic conditions with Vertisol and travertine development at that time (Dramis et al., 2003; Moeyersons et al., 2006; Sagri et al., 2008). Pietsch and Machado (2012) found evidence of soil formation under an open woodland cover during this period (near Yeha, Tigray). The *Podocarpus-Juniperus* forest around Lake Hayk was still intact (Darbyshire et al., 2003). Mixed forest including *Podocarpus*, *Juniperus*, *Celtis* and *Olea* covered the landscape, somewhat similar to the present montane forest of central Ethiopia (Darbyshire et al., 2003). During the 3rd millennium BCE (Late Bronze Age), paleosols indicate environmental stability (Pietsch and Machado, 2012).

5.4.2 Aggradation during the Pre-Axumite era

At the base of our sequence (Figure 5.7a), a first depositional unit (Figure 5.4, lower part) represents about 300 cm of aggradation, deposited after 1546 BCE. This corresponds with the beginning of the first degradation period of Machado et al. (1998). The base of the deposition (with an extrapolated deposition date of 1607 BCE) slightly precedes the start of colluvial activity and increasing ratio of monocotyledons/dicotyledons determined by Moeyersons et al. (2006), based on backfill and overfill deposits of tufa dams in Tigray from 1430–1260 BCE onwards. Pietsch and Machado (2012) identify slope degradation and high sediment yield during the second half of the 2nd millennium, corresponding to a decreased trees/shrub ratio after 1400-1100 BCE. Similarly, Bard et al. (2000) report increased sedimentation at the Meskilo River (near Mekele) after the early second millennium BCE.

The dates closely follow the introduction of cattle herding from Sudan in the North Ethiopian Highlands, at the beginning of the 2nd millennium BCE (Lesur et al., 2014). Indeed, the earliest evidence for domesticated cattle (*Bos taurus*) in North Ethiopia is dated to ~ 1800 BCE (Marshall and Negash, 2002). Simultaneously, during the 2nd millennium BCE, chiefdoms rose in the Ethiopian Highlands and in the Gash (D'Andrea et al., 2008). 'Pre-Axumite chiefdoms' might be the best term to describe these social organizations because, despite the existence of the Sabaean ruins of Yeha, there was never a centralized 'Pre-Axumite state' (the so-called 'Damaat') (Phillipson, 2009).

Aggradation was (still) active around 656 BCE, when a rapid decline of *Podocarpus* and Cupressaceae forests dated to 775–410 BCE occurred around Lake Hayk (Darbyshire et al., 2003). At that time, the mixed conifer forest was replaced by disturbed, secondary bushland vegetation. Pollen evidence for this first large-scale deforestation concerns more than one taxon, indicating a dominant human interference, including vegetation clearance with the use of fire (Darbyshire et al., 2003). As will be discussed in chapter 9, the forest decline corresponds with the migrations of Semitic or Sabaean peoples across the Red Sea during the eighth and fifth century BCE, along with the introduction of long horned zebu (*Bos indicus*) to the Ethiopian Highlands. In comparison, allochthonous sediment input in Lake Ashenge rises between 950 and 750 BCE (unpublished pollen data of Marshall et al., 2009). The large-scale deforestations happened about 600 years before deforestation in the Arsi and Bale Mountains (Hamilton, 1982), which suggests a decreasing anthropogenic impact as

one moves away from the Red Sea (Phillipson, 1985) (see Chapter 9). As discussed in chapter 7, the records of Lake Hayk and Lake Ashenge indicate overall dry conditions during this period, except for a wet period between 1300-1100 BCE and increased wetness during the second half of the first millennium BCE.

5.4.3 Geomorphic stability in the (Proto-)Axum era

Much slower aggradation rates were dated between ~600 BCE and ~400 CE, although no clear discordance was observed in the profiles. Compared to the faster aggradation before ~600 BCE, this period comprising 16 cm of aggradation must represent a phase of geomorphological stability. The phase corresponds with the soil formation period described by Machado et al. (1998) (~500 BCE-500 CE) and broadly coincides with the history of the Axumite state. French et al. (2009) indeed infer considerable landscape stability both during and prior to the Axumite Period, evidenced by the development of vertic-like soils. In *The History*, Herodotos of Halicarnassos (430 BCE) describes Ethiopia as a very rich civilization. Following an explosion of demand for South Indian products in the Roman Empire (Rome, later Byzantium), there was a strong expansion of the Indian Ocean trade through the Red Sea, giving rise to the urban Axum Empire (Burstein, 2001; Phillipson, 2012). As reported in the *Periplus of the Erythraean Sea,* Adulis was an important sea port. The hegemony over the Red Sea and the Upper Nile ensured trade with Persians, Nubians and Yemen, while achieving the monopoly over trade routes to central Africa (D'Andrea et al., 2008). It can be assumed that increased resources allowed reducing pressure on the lands, as Bard et al. (2000) claim that no reduction in soil productivity can be found over the Axumite era. Pietsch and Machado (2012) identify increased trees-to-shrub ratios over the Axumite times, as compared to the Pre-Axumite period. Following Ciampalini et al. (2008), there are the Proto-Axumite (from ~ 450 BCE), Early Axumite (from ~ 90 BCE) and Classic Axumite (from ~ 100 CE) eras. Erosion rates in the immediate surroundings of Axum, calculated for these three main intervals are relatively low, evidencing the strong positive impact of Axum's extensive soil and water conservation (dams and terraces) (Ciampalini et al., 2008) and long-term landscape management by the growing population (French et al., 2009). Generally, it is recognized that adoption and intensity of investments in water and soil conservation are positively dependent on land tenure security and farmers income (Kabubo-Mariara et al., 2006). During periods of social security, agricultural technology and

intensification prosper while long-term conservation issues prevail over short-term survival (Nyssen et al., 2004). As will be discussed in chapter 7, the records from Lake Hayk and Lake Ashenge point to wet conditions between 650 BCE and 450 CE.

5.4.4 Aggradation during the Post-Axumite era

More than 150 cm of sediment vertically filled the valley bottom during another phase of faster aggradation rates from ~400 CE onwards, approximately around the shift to a dryer climate around 450 CE (Marshall et al., 2009). Since we did not measure sediment volumes, the vertical aggradation depth only gives an indication of the amount of deposited sediment – volumetric increase rate is assumed to be many times more important, given the 'triangular' shape of the infilled valley bottom. Again, the ages correspond with the post-Axumite degradation period (~500-1000 CE) identified by Machado et al. (1998). At Lake Ashenge, pollen evidence points to an abrupt *Podocarpus* decline and enhanced soil erosion by 500 CE, under intensified land use (Marshall et al., 2009). At Lake Hayk, forest clearance further progressed after 900 CE (Darbyshire et al., 2003).

Arab expansions from the 6th century onwards brought in large amounts of short horned zebu (see chapter 9) and excluded Axum from the Indian Ocean trade system, which led to the decline of the empire (Pankhurst, 1990). Population continued to grow (McEvedy and Jones, 1978) and around 800 CE 'roving kingdoms' were rivaling over the Ethiopian plateau (Abebe, 1998) while famines and plagues culminated between 831-849 CE (Bard et al., 2000).

Machado et al. (1998) identified another period of low sediment activity (calibrated dates from 1013-1164 CE), which could have been left undetected in the May Tsimble record given its lower resolution. Brancaccio et al. (1997) also report on pedogenesis around 1250 and 970 BP. This Medieval Warm Period (750-1200 CE) is in North Ethiopia relatively dry (Lamb et al., 2008). However, the centralized Zagwe rule (1000-1250 CE) based in the Lasta region, was rather peaceful, stable and urban and was involved in long-distance trade from the port of Zayla (Pankhurst, 1997; Tekeste Negash, 2006). More datasets are required to investigate the specificities of human-environment interactions at that time.

5.4.5 The 'Medieval Times'

Faster aggradation rates were reported by Machado et al. (1998) after 1050 CE. As the stabilization phase discussed above (~ 1000-1050 AD) was undetected in the May Tsimble record, aggradation is dated up to ~1800 CE. Overall, the 'Medieval Warm Period' was dry in North Ethiopia (Lamb et al., 2007). Following intensification of grazing, grasslands were expanding around 1200-1400 CE (Darbyshire et al., 2003). European historical sources from the 'Early Medieval times' report on vast amounts of cattle and grasslands in Ethiopia (Pankhurst, 1990). There were frequent civil wars with rebelling vassals and pastoral Muslim lowlanders moving to the highlands during this unstable Solomonic dynasty. Lands were owned by noblemen or by the Church while reported in *Il Milione* by Marco Polo (from second hand information), trade was dominated by Arabs (and some Armenians). Instead of a fixed capital, there were 'moving camps', and there are many reports on crop plagues by locusts and rats (Pankhurst, 1990).

During the 'Late Medieval times', Darbyshire et al. (2003) identified a gradual reforestation of *Juniperus*-dominated dry Afromontane forest at Lake Hayk between 1400 and 1700 CE. Following the war between the Adal Sultanate and Ethiopia and Portugal, Oromo peoples moved to the Highlands and their nomadic lifestyle might have reduced pressure on the land (Darbyshire et al., 2003). Traditionally, Oromo are not allowed to cut trees and destroy forests (Taddesse Berisso, 1995). Simultaneously, the 'Little Ice Age' was a wet period in North Ethiopia (Lamb et al., 2007). Under the new capital of Gondar (1632) and commercialization of agriculture, the late 17th century was an urban period of renaissance, trading with Sudan and from the port of Massawa (Pankhurst, 1990). Little information on geomorphic activity is available for this period, although a phase of soil formation has been dated around 1641 CE in Adi Kolen (Bard et al., 2000). Pedogenesis was also dated from 1425-1445 CE till 1481-1660 CE, preceding a new phase of colluvial activity (thermoluminescence dated to 1714 CE) (Machado et al., 1998).

5.4.6 The 20th century

Finally, according to the semi-structured interviews with farmers around our study site, the May Tsimble stream incised and shifted its channel to the right (i.e. to the West) around the 1960s-1970s. Gully incision has been observed at regional scale during this period (Frankl et

al., 2011, 2013). In the modern channel, very recent re-incision is visible as a small intra-channel terrace. It might be the result of a clear-water effect after the large-scale implementation of conservation measures (including the dam pictured in Fig. 5.3), following increased sediment supply during the 1960s-1980s. These phases correspond well with the three main geomorphic periods over the 20th century discussed in chapter 3 and by Frankl et al. (2011). There is the *early feudal era*, with some widely implemented conservation structures (such as *dagets*) (Chapter 3), quite stable channels with an oversized inherited morphology and low sediment supply (Frankl et al., 2010). Following strongly increased runoff coefficients, an upstream incision phase was documented to start in the (late feudal) 1960s. It continued through the civil war, amplified by the effect of large droughts and a lack of investment in conservation during the 1980s (Frankl et al., 2011). Finally, there is the *post-war era*, with new conservation efforts, more equal land rights (Chapter 3) and again lower sediment supply and lower runoff response (Frankl et al., 2011).

Figure 5.7 (a) Base of the sequence (indicated by stick) (left); and (b) small waterfall parallel to our study site, with travertine identified (indicated by red arrow) (right).

5.5 Conclusions

In this study, we analyzed a number of paleo environmental records from the North Ethiopian Highlands and additionally used optically stimulated luminescence to date aggradation phases in the May Tsimble catchment (North Ethiopia). Interrupted by periods of low aggradation rates, we dated alluvial deposition around 1550 BCE, 650 BCE and 400 CE. The results are consistent with radiocarbon dating results from the Wechi, Adwa and May Kinetal catchments. We infer that the sequence of terraces in May Tsimble is resulting from subsequent depositional phases, followed by recent incision. Stable channels observable on mid-19th-century terrestrial photographs indicate at least one earlier incision phase. The onset of aggradation coincides with the introduction of cattle herding (*Bos taurus*) in the Highlands and climate records show correspondence with the aggradation phases (see Chapter 9).

Acknowledgements

This study would not have been possible without the enormous support, friendship and help of our translator Gebrekidan Mesfin, the important input on mineralogy from Florias Mees, the advice from Dimitri Vandenberghe, the support and kindliness of the farmers near the study site, the kind hospitality of the Luminescence Dating Laboratory of the University of Oxford, the funding of UGent Special Research Fund, as well as the logistical support through Belgian VLIR projects at Mekelle University (IUC and Graben TEAM).

5.6 References

Abebe, B., 1998. Histoire de L'Éthiopie d'Axoum à la revolution. Maisonneuve et Larose, Paris, France.

Aitken, M.J., 1985. Thermoluminescence Dating. Academic Press, New York, USA.

Adamiec, G., Aitken, M.J., 1998. Dose-rate conversion factors: new data. Ancient TL 16, 37-50.

Alexanderson, H., 2007. Residual OSL signals from modern Greenlandic river sediments. Geochronometria 26, 1-9.

Arnold, L., Bailey, R., Tucker, G., 2007. Statistical treatment of fluvial dose distributions from southern Colorado arroyo deposits. Quaternary Geochronology 2, 162-167.

Arnold, L., Roberts, R., Galbraith, R., DeLong, S., 2009. A revised burial dose estimation procedure for optical dating of young and modern-age sediments. Quaternary Geochronology 4, 306-325.

Avni, Y., Porat, N., Plakht, J., Avni, G., 2006. Geomorphic changes leading to natural desertification versus anthropogenic land conservation in an and environment, the Negev Highlands, Israel. Geomorphology 82 (3-4), 177-200.

Avni, Y., Zhang, J., Shelach, G., Zhou, L., 2010. Upper Pleistocene-Holocene geomorphic changes dictating sedimentation rates and historical land use in the valley system of the Chifeng region, Inner Mongolia, northern China. Earth Surface Processes and Landforms 35 (11), 1251-1268.

Avni, Y., Porat, N., Avni, G., 2012. Pre-farming environment and OSL chronology in the Negev Highlands, Israel. Journal of Arid Environments 86, 12-27.

Bailey, R., Arnold, L., 2006. Statistical modelling of single grain quartz D-e distributions and an assessment of procedures for estimating burial dose. Quaternary Science Reviews 25 (19-20), 2475-2502.

Banerjee, D, Murray, A S, Bøtter-Jensen, L, Lang, A., 2001. Equivalent dose estimation using a single aliquot of polymineral fine grains. Radiation Measurements 33, 73-94.

Bard K., Coltorti, M., Di Blasi, M., Dramis F., Fattovich, R., 2000. The environmental history of Tigray (Northern Ethiopia) in the Middle and Late Holocene: a preliminary outline. African Archaeological Review 17 (2), 65-86.

Botha, G., Wintle, A., Vogel, J., 1994. Episodic Late Quaternary palaeogully erosion in Northern Kwazulu Natal, South Africa. Catena 23 (3-4), 327-340.

Bøtter-Jensen, L., 1988. The automated Risø TL dating reader system. Nuclear Tracks and Radiation Measurements 14, 177–180.

Bøtter-Jensen, L., 1997. Luminescence techniques: instrumentation and methods. Radiation Measurements 27, 749–768.

Bøtter-Jensen, L., Bulur, E., Duller, G.A.T., Murray, A.S., 2000. Advances in luminescence instrument systems. Radiation Measurements 32, 523–528.

Bourke, M., Child, A., Stokes, S., 2003. Optical age estimates for hyper-arid fluvial deposits at Homeb, Namibia. Quaternary Science Reviews 22, 1099–1103.

Brancaccio, L., Calderoni, G., Coltorti, M., Dramis, F., 1997. Phases of soil erosion during the Holocene in the Highlands of Western Tigray (Northern Ethiopia): a preliminary report. In: Bard, K. (Ed.), The Environmental History and Human Ecology of Northern Ethiopia in the Late Holocene. Instituto Universitario Orientale, Napoli, Italy, 30 – 48.

Broothaerts, N., Verstraeten, G., Notebaert, B., Assendelft, R., Kasse, C., Bohncke, S., Vandenberghe, J., 2013. Sensitivity of floodplain geoecology to human impact: A Holocene perspective for the headwaters of the Dijle catchment, central Belgium. The Holocene 23 (10), 1403-1414.

Burstein, S., 2001. State formation in ancient Northeast Africa and the Indian Ocean Trade. Conference Proceeding of the American Historical Association: Interactions, Regional Studies, Global Processes, and Historical Analysis: 28 February 2001, Library of Congress, Washington D.C. Accessed on 02 December 2014 and available from: http://webdoc.sub.gwdg.de/ebook/p/2005/history_cooperative/www.historycooperative.org/proceedings/interactions/burstein.html

Bussert, R., Schrank, E., 2007. Palynological evidences for a latest Carboniferous-Early Permian glaciation in Northern Ethiopia. Journal of African Earth Science 49, 201-210.

Carnicelli, S., Benvenuti, M., Ferrari, G., Sagri, M., 2009. Dynamics and driving factors of late Holocene gullying in the Main Ethiopian Rift (MER). Geomorphology 103 (2), 541-554.

Chen, J., Dai, F., Yao, X., 2008. Holocene debris-flow deposits and their implications on the climate in the upper Jinsha River valley, China. Geomorphology 93 (3-4), 493-500.

Ciampalini, R., Billi, P., Ferrari, G., Borselli, L., 2008. Plough marks as a tool to assess soil erosion rates: A case study in Axum (Ethiopia). Catena 75, 18–27.

Collins, R., 1999. Macrohistory: Essays in Sociology of the Long Run. Stanford University Press, Redwood City, USA, 312 p.

Connah, G., 2001. African Civilizations: An Archaeological Perspective. Cambridge University Press, Cambridge, UK, 340 p.

Costas, I., Reimann, T., Tsukamoto, S., Ludwig, J., Lindhorst, S., Frechen, M., Hass, H., Betzler, C., 2012. Comparison of OSL ages from young dune sediments with a high-resolution independent age model. Quaternary Geochronology 10, 16–23.

D'Andrea, C., Manzo, A., Harrower, M., Hawkins, A., 2008. The Pre-Aksumite and Aksumite Settlement of NE Tigrai, Ethiopia. Journal of Field Archaeology 33, 151-176.

Darbyshire, I., Lamb, H., Umer, M., 2003. Forest clearance and regrowth in northern Ethiopia during the last 3000 years. The Holocene 13, 537–546.

Dramis, F., Umer M., Calderoni G., Haile M., 2003. Holocene climate phases from buried soils in Tigray (northern Ethiopia): Comparison with lake level fluctuations in the Main Ethiopian Rift. Quaternary Research 60, 274-283.

Duller, G., 2008. Luminescence dating: guidelines on using luminescence dating in archaeology. English Heritage, Swindon, UK.

Eipert, A., 2004. Optically stimulated luminescence (OSL) dating of sand deposited by the 1960 tsunami in south-central Chile. BA Thesis Carleton College, Northfield, Minnesota, USA, 35 p.

Eriksson, M., Olley, J., Payton, R., 2000. Soil erosion history in central Tanzania based on OSL dating of colluvial and alluvial hillslope deposits. Geomorphology 36 (1-2), 107-128.

Frankl, A., Nyssen, J., De Dapper, M., Haile, M., Billi, P., Munro, N., Deckers, J., Poesen, J., 2011. Linking long-term gully and river channel dynamics to environmental change using repeat photography (Northern Ethiopia). Geomorphology 129, 238-251.

Frankl, A., Poesen, J., Scholiers, N., Jacob, M., Mitiku Haile, Deckers, J., Nyssen, J., 2013. Factors controlling the morphology and volume (V) – length (L) relations of permanent gullies in the Northern Ethiopian Highlands. Earth Surf. Process. Landforms 38, 1672-1684.

French, C., Sulas, F., Madella, M., 2009. New geoarchaeological investigations of the valley systems in the Aksum area of northern Ethiopia. Catena 78 (3), 218–233.

Galbraith, R., Roberts, R., Laslett, G., Yoshida, H., 1999. Optical dating of single and multiple grains of quartz from Jinmium rock shelter, Northern Australia: Part I, experimental design and statistical models. Archaeometry 41 (2), 339–364.

Goudie, A., 2013. The Human Impact on the Natural Environment: Past, Present, and Future. John Wiley and Sons, Hoboken, New Jersey, USA.

Hamilton, A., 1982. Environmental history of East Africa. Academic Press, London, UK, 328 p.

Harvey, J., Pederson, J., Rittenour, T., 2011. Exploring relations between arroyo cycles and canyon paleoflood records in Buckskin Wash, Utah: Reconciling scientific paradigms. Geological Society of America Bulletin 123 (11-12), 2266-2276.

Herodotos of Halicarnassos, 430 BCE, The Histories: Muse 3, 114.1. In: The History, trans. George Rawlinson. Dutton, New York, USA, 1862 p.

Kabubo-Mariara, J., Linderhof, V., Kruseman, G., Atieno, R., Mwabu, G., 2006. Household Welfare, Investment in Soil and Water Conservation and Tenure Security: Evidence From Kenya. PREM Working Paper PREM 06/06, 87 p.

Keen-Zebert, A., Tooth, S., Rodnight, H., Duller, G., Roberts, H., Grenfell, M., 2013. Late Quaternary floodplain reworking and the preservation of alluvial sedimentary archives in unconfined and confined river valleys in the eastern interior of South Africa. Geomorphology 185, 54-66.

Lamb, H., Leng, M., Telford, R., Tenalem Ayenew, Umer, M., 2007. Oxygen and carbon isotope composition of authigenic carbonate from an Ethiopian lake: a climate record of the last 2000 years. The Holocene 17(4), 517–526.

Lang, A., Mauz, B., 2006. Towards chronologies of gully formation: optical dating of gully fill sediments from Central Europe. Quaternary Science Reviews 25 (19-20), 2666-2675.

Lehmkuhl, F., Hilgers, A., Fries, S., Hulle, D., Schlutz, F., Shumilovskikh, L., Felauer, T., Protze, J., 2011. Holocene geomorphological processes and soil development as indicator for environmental change around Karakorum, Upper Orkhon Valley (Central Mongolia). Catena 87 (1), 31-44.

Leigh, D.S., Kowalewski, S.A., Holdridge, G.H., 2013. 3400 Years of Agricultural Engineering in Mesoamerica: Lama-Bordos of the Mixteca Alta, Oaxaca, Mexico. Journal of Archaeological Science 40, 4107-4111.

Lesur, J., Hildebrand, E., Abawa, G., Gutherz, X., 2014. The advent of herding in the Horn of Africa: New data from Ethiopia, Djibouti and Somaliland. Quaternary International 343 (1), 148–158.

Machado, M., Pérez-González, A., Benito, G., 1998: Paleoenvironmental changes during the last 4000 yr in the Tigray, Northern Ethiopia. Quaternary Research 49, 312–21.

Marcus, H., 2002. A History of Ethiopia, Updated Edition. University of California Press, Berkeley, California, USA, 394 p.

Marshall, F., Negash, A., 2002. Early hunters and herders of northern Ethiopia: The fauna from Danei Kawlos and Baati Ataro rockshelters. Society for African Archaeologists Meeting. Tucson, Arizona, USA.

Marshall, M., Lamb, H., Davies, S., Leng, M., Zelalem Kubsa, Umer, M., Bryant, C., 2009. Climatic change in northern Ethiopia during the past 17,000 years: A diatom and stable isotope record from Lake Ashenge. Palaeogeography, Palaeoclimatology, Palaeoecology 279, 114–127.

McCann, J., 1997. The Plow and the Forest: Narratives of Deforestation in Ethiopia 1840-1992. Environmental History 2 (2), 138-159.

McEvedy, C., Jones, R., 1978. Atlas of World Population History (Hist Atlas). Puffin, London, UK, 368 p.

Mejdahl, V., 1979. Thermoluminescence dating: beta-dose attenuation in quartz grains. Archaeometry 21, 61-72.

Merla, G., Abbate, E., Azzaroli, A., Bruni, P., Canuti, P., Fazzuoli, M., Sagri, M. Tacconi, P., 1979. A Geological Map of Ethiopia and Somalia (1973). 1 : 2 000 000; and Comment. University of Florence, Firenze, Italy.

Moeyersons, J., Nyssen, J., Poesen, J., Deckers, J., Mitiku Haile, 2006. Age and backfill/overfill stratigraphy of two tufa dams, Tigray Highlands, Ethiopia: Evidence for Late Pleistocene and Holocene wet conditions. Palaeogeography, Palaeoclimatology, Palaeoecology 230 (1–2), 165–181.

Murray, A.S., Wintle, A.G., 2000. Luminescence dating of quartz using an improved single-aliquot regenerative-dose protocol. Radiation Measurements 32, 57-73.

Nicholson, S., Dezfuli, A., Klotter, D., 2012. A two-century precipitation dataset for the continent of Africa. Bull. Amer. Meteor. Soc. 93, 1219–1231.

Nyssen, J., Poesen, J., Moeyersons, J., Deckers, J., Mitiku Haile, Lang, A., 2004. Human impact on the environment in the Ethiopian and Eritrean highlands--a state of the art. Earth-Science Reviews 64 (3-4), 273-320.

Nyssen, J., Poesen J., Veyret-Picot, M., Moeyersons, J., Mitiku Haile, Deckers, J., Dewit, J., Naudts, J., Teka, K., Govers, G., 2006. Assessment of gully erosion rates through interviews and measurements: a case study from northern Ethiopia. Earth Surface Processes and Landforms 31 (2), 167–185.

Nyssen, J., Haile, M., Naudts, J., Munro, N., Poesen, J., Moeyersons, J., Frankl, A., Deckers, J., Pankhurst, R., 2009. Desertification? Northern Ethiopia re-photographed after 140 years. Sci Total Environ 407, 2749–2755.

Nyssen, J., Frankl, A., Mitiku Haile, Hurni, H., Descheemaeker, K., Crummey, D., Ritler, A., Portner, B., Nievergelt, B., Moeyersons, J., Munro, R.N., Deckers, J., Billi, P., Poesen, J., 2014. Environmental conditions and human drivers for changes to north Ethiopian mountain landscapes over 145 years. Science of the Total Environment 485-486, 164-179.

Pankhurst, R., 1990. A Social History of Ethiopia: The Northern and Central Highlands from Early Medieval Times to the Rise of Emperor Tewodros II. Addis Ababa University, Addis Ababa, Ethiopia, 371 pp.

Pankhurst, R., 1997. The Ethiopian Borderlands: Essays in Regional History from Ancient Times to the end of the 18th century. The Red Sea Press, Asmara, Eritrea.

Pelletier, J., Quade, J., Goble, R., Aldenderfer, M., 2011. Widespread hillslope gullying on the southeastern Tibetan Plateau: Human or climate-change induced? Geological Society of America Bulletin 123 (9-10), 1926-1938.

Phillipson, D. 1985. African archaeology. Cambridge University Press, Cambridge, UK, 234 p.

Phillipson, D., 2009. The First Millennium BC in the Highlands of Northern Ethiopia and South–Central Eritrea: A Reassessment of Cultural and Political Development". African Archaeological Review 26, 257–274.

Phillipson, D., 2012. Aksum and the Northern Horn of Africa. Archaeology International 15, 49-52.

Pietsch, D., Machado, M., 2012. Colluvial deposits – proxies for climate change and cultural chronology. A case study from Tigray, Ethiopia. Zeitschrift für Geomorphologie 58, 119-136.

Poesen, J., Vandekerckhove, L., Nachtergaele, J., Oostwoud Wijdenes, D., Verstraeten, G., van Wesemael, B., 2002. Gully erosion in dryland environments. In: Bull, L.J., Kirkby, M.J. (Eds.), Dryland Rivers: Hydrology and Geomorphology of Semi-Arid Channels. Wiley, Chichester, UK, 229–262 p.

Porat, N., Zilberman, E., Amit, R., Enzel, Y., 2001. Residual ages of modern sediments in an hyperarid region, Israel. Quaternary Science Reviews 20 (5-9), 795-798.

Prescott, J. R., Hutton, J. T., 1994. Cosmic ray contributions to dose rates for luminescence and ESR dating: large depths and long-term time variations. Radiation Measurements 23, 497–500.

Sagri, M., Bartolini, C., Billi, P., Ferrari, G., Benvenuti, M., Carnicelli, S., Barbano, F., 2008. Latest Pleistocene and Holocene river network evolution in the Ethiopian Lakes Region. Geomorphology 94, 79–97.

Schoff, W., 1912. The Periplus of the Erythraean Sea - Periplus maris Erythraei (English translation). Longmans, New York, USA.

Schütt, B., Frechen, M., Hoelzmann, P., Fritzenwenger, G., 2011. Late Quaternary landscape evolution in a small catchment on the Chinese Loess Plateau. Quaternary International 234, 159-166.

Shaw, A., Holmes, P., Rogers, J., 2001. Depositional landforms and environmental change in the headward vicinity of Dias Beach, Cape Point. South African Journal of Geology 101 (2), 101-114.

Summa-Nelson, M., Rittenour, T., 2012. Application of OSL dating to middle to late Holocene arroyo sediments in Kanab Creek, southern Utah, USA. Quaternary Geochronology 10, 167-174.

Taddesse Berisso, 1995. Deforestation and Environmental Degradation in Ethiopia: The case of Jam Jam Province. Northeast African Studies 2 (2), 139-155.

Teeuw, R., Rhodes, E., Perkins, N., 1999. Dating of quaternary sediments from western Borneo, using optically stimulated luminescence. Singapore Journal of Tropical Geography 20 (2), 181-192.

Tekeste Negash, 2006. The Zagwe period re-interpreted: post-Aksumite Ethiopian urban culture. Africa: Rivista Trimestrale di Studi e Documentazione 61 (1), 120-137.

Terwilliger, V.J., Eshetu, Z., Huang,Y., Alexandre,M., Umer, M. and Gebru,T., 2011. Local variation in climate and land use during the time of the major kingdoms of the Tigray Plateau in Ethiopia and Eritrea. Catena 85, 130–143.

Thomas, M., Murray, A., 2001. On the age and significance of Quaternary colluvium in eastern Zambia. Palaeoecology of Africa and the surrounding islands 27, 117-133.

Tooth, S., Hancox, P., Brandt, D., McCarthy, T., Jacobs, Z., Woodborne, S., 2013. Controls On the Genesis, Sedimentary Architecture, and Preservation Potential of Dryland Alluvial Successions In Stable Continental Interiors: Insights from the Incising Modder River, South Africa. Journal of sedimentary research 83 (7-8), 541 -561.

Vanmaercke M, Poesen J, Verstraeten G, Maetens W, de Vente J., 2011. Sediment yield as a desertification risk indicator. Science of the Total Environment 409, 1715-1725.

Vanmaercke, M., Poesen, J., Broeckx, J., Nyssen, J., 2014. Sediment Yield in Africa. Earth-Science Reviews 136, 350-368.

Wallinga, J., 2002. Optically stimulated luminescence dating of fluvial deposits: a review. Boreas 31 (4), 303-322.

Wintle, A.G. and Murray, A.S., 2006. A review of quartz optically stimulated luminescence characteristics and their relevance in single-aliquot regeneration dating protocols. Radiation Measurements 41, 369-391.

Zimmerman, D.W., 1971. Thermoluminescent dating using fine grains from pottery. Archaeometry 13, 29-50.

Chapter 6 Alluvial and lacustrine debris fans: indicators for subrecent land degradation and gully activity around Lake Ashenge

This chapter is modified from:

Lanckriet, S., Tesfaalem Asfaha, Frankl, A., Amanuel Zenebe, Nyssen, J., 2015. Sediment in alluvial and lacustrine debris fans as an indicator for land degradation around Lake Ashenge (Ethiopia). Land Degradation and Development, online early view. DOI: 10.1002/ldr.2424.

Abstract

Sediments deposited by (paleo) flash floods can hold valuable information on processes of environmental change, land degradation or desertification. In order to assess the suitability of flash flood deposits as proxies for land degradation, we monitored a representative gully segment in North Ethiopia (Ashenge catchment), investigated a sequence of alluvial debris fans downstream of this gully segment and dated a neighboring subaquatic debris fan using short-lived ^{210}Pb isotope counting. During one rainy season (July-September 2014), we measured daily rainfall, peak discharge, bed load transport, suspended sediment load and sediment deposition rates. The data show that sediment deposition in the debris fans is significantly dependent on micro-topography (net incision in micro-channels) ($p < 0.1$) and position within the sequence (net incision farther away from the lake) ($p < 0.05$). As sediment transfer to the lake and magnitude of downstream sediment transfer significantly depend on the balance between available water and sediment (ratio rainfall depth / bed load transport) ($p < 0.05$), we could reconstruct the hydro-sedimentary evolution of the gully over the past half century and validate it with aerial photographs and semi-structured interviews. The findings are consistent with the short-lived isotope count results, indicating increased sediment supply from the 1970s onwards, when little amounts of clay were deposited in the lake (< 5%), and a subrecent clear water effect that resulted in increased deposition rates of clay in the lacustrine debris fan. Our analysis indicates that debris fan sediments can be used to estimate past environmental degradation rates, if the contemporary water and sediment behavior is well understood. Overall, we find that phases of increased sediment deposition match with periods of decreased vegetation cover under insecure land tenure and large drought.

6.1 Introduction

Sediment transport can be used as a valuable research 'proxy' for the assessment of environmental degradation in regions with a strongly contrasted climate (alternating wet and dry seasons). For instance, Vanmaercke et al. (2011) employ sediment yield as an effective desertification risk indicator. Avni (2005) also shows that gully sediment dynamics under headcut retreat are a key factor for desertification in the Negev. In particular, it is recognized that sediment deposited in alluvial fans located downstream of ephemeral streams (Figure 6.1) can hold valuable information concerning environmental change and environmental degradation. Harvey (2012) claims that alluvial debris fans have not only a 'functional role' of control on sediment supply from hillslope gullies to stream channels, but have also a 'preservational role' as storage zones that contain information on (past) environmental change. Consequently, alluvial fan sediments could be equally useful as research 'proxies' for land degradation assessment, if their evolution responds to degradation in their catchments. Geomorphological studies on alluvial fans show that they are often built up (i) by sheetflood deposits (Sweeney and Loope, 2001), (ii) by sediment-charged flash floods (Blair, 1999, 2000), or (iii) by accumulation on the fan from supercritical standing waves of expanding sheetfloods (Blair, 2000).

Generally, the study of the driving forces of gullying is less developed in comparison with the study of their control technology and physical modelling (Carnicelli et al., 2009). Debate concerning the driving forces of the morphologic evolution of alluvial debris fans is ongoing. Late Holocene anthropogenic impact leading to alluvial debris fan development is a common theme. For example, Chiverrell et al. (2007) attribute the late Holocene increase in gullying activity in Lancashire (Great Britain) to population expansions, a growing rural economy, and an increased anthropogenic pressure on upland hill slopes that are crucial in priming hill slopes before major storm events. Also, Eriksson et al. (2000) found that the recent phase of floodout aggradation (< 1000 years) in central Tanzania is probably the result of the introduction or intensification of agriculture and livestock husbandry. Other studies focus on climate change as the cause of alluvial fan evolution. For example, Lafortune et al. (2006) found that alluvial fans in Canada have been deposited by torrential activity, due to increasing rainfall or other triggers that facilitate torrential activity. Also Grenfell et al. (2012) found floodouts in the semi-arid Karoo region (South Africa) formed

under increased precipitation. Others, such as Zygmunt (2009) attribute the development of alluvial fans to a combination of climatic changes and human impact. Additionally, some authors discuss the impact of gully's 'authigenic' factors, such as local conditions independent of external drivers, i.e. control of the hydraulic base level (Prosser et al., 1994; Bull, 1997; Carnicelli et al., 2009).

In North Ethiopia, the controlling factors of sediment dynamics in ephemeral streams are not yet fully understood. The flashfloods in these ephemeral streams have severe negative impacts on both the regional agricultural economy and human health. Overland flow and concentrated water flow can induce downstream flooding, high sediment concentration of the water and severe fluvial erosion. Unfortunately, measuring and modeling sediment transport in ephemeral streams is a rather difficult task, mainly due to the unpredictable nature of the flashfloods (Reid et al., 1996; 1998). Hydrological models are often equipped for predictions in perennial streams in the more temperate (humid) regions of the world, so they are often less accurate in areas with contrasted climatic conditions (Reid et al., 1995). Mechanisms of stream hydrology differ significantly between regions with different climates. For instance, Laronne & Reid (1993) show coarse bedload sediment transport in ephemeral channels, due to the peaks in ephemeral streams, can be up to 400 times more efficient than in humid perennial rivers.

For North Ethiopia in particular, several regional studies exist on the dynamics of suspended sediment transport (see Amanuel Zenebe, 2009; Vanmaercke et al., 2010), but to date few studies have been performed focusing on bed load transport. Further, it is not clear to what extent alluvial debris fans could be useful 'tools' to assess land degradation. Therefore, in this chapter we will present (i) a characterization of water and sediment dynamics at a gully system near Lake Ashenge (North Ethiopia); (ii) empirical relations to express water and sediment dynamics in terms of their controlling factors; (iii) short-lived isotope dating of a subaquatic debris fan; and (iv) a reconstruction of land degradation processes from a sequence of alluvial debris fans found downstream of the gully system.

6.2 Methods

6.2.1 Study catchment of Ashenge

Our study was performed within a gully catchment adjacent to Lake Ashenge (North-Ethiopia), close to the city of Korem (12°30'N, 39°31'E) within the region of Tigray (Figure 6.1). The first studied 'Menkere gully' (site 1) lies adjacent to the village of Menkere, to the East of the lake (Figure 6.2). Upstream, the gully incises rather shallow colluvium on steep slopes. Downstream, the gully incises a flat but thick alluvial-colluvial mantle. The gully catchment is mainly composed of croplands, with some areas of woody vegetation on the steeper slopes. In the gully, a sequence of three debris fans is evident (coded DF1 to DF3) and one additional fan extends into the lake (DF4, at the closest position by the lake) (Figure 6.1 & 6.2). Just Northeast of DF4, a conical spot of grazing lands most probably also corresponds to an inactive debris fan (Figure 6.2), although this could not be clearly substantiated on the field. Cross-sections of the debris fans show that they are built-up by stony debris (Figure 6.1b). The gully catchment has an area of 221 ha. The second studied 'Korem gully' (site 2), with a catchment of 193 ha, lies at the south of the lake, where a large underwater debris fan is present (Figure 6.2).

Figure 6.1 Alluvial debris fans along the Menkere gully, including (a) the fan adjacent to the lake (coded DF4 in Figure 6.2) (the lake is at the back of the photographer and euphorbia trees are approximately 3 m high); and (b) a profile on the stoniness of DF2. See the sheep for indication of scale.

6.2.2 Measurement campaign for hydrology and sediment trapping

Upstream of the depositional area, the Menkere gully was instrumented (Figure 6.2) in order to understand the contemporary sediment dynamics during flashfloods in the rainy season (July-September 2014). Measurements included (i) rainfall, (ii) peak discharge, (iii) bed load transport, (iv) suspended sediment load and (v) spatially distributed sediment deposition rates.

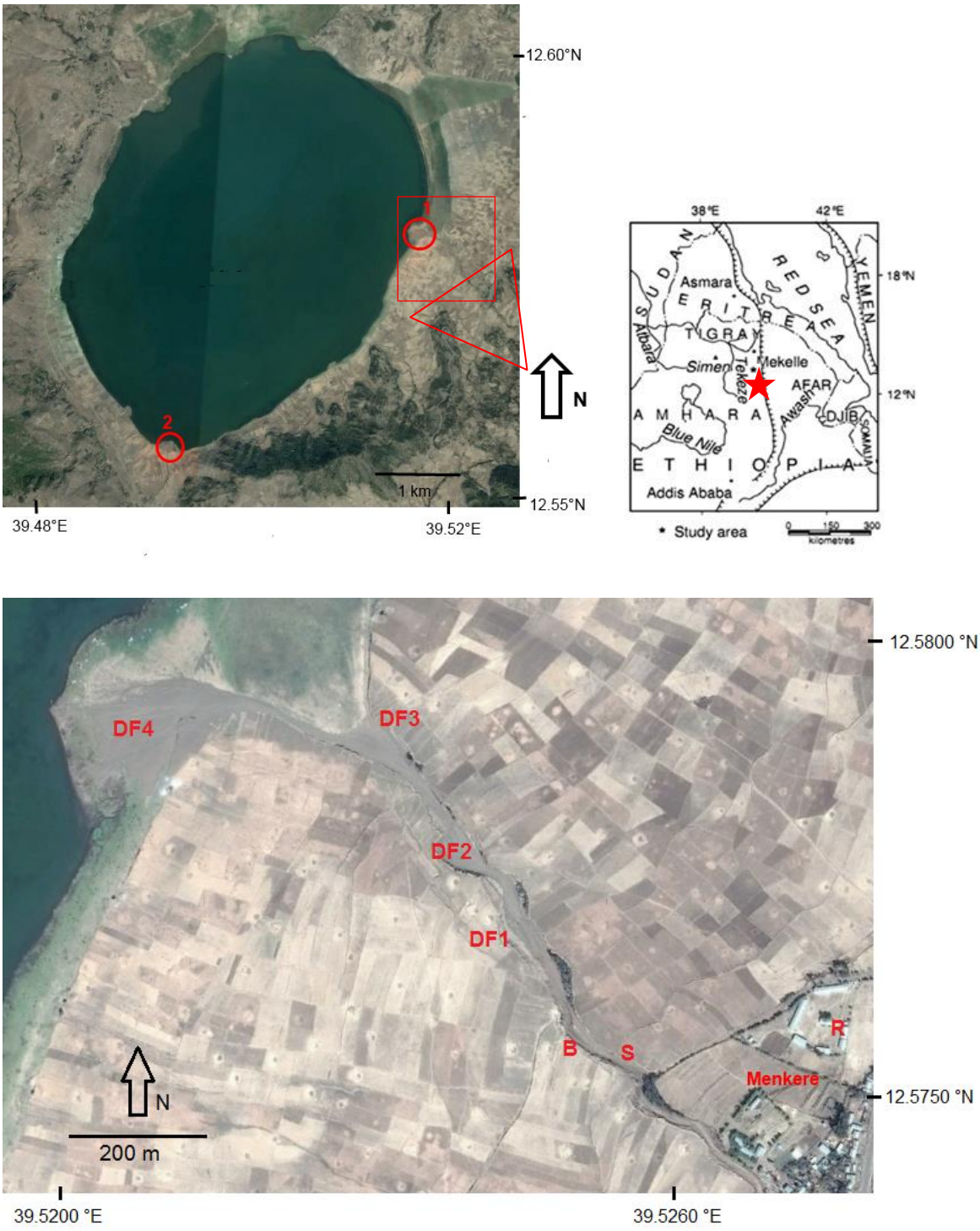

Figure 6.2 Location of the study area (indicated with red star) and the two study sites (1 indicates the Menkere gully and 2 indicates the Korem gully) (upper photo); and location of the debris fans (DF4, DF3, DF2, DF1) at study site 1 (lower image), where sediment deposition rates were monitored, as well as the location of the bed load trap (B), the staff gage and suspended sediment sampling (S) and the rain gage (R). Background is given by CNES-Astrium images (18/01/2014) and the village of Menkere is indicated. The area covered by Figure 6.9 is indicated by a red rectangle and the area covered by Figure 6.10 by a red triangle.

6.2.2.1 Rainfall measurements

Rainfall was measured by a rain gauge installed about 100 m from the gully channel (Figure 6.2) and monitored twice a day (at 8 AM and 6 PM). The standard rain gauge, made of a metal cylindrical funnel, was installed level and in an open field, far away from any obstacles (Figure 6.3a).

6.2.2.2 Peak discharge measurements

Due to the instantaneous nature of the floods, excessive velocities and accessibility problems, direct measurement of flash floods in ephemeral rivers is usually impractical when they occur. Peak discharges can, however, be indirectly estimated after floods using crest stage gauges (Tesfaalem et al., 2015). Peak flow height was therefore monitored for floods during July, August and September 2014 (Figure 6.3b). Peak discharge was recorded by a crest stage gauge with floating marker (sawdust) installed at a rectangular gully segment near the village (segment width 8.1 m) (S in Figure 6.2). We follow the recommendations made by Tesfaalem et al. (2015) by installing the gauge level in a straight, permanent and stable channel section. Small floods with flow heights less than 20 cm could not be measured, but the 20 cm was added when calculating peak depths. We computed peak discharges (Q_p; m^3/s) from peak depths using the Manning equation, with R the hydraulic radius (m), A the flow area (m^2), S the channel slope (0.02) and a roughness coefficient n estimated at 0.030 (Chow, 1959):

$$Q_p = \frac{AR^{2/3}\sqrt{S}}{n} \qquad (6.1)$$

6.2.2.3 Measurement and characterization of daily bed load transport

After every flood, the volume of transported bed load material was measured in a cemented sediment trap placed in the active gully channel (Figure 6.2). The construction (dimensions of 2.4 m by 0.4 and 0.5 m) consisted of three small traps (dimensions of 0.4 m by 0.4 m and 0.5 m) that occupied 37 % of the channel bottom width; this was done in order to minimize interference of the installation with the measurement of downstream bed load sediment deposition rates (Figure 6.3c). Measured sediment volumes (n = 30) were multiplied by a conversion parameter ζ calculated as the ratio of the length of the construction with the combined length of the traps. The construction was placed just downstream of the staff gauge, with the longest side perpendicular on the channel direction. We took three random

samples of the bedload sediment using Kopecky rings (5.1 cm height, 5 cm across, 100 cm^3 volume), in order to estimate sediment bulk density. We estimate the bedload sediment trapping efficiency of the traps at ~ 100 %, i.e. the fraction of the sediment that enters the trap and which is deposited in the trap (Verstraeten & Poesen, 2001). This is because the traps were never fully filled during one event and the combined trap volume of 0.24 m^3 > the measured volume of trapped sediments (always < 0.20 m^3, with only once an exception of 0.23 m^3). This sediment also included pebbles, so we counted the number of trapped pebbles (NTP) in the construction after every flood and following the Wentworth US Geological Survey grain size chart characterized them as cobbles (diameter > 6.4 cm), very coarse pebbles (diameter 3.2 – 6.4 cm) and coarse pebbles (diameter 3.2 – 1.6 cm).

6.2.2.4 Characterization of suspended sediment load

During two floods, three samples of suspended sediment load were taken in the flood at intervals of five minutes during the peak flood. For this purpose, two-liter bottles were installed on a long metal stake and a depth-integrated sample was taken in the middle of the water flow (Figure 6.2; Figure 6.3d). In order to avoid additional sediment flux into the bottle, the opening of the bottles was turned away from the direction of the water flow. All samples were filtered in a funnel with Whatman 42 filter paper (pore size of 2.5 µm), oven-dried and sediment was weighed in order to determine suspended sediment loads (Mekele University Soil Laboratory).

6.2.2.5 Vertical deposition rates and magnitude of downstream transfer

Vertical sediment deposition rates were determined by vertical measurements relative to 45 stable markers installed in the four depositional areas (DF1-DF4) (Figure 6.2; Figure 6.3e). Measurement was performed twice a week and hence debris fan volume changes could be calculated (mean vertical change multiplied with debris fan area; m^3). For every marker, the position in the gully bed was noted (in a micro channel or on a micro ridge), as well as the number of the debris fan in which it was located (coded DF1 to DF4). Analysis of variance allowed calculation of sediment deposition rates in terms of these factors. We also ranked all events on a scale of 'magnitude of downstream transfer' (MDT), with value 5 if overall deposition occurs in the lake (i.e. overall incision of all debris fans taken together) and values 1 to 4 if deposition is starting from DF1 to DF4 respectively onwards. Moreover, we coded all events according to their 'sediment transfer to the lake' (STL) (1 if the total debris fan volume change was negative, 0 if it was positive).

Figure 6.3 Monitoring installations for sediment dynamics, including (a) the rain gage, (b) the crest stage gage, (c) bedload trap, (d) sampler for suspended sediment load measurements, and (e) a stable vertical marker as indicated with blue paint. The sediment deposition was measured relative to the lowest line of blue paint.

6.2.3 Alluvial debris fan sequence

As stated before, a sequence of four alluvial fans was found downstream of the staff gauge. It is possible that these debris fans may deliver information on past land degradation upstream, if the contemporary sediment dynamics of the gully system are well understood.

We followed the methodology discussed in chapter 3, based on the AGERTIM method developed by Nyssen et al. (2006), in order to assess the temporal evolution of the fan complex. Semi-structured interviews in and around the gully sites were performed with 14 farmers. The farmers were interviewed independently and individually, during walks along the gully. The interviewees were asked to show and locate the features they were talking about. These included the occurrence and timing of appearance of, among others, boulders, alluvial fans, floods, gully incisions and terraces. Only if all interviewed farmers came independently and individually to the same conclusions were these insights used in the study.

In order to independently assess the chronology of the debris fan sequence development, aerial photographs of the area were obtained. These include aerial photographs taken in 1936, 1965, 1986 and recent images. It is worth shortly mentioning the 1936 aerial photographs, as they have been recently rediscovered (Nyssen et al., 2015). Each set of photographs contains one vertical photograph, two low-oblique photographs and one high-oblique photograph, taken simultaneously at a flight height of about 4000-4500 m a.s.l., resulting in a scale of about 1:16 000 - 1:18 000 (low-oblique photographs) (Nyssen et al., 2015). We used a low-oblique photograph of the study area and lakeshore (Table 6.1) which could be compared to the aerial photographs of 1965, 1986 and to high resolution CNES/Astrium images accessible on Google® Earth.

Table 6.1 Remote sensing images (aerial photographs and satellite images) used to study the alluvial fan sequence development.

Image	Date	Operator	Source	Resolution
109-103 (flight of 24-03-1936)	March 1936	Istituto Geografico Militare	Geography Department, Ghent University	ground resolution < 2 m
24OCT65-R-187-186 96	October 1965	Swedsurvey	Ethiopian Mapping Agency	ground resolution of ca. 1.9 m
13NOV86-S12-01-0043	November 1986	Swedsurvey	Ethiopian Mapping Agency	ground resolution of ca. 1.9 m
CNES/Astrium images	January 2014	GeoBasis – DE/BKG	Google® Earth	ground resolution of ca. 0.5 m

6.2.4 Subaquatic debris fan

Additional dating of debris fan dynamics around Lake Ashenge was derived from short-lived isotope counting. For logistical reasons, no subaquatic alluvial fan sample could be taken near the Menkere gully. Therefore, we focused on the second gully downstream of a gully system located at the South of the lake (Korem gully), where an underwater debris fan is present (Figure 6.2). Using a gravity corer (Uwitec, 2014) from a boat, a subaquatic debris fan sample was collected approximately 100 m from the shore and in alignment with the gully channel, over a depth of 16 cm (Figure 6.4). This core of shallow lake sediments was retrieved and sectioned upright with a fixed-interval sectioning device in 1-cm slices.

Figure 6.4 Location of the coring in the subaquatic debris fan (indicated with red star), aligned with the mouth of the Korem gully.

Using a high-purity Germanium detector (Centre d'Etudes Nordiques; Québec, Canada), supported isotopes of ^{210}Pb and non-supported ^{210}Pb were measured for samples taken at 2 cm intervals. Sediment age was estimated using the constant-rate-of-supply model, assuming a constant atmospheric lead flux under varying sediment supply (Appleby, 1978).

Sediment texture was determined for all 16 subsamples. Treatment with 35% hydrogen peroxide allowed removal of the organic matter, whereafter sand (>63 µm) was separated from silt and clay (<63 µm) by wet sieving of the sample with distilled water on a 63 µm sieve. The sandy fraction was measured, and some 2.5-3 g of the remaining silt and clay fraction was mixed with a 40 ml 0.2% sodium hexametaphosphate solution, and treated with ultrasound. Texture of the clayey and silty classes was then determined in the UGent sedimentology laboratory with X-ray sedigraphy (*SediGraph III Plus*), a methodology based on the combined laws of Beer-Lambert and Stokes. Reynolds numbers were held between

0.3 and 0.5 to ensure laminarity of the suspension (Micromeritics, 2014). In line with basic theory on sediment transportation, we can assume that with decreasing grainsize, critical stream velocity for deposition is less, and stream conditions are more stable (Hjulström, 1935).

6.3 Results

6.3.1 Characterization of the hydro-sedimentary regime

6.3.1.1 Rainfall distribution and peak discharges

Rainfall in 2014 was rather 'late', since the first real storms arrived only at the end of July (Figure 6.5). Apart from the delayed start, measured storms were quite typical for the region, with maximum daily rainfall amounts up to 40 mm. These values are generally in line with the data described by Nyssen et al. (2005), who measured for instance a maximum rain depth over 1 h (32 mm) that is only slightly less than that over 24 h (34 mm). Note that most rainfall was recorded as nighttime rain (*in casu* 3.4 times as much as compared to daytime rain) and that precipitation was highest in August (Figure 6.5a). There were also 10 dry days in the middle of the rainy season; a t-test showed that the average daily rainfall before (8.2 mm) and after (8.4 mm) this period was not significantly different ($p > 0.1$). Using the Manning method we calculated peak discharges that range between 4.65 and 19.00 m^3/s, with an average of 7.93 ± 5.46 m^3/s. There are only few peak discharge data ($n = 7$), partly due to theft of the gauge in the middle of the rainy season (one week of missing data). We could model peak discharges from the following significant relationship between peak discharge (Q_p) and R_{24} (cumulative rainfall over the past 24 hours):

$$Q_p = 0.3592 R_{24} \qquad (n = 7;\ p < 0.05;\ R^2 = 0.25) \qquad (6.2)$$

6.3.1.2 Suspended sediment and bed load transport

Suspended sediment load was measured for six samples during two floods and was on average 18.3 ± 10.9 g/l, which is broadly in the range of the suspended sediment load data

reported for ten catchments in the Highlands by Vanmaercke et al. (2010). Taking the average peak discharge into account (7.93 m^3/s), we estimate the average suspended sediment load at peak flood around 145.1 kg/s.

Sampled bed load was mostly sand and amounted to 3.1 m^3 over the entire rainy season; on average 0.10 ± 0.06 m^3 per flood. Taking into account the conversion parameter ζ of 2.67 and the average bulk density of 1.59 g/cm^3, this represents 13.2 tonnes over the rainy season or an average of 425 kg of bed load transport per flood (Figure 6.5). In total, 72 trapped pebbles were counted, of which most (43 %) were characterized as 'coarse pebbles', and the rest as 'cobbles' (31 %) and 'very coarse pebbles' (26 %). The pebbles account only for a very small portion of the total bed load volume and most pebbles were counted in August, except for a period of ten days with absence of any sediment and pebble activation during the already mentioned dry spell (4-13 August 2014) (Figure 6.5). T-tests showed that neither bed load sediment nor the number of trapped pebbles per day differed significantly ($p > 0.1$) before and after this dry spell.

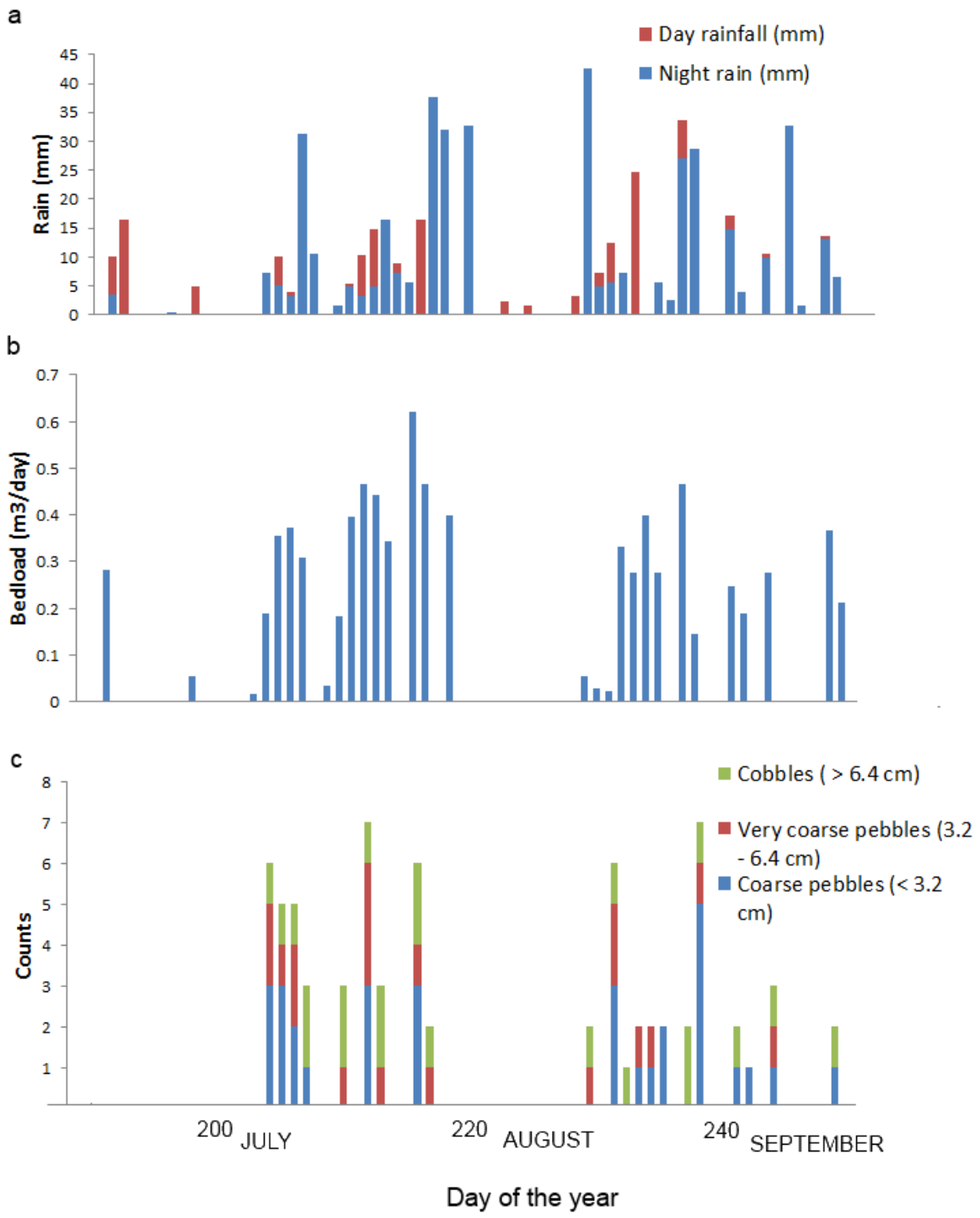

Figure 6.5 Temporal patterns (in 2014) of (a) daily rainfall (in mm/day); (b) computed bed load transport (m3/day); (c) number of trapped pebbles per day.

6.3.1.3 Sediment deposition rates in debris fans

Vertical depth measurements relative to the markers allowed identification of both erosion and deposition patterns within the debris fans. In general, the gully segment is in a rather stable geomorphic equilibrium, given that for all markers there was an average vertical evolution of - 0.17 cm per flood. Generally, most deposition occurred during the first big floods (the end of July), while important phases of erosion were common over the whole rainy season. As indicated by the mean vertical changes (cm) and debris fan volume changes (m^3) per event, depositional variability appears to be higher in the upper debris fans while eroded and deposited volumes are larger for DF4 (Figure 6.6).

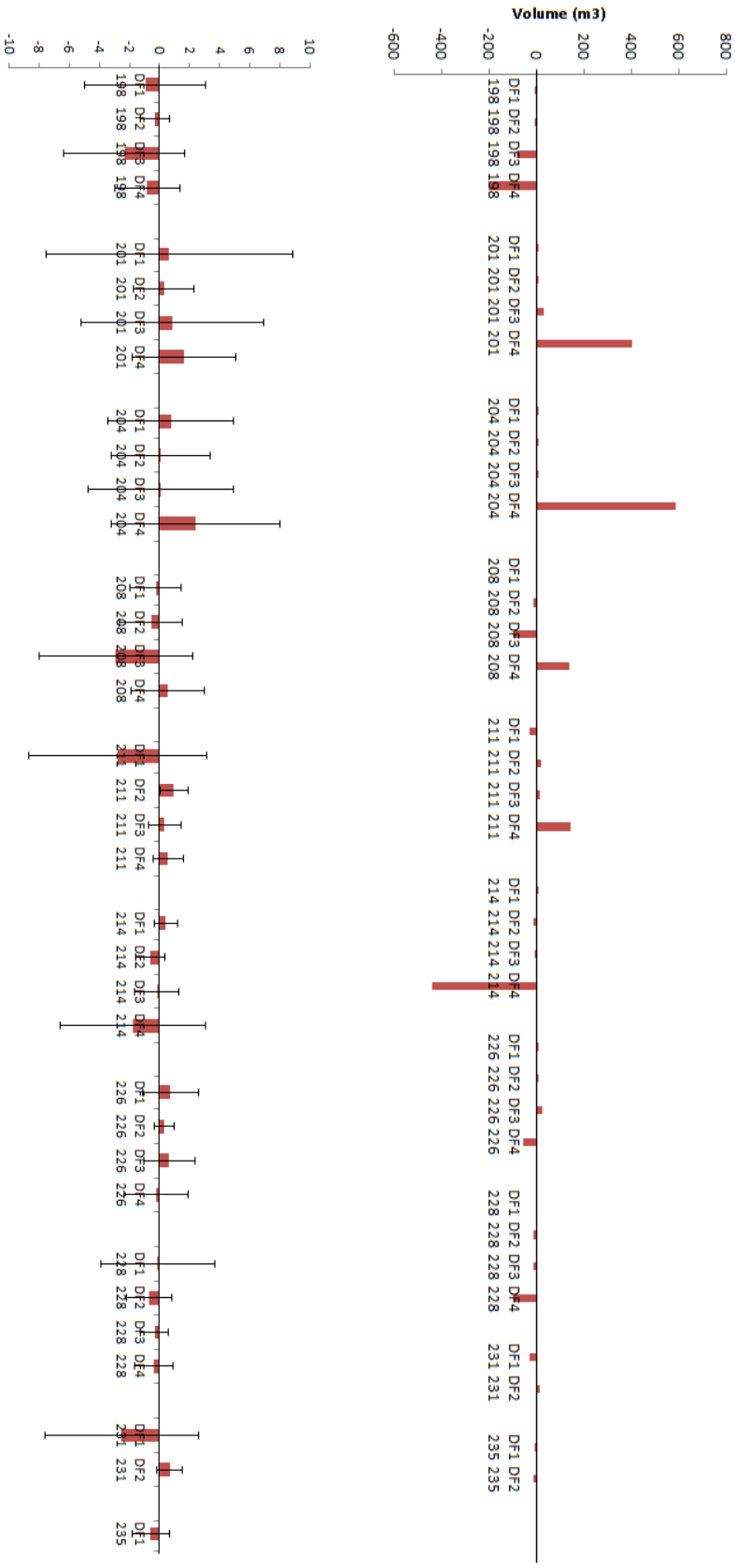

Figure 6.6 Mean vertical changes (cm) and volume changes (m3) on all debris fans, in days of the year with indication of standard deviation. Days 231 and 235 show some missing data.

6.3.2 Impact of discharge on sediment transport

There is a well-studied and strong relation between discharge Q and suspended sediment load (SSC) in the North Ethiopian Highlands (Amanuel Zenebe, 2009; Vanmaercke et al., 2010). We also find a very strong relation between peak discharge (Q_p) and the number of trapped pebbles NTP (Pearson product-moment correlation = 0.97). The following equation could be established:

$$NTP = 0.3751 Q_p + 0.0731 \qquad (R^2 = 0.94;\ p < 0.05) \qquad (6.3)$$

The relationships between Q_p and the number of trapped pebbles taking into account pebble sizes, as well as between Q_p and bed load transport (BT) (m^3) were weaker and not significant. Moreover, there is no tendency in bed load transport volumes apparent over the rainy season (Figure 6.5). However, a significant logarithmic relation was identified between 24h-rainfall (R_{24}) and bed load transport. Hence, even under relatively small amounts of rainfall (R_{24} < 10 mm), bed load transport can be substantial (Figure 6.7).

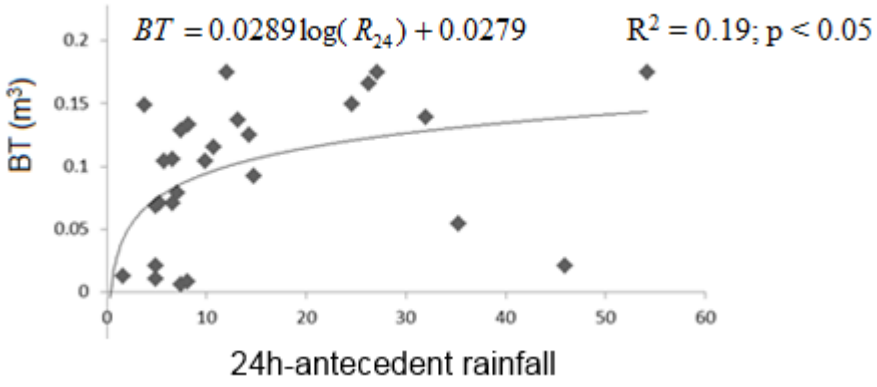

Figure 6.7 Bed load transport (BT) as a function of 24-hour antecedent rainfall.

6.3.3 Factors controlling sediment deposition

6.3.3.1 Sediment deposition as controlled by microtopography

Mean deposition per flood in micro channels was compared with mean deposition per flood on micro ridges, by means of a non-parametric t-test. Mean vertical change in micro-channels over the rainy season was - 0.49 cm per marker per flood (net incision), while it was + 0.07 cm per marker per flood (net aggradation) on the micro-ridges. The difference between both means is significant at the 0.1 level ($p = 0.09$).

6.3.3.2 Sediment deposition as controlled by fan location

Analysis of variance showed that mean deposition on at least one debris fan was significantly different from mean deposition on other debris fans ($p < 0.05$). Post-hoc analysis with non-parametric t-tests allowed further characterization. Mean deposition on DF4 was + 0.038 cm per marker per flood, while this was - 0.077 cm on DF3, - 0.005 cm on DF2 and - 0.059 cm on DF1. Only the difference between DF4 (overall net deposition) and the other debris fans (overall net incision) is significant ($p = 0.03$). Interestingly, the current deposition is in DF4 while the sediment is channeled through DF1, DF2 and DF3 that are eroded out. An upstream clear water effect can hence facilitate sediment deposition further downstream, a situation that was also observed on larger scale in the nearby Gra Kashu catchment (Tesfaalem et al., 2015).

6.3.3.3 Downstream transfer as controlled by the water-sediment balance

A t-test shows that the ratio rainfall depth / bed load transport is significantly higher during events with 'sediment transfer to the lake' (ratio = 55.7), as compared to events where the sediment is essentially deposited in the debris fans (ratio = 8.4) ($p < 0.05$). The 'magnitude of downstream transfer' is strongly and positively correlated with the ratio rainfall depth / bed load transport (Spearman rank-order correlation = + 0.78). Assuming equal intervals (presuming that the distances between ordinal scores are equal; Howell, 1997), linear regression facilitated explanation of the 'magnitude of downstream transfer' by the ratio rainfall depth / bed load transport ($p < 0.05$; $R^2 = 0.50$). Thus, significantly more sediment is transferred downstream or towards the lake if rainfall (modeled peak discharge) is high; or if the amount of mobilized bed load in the channels is relatively low ('clearer water').

6.3.4 Short-lived isotope counts

Changes in gully activity over 70 years could be derived from the short-lived isotope counting of the subaquatic lacustrine debris fan (Table 6.2). Overall, ^{210}Pb isotope values are low, probably resulting from the semi-arid climatic conditions. The unsupported ^{210}Pb, transported from the gully watershed, increases from the bottom of the core towards 7 cm, then stays roughly constant up to the top of the core. Assuming a constant-rate-of-supply, dates were calculated (Table 6.2). Mass-median-diameter (D_{50}), silty fractions and clay fractions give an indication of sediment flux activity (Figure 6.8). At 7-9 cm depth, there are higher abundances of coarser silty grains, while almost no clay is deposited at that time (~ 1980s). The deposition rates increase gradually over time and accelerate after the 1980s (Figure 6.8).

Table 6.2 ^{210}Pb dating results (based on the constant-rate-of-supply model) of the subaquatic lacustrine debris fan; as well as mass-median-diameter of the sediment (D_{50}, in µm).

Depth (cm)	^{210}Pb activity (Bq/g)	^{226}Ra daughters (Bq/g)	^{210}Pb unsupported (Bq/g)	Error ^{210}Pb unsupported (mBq/g)	*Pb age with error (CE)*	D_{50} (µm)
1	0.103245	0.008189	0.096452	12	2013	28.2
2						19.0
3	0.108447	0.005513	0.104454	11	2010 ± 2.1	21.4
4						33.3
5	0.115254	0.009735	0.107086	12	2005 ± 2.3	26.1
6						44.1
7	0.104155	0.004496	0.101165	12	1998 ± 2.5	24.7
8						35.3
9	0.082415	0.010037	0.073478	11	1989 ± 2.7	28.1
10						29.6
11	0.073760	0.008922	0.065830	10	1979 ± 3.0	46.5
12						29.9
13	0.067482	0.006705	0.061718	9	1966 ± 3.5	32.0
14	0.088819	0.005531	0.084597	11	1948 ± 4.5	34.3
15						39.2

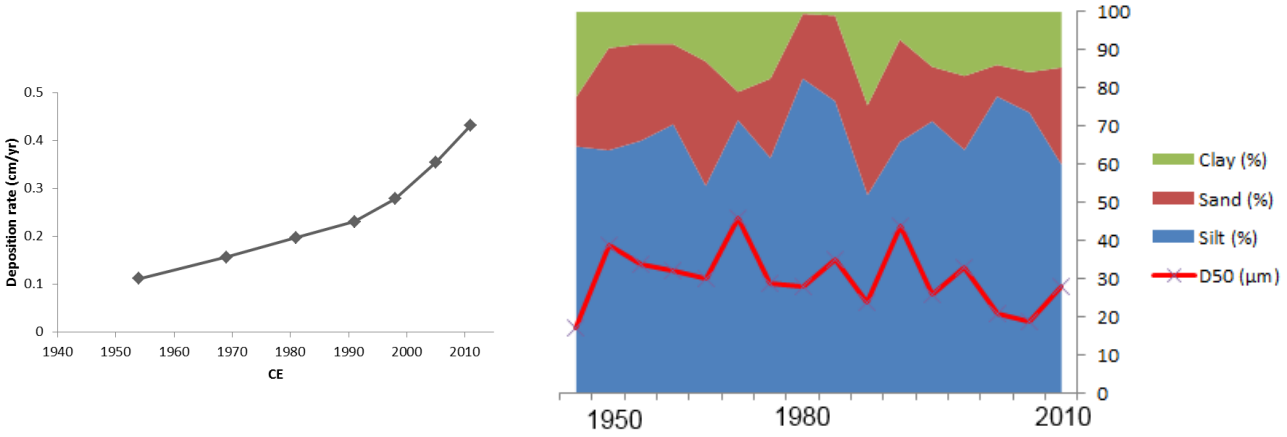

Figure 6.8 (left) Deposition rates (cm/yr) in function of time of deposition (middle of the time interval between two dates) show the recent effect of 'clearer water'; (right) D50 (µm), sandy, silty and clayey fraction (in %) in function of time show decreasing clay deposition around the 1980s.

6.3.5 Farmers' assessments on the age of debris fan deposition

No farmers remembered the earliest period (before 1950) and few farmers remembered the period before the 1970s or their answers were considered to be inconsistent. During the 1970s to the 1990s, the biggest debris fan adjacent to the lake (DF4) appeared. According to all farmers, DF4 is considered as the oldest deposit (~ 30-40 years). Several farmers state that a deep gully was then located at the place of DF1, DF2 and DF3. Later, around the year 2000, the second biggest debris fan (DF3) appeared, just upstream of DF4. The appearance of DF2 was estimated around 2005-2010, as was DF1.

To date, the debris fans remain active. The farmers point at a continuing growth of DF3 and DF4, among others by stating that 'DF3 was much smaller ten years ago, as it was partly a grazing land'; and that 'DF4 is becoming wider and wider over recent years'.

6.3.6 Changes to sediment deposition retrieved from aerial photographs

Lake Ashenge is visible on the earliest aerial photograph (1936). Around the lake, no debris fans can be seen while the photo also shows a house surrounded by trees just to the southwest of the studied gully. These are still visible on the 1965 photograph, while a shallow sediment accumulation (located at the current position of DF3) developed just downstream of a small channel incision near the house and along a line of euphorbias (Figure 6.9). These elements are no longer visible on the aerial photograph of 1986, depicting a debris fan further downstream at the lake shore. While there is no sign of other shallow zones or debris fans along the gully, a broader incision is present at the location

of the former sediment accumulation (DF3) that was visible on the 1965 photograph (Figure 6.9). Some farmlands that were visible near the lake on the 1965 photograph were covered with sediment in 1986. The CNES-Astrium images show the current situation, while DF3 reappears on the image, two other debris fans appear more upstream and DF4 covers a larger area than in 1986 (Figure 6.9).

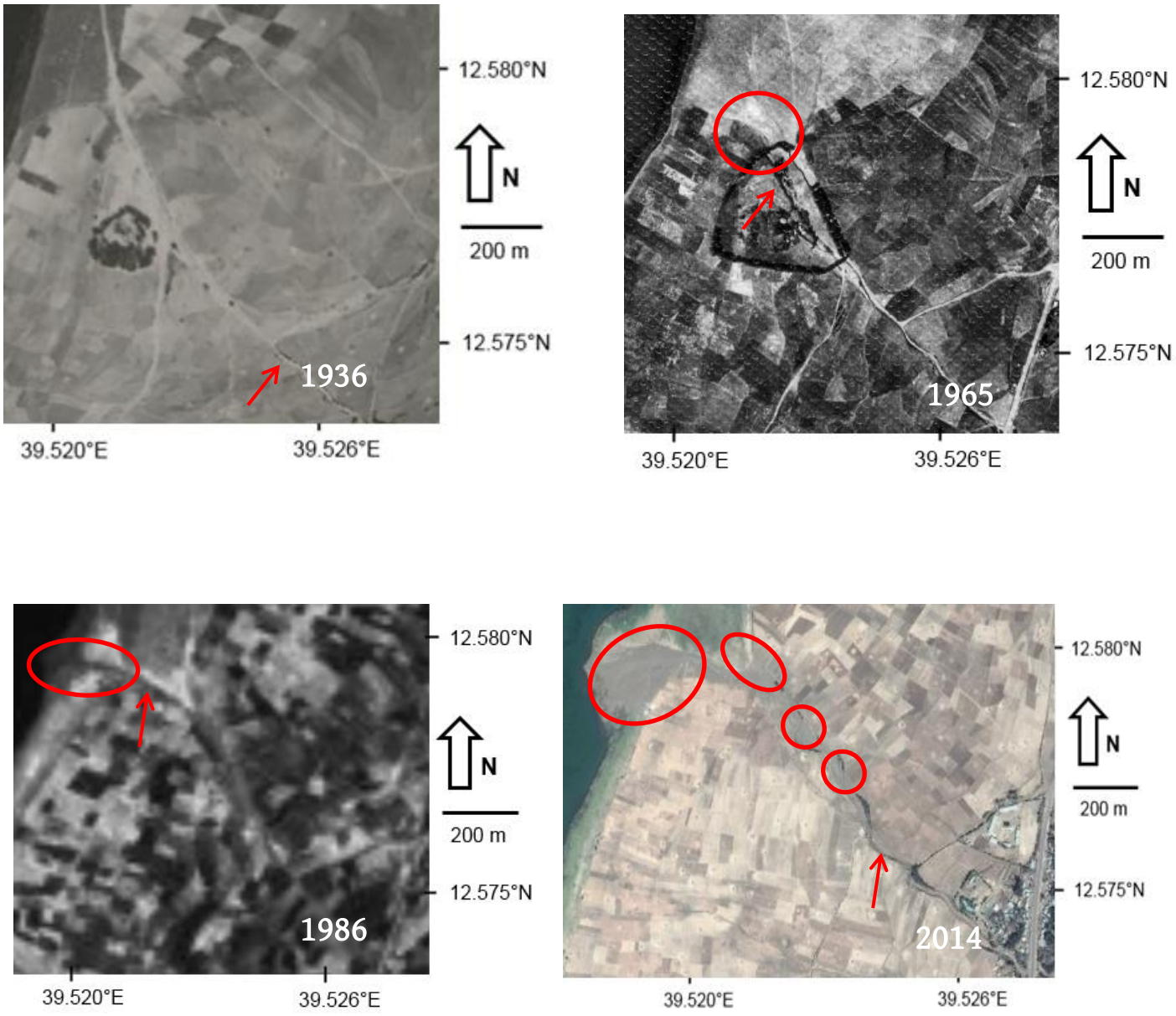

Figure 6.9 The Menkere gully as visible on the aerial photographs of 1936 (up left), 1965 (up right), 1986 (down left) and 2014 (down right). Minor flat zones (sediment accumulations) are indicated with red circles; active incisions with red arrows.

6.3.7 Chronology of alluvial debris fan evolution

Linking the semi-structured interviews, the sequence of aerial photographs, the ^{210}Pb isotope dating and the significantly positive relation between magnitude of downstream transfer and discharge/sediment, facilitates the reconstruction of the sedimentary evolution of the gully since the 1930s (Table 6.3). Conceptually, we identify five different sedimentary "periods"; in so doing, we show that flashflood sediments can be useful proxies for land degradation.

Table 6.3 Evidence for gully debris fan evolution since the 1930s.

Phase	Date	Available data	Sources
I	1930s-1950s	no debris fans apparent subaquatic clay deposition	aerial photograph 1936 short core
II	1960s-1970s	higher D_{50} in subaquatic core sediment accumulation	short core aerial photograph 1965
III	1970s-1990s	appearance of DF4 subaquatic silt deposition	aerial photograph 1986 / interviews short core
IV	2000s	upslope migrating debris fans subaquatic clay deposition	interviews short core
V	2010s	gully cut activity	field observations

6.3.7.1 Sedimentary Phase I (1930s – 1950s): low peak discharges

As there are no debris fans visible on the early aerial photograph, and given the relatively high proportions of clay in the shallow core (Figure 6.8), the first half of the 20th century was a period with relatively low peak discharges. According to Frankl et al. (2011), upslope gullies around Ashenge were stabilized during this period. Land use in the upper catchment was already dominated by cereal agriculture, but many trees and shrubs were present on lynchets, steep slopes and in the stream bed (Figure 6.10).

Figure 6.10 Terrestrial photograph of the upper catchment of Menkere gully in 1937 (courtesy of IAO Firenze). Upstream, from the road crossing, the top of the shrubs that grew in the gully are visible. Valley bottoms are under cereal agriculture, with many shrubs growing on the lynchets; many trees grow on steeper slopes. Menkere village was located essentially on the hill at centre left; larger trees surround the church.

6.3.7.2 Sedimentary Phase II (1960s – 1970s): increasing discharges and sediment supply

The mass-median-diameter of the shallow core peaks at 50 µm during the 1970s (Figure 6.8). The aerial photograph shows sediment accumulation along the gully at the current location of DF3 (Figure 6.9), although there is no sign of debris fans at the lake shore. This must have been a period with predominantly higher discharges and sediment supply from the catchment. Upslope gullies were still quite stable, with a position of the lower gully end similar to the 1930s (Frankl et al., 2011). These authors infer a drainage density of 22.26 m ha^{-1} in a nearby catchment around Lake Ashenge in 1965.

6.3.7.3 Sedimentary Phase III (1970s – 1990s): high discharges

The interview records on this period are in line with the appearance of DF4 on the aerial photograph of 1986, while the former sediment accumulation (DF3) gets incised. This indicates a period with predominantly high discharges and high amounts of sediment towards DF4 and the lake. During the 1980s, the subaquatic debris cone contains more coarse grains, shown by higher proportions of silty grains (up to 85 %) (Figure 6.8). At the same time, only a small proportion of clay was present in the core (< 10 %). These findings are in line with the observations of Frankl et al. (2011), who identify

incision in the lower valley floor with a sediment fan in a neighboring catchment by 1975. Eleven years later, the lowest gully end was located more downstream with a drainage density of 24.96 m ha^{-1}. A debris fan is then clearly visible (Frankl et al., 2011).

6.3.7.4 Sedimentary Phase IV (2000s): upslope migrating debris cones

Following the interviews and the appearance of DF1 and DF2, the debris fans are developing as an "upslope migrating" sequence, during a period with decreasing discharges. While DF4 continues to grow and DF3 reappears, the upper sections of the shallow lake core contain again higher relative amounts of clay (Figure 6.8). By 2009, the drainage density of the neighboring catchment was 24.59 m ha^{-1} (Frankl et al., 2011).

6.3.7.5 Sedimentary Phase V (2010's): observations of a clear water effect

We observed recent gully incision activity, indicative of even lower amounts of sediment supply towards the gully segment. In particular, DF1 and DF2 are incised by a channel, according to all farmers no older than 3 years. About 100 m upstream of DF1, this young channel incises the former gully bottom, resulting in a small terrace sculpted in the alluvio-colluvial mother mantle. Under decreased amounts of upstream sediment supply, a clear water effect can explain the increased deposition rates under decreased mass-median-diameters at the subaquatic Korem gully debris fan during this period (Figure 6.8), probably originating from activation of finer micro-channel material.

6.4 Discussion

6.4.1 Co-evolution of erosional and depositional phases

The evolution of alluvial fan sedimentation corresponds well with periods of gully erosion and drainage density of gully channels identified by Frankl et al. (2011, 2013). These authors could detect three broad periods of gully erosion over the 20th century, by studying historical terrestrial and aerial photographs: (i) a stage with stable first order channels 1886-1965; (ii) a stage with activation of first order streams 1965-2000; and (iii) a stage of de-activation of first order streams 2000-present (Frankl et al., 2011, 2013). Their first stage of first order channel stability correlates well with Phase I of our

sediment supply history; as is their second stage similar with our Phases II and III; and their third stage with our Phases IV and V. Such findings are also broadly in line with longer-term gully dynamics over the past millennia, as we related phases of downstream valley aggradation in the Northeastern Highlands with increases in sediment supply and upstream erosive activity (Chapter 5). Taking the co-evolution of erosional and depositional phases together, we conceive an 'accordion' system – illustrating the connectivity between both upstream and downstream channel ends. During periods with stable upstream channels, downstream no sedimentation occurs. During periods with active upstream channels and retreating gully heads, or when a clear water effect is present (eroding out the upstream debris fans), progressive downstream sedimentation occurs. Under an 'intermediate' regime, the system of debris fans can migrate downstream or upstream. This kind of geomorphic behavior is in line with general alluvial fan theory (Knighton, 1998; Graf, 2002). Broadly, alluvial fans develop when channel widening allows for channel migration (e.g. at the Ashenge shore) and when upland erosion increases the sediment supply (Graf, 2002). Indeed, the upland basin is the main sediment source for fan growth, notably when sediment production is high compared to sediment transport capacity (Knighton, 1998). These results are also in line with the theory of Exner (1920, 1925) that the rate erosion/deposition in a stream segment is proportional to the gradient of water flow velocity in the segment (Exner, 1925) and negatively related with the rate of bed load transport from upstream (Exner, 1920).

6.4.2 Relation with land policies, drought and the Ashenge lake level

The phases of alluvial fan accumulation as identified in this study and the phases of active gully erosion as identified by Frankl et al. (2011, 2013) also correlate well with changes in North Ethiopian land policies. In chapter 3, we described three main political-ecology eras (the late feudal era, the civil war and the post-revolution era), each with a specific configuration of land and conservation policies. Under the late feudal land system, tenure insecurity under the *mwufar* sharecropping system discouraged investments in land conservation and poor farmers had to farm on steeper slopes. Moreover, in the nearby Gra Kashu catchment, the proportion of cropland was at its maximum and occupied very steep slopes during the 1960s, when there was a minimum of woody vegetation (De Meyere et al., 2015). The pre-1980 appearance of sediment fans and the peaking mass-median-diameters in the subaquatic debris then result from the degraded socio-environmental situation inherited from that late-imperial period (Sedimentary Phase II).

Further, appearance of alluvial fans (Sedimentary Phase III) during the eighties coincided with the civil war, economic decline and a lack of investment in conservation efforts (Chapter 3). After a period of relatively high rainfall, a series of droughts struck the decade of the 1980s, as influenced by the interplay of several oceanic oscillations (Chapter 2). This must have had an impact on the Ashenge Lake level; Schuett and Busschert (2005) report high lake levels during the 1930s and 1960s, 10 m above present levels, based on oral evidence. The lake level was low during the 1980s with lake levels about 5 m lower than present (Figure 6.11). Hence, the hydraulic base level lowered, further facilitating gully incision. However, the position of the debris fans cannot be explained by lake levels as lake levels have been lower than the fans, at least since the 1970s. Today the lake has risen as indicated by drowned trees near the western shore (Schuett and Busschert, 2005). After the regime change in 1991, intensive conservation efforts (Chapter 3) clearly succeeded in a reduction and overall stabilization of sediment supply (Sedimentary Phases IV and V).

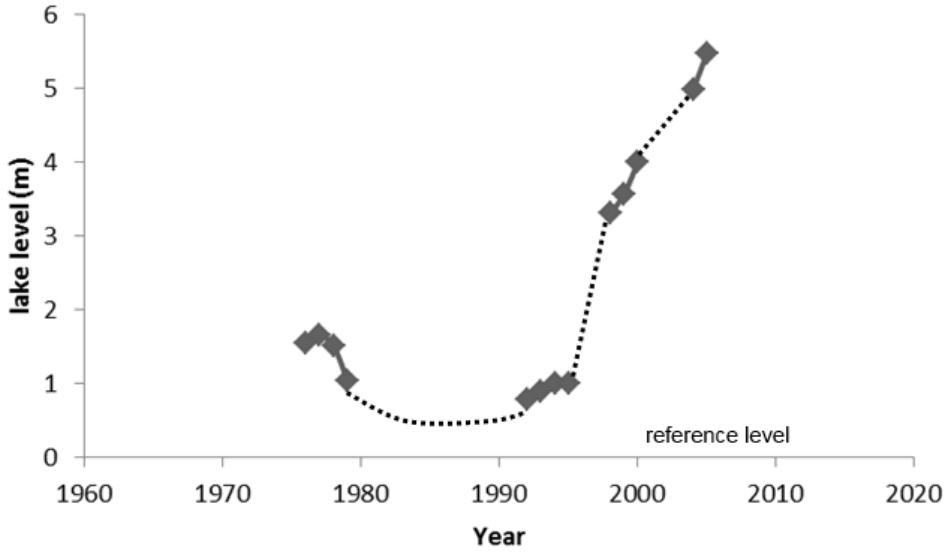

Figure 6.11 The lake level of Lake Ashenge (courtesy of Dr. Enyew Adgo, Bahir Dar University, based on data from the Ethiopian Ministry of Water and Energy).

6.5 Conclusions

In this chapter, we show that flashflood sediments can deliver information on the development of land degradation, if the contemporary relations between flashfloods and sediment are well

understood. We employed semi-structured interviews on debris fan activity, aerial photographs, short-lived ^{210}Pb isotope counting and the data from a measurement campaign (July-September 2014) in one gully system near Lake Ashenge. The monitoring, including rainfall, peak discharge, bed load transport, suspended sediment load and sediment deposition rates, shows that downstream sediment transfer significantly depends on the prevailing discharge-sediment balance. This allowed the reconstruction of the sedimentary evolution of the gully over the past half century. We identified five different sedimentary periods: (i) a period of sedimentary stability in the early 20th century; (ii) a period of sedimentary destabilization in the 1960s – 1970s; (iii) a phase of sedimentary instability in the 1970s – 1980s; (iv) a phase of upslope migrating debris cones in the 1990s – 2000s; and finally (v) a period with more clear water effects (2010s). During phases of retreating gully heads, progressive downstream sedimentation occurs in the alluvial debris fans; while 'clearer water' results in increased deposition of finer sediment particles in the lake. The periods of active gully sedimentation correlate well with periods of intensive gully erosion; and clearly co-evolve with periods of decreased vegetation cover under insecure land tenure, drought and lower base levels.

Acknowledgements

This study became possible thanks to the support of our translator Bereket and of Anthony Denaeyer, the support of our data collectors Hayelom and Meles, the help of Etefa Guyassa and the funding by UGent's Special Research Fund. Special thanks go to Dr. Sébastien Bertrand for his help on the lead dating, to the fishermen of Lake Ashenge for providing boat transport, to the Mekele University Soil Laboratory for the suspended sediment load analysis, to the UGent sedimentology laboratory and to the dating laboratory of the Centre d'Etudes Nordiques (Québec, Canada).

6.6 References

Amanuel Zenebe, 2009. Assessment of spatial and temporal variability of river discharge, sediment yield and sediment-fixed nutrient export in Geba River catchment, northern Ethiopia. Unpublished PhD thesis, KULeuven, Belgium.

Appleby, P., 1978. The calculation of lead-210 dates assuming a constant rate of supply of unsupported 210Pb to the sediment. Catena 5 (1), 1–8.

Avni, Y., 2005. Gully incision as a key factor in desertification in an arid environment the Negev highlands, Israel. Catena 63 (2-3), 185-220.

Blair, T., 1999. Sedimentology of the debris-flow-dominated Warm Spring Canyon alluvial fan, Death Valley, California. Sedimentology 46, 941-965.

Blair, T., 2000. Sedimentology and progressive tectonic unconformities of the sheetflood-dominated Hell's Gate alluvial fan, Death Valley, California. Sedimentary Geology 132, 233-262.

Bull, W., 1997. Discontinuous ephemeral streams. Geomorphology 19, 227–276.

Carnicelli, S., Benvenuti, M., Ferrari, G., Sagri, M., 2009. Dynamics and driving factors of late Holocene gullying in the Main Ethiopian Rift (MER). Geomorphology 103 (4), 541-554.

Chiverrell, R., Harvey, A., Foster, G., 2007. Hillslope gullying in the Solway Firth – Morecambe Bay region, Great Britain: Responses to human impact and/or climatic deterioration? Geomorphology 84, 317-343.

Chow, V., 1959. Open-channel hydraulics. McGraw-Hill, New York, USA, 680 p.

De Meyere, M., Tesfaalem G. Asfaha, Frankl, A., Mitiku Haile, Nyssen, J., 2015. Land cover trajectories and runoff response on the Ethiopian Rift Valley escarpment over the last eight decades. Geomorphology, submitted.

Eriksson, M., Olley, J., Payton, R., 2000. Soil erosion history in central Tanzania based on OSL dating of colluvial and alluvial hillslope deposits. Geomorphology 36, 107-128.

Exner, F., 1920. Zur physik der dunen. Akad. Wiss. Wien Math. Naturwiss. 129, 929-952.

Exner, F., 1925. Uber die Wechselwirkung zwischen Wasser und Geschiebe in Flussen. Akad. Wiss. Wien Math. Naturwiss. 134, 165-203.

Frankl, A., Nyssen, J., De Dapper, M., Haile, M., Billi, P., Munro, N., Deckers, J., Poesen, J., 2011. Linking long-term gully and river channel dynamics to environmental change using repeat photography (Northern Ethiopia). Geomorphology 129, 238-251.

Frankl, A., Poesen, J., Mitiku Haile, Deckers, J., Nyssen, J., 2013. Quantifying long-term changes in gully networks and volumes in dryland environments: the case of Northern Ethiopia. Geomorphology 201, 254–263.

Graf, W., 2002. Fluvial processes in dryland rivers. The Blackburn Press, Caldwell, USA.

Grenfell, S., Rowntree, K., Grenfell, M., 2012. Morphodynamics of a gully and floodout system in the Sneeuberg Mountains of the semi-arid Karoo, South Africa: Implications for local landscape connectivity. Catena 89, 8-21.

Harvey, A., 2012. The coupling status of alluvial fans and debris cones: a review and synthesis. Earth Surface Processes and Landforms 37, 64-76.

Hjulström, F., 1935. Studies on the morphological activity of rivers as illustrated by the river Fyris. Les Études rhodaniennes 11 (2), 255-256.

Howell, D., 1997. Statistical methods in psychology (4th ed.). Duxbury Press, Belmont, USA.

Knighton, D., 1998. Fluvial forms and processes, a new perspective. Hodder Education, London, UK.

Kurkura Kabeto, Aynalem Zenebe, Bheemalingeswara, K., Kinfe Atshbeha, Solomon Gebresilassie, Kassa Amare, 2012. Mineralogical and Geochemical Characterization of Clay and Lacustrine Deposits of Lake Ashenge Basin, Northern Ethiopia: Implication for Industrial Applications. Momona Ethiopian Journal of Science (MEJS) 4 (2), 111-129.

Lafortune, V., Filion, L., Hétu, B., 2006. Impacts of Holocene climatic variations on alluvial fan activity below snowpatches in subarctic Québec. Geomorphology 76, 375-391.

Laronne, J., Reid, I., 1993. Very high bedload sediment transport in desert ephemeral rivers. Nature 366, 148-150.

Merla, G., Abbate, E., Azzaroli, A., Bruni, P., Canuti, P., Fazzuoli, M., Sagri, M., Tacconi, P., 1979. A Geological Map of Ethiopia and Somalia (1973). 1:2000.000; and Comment. University of Florence, Firenze, Italy.

Micromeritics, 2014. Overview SediGraph III Plus. http://www.micromeritics.com/ (accessed on 14/05/2014)

Nyssen, J., Vandenreyken, H., Poesen, J., Moeyersons, J., Deckers, J., Mitiku Haile, Salles, C., Govers, G., 2005. Rainfall erosivity and variability in the Northern Ethiopian Highlands. J. Hydrology 311, 172–187.

Nyssen, J., Poesen, J., Veyret-Picot, M., Moeyersons, J., Mitiku Haile, Deckers, J., Dewit, J., Naudts, J., Kassa Teka, Govers, G., 2006. Assessment of gully erosion rates through interviews and measurements: a case study from northern Ethiopia. Earth Surface Processes and Landforms 31 (2), 167–185.

Nyssen, J., Petrie, G., Sultan Mohamed, Gezahegne Gebremeskel, Frankl, A., Stal, C., Seghers, V., Debever, M., Demaeyer, Ph., Kiros Meles Hadgu, Billi, P., Mitiku Haile, 2015. Historical aerial photographs of Ethiopia in the 1930s and their fusion with current remotely sensed imagery for retrospective geographical analysis. Journal of Cultural Heritage, submitted.

Prosser, I., Chappell, J., Gillespie, R., 1994. Holocene valley aggradation and gully erosion in headwater catchments, southeastern highlands of Australia. Earth Surface Processes and Landforms 19, 465–480.

Reid, I., Laronne, J., 1995. Bedload sediment transport in an ephemeral stream and comparison with seasonal and perennial counterparts. Water Resources Research 31, 773-781.

Reid, I., Powell, D., Laronne, J., 1996. Prediction of bedload transport by desert flash-floods. Journal of Hydraulic Engineering of the American Society of Civil Engineers 122, 170-173.

Reid, I., Laronne, J., Powell, D., 1998. Flash-flood and bedload dynamics of desert gravel-bed streams. Hydrological processes 12, 543-557.

Schuett, B., Busschert, R., 2005. Geomorphological reconstruction of palaeo Lake Ashengi, Northern Ethiopia. Lake Abaya Research Symposium Proceedings, Siegen, Germany. FWU Water Resources Publications, 51-57 p.

Sweeney, M., Loope, D., 2001. Holocene dune-sourced alluvial fans in the Nebraska Sand Hills. Geomorphology 38, 31-46.

Tesfaalem G. Asfaha, Frankl, A., Mitiku Haile, Nyssen, J., 2015. Catchment rehabilitation and hydro-geomorphic characteristics of mountain streams in the western Rift Valley escarpment of Northern Ethiopia. Land Degradation and Development, online early view. DOI: 10.1002/ldr.2267.

Uwitec, 2014. Uwitec Sampling Equipment. http://www.uwitec.at/ (accessed on 12/12/2014)

Vanmaercke, M., Amanuel Zenebe, Poesen, J., Nyssen, J., Verstraeten, G., Deckers, J., 2010. Sediment dynamics and the role of flash floods in sediment export from medium-sized catchments: a case study from the semi-arid tropical highlands in northern Ethiopia. Journal of Soils and Sediments 10 (4), 611-627.

Vanmaercke, M., Poesen, J., Verstraeten, G., Maetens, W., de Vente J., 2011. Sediment yield as a desertification risk indicator. Science of the Total Environment 409, 1715-1725.

Verstraeten, G., Poesen, J., 2001. Modelling the long-term sediment trap efficiency of small ponds. Hydrological Processes 15, 2797–2819.

Zygmunt, E., 2009. Alluvial fans as an effect of long-term man-landscape interactions and moist climatic conditions: A case study from the Glubczyce Plateau, SW Poland. Geomorphology 108, 58-70.

Chapter 7 Lakes records: indicators for hydroclimatic changes during the Holocene

This chapter is modified from:

Lanckriet, S., Rangan, H., Nyssen, J., Frankl, A., 2015. The influences of Holocene climatic shifts and cattle migrations on land cover and land use in the Ethiopian Highlands. Plos One, submitted.

Abstract

The Ethiopian Highland is very sensitive to the occurrence of periodic droughts, partly because of its location at the northern edge of the Intertropical Convergence Zone. This chapter presents a diachronic synthesis of hydroclimatic shifts in the Ethiopian Highlands from the late Pleistocene onwards. We integrate paleolacustrine records from the wider Horn of Africa to determine distinct past dry phases. Based on the datasets, we discern Late Pleistocene dry phases in the region during the Last Glacial Maximum, the Heinrich 1 event and the Younger Dryas. Additionally, we recognize six dry phases during the Holocene. These were Holocene 1 (Hol-1), between 6650 and 5850 BCE; Holocene 2 (Hol 2), between 4900 and 4800 BCE; Holocene 3 (Hol-3), between 3700 and 1300 BCE; Holocene 4 (Hol-4), between 1100 to 650 BCE; Holocene 5 (Hol-5), between 450 CE and 1200 CE; and Holocene 6 (Hol-6), between 1750 and 1900 CE. The hydroclimatic shifts seem associated with cooler equatorial Atlantic and western Indian Ocean sea surface temperatures. Overall, this chapter highlights the importance of integrating paleo-climatic and paleo-oceanic records for more accurate understanding of droughts in African drylands.

7.1 Introduction

Ethiopia is vulnerable to the regular occurrence of dry spells, to some extent since the country is situated at the northern boundary of the Intertropical Convergence Zone (Marshall et al., 2009). Studying climatic variability in the Ethiopian Highlands is important because of the strong interactions between long-term climatic variability, land degradation and hydrogeomorphic change taking place in the region (Frankl et al., 2011, 2013). Ethiopia is often perceived as a region plagued by drought, land degradation and famine. The linkages between climate, land degradation, surface water processes and crop production are quite complex (Rosell, 2011; Frankl et al., 2013). Ethiopia is sometimes named 'the water tower of Africa', since its' surface runoff waters account for about 85 % of the Nile flow (Yacob and Imeru, 2005; Tesfamichael Gebreyohannes et al., 2013). Notably, land degradation processes, such as severe erosion and water runoff, are very active in the North Ethiopian Highlands (Nyssen et al., 2004).

A significant number of paleo-climatic datasets from the region exists (see section 7.2.2) but these records lack overall integration (Umer, 2010). In order to synthesize the long-term patterns of hydroclimate in the Ethiopian Highlands, in this short chapter we integrate paleolacustrine datasets from the wider region.

7.2 Materials and methods

7.2.1 General approach

We reviewed a number of recently published paleoclimatic studies (n = 10) and paleo-oceanic studies (n = 5). We compiled the timing of events reported in these studies, usually derived from radiocarbon or ^{210}Pb dating. For reasons of consistency, we expressed all Pleistocene dates in 'ka BP' and all Holocene calibrated radiocarbon dates in '(B)CE'. We calibrated all non-calibrated radiocarbon dates with the CalPal-2007-Hulu curve, a radiocarbon calibration curve built with U/Th-dated coral data (see Weninger and Jöris, 2008). Following Walker et al. (2012), we set the Early-to-Middle Holocene division at 6200 BCE and the Middle-to-Late Holocene division at 2200 BCE.

7.2.2 Paleoclimatic datasets

7.2.2.1 Paleolacustrine records

Over the past few decades, several paleolacustrine records have been derived from lakes across Ethiopia (Figure 7.1). Given their high sensitivity to shifts in the regional precipitation/evaporation balance, paleolacustrine records (some from endorheic lakes) are the most suitable proxies for assessing past dry periods in the region. Because of the strong interactions between drought, agricultural production and hydrogeomorphic processes in the Highlands (Frankl et al., 2011; 2013), we focused on the variability of dry periods rather than on the temporal evolution of wet, cold or warm conditions. We determine the timing of Holocene dry phases as reported in 10 paleolacustrine studies from the Highland/Rift area (Lake Abhé, Ziway Shala, Ashenge, Tana, Tilo, Hayk and Abiyata) (Table 7.1). Most of the records are based on diatom and stable isotope analysis, while others are based on geophysical and geochemical analyses or geomorphological investigation to reconstruct paleo lake levels (Table 7.1). As we could not directly access the data from these studies, we based our synthesis on the interpretation of the records as reported in the publications. We delineated and coded all clearly demonstrated Holocene dry phases ('Hol-1' to 'Hol-6').

Table 7.1 Paleoenvironmental records in the Horn of Africa, with their temporal coverage and the main proxies involved.

Number on map (Figure 7.1)	Record	Temporal coverage	Number of radiocarbon dates for age control	Hydroclimatic proxies	Reference
1	Lake Tana (a)	~17000-year	17	magnetic and geochemical data	Marshall et al. (2011)
1	Lake Tana (b)	~19000-year	16	seismic data	Lamb et al. (2007b)
2	Lake Ashenge	~17000-year	10	diatom and oxygen isotope	Marshall et al. (2009)
3	Lake Hayk (a)	~2000-year	4[a]	oxygen and carbon isotope	Lamb et al. (2007a),
3	Lake Hayk (b)	~3500-year	22	stratigraphical and geomorphological analysis	Ghinassi et al. (2012)
4	Lake Abhé	~12000-year	37	diatoms	Gasse (2000)
5	Lakes Ziway Shala	~12000-year	18	diatoms	Gasse (2000)
6	Lake Abiyata (a)	200-year	3[b]	diatoms and salinity	Legesse et al. (2002)
6	Lake Abiyata (b)	~14000-year	11	diatoms	Chalié & Gasse (2002)
7	Lake Tilo	~9000-year	14	pollen and diatom and oxygen-isotopes	Lamb et al. (2000)

[a] Supplemented with 9 ^{210}Pb dates
[b] Supplemented with 24 ^{210}Pb dates

7.2.2.2 Marine records to synthesize hydroclimatic shifts on a regional scale

In order to validate whether dry periods are site-specific or reflect paleo-climatic shifts on a broader regional or global scale, we compared the paleo-lacustrine records with each other and considered a number of previously obtained marine records to geographically synthesize the timing of significantly dry periods. As the Ethiopian hydroclimate is extremely sensitive to changing sea surface temperatures (Lyon & DeWitt, 2012; Liebmann et al., 2014), marine records can help in validating the occurrence of region-wide hydroclimatic shifts. We incorporated 5 records, including a marine record of hydrogen isotopic composition of leaf wax (with enriched deuterium values pointing to drier conditions) that was recently retrieved from near the coast of Djibouti-Eritrea (Gulf of Aden), as well as foraminiferal records from the Atlantic and Indian Oceans (Table 7.2).

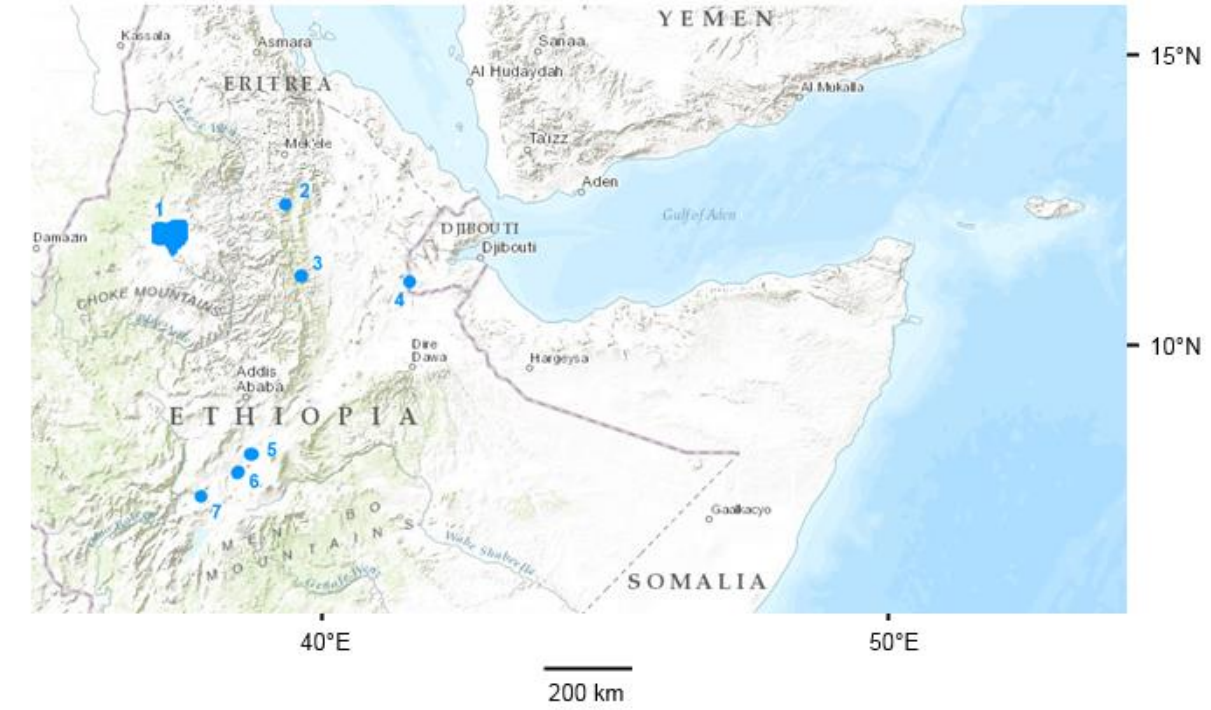

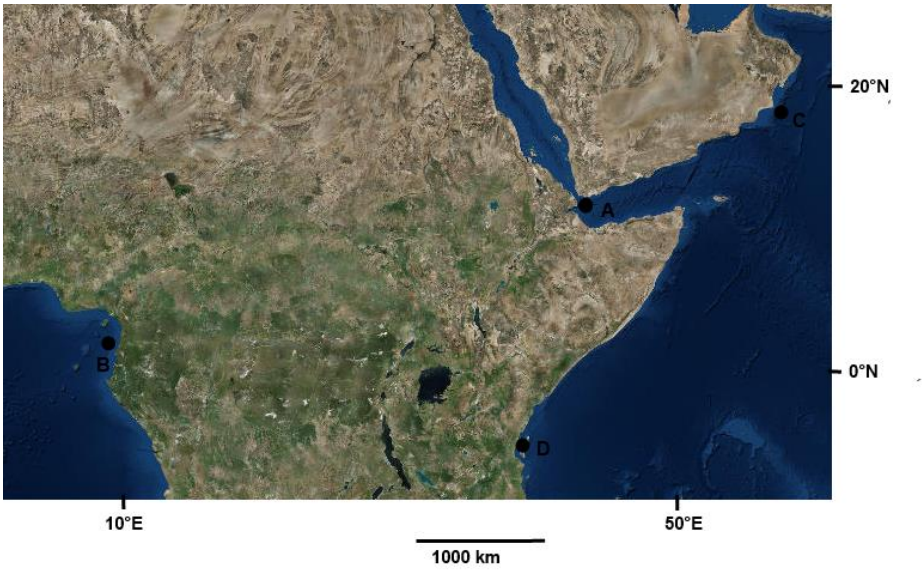

Figure 7.1 (upper figure) Study region with indication of investigated lakes (blue; numbers mentioned in Table 7.1). Background is given by the U.S. National Park Service (NPS) Natural Earth physical map; grey tone for relief and green for forest; dotted lines for disputed borders. (lower figure) Location of oceanic records (black; see Table 7.2 for codes). Background is given by GeoEye® satellite imagery.

Table 7.2 Marine records used to validate hydroclimatic shifts recorded in the lake sediments, with their temporal coverage and the main proxies involved.

Letter on map (Figure 7.1)	Record	Temporal coverage	Number of radiocarbon dates for age control	Hydroclimatic proxies	Reference
A	Gulf of Aden	~40000-year	20	hydroclimatic record of hydrogen isotope composition of leaf waxes	Tierney and de Menocal (2013)
B	Eastern Equatorial Atlantic	~22000-year	12	Mg/Ca sea-surface temperature record (Globigerinoides ruber foraminifera)	Weldeab et al. (2005)
C	Arabian Sea	~11000-year	11	record of monsoonal activity (Globigerina bulloides foraminifera)	Gupta et al. (2003)
	Indian Ocean	~400-year		synthesis of tropical coral archives	Tierney et al. (2015)
D	Western Indian Ocean	~10000-year		foraminiferal Mg/Ca ratios and $\delta^{18}O$	Kuhnert et al. (2014)

7.3 Results

7.3.1 Late Pleistocene dry periods

Records spanning back to the Late Pleistocene show that the Last Glacial Maximum (LGM; 26-19 ka BP) was generally dry. Hydrogen isotopic composition of leaf waxes in the Gulf of Aden gradually became more negative since ~ 40 ka BP and attained a low plateau during the LGM (Tierney and deMenocal, 2013).

Studies from the coastal zones to the Highlands of the Horn all show the persistence of dry conditions after 19 ka BP (Tierney and deMenocal, 2013; Marshall et al., 2009; Marshall et al., 2011; Lamb et al., 2007b). Tierney and deMenocal (2013) discern a sharp (more negative) drop in these hydrogen isotope values between 18-19 ka BP. A desiccation surface with stiff sediments was deposited in shallow waters at Lake Tana around ~ 18.7 ka BP across nearly the entire lake floor (Lamb et al., 2007b). Pollen evidence from Lake Tana pointed to abundances of xerophyte herbs

(Chenopodiaceae or Amaranthaceae) during this time. The Tana desiccation layer was also recognized by Marshall et al. (2011) as a deposition before 16.4 ka BP, followed by swampy conditions at the center of the lake between 16.4 and 15.9 ka BP and by peat development between 15.9 and 15.3 ka BP. The swampy conditions at Lake Tana overlapped with the lower level at Ashenge as inferred from diatoms from 17.2 to 16.2 ka BP.

Transition to the African Humid Period varied across the region. Increased abundances of *Cyclotella ocellata* in Lake Ashenge between 16.2 and 15.2 ka BP indicate early onset of humid conditions (Marshall et al., 2009). Swampy and peaty conditions at Lake Tana between 16.4 and 15.3 ka BP (Marshall et al., 2011) point to gradual rather than abrupt transition to wetter conditions. The wet conditions were also recognized by the input of allochthonous sediments in Lake Tana (Marshall et al., 2011) and increased karstic activity in the North Ethiopian Highlands from ~15.0 ka BP (Moeyersons et al., 2006). The record from the Gulf of Aden shows transition towards humid conditions at 14.7 ka BP (Tierney and de Menocal, 2013). This coincides with evidence of Lake Tana overflowing into the Blue Nile, dated to 14.8 ka BP, and testified by higher abundances of freshwater diatoms and inorganic sediments (Lamb et al., 2007b).

7.3.2 Dry events during the African Humid Period

As indicated by variations in lake water levels and hydrogen isotopic composition of leaf waxes, the transition from Late Pleistocene to Early Holocene during the African Humid Period was marked by several dry events in the region. The water level of Lake Tana lowered between 13.0 and 12.5 ka BP (Marshall et al., 2011), and Lake Ashenge experienced a water level drop between 13.6 and ~ 11.8 ka BP (Marshall et al., 2011). Both events were broadly matched by records of falling water levels of Lake Abhé and Lakes Ziway-Shalla, and a sharp decline in hydrogen isotopic composition of leaf waxes in the Gulf of Aden (Tierney and deMenocal, 2013).

Wet conditions resumed in the Early Holocene from 12.0 ka BP onwards, with evidence of rising water levels in Lakes Abyata, Abhé and Ziway Shala. The record from the Gulf of Aden showed a later start of humidification at 10.9 ka BP, possibly due to a shifting ^{14}C reservoir with changing Arabian Sea upwelling during deglaciation (Tierney and deMenocal, 2013).

The second dry event during the African Humid Period started around 8.7 ka BP. This was the first major drought that occurred in the Holocene. Water levels at Lake Ashenge declined between 11.8

and 7.6 ka BP (Marshall et al., 2009). Lake Tana registered similar trends dated between 6650 and 5850 BCE (Marshall et al., 2011) (Hol-1; see Table 7.3 for the summarized delineation of all Holocene dry phases). This ~6500 BCE event was also recognized in hydrogen isotope record from leaf waxes at Lake Tana (Costa et al., 2014); and at Lakes Abhé and Ziway Shala. Other records such as a peak in aeolian fluoride in the Kilimanjaro glacier (Thompson et al., 2002), and a dust strontium-neodymium record from the Arabian Sea also signal aridification around 6500 BCE (Jung et al., 2004).

7.3.3 Middle Holocene drying towards the 2200 BCE event

The records indicate considerable variation in the abruptness and timing of the ending of the African Humid Period in the Horn of Africa. Water levels at Lakes Abhé and Ziway-Shalla showed an initial short-lived decline around 6000 ^{14}C yrs BP, calibrated to ~4900 BCE (CalPal, 2015) (Hol-2). Lake Tana registered a gradual decline in wet conditions from 4850 BCE onwards. A similar gradual ending was detected at Lake Tilo, but starting at around 4500 ^{14}C yrs BP onwards, calibrated to 3200 BCE. Several records from other locations register abrupt endings over a long period. An abrupt transition occurred at Lake Ashenge around 3700 BCE. Lake Abyata became shallow rapidly after 3450 BCE. The Gulf of Aden registered a sudden end at around 3010 BCE.

The differences in the timing of endings are likely larger than standard errors on Holocene age models and hence significant (Costa et al., 2014). The African Humid Period most probably ended gradually, with site-specific outliers likely caused by non-linear vegetation or ocean feedbacks (Marshall et al., 2009). Since records from northern locations (e.g. Lake Tana) showed an earlier termination of the African Humid Period in comparison to records from southern locations (e.g. Lake Tilo) in the Highlands, this might indicate a North-South shift of the intertropical convergence zone (see de Menocal, 2015; Shanahan et al., 2015).

7.3.4 Dry and wet phases during the Late Holocene

Following the transition to dry conditions at Lake Ashenge around 3700 BCE, low values in magnetic parameters at Lake Tana from 2200 BCE onwards show that gradually diminishing rainfall reached a precipitation minimum (Marshall et al., 2011). The levels of Lakes Abhé and Ziway-Shala declined between 2200 and 2000 BCE, and remained low until around 1300 BCE (Hol-3) (Ghinassi et al., 2012).

Records from Lakes Hayk, Abhé and Ziway-Shala indicate that a short wet phase occurred after 1300 BCE, followed by another dry phase from ~1100 BCE to about 650 BCE (Hol-4).

Wet conditions resumed at Lake Hayk after 650 BCE (Ghinassi et al., 2012), with similar rise in levels in Lakes Abhé and Ziway-Shala. The diatom record from Lake Ashenge showed a dominance of freshwater diatom taxa between 350 BCE and 450 CE at Lake Ashenge (Marshall et al., 2009). Dry conditions returned to Lakes Ashenge and Abhé after 450 CE (Hol-5), overlapping in part with the dry 'Medieval Climatic Anomaly' that occurred between 800 and 1200 CE in northern Ethiopia (Lamb et al., 2007a). Wetter conditions prevailed from 1200 to 1700 CE, a period corresponding with the Little Ice Age. The isotope record from Lake Hayk indicates a very dry phase between 1750 and 1900 CE (Lamb et al., 2007a) (Hol-6), along with evidence of a dry event at Lake Abyiata around 1888–1892 (Legesse et al., 2002).

To summarize, the analysis of lacustrine and marine records revealed six major dry phases that occurred in the Ethiopia-Horn of Afica region during the Holocene (Table 7.3). These were Holocene 1 (Hol-1), between 6650 and 5850 BCE; Holocene 2 (Hol 2), between 4900 and 4800 BCE; Holocene 3 (Hol-3), between 3700 and 1300 BCE; Holocene 4 (Hol-4), between 1100 to 650 BCE; Holocene 5 (Hol-5), between 450 CE and 1200 CE; and Holocene 6 (Hol-6), between 1750 and 1900.

Table 7.3 Subsequent Holocene dry phases, including dates and references.

Period	Dates	Description
African Humid Period	~15 ka BP - 3700 BCE	African Humid Period with Early Holocene Hol-1 dry event registered at Lake Tana between 6650 and 5850 BCE (Marshall et al., 2011; Costa et al., 2014), at Lake Ashenge (Marshall et al., 2009) and at Lakes Abhé and Ziway Shala; and second dry event Hol-2 around ~4900 BCE registered at Lakes Abhé and Ziway Shala, when dryer conditions develop at Lake Tana (Marshall et al., 2011)
Hol-3	3700 - 1300 BCE	Transition to dry conditions at Lake Ashenge around 3700 BCE towards relatively maximal conductivity values around ~1600 BCE; precipitation minimum from 2200 BCE onwards at Lake Tana (Marshall et al., 2011), and simultaneous lowstands at Lake Abhé and Lake Ziway-Shala (Gasse, 2000)
Wet period	1300 - ~1100 BCE	Highstands after ~1300 BCE are recognized at Lake Hayk (Ghinassi et al., 2012), Lakes Ziway Shalla and Lake Abyata (Gasse, 2000); reduced conductivity at Lake Ashenge around ~1100 BCE
Hol-4	~1100 BCE – 650 BCE	Lowstands after ~1100 BCE are recognized at Lake Hayk (Ghinassi et al., 2012), Lakes Ziway Shalla and Lake Abyata (Gasse, 2000); increased conductivity at Lake Ashenge after ~800 BCE
Wet period	650 BCE - 450 CE	Shift to wetter conditions around 250 BCE at Lake Ashenge (Marshall et al., 2009), Lakes Abhé and Ziway Shala (Gasse, 2000) with an earlier high stand of Lake Hayk around 650 BCE (Ghinassi et al., 2012).
Hol-5	450-1200 CE	Dry after 450-550 CE (Marshall et al., 2009) followed by dry 'Medieval Warm Period' (750-1200 CE) (Lamb et al., 2007); phase of increased conductivity around ~1100 CE at Lake Ashenge
Wet period	1200-1650 CE	Isotopic evidence for a wet 'Little Ice Age' (Lamb et al., 2007); relatively low conductivity values at Lake Ashenge (Marshall et al., 2009)
Hol-6	1650-1900 CE	Drying from ~1650 CE onwards till ~1900 CE, with climax drought around 1750 CE (Lamb et al., 2007); earlier trend of increased conductivity at Lake Ashenge after ~1500 CE

7.4 Discussion

Overall, in North Africa, the most significant climatic episode of the Holocene was the precession-driven end of the African Humid Period. The drying of eastern Sahara happened several millennia before drying in the western Sahara; the Sudanese Sahara was completely dry by 1500 BCE (Lézine et al., 2011). Coupled climate–vegetation models estimated an overall reduction in summer precipitation of ~ 25 % for the Northern Ethiopian Highlands after the end of the African Humid Period. About one fifth of this effect is explained by a vegetation feedback of reduced canopy evapotranspirational cooling, which strengthened moisture export by the African easterly jet

(Rachmayani et al., 2015). Furthermore, the Ethiopian hydroclimate is very sensitive to shifting temperatures and tropospheric circulation patterns in the Atlantic and Indian Oceans (see Appendix A3). The hydrogen isotopic signal in the Tana record (Costa et al., 2014) and the oxygen isotopic signal in the Hayk record (Lamb et al., 2007a) show sensitivity to the Congo Air Boundary as the Ethiopian Highlands are squeezed between Indian and Atlantic circulation patterns (Verschuren and Russell, 2009). Weaker west-east temperature gradients in the Indian Ocean likely weaken the Walker circulation (Tierney et al., 2014). Long-term failures of the southwest monsoon in the Arabian Sea broadly correspond with cold events in the Atlantic, and long-term monsoon maxima with North Atlantic warm phases (Gupta et al., 2003).

7.4.1 Pleistocene climatic phases linked with the Atlantic and Indian Ocean

The Ethiopian records show strong correspondence with cold and warm events in the Atlantic basin. With respect to dry and wet periods in the Ethiopian region during the Pleistocene, the three stiff layers of high seismic reflectivity formed in Lake Tana might match with the Atlantic Heinrich layers H6 (60 ka BP), H4 (38 ka BP) and H3 (24 ka BP) (Lamb et al., 2007b). The dry conditions prevailing during the LGM after 19 ka BP in the Ethiopian region overlapped with North Atlantic Heinrich event 1 dated between 19 and 14.7 ka BP (Lamb et al., 2007b; Marshall et al., 2009; Marshall et al., 2011; Tierney and deMenocal, 2013). The aridification phase recorded in the Lake Ashenge and Gulf of Aden sediments between ~13.6 and 11.8 ka BP overlap with the North Atlantic Younger Dryas event between 12.8-11.5 ka BP, when equatorial Atlantic temperatures decreased to about 25°C (Weldeab et al., 2005).

The early onset of the African Humid Period overlaps with a period of Northern Hemisphere warming under a restarted Atlantic meridional overturning from 14.7 to 14.1 ka BP (Thiagarajan et al., 2014), also known as the Bølling interstadial. The rapid transition towards humid conditions at 14.7 ka BP matches the accepted timing of Heinrich event 1 termination at 14.7 ka BP (Tierney and de Menocal, 2013). During the African Humid Period, the effect of orbital forcing and rising greenhouse gases on summer precipitation was strengthened by equatorial Atlantic Ocean temperatures up to 27.5° (Weldeab et al., 2005) and by a northward shift of the savannah into the Sahara (Claussen and Gayler, 1997).

7.4.2 Holocene climatic phases linked with the Atlantic and Indian Ocean

The six Holocene dry phases for Ethiopia identified by lacustrine and marine records demonstrated strong overlap with decreased temperatures in the equatorial Atlantic and western Indian Ocean. Figure 7.2 shows the Holocene Sea Surface Temperature (SST) records for the eastern equatorial Atlantic and the western Indian Ocean, along with the timings of the dry phases (Table 7.3). Standardized z-scores of the Mg/Ca values are indicative of sea-surface temperature variability around the mean.

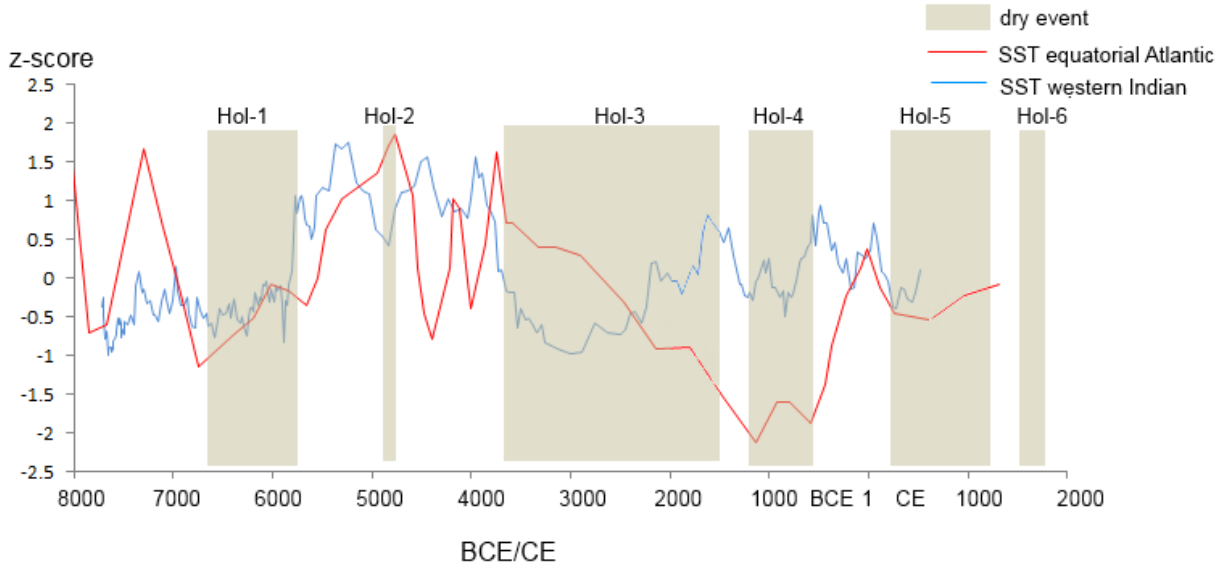

Figure 7.2 Sea-surface temperature (SST) records (z-scores of Mg/Ca values), in red from the equatorial Atlantic (Weldeab et al., 2005), in blue from the western Indian Ocean (Kuhnert et al., 2014), indicate similarities with six Holocene dry events (Hol-1 to Hol-6) recorded in lake sediments from Ethiopia (brown bars, see above). Dates are mentioned as (B)CE.

The first Holocene dry event between 6650 and 5850 BCE, shown as Hol-1, overlaps with reduced SST in the equatorial Atlantic and western Indian Ocean (Figure 7.2). The earlier start of drying in the Horn of Africa compared to the onset of North Atlantic signals (i.e., 6500 instead of 6200 BCE) may be attributed to a gradual suppression of the intertropical convergence zone to the north of 10°N (Tierney et al., 2013). It also overlaps with the outflow of Lake Agassiz in the Atlantic dated at 6520 BCE which preceded the 8.2 ka global cooling event (Alley and Ágústsdóttir, 2005). Speleothem evidence from a cave stalagmite in Oman (Cheng et al., 2008) shows a weakened southwest monsoon in the Arabian Sea during this period (Gupta et al., 2003).

The short Hol-2 dry phase between 4900 and 4800 BCE identified at Lake Tana, Abhé and Ziway-Shala marks the onset of the gradual ending of the African Humid Period. The phase corresponds with a short-lived drop in SST in the western Indian Ocean (Figure 7.2).

The rainfall decline between 3700 and 1300 BCE (Hol-3) overlaps with phases of weakened southwest monsoons around the Arabian Sea between 4250-3250 BCE, 2200 BCE, and 1550 BCE (Gupta et al., 2003). The phase corresponds with a period of gradually declining equatorial Atlantic SSTs and lower western Indian Ocean sea surface temperatures (Figure 7.2). The drought maxima inferred from Lakes Tana, Abhé and Ziway-Shala during 2200-2000 BCE match Atlantic Bond event 3 (Parker et al., 2006).

The dry phase Hol-4 (1100 BCE – 650 BCE) identified at Lake Hayk, Lakes Ziway Shalla and Lake Abyata matches with the lowest equatorial Atlantic sea surface temperatures of the record, as well as with a relative decline in western Indian Ocean sea surface temperatures. The wet period after 650 BCE indicated at Lakes Hayk, Abhé, Ziway-Shala and Ashenge corresponds with a sharp increase in equatorial Atlantic sea surface temperatures (Figure 7.2).

The decrease in equatorial Atlantic sea surface temperatures (Weldeab et al., 2005) after ~ 250 CE precedes a return to drier conditions at Lake Ashenge, Abhé and Hayk (Hol-5). The southwest monsoons around the Arabian Sea are weakened around 450 CE (Gupta et al., 2003). Finally, the very dry period between 1750 and 1900 CE (Hol-6) overlaps with decreased equatorial Atlantic temperatures between ~1700 and 1850 CE (~ minus 1°C as compared to current temperatures under increased frequencies of volcanic eruptions and solar variability), and with decreased Indian Ocean temperatures during the early 1800s (Tierney et al., 2015).

It should be indicated that Heinrich 1 is an exception to this pattern, because then the east-equatorial Atlantic was warmer (Weldeab et al., 2005), leading to lessened monsoon intensity and African drought (Lamb et al., 2007b). Interestingly, there also seem to be some similarities between the Holocene dry phases (Table 7.3), and several Holocene 'Bond events' (Bond et al., 2001).

7.4.3 Recent climatic variability linked with Tropical Ocean temperatures

Since 1979, the October–December wet season in the Horn of Africa has become wetter, which is likely the result of western Indian Ocean warming (Liebmann et al., 2014). The March–May season has become drier, especially after 1999 (Lyon & DeWitt, 2012), probably forced by a westward extension of the Walker circulation (Williams and Funk, 2011) in relation with an increased zonal sea-surface temperature gradient between Indonesia and the central Pacific (Liebmann et al., 2014; Lyon & DeWitt, 2012), i.e. a decadal cooling of the Eastern Pacific (Kosaka & Xi, 2013). Climate model ensembles project an average rainfall increase in the broader region over the course of the 21st century (de Wit and Stankiewicz, 2006), which is in line with projected warming of the tropical oceans (Williams and Funk, 2011).

7.5 Conclusions

In this chapter, we synthesized paleo-climatic datasets from the Horn of Africa with a particular focus on dry phases since the Late Pleistocene. Three Late Pleistocene dry phases included the Last Glacial Maximum, the Heinrich 1 event and the Younger Dryas. Moreover, analyses of lake sediments from Ethiopia revealed six Holocene dry phases. These included the events Holocene 1 (Hol-1), between 6650 and 5850 BCE; Holocene 2 (Hol 2), between 4900 and 4800 BCE; Holocene 3 (Hol-3), between 3700 and 1300 BCE; Holocene 4 (Hol-4), between 1100 to 650 BCE; Holocene 5 (Hol-5), between 450 CE and 1200 CE; and Holocene 6 (Hol-6), between 1750 and 1900 CE. Somewhat similar to the findings discussed in chapter 2, we discerned remarkable links between the occurrence of dry events in the study region and oceanic (temperature) patterns in the eastern-equatorial Atlantic and western Indian Ocean. Dryer conditions in Ethiopia corresponded with cooler sea surface temperatures in these oceanic target regions. While most tropical oceans are currently warming, we might anticipate increased average precipitation in the study region, which is confirmed by future climate model ensemble projections.

7.6 References

Alley, R., Ágústsdóttir, A., 2005. The 8k event: cause and consequences of a major Holocene abrupt climate change. Quaternary Science Reviews 24 (10-11), 1123–1149.

Bond, G., Kromer, B., Beer, J., Muscheler, R., Evans, M., Showers, W., Hoffmann, S., Lotti, R., Hajdas, I., Bonani, G., 2001. Persistent Solar Influence on North Atlantic Climate During the Holocene. Science 294 (5549), 2130–2136.

Chalié, F., Gasse, F., 2002. Late Glacial–Holocene diatom record of water chemistry and lake level change from the tropical East African Rift Lake Abiyata (Ethiopia). Palaeogeography Palaeoclimatology Palaeoecology 187 (3), 259-283.

Cheng, H., Fleitmann, D., Edwards, R., Burns, S., Matter, A., 2008. Timing of the 8.2-kyr event in a stalagmite from Northern Oman. PAGES News 16 (3), 29-30.

Claussen, M., Gayler, V., 1997. The Greening of the Sahara during the Mid-Holocene: Results of an Interactive Atmosphere-Biome Model. Global Ecology and Biogeography Letters 6, 369-377.

Conway, D., 2000. Some aspects of climate variability in the North East Ethiopian highlands—Wollo and Tigray. Sinet. Ethiopian Journal of Science 23 (2), 139– 161.

Costa, K., Russell, J., Konecky, B., Lamb, H., 2014. Isotopic reconstruction of the African Humid Period and Congo Air Boundary migration at Lake Tana, Ethiopia. Quaternary Science Reviews 83, 58-67.

de Menocal, P., 2015. Palaeoclimate: End of the African Humid Period. Nature Geoscience 8, 86–87.

de Wit, M., Stankiewicz, J., 2006. Changes in Surface Water Supply Across Africa with Predicted Climate Change. Science 311 (5769), 1917-1921.

Elshamy, M., Seierstad, A., Sorteberg, A., 2009. Impacts of climate change on Blue Nile flows using bias-corrected GCM scenarios. Hydrol. Earth Syst. Sci. 13, 551–565.

Frankl, A., Nyssen, J., De Dapper, M., Haile, M., Billi, P., Munro, N., Deckers, J., Poesen, J., 2011. Linking long-term gully and river channel dynamics to environmental change using repeat photography (Northern Ethiopia). Geomorphology 129, 238-251.

Frankl, A., Jacob, M., Haile, M., Poesen, J., Deckers, J., Nyssen, J., 2013. The effect of rainfall on spatio-temporal variability in cropping systems and duration of crop cover in the Northern Ethiopian Highlands. Soil Use and Management 29 (3), 374–383.

Gasse, F., 2000. Hydrological changes in the African tropics since the Last Glacial Maximum. Quaternary Science Reviews 19, 189-211.

Ghinassi, M., D'Oriano, F., Benvenuti, M., Awramik, S., Bartolini, C., Fedi, M., Ferrari, G., Papini, M., Sagri, M., Talbot, M., 2012. Shoreline fluctuations of Lake Hayk (northern Ethiopia) during the last

3500 years: Geomorphological, sedimentary, and isotope records. Palaeogeography, Palaeoclimatology, Palaeoecology 365, 209–226.

Gupta, A., Anderson, D., Overpeck, J., 2003. Abrupt Changes in the Asian Southwest Monsoon during the Holocene and Their Links to the North Atlantic Ocean. Nature 421, 354-357.

Jung, S., Davies, G., Ganssen, G., Kroon, D., 2004. Stepwise Holocene aridification in NE Africa deduced from dust-borne radiogenic isotope records. Earth and Planetary Science Letters 221 (1-4), 27-37.

Kosaka, Y., Xie, S., 2013. Recent global-warming hiatus tied to equatorial Pacific surface cooling. Nature 501, 403–407.

Kuhnert, H., Kuhlmann, H., Mohtadi, M., Meggers, H., Baumann, K., Pätzold, J., 2014. Holocene tropical western Indian Ocean sea surface temperatures in covariation with climatic changes in the Indonesian region. Paloceanography 29 (5), 423–437.

Lamb, A., Leng, M., Lamb, H., Umer, M., 2000. A 9000-year oxygen and carbon isotope record of hydrological change in a small Ethiopian crater lake. The Holocene 10, 167-177.

Lamb, H., Leng, M., Telford, R., Tenalem Ayenew, Umer, M., 2007a. Oxygen and carbon isotope composition of authigenic carbonate from an Ethiopian lake: a climate record of the last 2000 years. The Holocene 17(4), 517–526.

Lamb, H., Bates, R., Coombes, P., Marshall, M., Umer, M., Davies, S., Dejen, E., 2007b. Late Pleistocene desiccation of Lake Tana, source of the Blue Nile. Quaternary Science Reviews 26, 287–299.

Legesse, D., Gasse, F., Radakovitch, O., Vallet-Coulomb, C., Bonnefille, R., Verschuren, D., Gibert, E., Barker, P., 2002. Environmental changes in a tropical lake (Lake Abiyata, Ethiopia) during recent centuries. Palaeogeography, Palaeoclimatology, Palaeoecology 187 (3-4), 233-258.

Lézine, A., Hély, C., Grenier, C., Braconnot, P., Krinner, G., 2011. Sahara and Sahel vulnerability to climate changes, lessons from Holocene hydrological data. Quaternary Science Reviews 30, 3001-3012.

Liebmann, B., Hoerling, M., Funk, C., Bladé, I., Dole, R., Allured, D., Quan, X., Pegion, P., Eischeid, J., 2014. Understanding Recent Eastern Horn of Africa Rainfall Variability and Change. J. Climate 27, 8630–8645.

Lyon, B., DeWitt, D., 2012. A recent and abrupt decline in the East African long rains, Geophys. Res. Lett. 39, L02702.

Marshall, M., Lamb, H., Davies, S., Leng, M., Zelalem Kubsa, Umer, M., Bryant, C., 2009. Climatic change in northern Ethiopia during the past 17,000 years: A diatom and stable isotope record from Lake Ashenge. Palaeogeography, Palaeoclimatology, Palaeoecology 279, 114–127.

Marshall, M., Lamb, H., Dei Huws, Davies, S., Bates, R., Bloemendale, J., Boylee, J., Leng, M., Umer, M., Bryant, C., 2011. Late Pleistocene and Holocene drought events at Lake Tana, the source of the Blue Nile. Global and Planetary Change 78 (3–4), 147–161.

Moeyersons, J., Nyssen, J., Poesen, J., Deckers, J., Mitiku Haile, 2006. Age and backfill/overfill stratigraphy of two tufa dams, Tigray Highlands, Ethiopia: Evidence for Late Pleistocene and Holocene wet conditions. Palaeogeography, Palaeoclimatology, Palaeoecology 230 (1–2), 165–181.

Mohtadi, M., Prange, M., Oppo, D., De Pol-Holz, R., Merkel, U., Zhang, X., Steinke, S., Lückge, A., 2014. North Atlantic forcing of tropical Indian Ocean climate. Nature 509, 76–80.

Nyssen, J., Poesen, J., Moeyersons, J., Deckers, J., Mitiku Haile, Lang, A., 2004. Human impact on the environment in the Ethiopian and Eritrean highlands - a state of the art. Earth-Science Reviews 64 (3-4), 273-320.

Parker, A., Goudie, A., Stokes, S., White, K., Hodson, M., Manning, M., Kennet, D., 2006. A record of Holocene climate change from lake geochemical analyses in Southern Arabia. Quat. Res. 66 (3), 465-476.

Rosell, S., 2011. Regional perspective on rainfall change and variability in the central highlands of Ethiopia, 1978–2007. Applied Geography 31 (1), 329–338.

Shanahan, T., McKay, N., Hughen, K., Overpeck, J., Otto-Bliesner, B., Heil, C., 2015. The time-transgressive termination of the African Humid Period. Nature Geoscience 8, 140–144.

Tesfamichael Gebreyohannes, De Smedt, F., Walraevens, K., Solomon Gebresilassie, Abdelwasie Hussien, Miruts Hagos, Kasa Amare, Deckers, J., Kindeya Gebrehiwot, 2013. Application of a spatially distributed water balance model for assessing surface water and groundwater resources in the Geba basin, Tigray, Ethiopia. Journal of Hydrology 499, 110–123.

Thiagarajan, N., Subhas, A., Southon, J., Eiler, J., Adkins, J., 2014. Abrupt pre-Bølling–Allerød warming and circulation changes in the deep ocean. Nature 511, 75–78.

Tierney, J., deMenocal, P., 2013. Abrupt Shifts in Horn of Africa Hydroclimate Since the Last Glacial Maximum. Science 342 (6160), 843-846.

Tierney, J., Smerdon, J.,Anchukaitis, K., Seager, R., 2014. Multidecadal variability in East African hydroclimate controlled by the Indian Ocean. Nature 493, 389–392.

Tierney, J., Abram, N., Anchukaitis, K., Evans, M., Giry, C., Kilbourne, K., Saenger, C., Wu, H., Zinke, J., 2015. Tropical sea surface temperatures for the past four centuries reconstructed from coral archives. Paleoceanography, in press. DOI: 10.1002/2014PA002717.

Thompson, L., Mosbey-Thompson, E., Davis, M., Henderson, K., Brecher, H., Zagorodnov, V., Mashiotta, T., Lin, P., Mikhalenko, V., Hardy, D., Beer, J., 2002. Kilimanjaro ice core records. Evidence of Holocene climate change in tropical Africa. Science 298, 589-593.

Umer, M., 2010. Regional Integration of Past Records For Management of Modern Resources and Landscapes In East and NE Africa. Available at: http://www.pages-igbp.org/download/docs/meeting-products/presentations/2010-regionalintegration-wshop/PAGES_F4RI_Umer.pdf.

Verschuren, D., Russell, J., 2009. Paleolimnology of African lakes: Beyond the exploration phase. PAGES news 17 (3), 112-116.

Walker, M., Berkelhammer, M., Björck, S., Cwynar, L., Fischer, D., Long, A., 2012. Formal subdivision of the Holocene Series/Epoch: a Discussion Paper by a Working Group of INTIMATE (Integration of ice-core, marine and terrestrial records) and the Subcommission on Quaternary Stratigraphy (International Commission on Stratigraphy). Journal of Quaternary Science 27 (7), 649-659.

Weldeab, S., Schneider, R., Kölling, M., Wefer, G., 2005. Holocene African droughts relate to eastern equatorial Atlantic cooling. Geology 33 (12), 981-984.

Weninger, B., Jöris, O., 2008. A 14C age calibration curve for the last 60 ka: the Greenland-Hulu U/Thtimescale and its impact on understanding the Middle to Upper Paleolithictransition in Western Eurasia. Journal of Human Evolution 55, 772-781.

Williams, A., Funk, C., 2011. A westward extension of the warm pool leads to a westward extension of the Walker circulation, drying eastern Africa. Clim. Dyn. 37, 2417–2435.

Yacob, A., Imeru, T., 2005. Ethiopia and the Eastern Nile Basin. Aquatic Sciences: Research Across Boundaries 67 (1), 15-27.

Chapter 8 Endorheic lake sediments: 400 years of land degradation dynamics around Lake Ashenge

This chapter is modified from:

Lanckriet, S., Rucina, S., Frankl, A., Ritler, A., Gelorini, V., Nyssen, J., 2015. Nonlinear vegetation cover changes in the North Ethiopian Highlands: evidence from the Lake Ashenge closed basin. Science of the Total Environment 536, 996-1006.

Abstract

Vegetation cover changes in African drylands are often thought to result from population growth, social factors and aridification. Here we show that long-term vegetation proxy records can help disentangling these main driving factors. Taking the case of North Ethiopia, we performed an integrated investigation of land cover changes over the last four centuries around the endorheic Lake Ashenge, as derived from pollen analysis and repeat photography complemented with information from historical sources. Pollen and sediment analysis of radiocarbon-dated lake deposits shows a phase of environmental destabilization during the 18th century, after a more stable previous period. This is evidenced by decreases of tree pollen (*Juniperus*, *Olea*, *Celtis*, *Podocarpus* < 5 %), increases in Poaceae (> 40 %) and deposition of coarser silt lake sediments (> 70 %). Quantitative analysis of 30 repeated landscape photographs around the lake indicates a gradual decline of the vegetation cover since a relative maximum during the mid-19th century. Vegetation cover declined sharply between the 1950s and the 1980s, but has since begun to recover. Overall, the data from around Lake Ashenge reveal a nonlinear pattern of deforestation and forest regrowth with several periods of vegetation cover change over the past four centuries. While there is forcing of regional drought and the regional land tenure system, the cyclic changes do not support a simplified focus on population growth.

8.1 Introduction

Discussion on the nature and the driving forces of deforestation and land degradation in African drylands is still ongoing. Some researchers describe the forest cover evolution in semi-arid environments 'as being determined mainly by ecological factors' (Easdale & Domptail, 2014). The consequences of the late 20th century Sahel drying trend can be viewed within this perspective (Adger et al., 2001). Others link deforestation with population growth (DeFries et al., 2010; Meadows et al., 1972). This neo-Malthusian discourse depicts overpopulation in dry lands as the main driver of decline of the forest cover (Stocking, 1995). Population growth would also lead to increasing soil degradation due to changes in land cover, particularly large-scale deforestation (Wøien, 1995, Tekle Kebrom & Hedlund, 2000). Despite the conceptual clarity of these two narratives, empirically disentangling the effects of population pressure and climatic factors is a difficult task (Adger et al., 2001). In fact, disentangling the effects of drivers of environmental change may only be achieved through the compilation of long-term environmental histories (Batterbury et al., 1997). Batterbury & Bebbington (1999) add that historical investigation is central for understanding changes, since most of the socioeconomic and environmental processes involved act only very slowly over time. Hence, historical analysis of land cover changes, climate as well as of human factors is required (Preston et al., 1997). Such historical approaches can bring important insights on environmental change and its relation with the main driving factors (i.e. land cover, climate, society) (Batterbury & Bebbington, 1999). However, compiling environmental histories in some environments can be a difficult task, in particular when there is a lack of historical documents and data. Therefore, researchers often turn to lake records for their historical-environmental reconstructions. Lake sediments can store important historical-environmental information (Marshall et al. 2009; Roberts et al., 2011). Terrestrial pollen in such sediments is amongst the most useful indicators for assessing human-environment interactions (Roberts, 2014).

8.2 Regional case-study and aim

We turn to the North Ethiopian Highlands, where climate drying started around eight million years ago, most probably in relation to the Pliocene and Pleistocene tectonic uplift that led to an important change in atmospheric circulation (Sepulchre et al., 2006). After this early onset of aridification, relatively dry periods alternated with wetter periods. During the Early Pleistocene, three humid periods occurred in East Africa, a first period (2.7-2.5 Ma) related to the intensification of the Northern Hemisphere Glaciation; a second period (1.9-1.7 Ma) related to an intensification of the Walker circulation; and a third period (1.1-0.9 Ma) related to the global shift in pattern from glacial cycles of 41 ka to cycles of 100 ka (Trauth et al., 2005). The last glaciation in Ethiopia was quite dry and cold (Hendrickx et al., 2014; Nyssen et al., 2004). Then, around 10 ka, peak northern hemisphere precession-driven summer solar insolation enhanced the ocean-continent temperature contrast, which strengthened the monsoons (Marshall et al., 2009; Roberts, 2014). However, around 5.6 ka, a non-linear vegetation-ocean-precipitation response to precessionally forced insolation changes resulted in drier climate (Marshall et al., 2009). Around 500 CE, there was a shift to even dryer climate (Marshall et al., 2009). Later, there was a brief period of abundant rainfall (700 CE), followed by less rainfall during the (European) Medieval Warm Period (800-1200 CE). After the dryer Medieval Warm Period, the Little Ice Age (1200-1700 CE) was a relatively wet period for Ethiopia (Lamb et al., 2007), which is in line with findings for east-equatorial East Africa (De Cort et al., 2013). The overall rainfall trend during the 20th century is stable (Funk et al., 2012). Rainfall varies inter-annually in response to oceanic forcing (Chapter 2).

In North Ethiopia, historical sources concerning the landscape and land cover of the last centuries are often lacking. There are some perfunctory claims that deforestation was catastrophic since the beginning of the 20th century (Parry, 2003; Ritler, 2003; Allen-Rowlandson, 1989; Robinson et al., 1995), which McCann (1997) calls the "Narrative of Deforestation". By contrast, Darbyshire et al. (2003) and Nyssen et al. (2009a) show that intense deforestation occurred well before the 19th century, inferring a more gradual environmental change. However, detailed datasets of the land cover during the pre-20th century are scarce (Frankl et al., 2011). Several lake coring studies were performed in North Ethiopia, but these are concentrated in the Main Ethiopian Rift Valley in central Ethiopia (e.g. Chalié and Gasse, 2002), in the Danakil depression (e.g. Fritz et al., 1999) or in the southern highlands (e.g. Umer et al., 2007). Moreover, these studies are not particularly relevant to

questions about land-cover changes of the last few centuries, as they focus on longer-term environmental changes or analyze diatoms rather than terrestrial pollen (e.g. Marshall et al., 2009; at Lake Ashenge).

We focus on the endorheic Lake Ashenge, with a hydrological budget that is highly sensitive to monsoonal variability and climate changes since the lake is located at the northernmost limit of the Intertropical Convergence Zone (Marshall et al., 2009). Apart from a Holocene diatom sequence from this lake (Marshall et al., 2009), no paleo-environmental reconstructions based on lake coring data exist in the North Ethiopian Highlands (region of Tigray). Given the overall lack of environmental understanding of the last centuries in the Northern Highlands, the aim of this research is to gather and integrate information from around Lake Ashenge to fill this data gap.

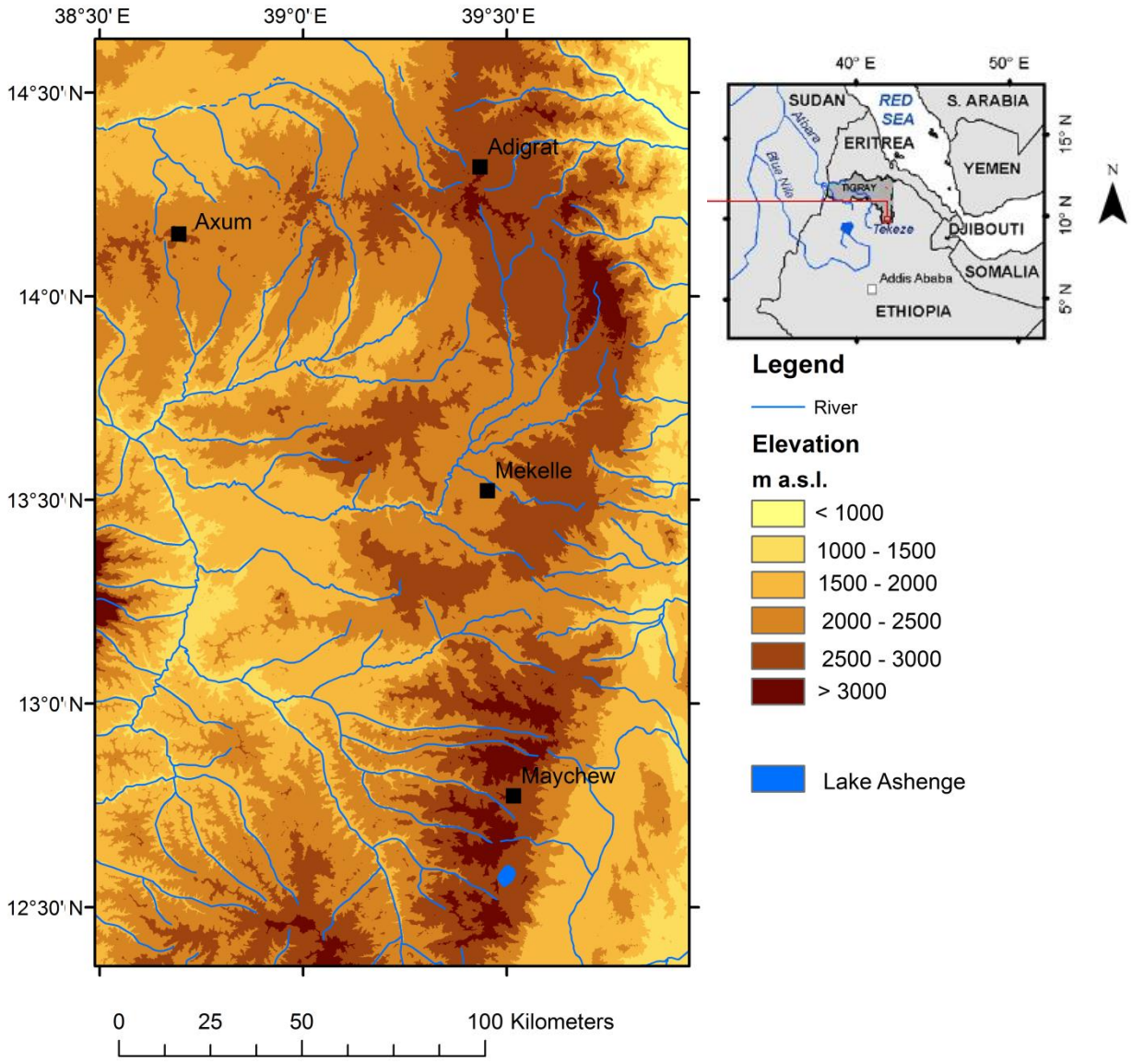

Figure 8.1 General setting of Lake Ashenge in the North Ethiopian Highlands.

8.3 Methods

8.3.1 Study lake and scientific approach

Our study was performed in and around Lake Ashenge (12°35'N, 39°29'E; 2440 m a.s.l.; lake surface area of approximately 1540 ha) (Figure 8.2), located in a marginal graben near the Ethiopian Rift valley, on the western side of the triple-junction between the Nubian, Somali and Arabian plates. Geology comprises deeply weathered Tertiary volcanics, *in casu* the black alkali olivine basalts and tuffs of the Ashangi group. These basalts are often interbedded with lacustrine deposits of silicified limestone and diatomite with gastropods (Merla et al., 1979). Lake Ashenge is moderately saline with conductivities near to 1600 µS cm^{-1} and a relatively high pH of ~8.8 (Marshall, 2006). Crusts of microbialite are, as witnesses of high past lake levels, found between 1 and 30 m above the lake (Marshall et al., 2009). The Ashenge level was low at the time of Heinrich event 1, rose between 16.2 and 15.2 cal kyr BP, and was again lower between 13.6 and ~ 11.8 cal kyr BP, coinciding with the Younger Dryas. There was an early Holocene low stand, after which the lake filled to its overflow during the African Humid Period (7.6 - 5.6 cal kyr BP). The lake responded to the dryer conditions after 5.6 ka, to a possible wet pulse around 200 BCE and to the dryer conditions after 500 CE (Marshall et al., 2009). Schuett and Busschert (2005), based on local reports, infer higher Ashenge lake levels from the 1930s to the 1960s, lower levels during the 1980s and a recent rise of the level over the past decade(s). Several gullies arrive at the flat valley bottom, where thick alluvial-colluvial sediments are present. Their catchments have shallow colluvial soils and relatively steep slopes (Frankl et al., 2011). Stabilized gullies were already present before the 1930s, with a network rather similar to the contemporary one. After 1965, the gullies became highly active, with higher peak floods and an upslope extension of the gully head cuts. To date, the gully channels are de-activating (Frankl et al., 2011).

To reconstruct the past four centuries of land cover change around Lake Ashenge, we use an integrated approach, using proxy records such as deep lake coring, repeat photography, and historical sources (Table 8.1).

Table 8.1 Integrated setup for covering four centuries of land cover; with temporal coverage of the proxy records, specific analysis and dating method.

Temporal coverage	*Proxy*	*Analysis/Method*	*Dating*
18^{th} – 20^{th} century	deep lake core (pollen)	loss-on-ignition sieving and X-ray sedigraphy pollen analysis	radiocarbon dating
1868 - 2010	vegetation cover on repeat photography	quantification of expert rates	photograph dates
17^{th} – 19^{th} century	historical sources on the environment	critical qualitative analysis of traveler and army reports	reported in source

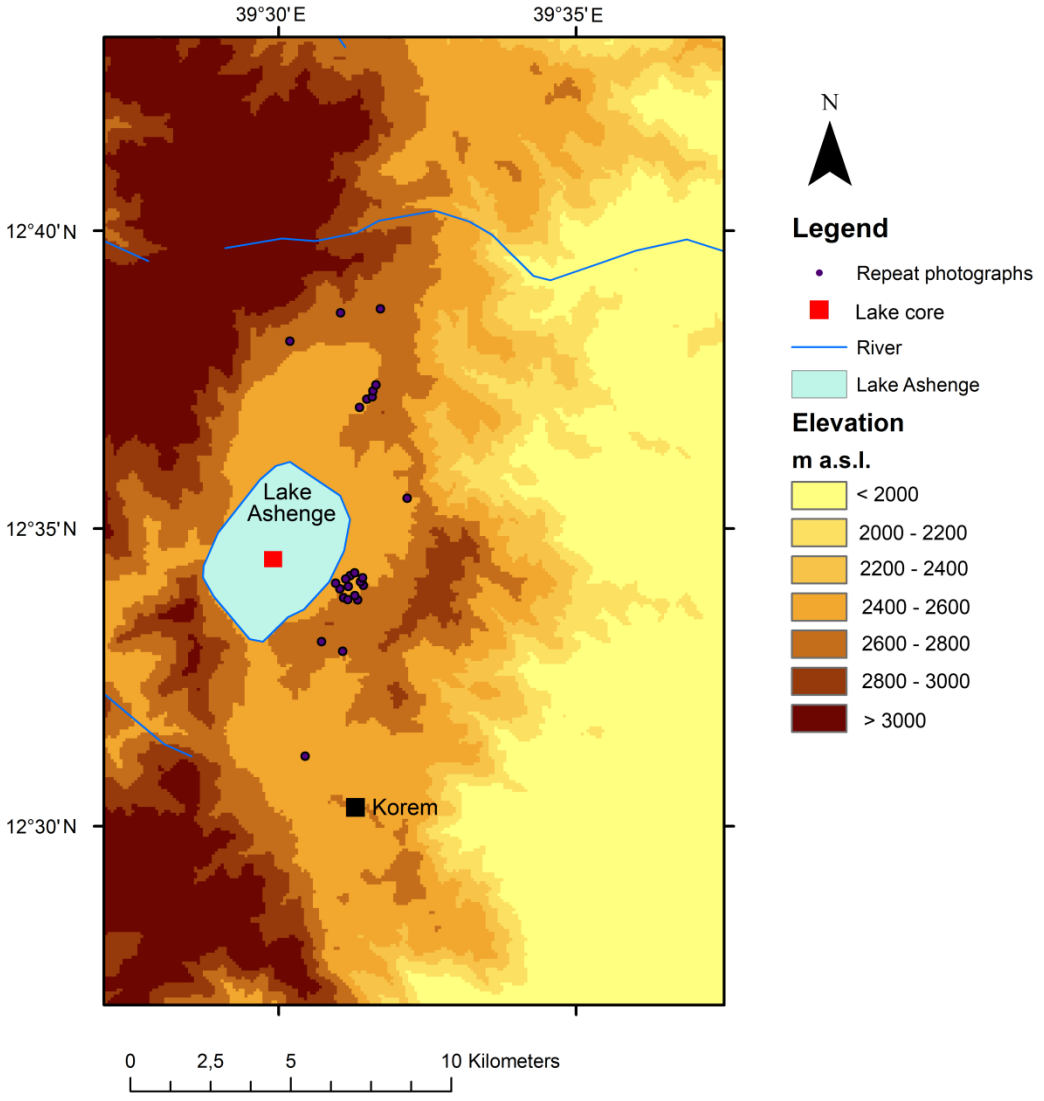

Figure 8.2 Lake Ashenge, with indication of the location of the repeat photographs and lake core.

8.3.2 Lake-sediment core

At the deepest part of the lake (21 m), a short lake core was collected using a gravity corer (Uwitec, 2014). This allowed retrieval of 31 cm of sediments, which were sectioned in 1-cm slices into *Whirl-Pack* bags. Sediment texture was determined for all 31 subsamples by first separating sand (>63 µm) from silt and clay (<63 µm) by wet sieving of the sample with distilled water on a 63 µm sieve. Some 2.5 g of the silt and clay fraction was mixed with a 40 ml 0.2% sodium hexametaphosphate solution

and treated with ultrasound. Mass distributions were determined with X-ray sedigraphy (*SediGraph III Plus*), with Reynolds numbers held between 0.3 and 0.5 (Micromeritics, 2014) (Sedimentology Laboratory, Ghent University).

Further, thermogravimetric analysis by loss-on-ignition was performed. This included treatment in a temperature-controlled furnace, by drying at 105 °C, burning at 550 °C and ashing at 1000 °C. This was in order to estimate porosity (wet minus dry weight), water content (porosity/wet weight), organic matter (based on the weight loss from 100-550°C), calcium carbonate (based on the weight loss from 550-1000°C) and inorganic material (100 minus organic matter minus calcium carbonate). The weight loss between 105 and 550 °C might slightly overestimate the organic material because of water loss from clay minerals (SCAR, 2014). Clay has a large share in the samples but the clay in the Lake Ashenge basin is mainly composed of kaolinite, microcline and muscovite minerals (Kurkura Kabeto et al., 2012).

In order to perform pollen analysis, following Faegri and Iversen (1975), we consistently combined two adjacent 1-cm thick slices from the core to prepare the pollen subsample (sample volumes of 116 cm^3). The 2-cm thick slices were chemically pretreated in order to remove the non-palynomorph components (Limnology Laboratory, Ghent University). The samples were boiled in 10% KOH and 10% Na pyrophosphate, dehydrated with 96% acetic acid and treated with a heated acetolysis mixture of H_2SO_4 and acetic anhydride. Subsequently, samples were treated with 96% ethanol, heavy liquid bromoformethanol mixture and again 96% ethanol. The samples were put in glycerine, dried, mounted and pollen were counted under the microscope (National Museum of Kenya, Nairobi). Based on a method of incremental sum of squares, stratigraphically constrained cluster analysis was performed using the CONISS package. We inferred changes in woody vegetation cover from variations in the ratio of arboreal pollen to non-arboreal pollen (AP/NAP), and also identified several indicator species. For instance, following Darbyshire et al. (2003) and Bonnefille & Buchet (1987), *Rumex* can be interpreted as a ruderal species, higher abundances of Cyperaceae can point to the occurrence of drought (Darbyshire et al., 2003) and *Dodonea* and Asteraceae are common in recently established exclosures (areas from which livestock and uncontrolled wood cutting are excluded) (Reubens et al., 2009). The pollen sum includes trees and shrubs, herbs, miscellaneous taxa (e.g. *Tarenna* and *Euphorbia*) and cultivated/exotic plants (e.g. *Zea* and *Pinus*), while ferns and aquatics were excluded.

Radiocarbon dating was performed on the bulk organic matter. Three samples (ULA-4455 to ULA-4457) were pretreated with HCl and fractionated in their different carbon components, followed by oxidation to CO_2 and subsequent conversion to graphite. The graphite was analyzed using Accelerator Mass Spectrometry (Centre d'Etudes Nordiques, Université Laval, Canada). Additionally, stable isotope $\delta^{13}C$ values were calculated relative to standards traceable to Pee Dee Belemnite, using a Thermo Finnigan Delta Plus stable isotope ratio mass spectrometer (IRMS) with Gas Bench input. The carbon dates were calibrated using the CalPal-2007-Hulu calibration curve. The age-depth model is based on linear interpolation between the median calibrated ages.

8.3.3 Repeat photography and historical sources

Between 2006 and 2011, 30 photographs were taken of different landscapes around the Ashenge catchment, replicating photographs taken in 1868 (3 photos), the 1930s (17 photos), the 1960s (2 photos), the 1970s (4 photos), the 1980s (2 photos) and the 1990s (2 photos) (Appendix A4). All were taken at the same angle and approximately in the same season as the original photograph (Nyssen et al., 2014) (Figure 8.3; all photographs are presented in the Supplement). All paired photographs were analyzed by 6 to 12 environmental scientists with longstanding experience in Ethiopia and elsewhere. They evaluated 'total woody vegetation' for all paired photographs, by assigning each pair a score (from +2 for 'much higher' to -2 for 'much less' woody vegetation in historical times). In this way a trendline for changes to vegetation cover since the late 19th century could be established. We validated the repeat photography with information from historical sources, mainly landscape descriptions from traveler and army reports since 1850 CE near Lake Ashenge (analyzed by Ritler, 2003) and since the 1600s in the broader Tigray (analyzed by Stähli, 2000). Despite the obvious limitations of travel reports, they do provide a wealth of information on the landscape if the reporting quality is rigorously checked (Ritler, 2003). Surprisingly, travel reports after 1900 CE were less detailed than those from the 19th century, presumably because of the time limitations of the travelers (Ritler, 2003).

Figure 8.3 Lake Ashenge, looking to the North along the Eastern shore in 1937 (Source AOI Archives, Firenze) (66AOI-4B).

8.4 Results

8.4.1 Land cover changes derived from the deep lake core

The radiocarbon dates indicate that the sediment core spans a period since ~1700 CE (Table 8.2; Figure 8.4). Porosity increases quite sharply at the top 8 cm of the core (Figure 8.5). The mass-median-diameter (D50) remains rather stable throughout the core (~ 2 µm), although it increases at the depth of 27 cm (and at 17 cm and in the upper parts of the core) representing relatively coarse particles at those depths (Figure 8.6). The proportions of clay are relatively low (<30%) at those depths.

Table 8.2 Radiocarbon dates including $\delta^{13}C$ (‰), $\Delta^{14}C$ (‰), ^{14}C age and calibrated date ± 2σ.

Code	Depth (cm)	$\delta^{13}C$ (‰)	±	Modern fraction	±	$\Delta^{14}C$ (‰)	±	^{14}C age (BP)	Calibrated date (CE) ± 2σ
ULA-4455	26	-17.9	0.1	0.9710	0.0022	-29.0	2.2	235 ± 20	1715 ± 68
ULA-4456	21	-16.9	0.1	0.9903	0.0022	-9.7	2.2	80 ± 20	1807 ± 96
ULA-4457	15	-14.4	0.1	1.0129	0.0023	12.9	2.3	modern	1950

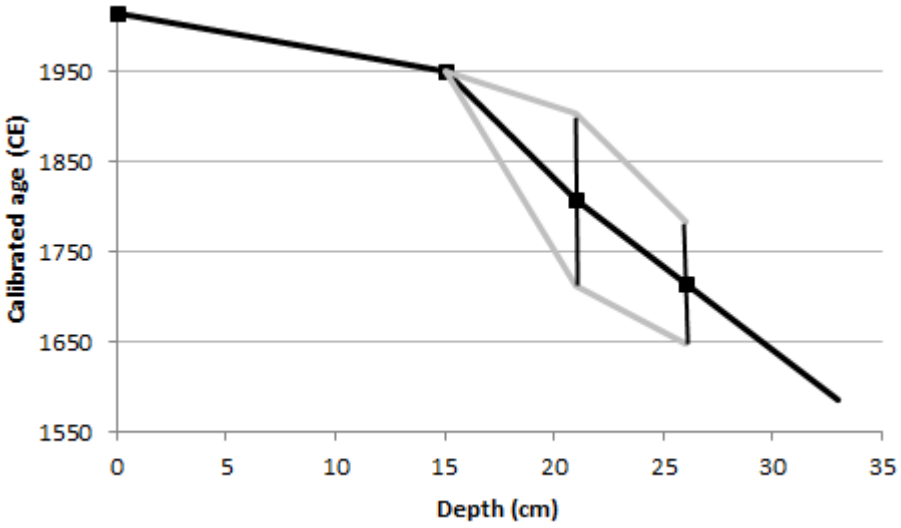

Figure 8.4 Age-depth model based on the calibrated radiocarbon dates (black line) and their lower and upper 2σ limits (bars and gray line) as a function of core depth (cm).

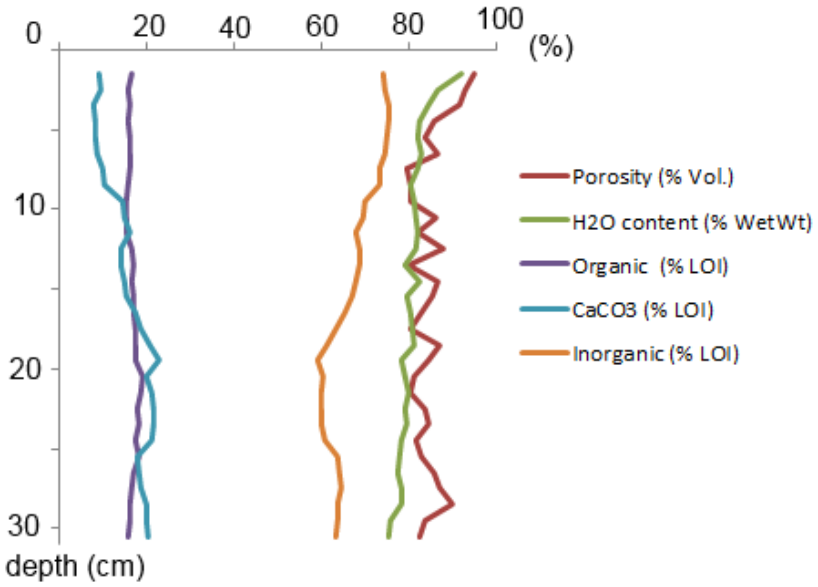

Figure 8.5 Loss-on-ignition with indication of porosity (% vol.), water content (% wet weight), organic and inorganic matter as well as CaCO3 (% of LOI – loss on ignition after oven-drying).

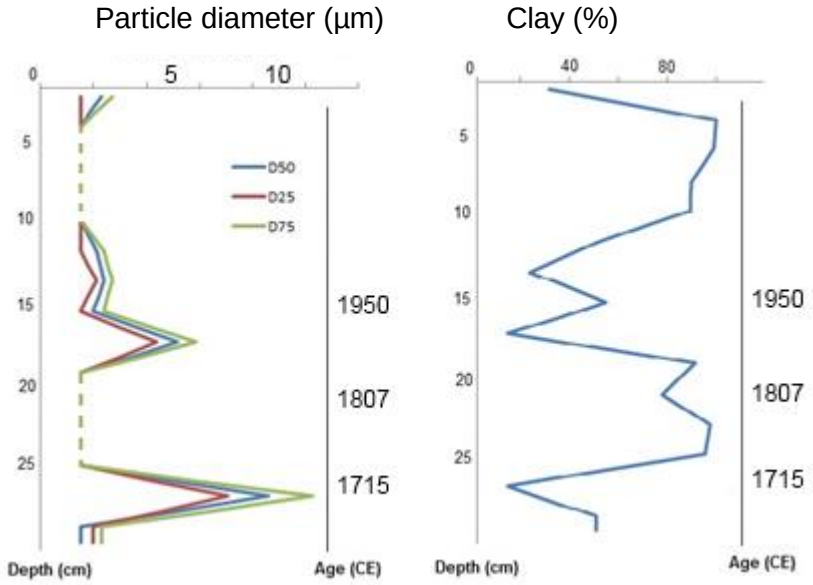

Figure 8.6 Texture analysis (D75, D50, D25 (left) and % of clay (right)) for the deep lake core (with indication of the calibrated dates (CE)). A dotted line indicates that D25/D50/D75 are < 2 µm.

In the deep lake core, 78 distinct pollen taxa were identified and a percentage-diagram was constructed (Figure 8.7). Note that the pollen sums are dominated by the occurrence of Cyperaceae and Poaceae and that the depths 0-2/2-4 cm and 4-6/6-8 cm were joined because of the low pollen sum, possibly related to the organic character of this sediment. Based on the stratigraphic cluster analysis and the plot of arboreal pollen percentages versus non-arboreal percentages (AP/NAP) (Figure 8.8), we identified five broad vegetation zones (Ashenge zones 1 to 5).

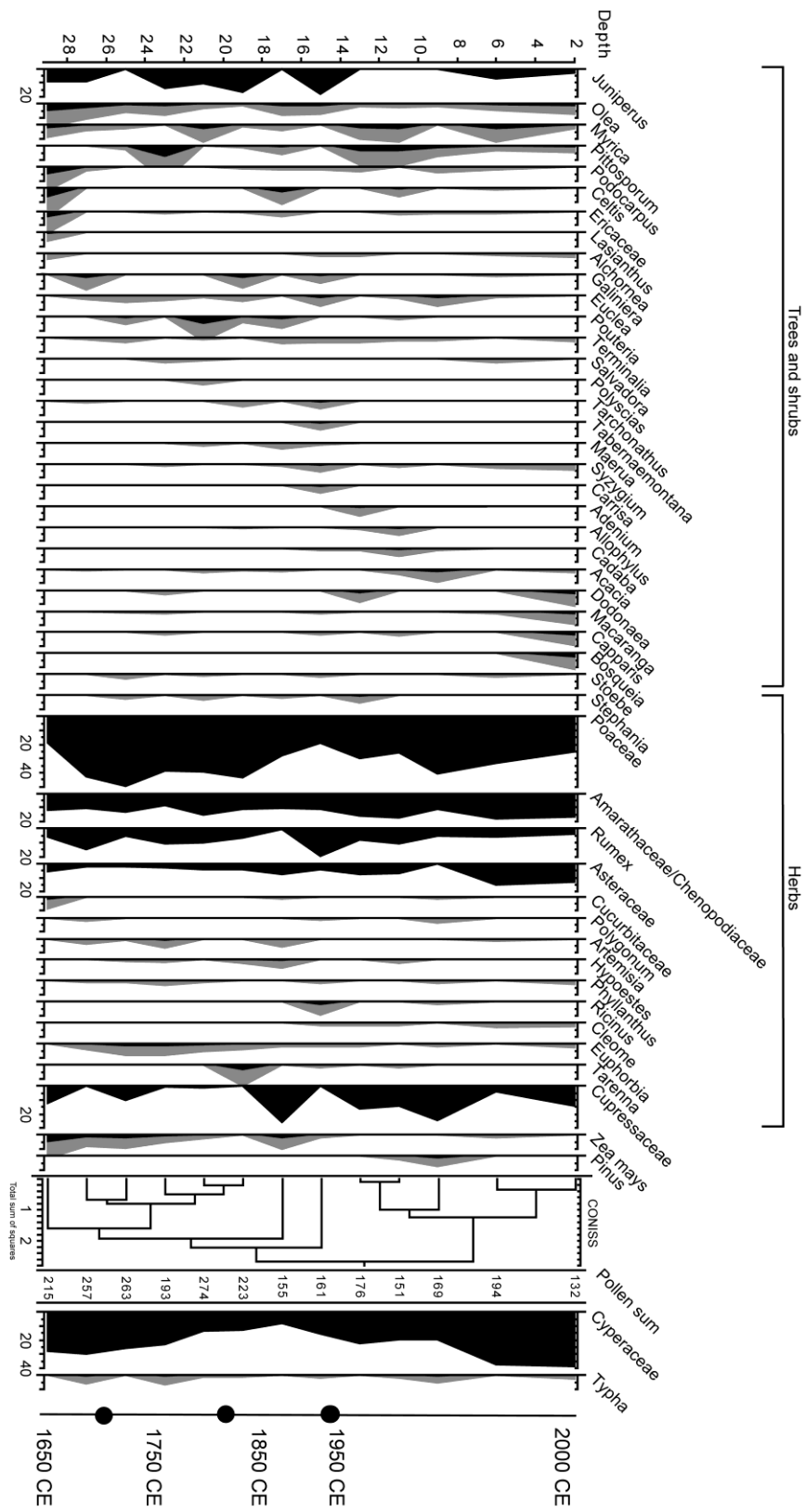

Figure 8.7 Percentage pollen diagram for the deep lake core, with calibrated radiocarbon dates indicated as black dots and depth in cm. The gray curves are magnified by factor 3. We separated exotic plants (*Zea*, *Pinus*) from indigenous trees, shrubs or herbs.

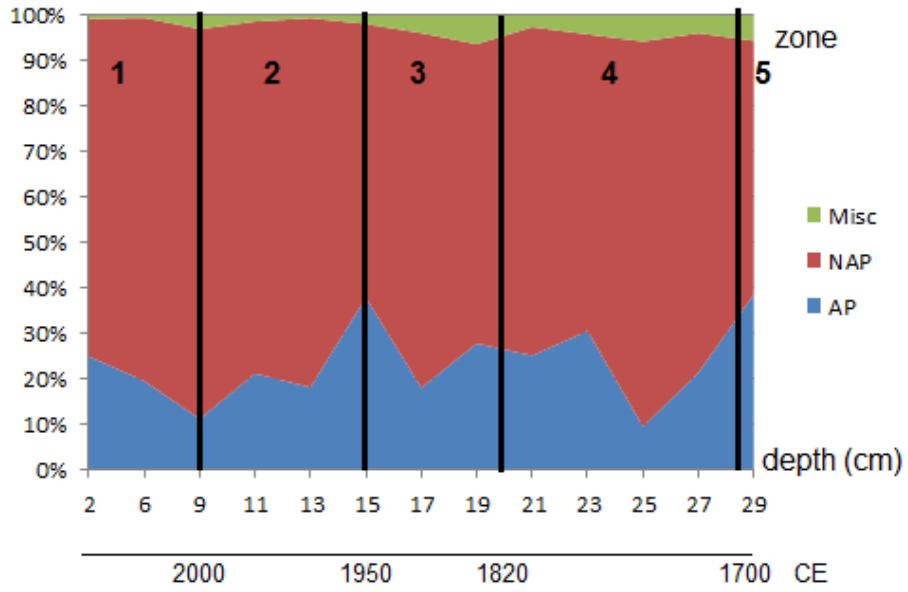

Figure 8.8 Relative pollen abundances of non-arboreal species (NAP) plotted against relative pollen abundances of arboreal species (AP) or miscellaneous species (Misc), with indication of zones 1 to 5 (see also Table 8.3) and their estimated ages.

Ashenge zone 5 (before ~1700 CE) encompasses the lowest parts of the core (> 28 cm) and contains the highest AP/NAP ratio of the entire core (Figure 8.8), pointing to a relatively high degree of forest cover. The bottom of the core features high abundances of *Juniperus* (~ 10 %), *Olea* (5-10 %), *Celtis* (5-10 %) and *Podocarpus* (5-10 %) (Figure 8.7). There is also high abundance of Cyperaceae (> 20 %), relatively low abundances of Poaceae and appearance of maize pollen (Figure 8.7).

Ashenge zone 4 (28-20 cm) (~1700-1820 CE) represents a distinct stratigraphic cluster of five layers (total sum of square < 1) (Figure 8.7). The zone starts with a sharply falling AP/NAP ratio (Figure 8.8) which points to a period of broad deforestation. There is a decline in *Olea*, *Celtis* and *Podocarpus* and a corresponding increase in *Poaceae* (> 40 %) (Figure 8.7).

Ashenge zone 3 (20-15 cm) (~1820-1950 CE) shows a recovered AP/NAP ratio (Figure 8.8) suggesting a small increase in woody vegetation cover. A decline in Poaceae (to < 20 %) is apparent, along with small increases in *Olea* and *Celtis* (Figure 8.7).

From 15 to 10 cm (*Ashenge zone 2*) (after 1950 CE), the AP/NAP ratio declines again (Figure 8.8), which points to a reduction in woody vegetation cover. There are relatively high percentages of *Rumex* (10

%), as well as a gradual increase in Poaceae (~40%) and a sharp decrease in *Juniperus* (to < 2 %) (Figure 8.7).

The sediments in the upper 10 cm of the core (*Ashenge zone 1*) (~ subrecent) are characterized by a rise in the AP/NAP ratio (Figure 8.8) due to increasing *Juniperus* and decreasing Poaceae (Figure 8.7). There is also an increase in the percentage of *Dodonea* and Asteraceae pollen.

8.4.2 Land cover changes derived from repeat photography

Based on the median scores given by 5-12 experts, a gradual decline of vegetation cover from 1868 towards the 1980s is evident on the historical photographs (Figure 8.9). For 1868, more woody vegetation is inferred while for the early 20th century less woody vegetation is deduced. Woody vegetation cover was particularly low starting in the 1950s, with minimum values occurring during the 1980s, followed by a rapid recovery. Hence, woody vegetation cover is rising in recent decades (Figure 8.9). The higher variance in the vegetation cover scores for the older photographs can be explained by (1) the fact that only three photographs were available for the older period (1868) of which one diverged strongly from the others, (2) the lower resolution of these older photographs, and (3) occurrence of land cover types (such as fallow land) that do not occur anymore nowadays, what makes the interpretation more difficult as compared to more recent photographs.

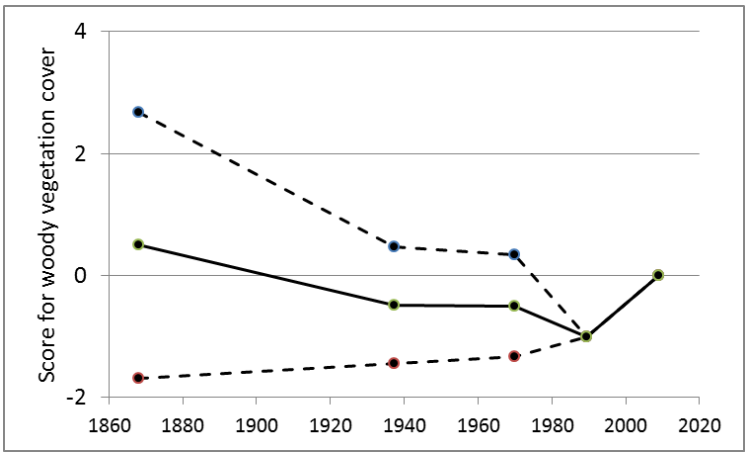

Figure 8.9 Interpretation of terrestrial photographs in the surroundings of Lake Ashenge (see location on map). Medians of scores given by 6-12 geographers and other environmental scientists for woody vegetation cover depicted on the photographs (-2 much less than on the recent photograph; 0 similar; +2 much more) were averaged per time period. All recent photographs received a score of 0 as it was the standard against which the historical scenery was interpreted. Dotted lines for average +/- one standard error. Photographs and their metadata are presented in Appendix A4.

8.4.3 Land cover changes derived from reports

8.4.3.1 General descriptions

According to the travel reports analyzed by Ritler (1997) and Stähli (2000), the Highlands were largely deforested by the 19th century, except in church forests, along rivers in deep valleys and on inaccessible steep slopes. It can further be assumed that the grassy bushland landscape of the 18th and 19th century did not greatly differ from that of the 16th and 17th centuries, as Stähli (2000) did not infer large forest declines over these periods. Exceptions are the bigger river valleys and the surroundings of cities such as Axum (see section 8.4.3.3).

According to the travel reports described by Ritler (2003), the main land use in the region between 1865 and 1930 was cereal agriculture, especially between 1500 and 3500 m a.s.l. Feudal taxes and levies impeded agricultural innovation and productivity increases (Ritler, 2003). Remnants of shrubs and forest were still only found in remote areas (e.g. steep slopes). Based on these reports, Ritler (2003) concludes that these spots of forest continued to decline from 1865 till the mid-20th century. Eucalyptus was probably introduced from 1895 onwards in the newly founded capital Addis (Ritler, 2003).

8.4.3.2 The surroundings of Lake Ashenge

The lands around Lake Ashenge, located along an important North-South travel route, have been described in several reports. Just to the East of the lake, on the slopes to the lower parts of the highland, Oromo people were living. Abargues de Sostén observed in 1883 that most of these Oromo were nomadic and Simon (reported in Ritler, 2003) at the same time also stated that some of them cultivated millet and cotton in the graben. The lands adjacent to the lake itself were cultivated. By 1868, there were vegetated terraces in-between fields, as well as small gullies and drainage ditches (supplementary data). Rohlfs mentions in 1869 the presence of irrigation systems around the lake, as well as cultivation of tobacco and pea nearby.

8.4.3.3 Spatiotemporal vegetation dynamics in the Northern Highlands

Cities like Axum were described as relatively green, having church forests and courtyards with trees, shrubs and hedges during the 18th and 19th century. The immediate surroundings of the two cities were usually described as treeless, with meadows, pastures and bushlands. Stähli (2000) reports explicitly that tree and forest cover increased with distance from these cities. Indeed, the broad

regions between Adigrat and Axum and around the bigger rivers were described as quite forested during the 18th century; with trees and forests not only in the valleys, but also on terraces, ridges and hills. These relatively large forests disappeared in the course of the 19th century and towards the end of the 19th century, the regions had become sparsely wooded (Stähli, 2000).

More semi-peripheral regions have been described as poor in woody vegetation, with prevailing grasslands and bushlands and characterized by a high absence of trees and forests. Stähli (2000) infers that the more peripheral and the less influenced by people, the more forest was still present. Peripheral river valleys for instance remained largely untouched by humans and were spared from military turmoil (Stähli, 2000).

8.5 Discussion

8.5.1 Periods of land cover change

The Ashenge lake record contradicts the already contested claims that deforestation in North Ethiopia occurred mainly during the 20th century (Narrative of Deforestation) (Nyssen et al., 2009a): the pollen data suggest that deforestation occurred in a nonlinear-cyclic instead of a gradually-accelerating pattern. For the last 150 years, we could compare the pollen assemblages with the patterns derived from the photographic and descriptive historical records. By doing so, and following Lishawa et al. (2013), pollen analysis was validated as an effective way for identifying vegetation cover changes in the Ashenge closed basin. Based on the proxy records, we discuss five broad periods of land cover, summarized in Table 8.3. These include (i) the pre-18th century; (ii) the civil war (*Zemene Mesafint*) coinciding with a large-scale regional drought; (iii) the early-feudal era; (iv) the late-feudal and civil war period coinciding with a severe drought; and (v) the post-revolution period (after 1991).

Table 8.3 Land cover periods as identified from the proxy records.

Ashenge zone	*Years*	*Period*	*Society*	*Population density*	*'Climate'*	*Proxy record*
1	1990s-2000s	Post-revolution	Equal land rights, conservation	High	periodic droughts	Repeat photos
2	1950-1990	Late-Feudal era and civil war	Lack of agricultural investments	Medium	dry 1980s	Repeat photos
3	1820-1950	Early-Feudal era	Unification	Low	periodic droughts	Repeat photos Deep lake core Historical sources
4	1700-1820	Decline and civil war	*gult* land tenure	Low	dryer 18th century	Deep core Historical sources
5	Pre-1700	Gondar Period	Centralization	Low	'wet Little Ice Age'	Literature Deep lake core

8.5.1.1 Pre-18th century forestation (Ashenge zone 5)

The relatively high AP/NAP ratio (Figure 8.8) and the abundance of *Juniperus*, *Olea*, *Celtis* and *Podocarpus* (Figure 8.7) at the lowest parts of the core (< 28 cm) indicate a relatively large extent of montane forest before ~ 1700 CE. This is in line with the *Juniperus*, *Olea* and *Celtis* forest expansion between 1400 and 1700 CE reported by Darbyshire et al. (2003) at Lake Hayk, when – as compared to previous centuries – the nomadic and pastoral lifestyle of Oromo immigrants reduced pressure on the land (Kelbessa, 2005). Ritler (1997) infers for instance that forests in areas settled by Oromos were significantly larger, due to the cultural importance of trees for Oromo. The surroundings of Lake Ashenge were indeed also occupied by Oromo (Ritler, 2003).

The occurrence of some species in the pollen diagram can inform us on past agro-ecological practices. There is for instance maize pollen at the bottom of our core. Maize was introduced to

Ethiopia in the 16th century (Huffnagel, 1961; Bedada et al., 2011), following Portuguese explorations of the Indian Ocean. Maize pollen was also identified from 1650 CE onwards in Lake Naivasha (Kenya) (Lamb et al., 2003). Some other (forest) species have been popular for medicinal use (e.g. *Celtis*) or as timber (*Podocarpus*, *Juniperus*).

In the North Ethiopian Highlands, the Little Ice Age was a generally wet period (Lamb et al., 2007) but also markedly cooler (Bonnefille & Umer, 1994). The occurrence of Ericaceae pollen in the bottom of the core (~ 5%) might thus point to a lowering of the *Erica* belt (Jacob et al., 2015a) following the colder conditions.

8.5.1.2 Deforestation during the civil war (~1700-1820 CE) (Ashenge zone 4)

The period from ~1700 to 1820 featured declining *Olea*, *Celtis*, and *Podocarpus*, increasing Poaceae (Figure 8.7), and a sharp decline in AP/NAP (Figure 8.8). This is consistent with the pollen evidence. Again, this is in line with the pollen evidence of Darbyshire et al. (2003) who identify a strong decrease in Cupressaceae, *Olea* and *Celtis* at Lake Hayk since 1700 CE, together with a rise in *Dodonaea*, Poaceae and *Rumex* as evidence for a conversion of forest towards bushlands and grasslands. The peak in mass-median-diameter of the sediment particles (at 27 cm depth) indicates an increase in the influx of coarse particles during the early 18th century (D50 of ~ 10 µm). Proportions of clay, indicative of landscape stability, drop sharply at this depth (< 20 %). Similarly, Darbyshire et al. (2003) find a rise in sediment magnetic susceptibility during this period (Lake Hayk core).

The 18th century is a period of political turmoil and civil war in North Ethiopia, including the complete destruction of certain regions (*Zemene Mesafint*) (Pankhurst, 1990). There is the decline of the centralized Gondar monarchy (accelerated since the death of Joshua I in 1706), giving rise to a period of Provincial Rulers lasting until the coronation of Tewodros II in 1855. In Tigray, *Mikael Sehul* ruled the region with Adwa at its centre. Roving chiefdoms caused devastating long-term environmental changes as "they would establish themselves in settlements with fertile fields and depart when the surrounding lands could no longer produce crops" (Abebe, 1998; Tsige Gebru et al., 2009). New regional capitals arose, although the numerous wars and political turmoil resulted in their abandonment or destruction towards the end of the 19th century (Stähli, 2000). Land tenure was organized in an unequal *gult* system (Ståhl, 1974), with lands granted to landlords in exchange for military or administrative services. The *gult* right was the right for the ruling elite (nobility, Church and privileged farmers) to demand work and taxes from the subjects in certain allocated regions

(Ritler, 2003). The Church owned a large part of the lands and there were three classes of farmers, including small peasants, rich proprietors and farm wage labourers (Pankhurst, 1990). During the early-19th century, the farm wage labourers consisted of woodcutters, grass cutters and *kofari* or 'diggers' who had to dig and clear vegetated lands on steep slopes for cultivation (Pankhurst, 1990). The German explorer Eduard Rüppell reports the use of fallowing every other year while locust pests were frequent (Pankhurst, 1990). The French scientific mission and the British expedition against Tewodros report a complete absence of trees in the landscape (Pankhurst, 1990), which is in line with findings from a quantitative analysis based on repeated photographs from 1868 in Tigray (Nyssen et al., 2014). Stähli (2000) asserts that the main drivers of vegetation clearances in Tigray during the 18th and 19th century were (i) the exploitative feudal ruling class and *gult* land tenure system, (ii) the vortex of various military conflicts under a legally and politically unstable situation, and (iii) epidemics and locusts. As will be discussed in section 8.5.3, there was also a tendency to dryer conditions over the early 18th century with a climax drought around 1750 CE (Lamb et al., 2007).

8.5.1.3 Gradual changes in the early-feudal era (1820s – 1950s) (Ashenge zone 3)

The small increases in *Olea* and *Celtis* corresponding to the decline in Poaceae pollen (20-15 cm) (Figure 8.7) and relatively elevated AP/NAP ratio in 1820-1950 (Figure 8.8) suggest a minor and local increase in forest cover. Indeed, woody vegetation cover around the lake was relatively abundant during the mid-19th century and was even greater than today (as indicated by median expert scores of ~ + 0.5) (Figure 8.9). Starting around 1865, however, woody vegetation cover began to decrease gradually (Figure 8.9). Simon for instance reports in 1885 deliberate forest burning to the North of Lake Ashenge by the troops of Yohannes IV, in order to avoid ambushes by Oromo groups. Forest burning continued up to the 1970s (Nyssen et al., 2009b), and Nyssen et al. (2009b) even report that forest burning continues at present. Overall, woody vegetation cover increased in the North Ethiopian Highlands from 1865 to 1950 with a relative optimum in the 1930s (Nyssen et al., 2014).

Resulting from the decline in imperial power after the 18th century (*Zemene Mesafint*), *gult* rights increasingly became inherited rights (*rist* rights), especially during and after the first third of the 20th century (Ritler, 2003). Ståhl (1974) describes this as the late-19th century transition from a 'tributary' towards an 'early-feudal' agro-system. Subsequently, after the reunification by Tewodros II, noblemen owned most of the lands by ancestral descent (*rist* lands). In particular the larger, low-lying and level parcels were owned by aristocrats. Gradually, more and more poor farmers had to establish their farms on marginal terrains, such as steep slopes in dry areas and marshes in cold and

humid areas, leading to increased catchment water runoff and degradation (Chapter 3). The *rist* lands were lent out in a sharecropping system (Thomas et al., 1991), locally named *mwufar*, which made them less appropriate for long-term soil and water conservation investments due to tenure insecurity (Chapter 3). Such feudal environmental degradation indeed relies on the lord-peasant relationship, over time limiting reinvestment in the lands (Moore, 2002).

8.5.1.4 Minimum cover during the late-feudal era (1950-1990) (Ashenge zone 2)

Since the 1950s, woody vegetation cover dropped towards a minimum, indicated by median expert scores ~ -0.5 (Figure 8.9) and a low AP/NAP ratio (Figure 8.8). The relatively high percentages of *Rumex* with the gradual increase in Poaceae and decrease in *Juniperus* (15 to 10 cm) also correspond to this period. This is in line with the findings of De Meyere et al (2015) who found a peak in cropland cover and a minimum of woody vegetation at the end of the 1960s at the nearby Rift Escarpment. This reflects the worsened environmental situation inherited from stagnated agricultural investments under a highly unequal late-feudal land tenure system (Chapter 3). From case studies across the Tigray Highlands, Kassa Teka Belay et al. (2014) calculated that average forest and dense bushland cover evolved from 18.5% in 1965 to 2.7% in 1994 (and 3.2% in 2007). Additionally, there is the impact of the civil war, further destabilizing the agricultural economy. Simultaneously, during the 1980s, a succession of strong droughts was caused by atmospheric responses to the interplay of the El Niño Southern Oscillation, the Indian Ocean Dipole and the South West Monsoons (Chapter 2). As a consequence, during the 1980s large alluvial debris fans developed around Lake Ashenge, evidencing increased gully sediment supply (Chapter 6).

8.5.1.5 Forest transition after the regime change (after 1991) (Ashenge zone 1)

Woody vegetation cover has risen over the last two decades, such that it is approaching the levels of the late 19th century (Figure 8.9). Increases in the AP/NAP ratio (Figure 8.8) and in *Juniperus*, with decreases in Poaceae in the upper 10 cm of the core (Figure 8.7), point to a forest transition over the past two decades. Under the Derg regime, *Juniperus* forests have been planted in the Ashenge basin (Figure 8.10). The rise in pollen of *Dodonea* and Asteraceae (Figure 8.7) points to the large-scale establishment of exclosures. We have observed that gully check dams are now stabilizing gullies around the lake. From 2000 CE onwards, large-scale terracing of the catchment's slopes has been leading to lower sediment supply towards the lake (Frankl et al., 2011). The post-revolution government initiated a large-scale land reform in the early 1990s, when all farmers received an

approximately equal share in the amount of cropland (roughly three plots). As a result of massive land management and conservation investments, and overriding the impacts of climate variability, the North Ethiopian Highlands are now greener than at any time in the last 145 years (Nyssen et al., 2014).

Figure 8.10 Example of a *Juniperus/Eucalyptus* forest on a hill near Lake Ashenge, which was planted and regenerated since the 1980s.

8.5.2 Population growth as a driver of vegetation cover?

Based on traveler estimations, Ritler (2003) claims that population in central-northern Ethiopia grew from 4 million inhabitants (mid-nineteenth century) to 6 to 8 million in 1930 in the same area. Our records indicate that such overall population growth is not in phase with the more cyclic evolution of vegetation cover. Environmental degradation during the 18th century, evidenced by the declining AP/NAP ratio, increasing abundance of Poaceae, and higher inputs of coarse-textured sediments in the lake core, is at odds with the low population densities at that time (estimated at less than 10 inhabitants per km^2) (Nyssen et al., 2014). Moreover, the greening of the North Ethiopian landscape over the last two decades contrasts with the very high population densities of today (over 100 inhabitants per km^2). The vegetation proxies gathered in this study thus do not deliver convincing evidence for a neo-Malthusian interpretation of deforestation in the Highlands. This is in line with the findings of Jacob et al. (2015b), and with Nyssen et al. (2014), who identified more intensive recent vegetation increases in North Ethiopian regions with higher population densities. The fact that high human populations are associated with landscape greening rather than deforestation does not support a neo-Malthusian forcing of population-vegetation dynamics in the Highlands (Jacob et al., 2015b; Leach and Fairhead, 2000).

8.5.3 The impact of past climate change

Yilma & Demarée (1995) and Camberlin (1994) suggested that the North Ethiopian Highland has become drier over the last decades, but this is contradicted by meteorological studies (e.g. Conway, 2000; Cheung et al., 2008). However, the stable isotope record from Lake Hayk (Lamb et al., 2007) indicates that the Ethiopian Highlands periodically experience large temporal drought. The Highlands were relatively wet during the Little Ice Age (Ashenge zone 5) and became dryer during the 18th century (Ashenge zone 4), with a climax drought around 1750 CE (Lamb et al., 2007). This climatic change towards dry conditions might also be reflected in our record by higher abundances of Cyperaceae (Figure 8.7) pointing to a lowering of the lake level that allows sedges to increase in the littoral zone (Darbyshire et al., 2003). Regional drought was also widespread at the end of the 18th century in East Africa, as shown from lake sediments in Kenya (Lake Turkana, Lake Baringo, the Naivasha lakes, Lake Challa) and Uganda (Lake Victoria and some crater lakes) (De Cort et al., 2013). Additionally, a number of region-wide droughts are indicated by wetness proxies for the Sahel/Soudan and East Africa (Nicholson et al., 2012) during the early 19th century. Following Tierney et al. (2013), such decade-scale drought variability can result from sea surface temperature variability in the Indian Ocean. Thus, the deforestation that took place during the early 18th century and the 1950s-1980s was likely exacerbated by the dry conditions that occurred during those intervals. The clear chronological overlap between climatic shifts, social upheaval and deforestation phases during both the early 18th century and the 1950s-1980s suggests that positive climate-human-vegetation feedbacks can occur that amplify the effects of drought.

8.6 Conclusions

Until quite recently, there was a widespread perception that in the early 1900s, the Highlands of Ethiopia were covered by a vast forest that rapidly disappeared over the course of a few decades. The forest clearance would have resulted in severe land degradation and recurrent famine during the late 20th century. However, this hypothesis is not very persuasive because historical landscape photographs from the 19th century show a land that was already barren without much of woody vegetation. We analysed sediments from Lake Ashenge to show that the events of the late 20th

century were indeed not exceptional: the Highlands experienced environmental shifts before. Around 1700 CE, forest extent was relatively large, possibly in relation to the lifestyle of Oromo people. Pollen evidence suggests that deforestation occurred during the (early) 18th century, influenced by the dryer conditions of that time. Later, there were gradual vegetation cover changes during the early-feudal period. During the late-feudal period and the civil war, vegetation cover was at a minimum (1950 – 1990), as impacted by a number of dry spells during the 1980s. The recent rises in pollen of planted *Dodonea* and pioneer Asteraceae exemplify the large-scale investments in reforestation, rendering the Highlands greener than long time before. Overall, we show that climate-human ecosystems in the Ethiopian Highlands pass through complex and nonlinear changes, mediated by land policies and the periodic occurrence of dry spells. In line with a 'political ecology' perspective of land degradation in the Highlands, we call into question the simplistic 'narratives' concerning drivers of vegetation cover (population growth in particular) that still misinform modern agro-ecological policy.

Acknowledgements

This study would not have been possible without the friendship and help of our translator Gebrekidan Mesfin, the support and kindliness of the fishermen of Lake Ashenge who were willing to assist us on the lake, the support and material assistance of the research units Physical Geography, Sedimentology and Limnology at Ghent University, the support of the radiochronology laboratory of the Centre d'Etudes nordiques (Laval University), the help from the Belgo-Ethiopian VLIR MU-IUC programme and funding through a scholarship of Ghent University (BOF). Thanks go also to Mitiku Haile, Hans Hurni, Katrien Descheemaeker, Donald Crummey, Brigitte Portner, Bernhard Nievergelt, Jan Moeyersons, Neil Munro, Jozef Deckers, Paolo Billi and Jean Poesen for the interpretation of the repeated photographs. Constructive comments by two anonymous reviewers are acknowledged.

8.7 References

Abargués de Sostén, 1885. Voyage en Abyssinie, dans le Zeboul et les Wallo-Gallas. Bulletin de la Société Khédiviale de Géographie II 6, Cairo, Egypt.

Abebe, B., 1998. Histoire de L'Éthiopie d'Axoum à la revolution. Maisonneuve et Larose, Paris, France.

Adger, N., Benjaminsen, T., Brown, K., Svarstad, H., 2001. Advancing a Political Ecology of global environmental discourses. Development and Change 32, 681-715.

Allen-Rowlandson, T., 1989. A new approach to wildlife conservation in Ethiopia and its relevance to the control of desertification. In: Verwey W.D., editor. Nature management and sustainable development. IOS Press, Amsterdam, The Netherlands, 307-315 p.

Bard, K., 1996. Ancient Egyptians and the issue of race. In: M.R. Lefkowitz, G.M. Rogers (Eds.), The Black Athena Revisited, University of North Carolina Press, Chapel Hill, NC, USA, 103–111 p.

Batterbury, S., Forsyth, T., Thomson, K., 1997. Environmental transformations in developing countries: hybrid research and democratic policy. Geographical Journal 163 (2), 126-132.

Batterbury, S., Bebbington, A., 1999. Environmental histories, access to resources and landscape change: an introduction. Land Degradation and Development 10 (4), 279-289.

Bedada, L., Seth, M., Runo, S., Tefera, W., Machuka, J., 2011. Plant Regeneration of Ethiopian Tropical Maize (Zea mays L.) Genotypes. Biotechnology 10, 506-513.

Bonnefille R., Buchet G., 1987. Contribution palynologique à l'histoire récente de la forêt de Wenchi (Ethiopie). Mémoires et Travaux de l'Ecole Pratique des Hautes Etudes de Montpellier 17, 143-158.

Bonnefille, R., Umer, M., 1994. Pollen inferred climatic fluctuations inEthiopia during the last 3000 years. Palaeogeography, Palaeoecology, Palaeoclimatology 109, 331–343.

Camberlin, P., 1994. Les précipitations dans la corne orientale de l'Afrique: climatologie, variabilité et connexions avec quelques indicateurs océano-atmosphériques. PhD dissertation, Université de Bourgogne, Dijon, France, 379 p.

Chalié, F., Gasse, F., 2002. Late Glacial-Holocene diatom record of water chemistry and lake level change from the tropical East African Rift Lake Abiyata (Ethiopia). Palaeogeogr. Palaeoclimatol. Palaeoecol. 187, 259–283.

Cheung, W., Senay, G., Singh, A., 2008. Trends and spatial distribution of annual and seasonal rainfall in Ethiopia. Int J Climatol 28, 1723–1734.

Conway, D., 2000. Some aspects of climate variability in the North East Ethiopian highlands—Wollo and Tigray. Ethiopian Journal of Science 23 (2), 139– 161.

Darbyshire, I., Lamb, H., Umer, M., 2003. Forest clearance and regrowth in northern Ethiopia during the last 3000 years. The Holocene 13 (4), 537–546.

De Cort, G., Bessems, I., Keppens, E., Mees, F., Cumming, B., Verschuren, D., 2013. Late-Holocene and recent hydroclimatic variability in the central Kenya Rift Valley: The sediment record of hypersaline lakes Bogoria, Nakuru and Elementeita. Palaeogeography, Palaeoclimatology, Palaeoecology 388, 69–80.

DeFries, R., Rudel, T., Uriarte, M., Hansen, M., 2010. Deforestation driven by urban population growth and agricultural trade in the twenty-first century. Nature Geoscience 3, 178-181.

De Meyere, M., Tesfaalem G. Asfaha, Frankl, A., Mitiku Haile, Nyssen, J., 2015. Land cover trajectories and runoff response on the Ethiopian Rift Valley escarpment over the last eight decades. Geomorphology, submitted.

Easdale, M., Domptail, S., 2014. Fate can be changed! Arid rangelands in a globalizing world - A complementary co-evolutionary perspective on the current 'desert syndrome'. Journal of Arid Environments 100, 52-62.

Faegri, K., Iverson, J., 1975. Text Book of Pollen Analysis. 3rd revised edition by K. Faegri. Munksgaard, Copenhagen, Denmark, 295 p.

Frankl, A., Nyssen, J., De Dapper, M., Mitiku Haile, Billi, P., Munro, R., Deckers, J., Poesen, J., 2011. Linking long-term gully and river channel dynamics to environmental change using repeat photography (North Ethiopia). Geomorphology 129 (3-4), 238-251.

Fritz, S.C., Cumming, B.F., Gasse, F., Laird, K., 1999. Diatoms as indicators of hydrologic and climate change in saline lakes. In: Stoermer, E.F., Smol, J.P. (Eds.), The Diatoms: Applications for Environmental and Earth Sciences. Cambridge University Press, Cambridge, UK, 41–72 p.

Funk, C., Rowland, J., Eilerts, G., Emebet Kebebe, Nigist Biru, White, L., Gideon Galu, 2012. A Climate Trend Analysis of Ethiopia. Famine Early Warning Systems Network—Informing Climate Change Adaptation Series: Fact Sheet 3053.

Hendrickx, H., Jacob, M., Frankl, A., Etefa Guyassa, Nyssen, J., 2014. Quaternary glacial and periglacial processes in the Ethiopian Highlands in relation to the current afro-alpine vegetation. Zeitschrift für Geomorphologie 59 (1), 1-21.

Huffnagel, H., 1961. Agriculture in Ethiopia. Food and Agriculture Organization of the United Nation Organization, Rome, Italy, 465 p.

Jacob, M., Frankl, A., Beeckman, H., Gebrekidan Mesfin, Hendrickx, M., Etefa Guyassa, Nyssen, J., 2015a. North Ethiopian Afro-Alpine tree line dynamics and forest-cover change since the early 20th century. Land Degradation and Development 26 (7), 654–664.

Jacob, M., Romeyns, L., Frankl, A., Tesfaalem Asfaha, Beeckman, H., Nyssen, J., 2015b. Land use and cover dynamics since 1964 in the Afro-Alpine vegetation belt: Lib Amba mountain in North Ethiopia. Land Degradation and Development, online early view. DOI: 10.1002/ldr.2396.

Kassa Teka Belay, Van Rompaey, A., Poesen, J., Van Bruyssel, S., Deckers, J., Kassa Amare, 2014. Spatial analysis of land cover changes in Eastern Tigray (Ethiopia) from 1965–2007: are there signs of a forest transition? Land Degradation and Development 26 (7), 680-689.

Kelbessa, W., 2005. The utility of ethical dialogue for marginalized voices in Africa. Discussion Paper 'Sharpening policy tools for marginalized managers of natural resources'. Addis Ababa University, Addis Ababa, Ethiopia, 45 p.

Kurkura Kabeto, Aynalem Zenebe, Bheemalingeswara, K., Kinfe Atshbeha, Solomon Gebresilassie, Kassa Amare, 2012. Mineralogical and geochemical characterization of clay and lacustrine deposits of Lake Ashenge basin, Northern Ethiopia: implication for industrial applications. Momona Ethiopian Journal of Science 4 (2), 111-129.

Lamb, H., Darbyshire, I., Verschuren, D., 2003. Vegetation response to rainfall variation and human impact in central Kenya during the past 1100 years. The Holocene 13 (2), 285-292.

Lamb, H., Leng, M., Telford, R., Tenalem Ayenew, Umer, M., 2007. Oxygen and carbon isotope composition of authigenic carbonate from an Ethiopian lake: a climate record of the last 2000 years. The Holocene 17 (4), 517–526.

Leach, M., Fairhead, J., 2000. Challenging Neo-Malthusian Deforestation Analyses in West Africa's Dynamic Forest Landscapes. Population and Development Review 26 (1), 17–43.

Lishawa, S., Treering, D., Vail, L., McKenna, O., Grimm, E., Tuchman, N., 2013. Reconstructing plant invasions using historical aerial imagery and pollen core analysis: Typha in the Laurentian Great Lakes. Diversity and Distributions 19 (1), 14-28.

Marshall, M.H., 2006. Late Pleistocene and Holocene palaeolimnology of Lakes Tana and Ashenge, Northern Ethiopia. Unpublished Ph.D Thesis, Univ. Wales Aberystwyth, Ceredigion, Wales, UK, 324 p.

Marshall, M., Lamb, H., Davies, S., Leng, M., Zelalem Kubsa, Umer, M., Bryant, C., 2009. Climatic change in northern Ethiopia during the past 17,000 years: A diatom and stable isotope record from Lake Ashenge. Palaeogeography, Palaeoclimatology, Palaeoecology 279, 114–127.

McCann, J., 1997. The Plow and the Forest: Narratives of Deforestation in Ethiopia 1840-1992. Environmental History 2 (2), 138-159.

Meadows, D., Meadows, D., Randers, J., Behrens, W., 1972. Limits to growth. Universe Books, New York, USA.

Merla, G., Abbate, E., Azzaroli, A., Bruni, P., Canuti, P., Fazzuoli, M., Sagri, M. Tacconi, P., 1979. A Geological Map of Ethiopia and Somalia (1973). 1:2000.000; and Comment. University of Florence, Firenze, Italy.

Micromeritics, 2014. Overview SediGraph III Plus. http://www.micromeritics.com/ (accessed on 14/05/2014)

Moore, J., 2002. The crisis of feudalism - An environmental history. Organization & Environment 15 (3), 301-322.

Muller, T., 2013. The Ethiopian famine revisited: Band Aid and the antipolitics of celebrity humanitarian action. Disasters 37 (1), 61-79.

Nicholson, S., Dezfuli, A., Klotter, D., 2012. A two-century precipitation dataset for the continent of Africa. Bull. Amer. Meteor. Soc. 93, 1219–1231.

Nyssen, J., Poesen, J., Moeyersons, J., Deckers, J., Mitiku Haile, Lang, A., 2004. Human impact on the environment in the Ethiopian and Eritrean highlands - a state of the art. Earth-Science Reviews 64 (3-4), 273-320.

Nyssen, J., Mitiku Haile, Naudts, J., Munro, N., Poesen, J., Moeyersons, J., Frankl, A., Deckers, J., Pankhurst, R., 2009a. Desertification? Northern Ethiopia re-photographed after 140 years. Science of the Total Environment 407 (8), 2749-2755.

Nyssen, J., Getachew Simegn, Nurhussen Taha, 2009b. An upland farming system under transformation: Proximate causes of land use change in Bela-Welleh catchment (Wag, Northern Ethiopian Highlands). Soil and Tillage Research 103 (2), 231–238.

Nyssen, J., Frankl, A., Mitiku Haile, Hurni, H., Descheemaeker, K., Crummey, D., Ritler, A., Portner, B., Nievergelt, B., Moeyersons, J., Munro, R.N., Deckers, J., Billi, P., Poesen, J., 2014. Environmental conditions and human drivers for changes to north Ethiopian mountain landscapes over 145 years. Science of the Total Environment 485-486, 164-179.

Pankhurst, R., 1990. A Social History of Ethiopia: The Northern and Central Highlands from Early Medieval Times to the Rise of Emperor Tewodros II. Addis Ababa University, Addis Ababa, Ethiopia, 371 p.

Parry, J., 2003. Tree choppers become tree planters. Appropriate Technology 30(4), 38-39.

Preston, D., Macklin, M., Warburton, J., 1997. Fewer people, less erosion: the twentieth century in southern Bolivia. The Geographical Journal 163, 198–205.

Reubens, B., Poesen, J., Nyssen, J., Leduc, Y., Abraha, A. Z., Tewoldeberhan, S., Muys, B., 2009. Establishment and management of woody seedlings in gullies in a semi-arid environment (Tigray, Ethiopia). Plant and Soil 324 (1-2), 131-156.

Ritler, A., 1997. Land Use, Forests and the Landscape of Ethiopia, 1699-1865. Soil Conservation Research Programme Ethiopia, Research Report 38, 222 p.

Ritler, A., 2003. Forest, land use and landscape in the Central and Northern Ethiopian Highlands, 1865-1930. PhD dissertation, Institute of Geography, Universität Bern, Bern, Switzerland.

Roberts, N., Eastwood, W., Kuzucuoglu, C., Fiorentino, G., Caracuta, V., 2011. Climatic, vegetation and cultural change in the eastern Mediterranean during the mid-Holocene environmental transition. Holocene 21 (1), 147-162.

Roberts, N., 2014. The Holocene, an environmental history (Third Edition). Blackwell Publ, Oxford, UK.

Robinson, I., MacKay, R., Afwerki Solomon, Yragelem Afwerki, 1995. A Review of the Agricultural Rehabilitation Programmes of Eritrea Bangor: Centre for Arid Zone Studies. University of Wales, Bangor, Wales, UK.

Rohlfs, G., 1883. Meine Mission nach Abessinien. Auf Befehl Sr. Maj. des Deutschen Kaisers im Winter 1880/81, Leipzig, Germany.

SCAR (Scientific Committee on Antarctic Research), 2014. Loss on Ignition. Available from: www.scar.org:8000/facilities/laboratories/techniques/loi.doc (accessed on 14/05/2014)

Schuett, B., Busschert, R., 2005. Geomorphological reconstruction of palaeo Lake Ashengi, Northern Ethiopia. Lake Abaya Research Symposium, Siegen, Germany. FWU Water Resources Publications, 51-57 p.

Sepulchre, P., Ramstein, G., Fluteau, F., Schuster, M., Tiercelin, J., Brunet, M., 2006. Tectonic uplift and Eastern Africa aridification. Science 313, 1419-1423.

Simon, G., 1885. Voyage en Abyssinie et chez les Gallas-Raias. L'Éthiopie, ses moeurs, ses traditions, le négouss Iohannès, les églises monolithes de Lalibéla. Victor Magen, Paris, France.

Ståhl, M., 1974. Ethiopia: political contradictions in agricultural development. Rabén & Sjögren, Stockholm, Sweden, 186 p.

Stähli, P., 2000. Historische Landschaftsveränderungen in Tigray (Äthiopien), 1520-1900. Master Thesis, Universität Bern, Bern, Switzerland.

Stocking, M., 1995. Soil erosion in developing countries: where geomorphology fears to tread! Catena 25 (1–4), 253-267.

Tekle Kebrom, Hedlund, L., 2000. Land cover changes between 1958 and 1986 in Kalu district, Southern Wello, Ethiopia. Mountain Research and Development 2, 42-51.

Thomas, P., Ofcansky, B., LaVerle, B., 1991. Ethiopia: A Country Study. GPO for the Library of Congress, Washington, USA.

Tierney, J., Smerdon, J.,Anchukaitis, K., Seager, R., 2013. Multidecadal variability in East African hydroclimate controlled by the Indian Ocean. Nature 493, 389–392.

Trauth, M., Maslin, M., Deino, M., Deino, A. Strecker, M., 2005. Late Cenozoic moisture history of East Africa. Science 203, 2051-2053.

Tsige Gebru, Zewdu Eshetu, Huang, Y., Taddese Woldemariam, Strong, N., Umer, M., DiBlasi, M. Terwilliger, V., 2009. Holocene palaeovegetation of the Tigray Plateau in northern Ethiopia from charcoal and stable organic carbon isotopic analyses of gully sediments. Palaeogeography, Palaeoclimatology, Palaeoecology 282 (1–4), 67–80.

Umer, M., Lamb, H.F., Bonnefille, R., Lézine, A.-M., Tiercelin, J.-J., Gibert, E., Cazet, J.-P., Watrin, J., 2007. Late Pleistocene and Holocene history of the Bale Mountains, Ethiopia. Quat. Sci. Rev. 26, 2229–2246.

Uwitec, 2014. Uwitec Sampling Equipment. http://www.uwitec.at/ (accessed on 12/12/2014)

Wøien, H., 1995. Deforestation, information and citations: a comment on environmental degradation in Highland Ethiopia. Geojournal 37 (4), 501-512.

Yilma S, Demarée G., 1995. Rainfall variability in the Ethiopian and Eritrean highlands and its links with the Southern Oscillation Index. J. Biogeogr. 22, 945–952.

Part III

Chapter 9 General discussion

Abstract

By confronting the results of chapter 2 to 8 with other paleo-environmental studies from the broader Horn of Africa, we here develop a model of Late-Holocene geomorphological change in the Ethiopian Highlands. We show that long-term land degradation changes in the Ethiopian highlands do not conform to a linear model of environmental degradation under rapid population growth. However, we establish a significant relation between major climate changes and land degradation cycles that was mediated through pastoralism and political conflict. Land resilience has been observed in recent decades, which suggests that the regional ecosystem may be robust and elastic, with fast recovery. The strong associations between climate changes, land cover and sediment activity were used to develop climate-resilient land management strategies under conditions of future climate change.

9.1 Nonlinear hydrogeomorphological changes

"New scientific ideas about climate-human-ecosystem interaction inspire a complex theory related to concepts of nonlinear change, feedback processes and regime shifts, instead of a simplified dichotomy between climatic determinism and human resource exploitation." (Gelorini and Verschuren, 2013).

As discussed in the previous chapters, there is no evidence to assume a linear drying trend or steadily accelerating pressure from population growth in the Ethiopian Highlands, as the late 20th century degradation period was merely one of the many periodic shifts that occurred during the course of the Holocene. Following Roberts (2006), Holocene environmental changes often do not follow a gradual trajectory but ought to be understood as a series of metastable equilibrium states (steady states), only interrupted by rapid environmental shifts when certain thresholds are crossed. Our Ethiopian paleoenvironmental data suggest a similar pattern of long-term hydrogeomorphological 'equilibrium states' with 'rapid transitions'. In Figure 9.1, we indicated several of these equilibrium states and transition periods, together with some important drivers. This flow chart may help the reader to explore this chapter.

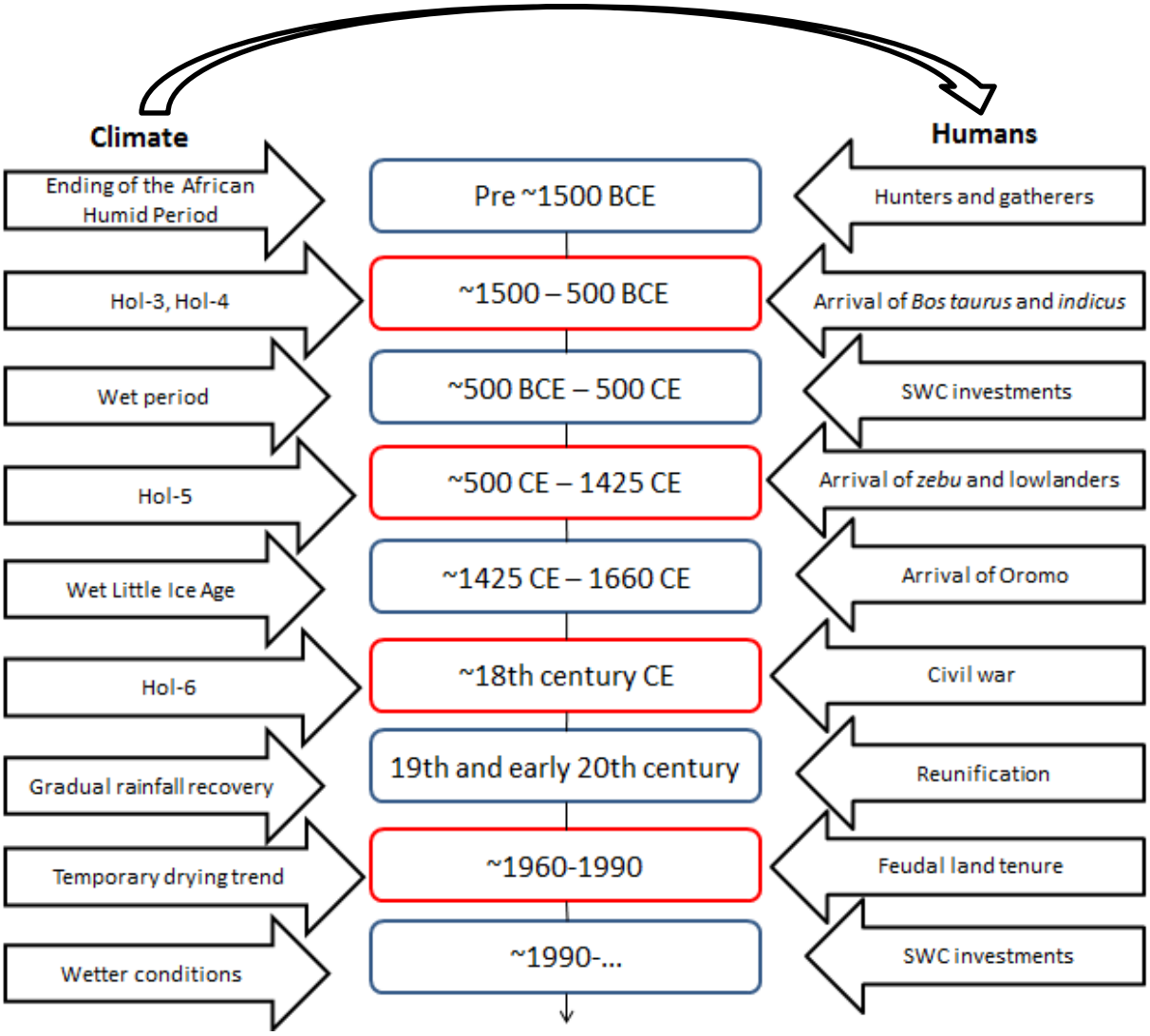

Figure 9.1 Flow chart indicating Late Holocene equilibrium states (in blue) and transition/degradation periods (in red), together with some important drivers (black arrows). The arrow between climatic and human drivers indicates likely climate-humans-ecosystem feedback.

By integrating different land-cover and hydrogeomorphic data, we can infer a nonlinear temporal pattern of hydrogeomorphological change in the Highlands (Figure 9.2). Dated evidence for a phase of Vertisol development, pedogenesis or travertine development (landscape stability) during the Mid-Holocene is abundant (Semmel, 1971; Verheye, 1978; Hurni, 1982; Brancaccio et al., 1997; Nyssen et al., 2004; Ogbaghebriel et al., 1997) (Figure 9.2). Then, sediment transport to floodplains in the Northern Highlands markedly increased from 1550-1500 BCE onwards (Machado et al., 1998; Chapter 5). This approximates the dates for increased colluvial activity obtained by Moeyersons et al. (2006) (1430-1260 BCE), when the ratio of phytolithic monocotyledons/dicotyledons sharply increased

(from 9% to 74%). It also matches the decrease in trees/shrub ratio after 1400-1100 BCE identified by Pietsch and Machado (2014) in the Northern Highlands (Yeha).

The landscape in the Highlands further transformed during the first millennium BCE, when May Tsimble was (still) aggrading (Chapter 5). There was rapid decline of the *Podocarpus-Juniperus* forest that was replaced by shrubs and grasslands between 800-500 BCE (Darbyshire et al., 2003). Slightly before the sharp decline of arboreal pollen at Lake Hayk, a steep increase of allochthonous material between 950 and 750 BCE pointed to anthropogenic soil erosion under agricultural activity in the Ashenge catchment (unpublished pollen data of Marshall et al., 2009). Decline of forest in the southern highlands (Bale Mountains) is identified from pollen analysis and dated about 600 years later (Umer et al., 2007).

As inferred by French et al. (2009), there is clear geoarcheological and geomorphic evidence for landscape stabilization in North Ethiopia during the Axumite times. Geomorphic stability was evidenced from Vertisol development (French et al., 2009), decreased soil erosion rates (Ciampalini et al., 2008) and diminished sediment supply from 500 BCE to 400 CE (Machado et al., 1998; Chapter 5). Pietsch and Machado (2014) identify an increased ratio of trees/shrubs during this period.

After 400 CE, the landscape in the Highlands became relatively degraded as evidenced by fluvial destabilization (Machado et al., 1998) and a dominance of grassland vegetation in the northern Highlands (Darbyshire et al., 2003) and higher sediment supply in the eastern Highlands (Chapter 5). Local increases of forest cover occurred from 1400 to 1700 CE, as indicated by the pollen records of Lake Hayk (Darbyshire et al., 2003) and Lake Ashenge (Chapter 8), and the start of a phase of soil formation in the Northern Highlands was dated to 1425-1445 CE, lasting till 1481-1660 CE (Machado et al., 1998). Thereafter, a new wave of large-scale forest decline and grassland expansion occurred across the Ethiopian Highlands after 1700 CE. This is reflected in the occurrence of alluvial aggradation in the northern and eastern highlands (Machado et al., 1998; Chapter 5); significant declines in the ratio of arboreal to non-arboreal pollen (AP/NAP) (Chapter 8; Darbyshire et al., 2003), and in Cupressaceae (Darbyshire et al., 2003) to the south (Lake Hayk and Ashenge) where forest recovery had previously occurred. Strong human or pastoral influence on forest decline and grassland expansion during the 18th century is evident from the significant increase of Poaceae (Chapter 8; Darbyshire et al., 2003) and *Rumex* (Darbyshire et al., 2003) in the pollen record. Thick gravelly slope deposits (dated with thermoluminescence to 1714 CE) inclusive of boulders with plough marks point to a phase of intensive soil erosion resulting from occupation of marginal steep

lands (Machado et al., 1998). Oversized gully morphology is visible on early 19th century photographs, indicative of a prior activation phase (Frankl et al., 2011). After the 18th century, landscape changes were rather gradual (Machado et al., 1998; Chapter 8), with a degradation period between 1960 and 1990 CE (Chapter 6).

9.2 Hydrogeomorphological evolution and model

In line with findings from the western Sahel (Yamé valley, Mali) (Lespez et al., 2011) and Tunisia (Zielhofer & Faust, 2008), there are remarkable chronological links between Late Holocene climatic shifts and hydrogeomorphological changes (Figure 9.2). Based on the method explained in Appendix A2, we find a significant and very strong association between dry phases and phases of land degradation ($p = 0.001$, $\chi^2 = 19.71$, Cramér's $V = 0.69$; $n = 41$) on the Late Holocene timescale. On the century-based timescale, we find a significant and strong correlation between the AP/NAP values and their corresponding interpolated $\delta^{18}O$ estimates (Pearson product-moment correlation = -0.63; $p = 0.047$; $n = 8$) (Figure 9.2). On the decade-based timescale, the correlation between clay-content of the alluvial debris fans and JJAS-rainfall data is not significant (Pearson product-moment correlation = 0.06; $p = 0.44$) (Figure 9.2). The associations show that long-term hydrogeomorphological dynamics were significantly affected by climatic rainfall reductions (of less than 25 %; Chapter 7) over the course of the Holocene. Indeed, contrasting with fluvial evidence from regions with a temperate climate, under drier climate conditions degradation and sedimentation increases in (semi)arid regions, while grasslands expand (Zielhofer & Faust, 2008).

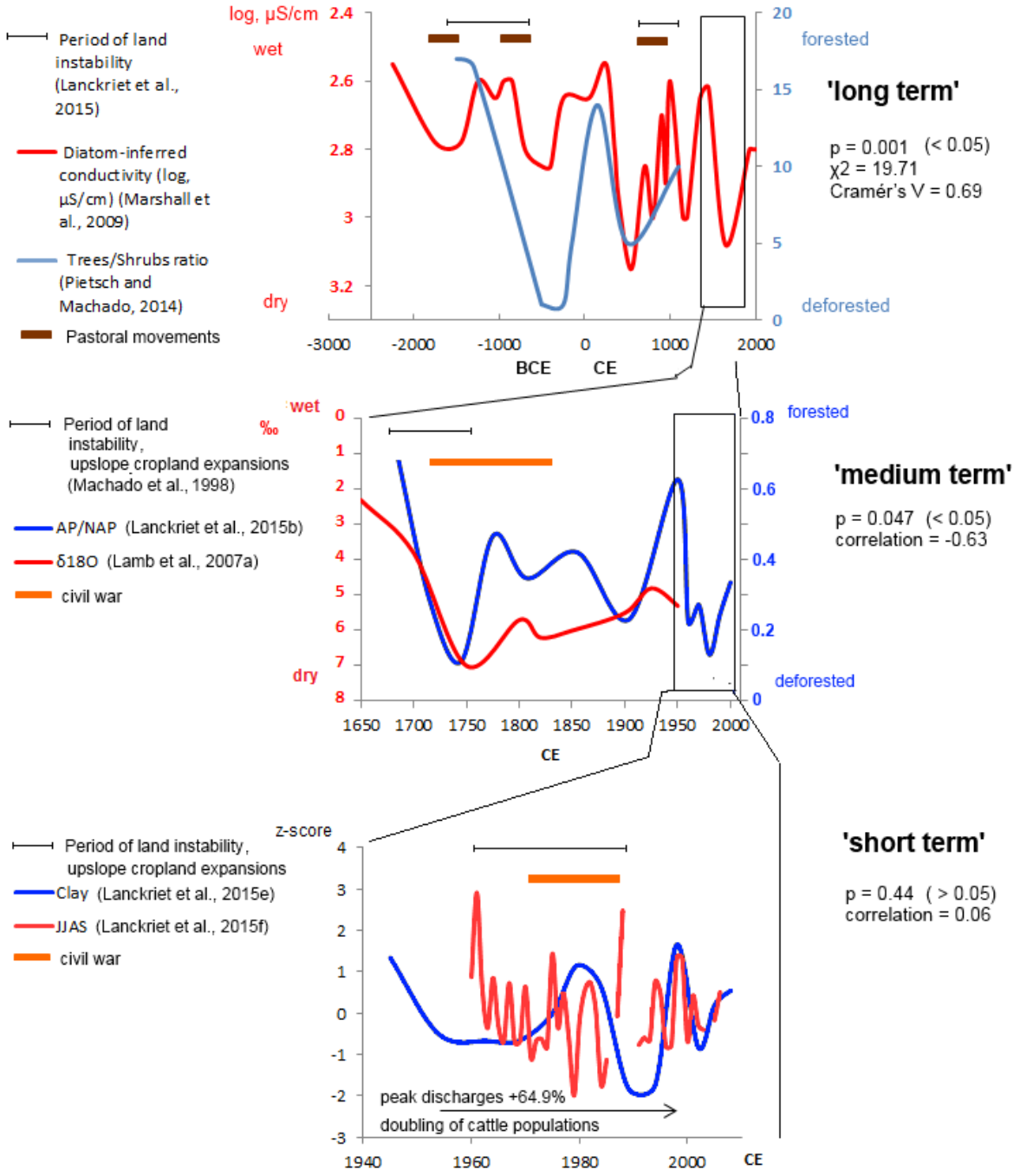

Figure 9.2 Temporal associations between hydroclimate (red lines), land cover and sediment activity (blue lines) are strong on the longer timescales. (upper) Conductivity record of Lake Ashenge (visual estimation from Marshall et al., 2009; red) plotted against trees/shrubs ratio (visual estimation from Pietsch and Machado, 2014) and phases of increased sediment supply (Chapter 5). (middle) Ratio of arboreal versus non-arboreal pollen (AP/NAP) as a proxy of forest cover around Ashenge (Chapter 8) and oxygen isotope composition of authigenic carbonate ($\delta^{18}O$) as an indicator of drought (visual estimation from Lamb et al., 2007). (lower) Clay content in a debris fan near Lake Ashenge (^{210}Pb dates) as a proxy for geomorphic stability (Chapter 6) and June-to-September rainfall (JJAS) as a hydroclimatic indicator (z-scores) (Chapter 2). See Appendix A2 for associations.

These associations provide the basis for postulating successive hydrogeomorphological phases that were affected by climatic variability and agro-pastoral expansions over the course of the Holocene. Below we will discuss the impact of climate and expansions of pastoral practices and grassland. Further, we discuss a conceptual geomorphic model of land degradation during the Late Holocene.

9.2.1 The 2200 BCE event and expansion of pastoralism from the North

It is likely that hunter-gatherers were thriving in the Early-to-Mid-Holocene forests of the Horn of Africa during the African Humid Period (Brandt, 1986; Umer & Negash, 2012; Menard et al., 2014). As suggested by lithic artefacts, Early Holocene high-standing lakes also allowed the establishment of fishing economies (Menard et al., 2014).

Remarkably, the gradual ending of the African Humid Period, from 4850 BCE towards the drought maximum at 2000-2200 BCE (Hol-3), coincides with population dynamics across North Africa. The drying in the eastern Sahara happened several millennia before drying in the west, while the Sudanese Sahara was completely dry by 1500 BCE (Lézine et al., 2011). A population simulation by Manning & Timpson (2014) shows a spatiotemporal demographic pattern that mimics the drying trend, with the disappearance of herding economies that were fully developed by 4200 BCE across Nubia in present-day Sudan. The 'out-of-Sudan' migrations would have occurred during the Mid-Holocene desiccation accelerated by the 2200 BCE event (Umer & Negash, 2012). Livestock keeping expanded slowly southward from the drying Sudanese plains towards the Highlands of the Horn (Lesur et al., 2014).

Consequently, in North Ethiopia, the very earliest remains of *Bos taurus* were dated to ~1800 BCE (Lesur et al., 2014). Near the end of the dry phase (Hol-3) and just slightly after the first evidence for pastoralism in the Northern Highlands, significant environmental changes were identified in all geomorphological records covering that period in the Northern Highlands (Machado et al., 1998; Chapter 5; Moeyersons et al., 2006; Pietsch and Machado, 2014; Gebru et al., 2009). Specifically, during the second half of the second millennium BCE, sediment supply increased (after 1500 BCE) (Machado et al., 1998), floodplain accumulation increased (after 1550 BCE) (~3 mm/yr; see Chapter 5), colluvial activity and monocotyledons increased (1430-1260 BCE) (Moeyersons et al., 2006), there was a

decrease in trees/shrub ratio (after 1400-1100 BCE) (Pietsch and Machado, 2014) and C4 plants became increasingly abundant (1350 BCE) (Gebru et al., 2009). The Late Holocene evidence for land degradation and vegetation change in the North Ethiopian Highlands thus matches the introduction of herding from the Nile valley between 1800 and 1300 BCE, following the drying of the Sahara.

9.2.2 Drying of the Arabian Peninsula and expansion of agro-pastoralism and *zebu* from the East

The late expansion of domesticated crops in the Highlands during the first millennium BCE (Harrower et al., 2010) matches the dates for Semitic movements from and interactions with Arabia and Yemen during another dry phase (Hol-4). Indeed, using Bayesian phylogenetic techniques, Kitchen et al. (2009) date Semitic arrival in the Horn of Africa at ~850 BCE. This is confirmed by Pagani et al. (2012), who date Semitic gene flow (SLC24A5 allele) into Ethiopia at ~1000 BCE. There are significant land cover changes apparent from the two land cover records comprising that period in the northern rift valley (Lake Ashenge, Marshall et al., 2009; Lake Hayk, Darbyshire et al., 2003), as the first spike of soil erosion around Lake Ashenge and forest decline with grassland expansions around Lake Hayk match this timing. The events are preceded by the Semitic migration from the Levant to southern Arabia between ~3000 and 1000 BCE, following the onset of aridification in the peninsula (Chiaroni et al., 2010). There are several *Bos* remains dated to this period and the earliest radiocarbon-dated crop evidence (first millennium BCE) includes explicitly drought-resistant crops (e.g. *Cicer arietinum*) (Harrower et al., 2010). Additionally, a number of genetic studies demonstrate that long-horned zebu cattle (*Bos indicus*) were introduced from India and the southern Arabian Peninsula into Eastern Africa during this period (first millennium BCE) (Paynes and Hodges, 1997; Boivin and Fuller, 2009). The earliest evidence available for zebu in East Africa comes from a short horn breed in southern Kenya dated to 810 – 410 BCE (Umer & Negash, 2012). Genetic variation as studied with autosomal microsatellite markers evidences that the introgression started from along the coast of East Africa, while admixture values suggest a maritime or South Arabian transport mode (Hanotte et al., 2000). According to Ehret & Posnansk (1982), *Bos indicus* is better adapted to arid conditions as compared to *Bos taurus*, because it has lower water requirements and can store fat in its humps. The introduction of *zebu* to the Northern Highlands is most likely to have followed the Semitic migrations (Ehret and Posnansk, 1982). An earlier introduction of cervicothoracic humped

zebu into Ethiopia during the 2nd millennium BCE is suggested but lacks adequate evidence (Caramelli, 2006).

When comparing all available dated evidence for the onset of forest decline, grassland expansion and land destabilization in our study region, we can infer a north-south gradient of human impacts proceeding from the Red Sea area and into the interior (Figure 9.3). Landscape destabilization in North Ethiopia precedes forest clearance around Lake Ashenge and Lake Hayk, followed by forest decline in the southern highlands (Arsi and Bale Mountains) about 600 years later (Umer et al., 2007) (Figure 9.3). In the southwestern Ethiopian Highlands, early evidence for herding and pottery is dated to the late 1st millennium BCE (Lesur et al., 2014).

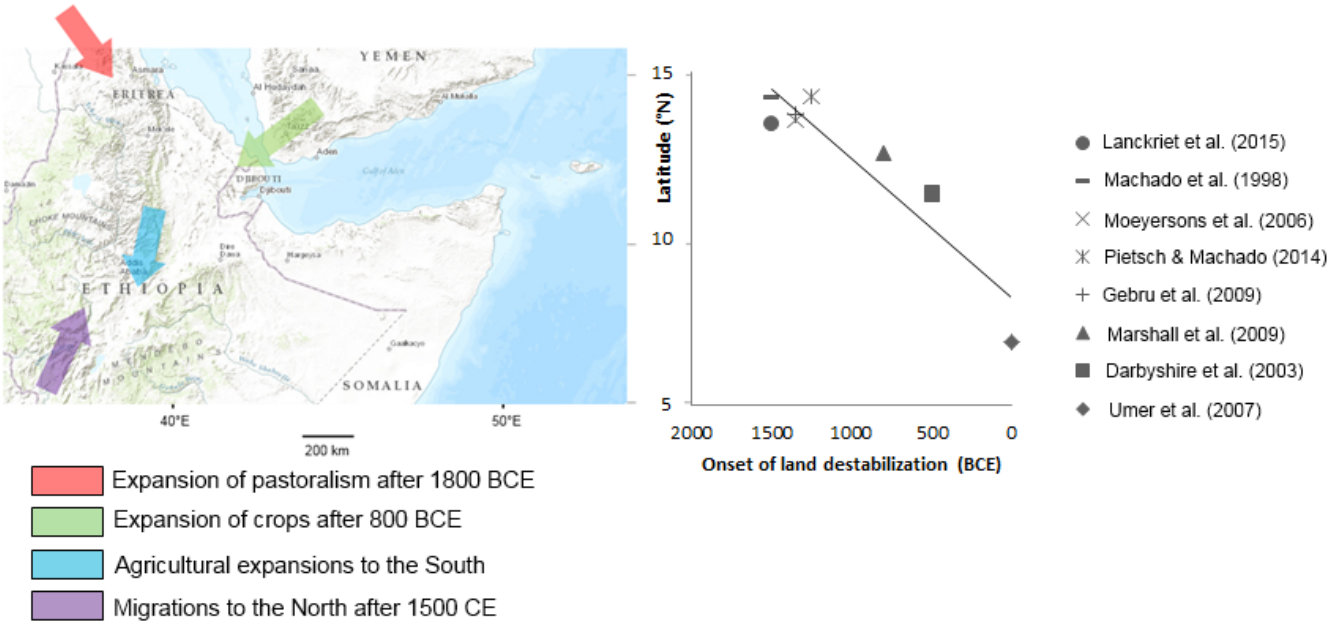

Figure 9.3 (left) Scenario of agro-pastoral expansions, associated grassland expansion and early land destabilization including the early expansion of pastoralism from the Nile valley after 1800 BCE (red), the expansion of domesticated crops and Bos (and possibly Zebu) from the Arabian Peninsula after 800 BCE (green), and gradual agro-pastoral proliferation to the south (blue). We also depict the Oromo movements from the southern Horn of Africa after 1500 CE (section 9.2.4) (purple). Background is given by the U.S. National Park Service (NPS) Natural Earth physical map; grey tone for relief and green for forest; dotted lines for disputed borders. (right) Earliest dates for land degradation show a gradient from the Red Sea to the south.

9.2.3 The Axumite wet phase and sedimentary stability

The shift to a wetter climate in the North Ethiopian Highlands (350 BCE - 450 CE) happened around the Proto-Axumite phase (from ~ 450 BCE; Ciampalini et al., 2008). Climate did not cause the rise of Axum but, among other factors, it did provide favorable agricultural boundary conditions (Marshall et al., 2009). After 100 CE, the Axumite era was a period of agro-intensification with increased access to external resources through Indian Ocean trade. While trading products from the African interior – incense, gold and ivory – in the Indian Ocean trade network, the empire formed a key link between Rome and India (Phillipson, 2012). There was also an extensive maritime trade network between the African interior, Persia and Sri Lanka through the ports of Axum and, as suggested by Han dynasty records, even further away with China (Munro-Hay, 1991). Shrubland vegetation in the Highlands persisted at that time (pollen evidence from Darbyshire et al., 2003; Gebru et al., 2009) although Pietsch and Machado (2014) find an increased ratio of trees/shrubs. The evidence of landscape stability (Machado et al., 1998) and lower floodplain accumulation rates (~0.16 mm/yr; Chapter 5) would also have been due to the extensive terracing in the Axum empire (Ciampalini et al., 2008).

9.2.4 Post-Axumite aridity and grassland expansion

The decline of the Axumite Empire is suggested as been linked with the rapid increase in aridity after 450 CE (Hol-5) (Marshall et al., 2009). The Arab expansions that cut Axum from its major trade routes also played a role, following the climatic deterioration that occurred when Axum was at its maximal expansion (Marshall et al., 2009). Along with the Arab expansions, there were large influxes of short horned *zebu* to the Ethiopian Highlands after ~670 CE (Epstein, 1971; McCann, 1999). Degradation processes resumed (Machado et al., 1998) and floodplain accumulation rates increased (~1 mm/yr; Chapter 5) during the dry 'Medieval Warm Period' (Lamb et al., 2007) (Hol-5). Lowlander cattle herders moved for pasture from Somalia and Afar to the Highlands from the 13th century onwards (Marcus, 2002), when grasslands expanded (1200-1400 CE) (Darbyshire et al., 2003). Increases of forest cover occurring from 1400 to 1700 CE at Lake Hayk (Darbyshire et al., 2003) and Lake Ashenge (Chapter 8) match the wet 'Little Ice Age' and the phase of soil formation in the Northern Highlands starting from the early 15th century till 1481-1660 CE (Machado et al., 1998). Lakes Hayk and Ashenge are also located along the northward track of Oromo movements following the rift valley. Filling the power vacuum that resulted from the Arab-Ethiopian wars in the 16th century, Oromo moved

northwards during the late 16th and 17th century, as did their nomadic lifestyle and participative approach to forest and natural resource management (Pankhurst, 1990).

The early 18th century phase of decreasing woody vegetation and grassland expansion broadly matches the increased colluvial activity dated by Machado et al. (1998) during an era of declining imperial power in Ethiopia and civil war in the north (Pankhurst, 1990; Chapter 8). However, it also coincides with a very rapid rainfall decline since 1700 CE just prior to the very dry period after 1750 CE, as recognized from the Lake Hayk record (Lamb et al., 2007) (Hol-6) (Figure 9.2). This points to the occurrence of positive climate-human-vegetation feedbacks as, following Nyssen et al. (2004), in times of harsh drought, social insecurity and stagnating agricultural production, human survival takes over on longer-term land management investment. Additionally, during the early-19th century wage labourers (woodcutters and 'diggers') started to clear vegetation on the steepest slopes (Pankhurst, 1990) while land tenure became consolidated around a very unequal feudal system (Ståhl, 1974), which triggered increased catchment runoff by forcing poorer farmers towards lands on steep slopes (Chapter 3).

9.2.5 The last century

Subrecent patterns of environmental degradation bear the imprints of the distant past, partly because land-cover changed only gradually or little during the 19th century and earlier 20th century (Chapter 8). Following Machado et al. (1998), after the early 18th century colluvial activation phase, there was relative land stability from the late 18th century to the early 20th century. In fact, the feudal land tenure system persisted up to the mid-1970s, resulting in the accumulation and even export of large volumes of cereals despite the recurrent occurrence of drought and famine (Holmberg, 1977; Nyssen et al., 2015). Overall, the feudal land system facilitated renewed decreases of woody vegetation cover that occurred across the Highlands (1950-1990 CE), following a climax of woody vegetation cover during the 1930s (Nyssen et al., 2014). At that time, severe periodic droughts occurred (Chapter 2), landscape denudation rates were high (Hagos et al., 2002) and gully networks were highly active across the northern Highlands (Frankl et al., 2011, 2013). Increased supply of coarse sediments during 1965–1990 CE is also evidenced by short-lived isotope dating and remote sensing imagery of alluvial debris fan sediments around Lake Ashenge (Figure 9.2) (Chapter 6). Indeed, near Lake Ashenge runoff responses and peak discharges were maximal at the end of the

1960s and early 1970s (final feudal era) in line with the maximal upslope extent of croplands at that time (De Meyere et al., 2015).

9.2.6 The last two decades

The new regime (after 1991) reformed the feudal land tenure system and made large investments in soil and water conservation structures (e.g. exclosures, stone bunds, check dams, reservoirs) as well as in agricultural inputs such as fertilizers and improved seeds. Coffee and vegetable exports are now higher than ever (Nyssen et al., 2015) and food productivity is outpacing levels of other countries in Africa South of the Sahara (World Bank, 2015). The export of Ethiopian agricultural products to the EU for instance has more than doubled, from less than 200 million euros in 2004 to about 500 million euros in 2014 (European Commission, 2015). Yet, the occurrence of large droughts (1997-1999, 2003, 2009, 2011) is regularly driving up food price inflation and hampering GDP growth (Conway and Schipper, 2011).

The investments in soil and water conservation were implemented in the framework of the ADLI (Agricultural Development Led Industrialization) strategy (Chapter 3). While the former regimes in Ethiopia followed a development strategy based on *Import Substituted Industrialization*, the focus of ADLI shifted to 'agriculture first' (Zewdu & Malek, 2010). Public expenditures in the agricultural sector have been large (Tewodaj et al., 2008; Mitik, 2010), driven by large agro-conglomerates that provided venture capital (EFFORT in Tigray, Tiret in Amhara; Vaughan & Mesfin, 2011) and backed by a policy of gradual depreciation of the Birr (Mehari & Holden, 2014). Overall, as impacted by these conservation investments, the Highlands are now 'greener' than long before (Chapter 8; Nyssen et al., 2014).

9.3 Geomorphic model

9.3.1 Conceptual model

We constructed a conceptual geomorphic model (Figure 9.4), under the reasonable assumption that aggradation periods correspond with phases of increased sediment supply from slopes into the

valley, during periods of active degradation in the upper catchment. As a matter of fact, in North Ethiopian ephemeral catchments, decreasing woody vegetation cover following land clearings upstream leads to sediment accumulations downstream (Frankl et al., 2011). Indeed, following the equations of Knighton (1998), channel aggradation (d^-) results from an increase in sediment supply (Q_s^+) (and/or a decrease in runoff Q^-). Simultaneously, channel incision (d^+) follows an increase in water runoff (Q^+) and/or a decrease in sediment load (Q_s^-). An early phase of incision is still visible on late 19th century historical photographs, possibly following the 18th century degradation phase, and a second incision phase is clearly attributed to the late 20th century (Figure 9.4).

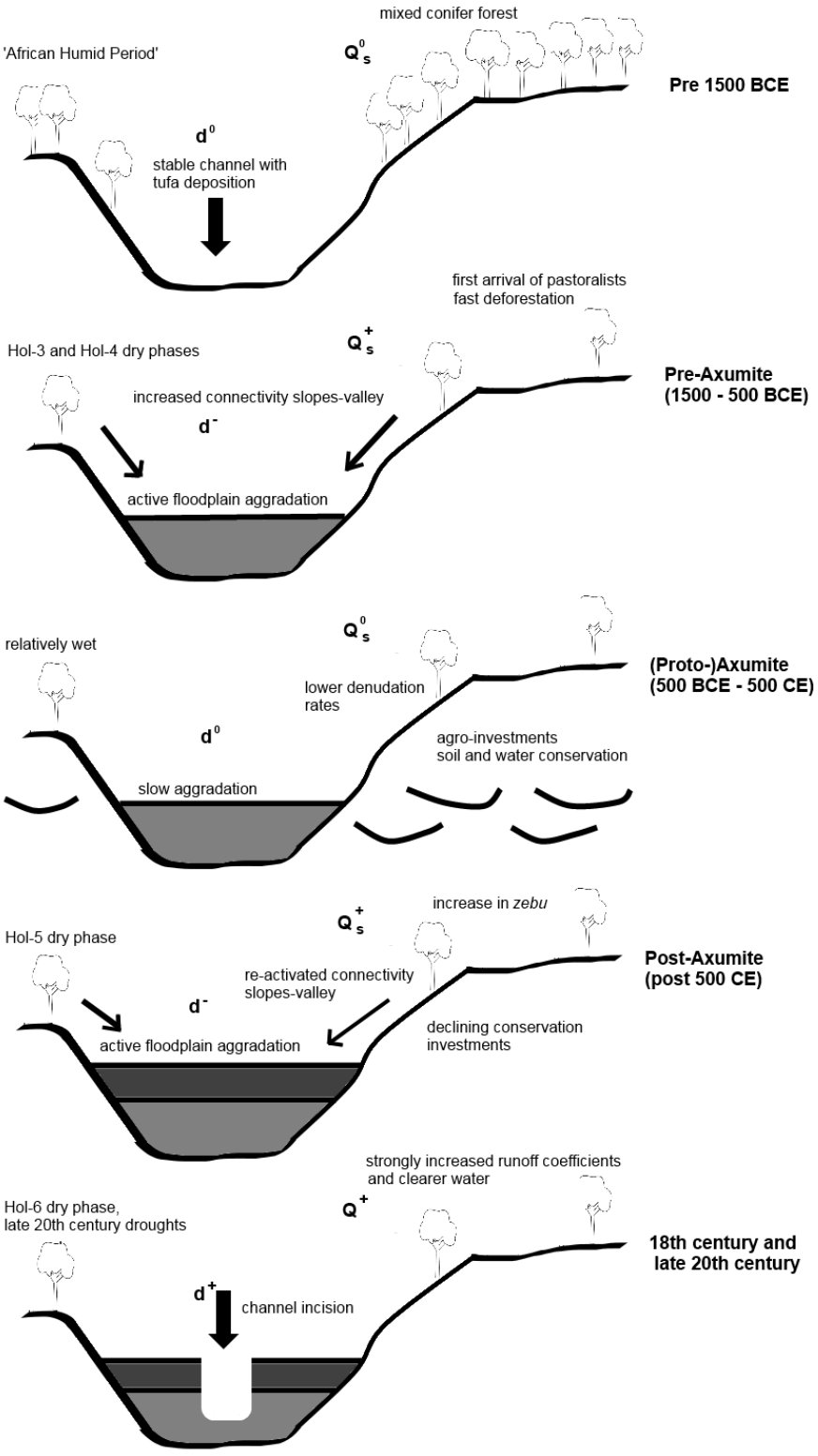

Figure 9.4 Conceptual geomorphic model of water and sediment supply responses to human impacs and climate changes over the Late Holocene. The figure indicates channel aggradation (d^-), increase in sediment supply (Q_s^+), channel incision (d^+), increase in water runoff (Q^+) and a decrease in sediment load (Q_s^-). Indication of 0 stands for a stable situation.

9.3.2 Role and influence of human and cattle populations

Reliable population records for the study area are limited to the last few decades, as censuses started in the 1950s (Nyssen et al., 2014). Nevertheless, there are demographic estimates of 4 million inhabitants (Ritler, 2003) with population densities of less than 10 inhabitants per km^2 (Nyssen et al., 2014) for the mid-nineteenth century in central-northern Ethiopia. Population size increased towards 6 up to 8 million inhabitants in 1930 in the same area (Ritler, 2003), and continued to increase strongly thereafter (Nyssen et al., 2014).

As shown by the geomorphic model above, our longer term analysis shows phases of significant land degradation prior to census taking in Ethiopia. As pointed out in Chapter 8, a simplified explanation of population growth and poverty does not hold. Additionally, relative land resilience during the Axumite period (Chapter 5) occurred when there was high population density in towns and ports (Phillipson, 2012). This is somehow reminiscent of the recent phase of land resilience during the last two decades that contrasts with the very high population densities of today (over 100 inhabitants per km^2) (Nyssen et al., 2014).

Clearly, other factors come into play. In chapter 3, we linked gully dynamics over the past decades with the occurrence of periodic droughts, changing cropland management and feudal land policies and land tenure. Considering the past century, land degradation was most severe during the period 1960-1990 CE (Chapter 6). There were less communal lands and a highly unequal distribution of croplands that were at their maximal areal extent and were basically in private hands of noblemen or the Church (Chapter 3). Then, the weak feudal state hardly supported farmers to maintain and expand the common resources (forests, grazing land, water supply sources) and public investments in infrastructure (integrated soil and water conservation, managing the grazing systems) were very limited.

In the discussion of the population growth – land degradation nexus, cattle populations should be considered too. As stated in chapter 3, cattle populations in Ethiopia (including the area of Eritrea) have increased from 24.9 million in 1961, to 31.1 million in 1995 and 56.1 million in 2013 (FAO, 2015). This is broadly in phase with the increase in human population from ~25 million in

1960 to well over 80 million in 2013 in Ethiopia (Nyssen et al., 2014). Clearly, cattle populations and grazing systems could have impacted degradation during the second half of the 20th century (Chapter 4) and this is an important issue for understanding and tackling land degradation in Ethiopia.

Indeed, the conceptual geomorphic model signals a potentially strong but unexplored relationship between cattle populations and migrations, climate and land degradation in the Ethiopian highlands. The major cattle migrations, first, of *Bos taurus* from the north (Sudan, Egypt, Levant) between 2000-1800 BCE occurred during a dry phase (Hol-3), followed by a period of land degradation with increases of monocots. Second, the arrival of long-horned *Bos indicus* with the Semitic peoples from the east occurred during the following dry phase (Hol-4) and overlapped with a period of land degradation and grass expansions. Third, the onset of dry phase Hol-5 corresponded with renewed land degradation, followed by introductions of short-horned *Bos indicus* after 670 CE. Grasslands further expanded between 1200 and 1400 CE, when pastoralists moved from Somalia and Afar to the Highlands. Finally, Pankhurst (1990) reports on increased cattle densities from the 18th century onwards, which corresponded with dry phase Hol-6 and increased Poaceae abundances and land degradation.

This argument is in line with contemporary and empirical studies of the impact of cattle grazing on land degradation. For instance, Mwendera et al. (1997) have shown that livestock grazing has a very significant impact on surface runoff and soil erosion in the Ethiopian Highlands, most notably on the erodible steeper slopes during the rainy season. Additionally, even on shorter timescales it is well known that pastoralists in Northeastern Ethiopia move to mountainous areas under dryer conditions. In the open fields of Tigray, transhumance is practiced on a seasonal basis, towards destination zones that have more water resources and vegetation and away from cropland (Nyssen et al., 2009). Also Afar pastoralists are known to migrate towards the 'wetter' graben floors, hills and mountains of the nearby areas of Tigray and Amhara in times of drought (Guinand, 2000). Lenaerts (2013) states in this perspective: "[...] when rains are failing and feed in the lowlands gets scarce, Afar people negotiate agreements with Tigray people and mostly gain access to the *hezati* [protected grazing lands] after the oxen have grazed."

9.4 Climate-resilient land management

9.4.1 Future environmental changes

Our paleo-environmental findings may have implications for future environmental management. As shown by the rapid transition from a relatively wet climate in 1650 CE to a dry climate in 1750-1900 CE, major climatic shifts can develop relatively rapidly in the region (< 100 yrs) (Figure 9.2). The Hayk climate record suggests that rainfall during the 20th century was less than average during the past 2000 years, as still recovering from the dry period (1750-1900 CE) (Lamb et al., 2007) when cooler tropical ocean temperatures prevailed (Tierney et al., 2015). Following this 'rapid climatic shift' scenario, and in line with multi-model projections of increased (year-to-year) hydroclimatic variability in Ethiopia (McSweeney et al., 2010), we may anticipate significant regional climate change by the end of this century. In particular, model ensembles project increased average rainfall across the Horn of Africa under warming oceans and strengthened Hadley circulation (de Wit and Stankiewicz, 2006), including a simulated 15% average rainfall increase in the Northern Highlands (GISS model II simuation; Lanckriet et al., 2012). At the same time, however, the intensity of drought is expected to increase (due to increased evapotranspiration and possibly El Niño amplification) while the average rainfall increase would be largely due to increased precipitation intensity (McSweeney et al., 2010). Globally, we can expect significant future changes in conditions of aridity across different regions around the world (see Appendix A6).

Further, the pollen data from Lake Hayk and Lake Ashenge show that large regional environmental changes can relatively rapidly develop and respond to climate changes (several decades) (Figure 9.2). Indeed, to date the Highlands have more woody vegetation cover than ever during the past 150 years, in an ongoing land cover transition since about two decades (Kassa Teka Belay et al., 2014; Nyssen et al., 2014). We can expect considerable hydrogeomorphic reactions to this landscape greening in the near future, as it is established that even a small increase of upslope forest cover leads to rapid and important runoff decreases in the steep catchments of the Ethiopian Highlands (De Meyere et al., 2015; Tesfaalem et al., 2015).

9.4.2 To a climate-resilient green economy?

The Ethiopian economy remains vulnerable to rainfall variability, which is illustrated by the significant correlation between average rainfall and GDP growth (one-year-lag) (Conway and Schipper, 2011). Additionally, increased hydroclimatic variability expected under future climate change would further restrain economic growth (World Bank, 2008). To prepare for future climate change, and to restrict annual greenhouse gas emissions around 150 Mt CO_2e, the Federal Government wants to develop a 'Climate-Resilient Green Economy' by 2025 (FDRE, 2011). The general aim is to invest around 150 billion US dollar, 80 % of which could be raised from carbon credit schemes (FDRE, 2011). In line with the strategy, high-input hydro-agricultural projects (i.e. large dams and irrigation schemes) are key to adapting to hydroclimatic changes in the Ethiopian Highlands. By doing so, 'climate change' becomes central for vindicating Ethiopia's 'hydroagricultural state-building agenda' and Ethiopia's control over the headwaters of the Nile (Verhoeven, 2013).

Yet, Pender and Gebremedhin (2008) show that the comparative advantage of the Tigray Highlands does not lie in high-input agriculture, given the low returns on investment for fertilizers and credit schemes (that are often monopolized by state companies, such as the Agricultural Inputs Supply Enterprise). Instead, the advantage lies in low-external-input production, including non-cereal activities, improved livestock and grazing management and reduced tillage (Pender and Gebremedhin, 2008). For instance, the establishment of exclosures by excluding livestock from some grasslands not only generates non-timber forest products (honey, incense) and sequestered carbon dioxide (on average 246 tonnes CO_2-e per hectare in Tigray), but also contributes to greater green water and soil nutrient availability for farmers (Mekuria et al., 2011). Similarly, Lanckriet et al. (2012) find that agro-ecological techniques such as reduced tillage in complement with standing stubble deliver convincing test results for reducing runoff and soil loss. Although farmer's acceptance and cattle grazing remain major bottlenecks for large-scale implementation, reduced tillage and standing stubble have a high market potential in North Ethiopia (Lanckriet et al., 2014). Future management scenarios were developed and calibrated by Lanckriet et al. (2012) to account for the effects of land management (no management; soil and water conservation; reduced tillage) under expected climate change (Table 9.1). Under a scenario of climate change, a sharp increase of annual soil loss was simulated as compared to the current situation (Table 9.2). Under a steady climate, soil loss and runoff from farmlands is greatly altered by applying conservation measures (stone bunds, exclosures

and check dams), and most notably by applying reduced tillage. Especially under a changing climate, reduced tillage is highly efficient in reducing soil loss (i.e. full compensation of the climate effect if reduced tillage is applied) (Table 9.2). In fact, under sustainable intensification, the future increase in precipitation could act in a beneficial way with greater green water availability for smallholder farmers (Lanckriet et al., 2012).

Table 9.1 Six scenarios, depending on climate situation and land management applied. Catchment management accounts for non-grazing policy, stone bunds, exclosures and check dams.

	Plain tillage, few conservation measures	Plain tillage with catchment management	Catchment management with conservation agriculture
Current average precipitation	Scenario I	Scenario III	Scenario V
15% increase in precipitation (IPCC A1F1 for 2041-2050)	Scenario II	Scenario IV	Scenario VI

Moreover, Tesfay et al. (2015) show that under reduced tillage on terraced fields, cereal yields are 35% higher as compared to conventional agriculture (9-years average), which is in line with the figures established by Pender and Gebrehmedhin (2009). Baudron et al. (2015) find that application of zero-grazing in farmlands leads to significantly increased soil organic matter and increased tef yields of 70%, as compared to open grazing farmlands. Conversely, crop yields on fields with stone terraces are *ceteris paribus* only 23% higher, while fertilizer and compost use leads to yield increases of 14% and 13% respectively (Pender and Gebrehmedhin, 2009). Clearly, lower-input production strategies such as reduced tillage are a very cost-efficient way to control water and sediment supplies in dryland regions and can boost food production, particularly under conditions of climate change. In the catchments of the Ethiopian Highlands, a 15% increase in future (daily) precipitation by 2040 (Lanckriet et al., 2012) would lead to an increase of the total yearly runoff volume by 54% (Curve Number = 81.1 for 2006 rainfall; see Figure 4.6 and Equation 4.4). Similarly, a hypothetical 15% decrease in future (daily) precipitation would lead to a decrease of the total yearly runoff volume by 38%.

Table 9.2 Effects of the six scenarios on soil–water behavior in May Zeg-zeg catchment (= indicates no change; + indicates increase; blank is not estimated). See Lanckriet et al. (2012) for calculations; CN = Curve Number.

	Rainfall (mm yr^{-1}) [a]	Soil loss (t ha^{-1} yr^{-1})	CN farmland [b]	CN catchment	Catchment runoff (mm) [c]	Ponding	Sediment yield (t yr^{-1})	Hydraulic conductivity	Organic matter
Scenario I	704	22.8	79.9 (A)	78.5	52.8	=	1591	=	=
Scenario II	970	30.2	79.9 (A)	78.5	>52.8	=		=	=
Scenario III	704	22.8	77.3 (F)	68.9	27.9	=	357	=	=
Scenario IV	970	30.2	77.3 (F)	68.9	>27.9	=		=	=
Scenario V	704	9.4	74.4 (F)	67.2	23.5	+	241	=	+
Scenario VI	970	12.4	74.4 (F)	67.2	>23.5	+		=	+

[a] Rainfall for scenarios I, III and V was calculated as the average of the yearly rainfall of 2005, 2008 and 2010.
[b] Farmland type A is cropland with free grazing policy and no stone bunds; farmland type F is cropland with zero grazing and good stone bunds.
[c] Catchment runoff was calculated by applying the area-weighed CN at daily scale with the rainfall values of 2011.

9.5 References

Baudron, F., Aynalem Mamo, Dereje Tirfessa, Mekuria Argaw, 2015. Impact of farmland exclosure on the productivity and sustainability of a mixed crop-livestock system in the Central Rift Valley of Ethiopia. Agriculture, Ecosystems & Environment 207, 109–118.

Boivin, N., Fuller, D., 2009. Shell middens, ships and seeds: Exploring coastal subsistence, maritime trade and the dispersal of domesticates in and around the ancient Arabian Peninsula. Journal of World Prehistory 22 (2), 113 - 180.

Brancaccio, L., Calderoni, G., Coltorti, M., Dramis, F., 1997. Phases of soil erosion during the Holocene in the highlands of Western Tigray (Northern Ethiopia): a preliminary report. In: Bard, K. (Ed.), The

environmental history and human ecology of Northern Ethiopia in the Late Holocene. Istituto Universitario Orientale, Napoli, Italy, 30-48.

Brandt, S., 1986. The Upper Pleistocene and early Holocene prehistory of the Horn of Africa. African Archaeological Review 4 (1), 41-82.

Caramelli, D., 2006. The origins of domesticated cattle. Human Evolution 21, 107–122.

Chiaroni, J., King, R., Myres, N., Henn, B., Ducourneau, A., 2010. The emergence of Y-chromosome haplogroup J1e among Arabic-speaking populations. Eur J Hum Genet 18, 348-353.

Ciampalini, R., Billi, P., Ferrari, G., Borselli, L., 2008. Plough marks as a tool to assess soil erosion rates: A case study in Axum (Ethiopia). Catena 75, 18–27.

Conway, D., Schipper, L., 2011. Adaptation to climate change in Africa: Challenges and opportunities identified from Ethiopia. Global Environmental Change 21 (1), 227–237.

Darbyshire, I., Lamb, H., Umer, M., 2003. Forest clearance and regrowth in northern Ethiopia during the last 3000 years. The Holocene 13 (4), 537–546.

De Meyere, M., Tesfaalem G. Asfaha, Frankl, A., Mitiku Haile, Nyssen, J., 2015. Land cover trajectories and runoff response on the Ethiopian Rift Valley escarpment over the last eight decades. Geomorphology, submitted.

de Wit, M., Stankiewicz, J., 2006. Changes in Surface Water Supply Across Africa with Predicted Climate Change. Science 311 (5769), 1917-1921.

Ehret, C., Posnansk, M., 1982. The Archaeological and Linguistic Reconstruction of African History. University of California Press, 299 p.

Epstein, H., 1971. The Origin of the Domestic Animals of Africa. Africana, New York, USA, 719 p.

European Commission, 2015. European Union, Trade in goods with Ethiopia. http://trade.ec.europa.eu/doclib/docs/2011/january/tradoc_147265.pdf (accessed on 26/06/2015).

FAO (Food and Agriculture Organization of the United Nations, Statistical division), 2015. Available on: http://faostat.fao.org/site/573/DesktopDefault.aspx?PageID=573#ancor (Accessed on 27/11/2015).

FDRE (Federal Democratic Republic of Ethiopia), 2011. Ethiopia's Climate-Resilient Green Economy, Green economy strategy. http://www.undp.org/content/dam/ethiopia/docs/Ethiopia%20CRGE.pdf (accessed on 29/10/2015)

Frankl, A., Nyssen, J., De Dapper, M., Haile, M., Billi, P., Munro, N., Deckers, J., Poesen, J., 2011. Linking long-term gully and river channel dynamics to environmental change using repeat photography (Northern Ethiopia). Geomorphology 129, 238-251.

Frankl, A., Poesen, J., Scholiers, N., Jacob, M., Mitiku Haile, Deckers, J., Nyssen, J., 2013. Factors controlling the morphology and volume (V) – length (L) relations of permanent gullies in the Northern Ethiopian Highlands. Earth Surf. Process. Landforms 38, 1672-1684.

French, C., Sulas, F., Madella, M., 2009. New geoarchaeological investigations of the valley systems in the Aksum area of northern Ethiopia. Catena 78 (3), 218–233.

Gebru, T., Zewdu Eshetu, Yongsong Huang, Taddese Woldemariam, Strong, N., Umer, M., DiBlasi, M., Terwilliger, V., 2009. Holocene palaeovegetation of the Tigray Plateau in northern Ethiopia from charcoal and stable organic carbon isotopic analyses of gully sediments. Palaeogeography, Palaeoclimatology, Palaeoecology 282 (1–4), 67–80.

Gelorini, V., Verschuren, D., 2013. Historical climate-human-ecosystem interaction in East Africa: a review. African Journal of Ecology 51 (3), 409–421.

Guinand, Y., 2000. Afar Pastoralists Face Consequences of Poor Rains; Rapid Assessment Mission: 19-24 April 2000. UN-Emergencies Unit for Ethiopia, Addis Abeba, Ethiopia.

Hagos, F., Pender, J., Gebreselassie, N., 2002. Land Degradation and Strategies for Sustainable Land Management in the Ethiopian Highlands: Tigray Region. International Livestock Research Institute Working Papers 25, 1-75.

Hanotte, O., Bradley, D., Ochieng, J., Verjee, Y., Hill, E., Rege, E., 2002. African Pastoralism: Genetic Imprints of Origins and Migrations. Science 296, 336-339.

Harrower, M., McCorriston, J., D'Andrea, C., 2010. General/Specific, Local/Global: Comparing the Beginnings of Agriculture in the Horn of Africa (Ethiopia/Eritrea) and Southwest Arabia (Yemen). American Antiquity 75 (3), 452-472.

Holmberg, J., 1977. Grain marketing and land reform in Ethiopia: an analysis of the marketing and pricing of food grains in 1976 after the land reform. Research report. Nordiska Afrikainstitutet, Uppsala, Sweden.

Hurni, H., 1982. Klima und Dynamik der Hohenstufung von der letzten Kaltzeit bis zur Gegenwart. Hochgebirge von Semien - Athiopien. Geographica Bernensia 13, 198 p.

Kassa Teka Belay, Van Rompaey, A., Poesen, J., Van Bruyssel, S., Deckers, J., Kassa Amare, 2014. Spatial analysis of land cover changes in Eastern Tigray (Ethiopia) from 1965–2007: are there signs of a forest transition? Land Degradation and Development 26 (7), 680-689.

Kitchen, A., Ehret, C., Assefa, S., Mulligan, C., 2009. Bayesian phylogenetic analysis of Semitic languages identifies an early Bronze Age origin of Semitic in the Near East. Proc Biol Sci. 276, 2703–2710.

Knighton, D., 1998. Fluvial Forms and Processes — A New Perspective. Hodder Education, London, UK.

Lamb, H., Leng, M., Telford, R., Tenalem Ayenew, Umer, M., 2007. Oxygen and carbon isotope composition of authigenic carbonate from an Ethiopian lake: a climate record of the last 2000 years. The Holocene 17(4), 517–526.

Lanckriet, S., Tesfay Araya Weldeslassie, Cornelis, W., Verfaillie, E., Poesen, J., Govaerts, B., Bauer, H., Deckers, J., Mitiku Haile, Nyssen, J., 2012. Impact of conservation agriculture on catchment runoff and soil loss under changing climate conditions in May Zeg-zeg (Ethiopia). Journal of Hydrology 475, 336-349.

Lanckriet, S., Tesfay Araya, Derudder, B., Cornelis, W., Bauer, H., Govaerts, B., Deckers, J., Mitiku Haile, Naudts, J., Nyssen, J., 2014. Toward Practical Implementation of Conservation Agriculture: A Case Study in the May Zeg-zeg Catchment (Ethiopia). Agroecology and Sustainable Food Systems 38 (8), 913-935.

Lenaerts, L., 2013. Insights into agency and social interactions in natural resource management: extended case studies from Northern Ethiopia. Unpublished PhD thesis, KULeuven, Leuven, Belgium, 126 p.

Lespez, L., Le Drezen, Y., Garniera, A., Rassec, M., Eichhorn, B., Ozainnee, A., Ballouchef, K., Neumann, K., Huysecom, E., 2011. High-resolution fluvial records of Holocene environmental changes in the Sahel: the Yamé River at Ounjougou (Mali, West Africa). Quaternary Science Reviews 30 (5–6): 737–756.

Lesur, J., Hildebrand, E., Gedef Abawa, Gutherz, X., 2014. The advent of herding in the Horn of Africa: New data from Ethiopia, Djibouti and Somaliland. Quaternary Science Reviews 343 (1), 148–158.

Lézine, A., Hély, C., Grenier, C., Braconnot, P., Krinner, G., 2011. Sahara and Sahel vulnerability to climate changes, lessons from Holocene hydrological data. Quaternary Science Reviews 30, 3001-3012.

Machado, M., Pérez-González, A., Benito, G., 1998. Paleoenvironmental changes during the last 4000 yr in the Tigray, Northern Ethiopia. Quaternary Research 49, 312–21.

Malthus, T., 1798. An Essay on the Principle of Population. Johnson, London, UK.

Manning, K., Timpson, A., 2014. The demographic response to Holocene climate change in the Sahara. Quaternary Science Reviews 101, 28-35.

Marcus, H., 2002. A History of Ethiopia, Updated Edition. University of California Press, Berkeley, California, USA, 394 p.

Marshall, M., Lamb, H., Davies, S., Leng, M., Zelalem Kubsa, Umer, M., Bryant, C., 2009. Climatic change in northern Ethiopia during the past 17,000 years: A diatom and stable isotope record from Lake Ashenge. Palaeogeography, Palaeoclimatology, Palaeoecology 279, 114–127.

McCann, J., 1999. Green land, brown land, black land: an environmental history of Africa. James Currey, Oxford, UK, 193 p.

McSweeney, C., New, M., Lizcano G., 2010. The UNDP Climate Change Country Profiles: improving the accessibility of observed and projected climate information for studies of climate change in developing countries. Bulletin of the American Meteorological Society 91, 157–166.

Mehari, T., Holden, K., 2014. Financing The Public Deficit In Ethiopia: Empirical Modelling and Policy Simulations. Occasional Papers in Economics 2000-2004, The Nottingham Trent University, Nottingham, UK.

Mekuria, W., Veldkamp, E., Tilahun, M., Olschewski, R., 2011. Economic valuation of land restoration: the case of exclosures established on communal grazing lands in Tigray, Ethiopia. Land Degradation and Development 22, 334-344.

Menard, C., Bon, F., Asamerew Dessie, Bruxelles, L., Douze, K., Fauvelle, F., Khalidi, L., Lesur, J., Mensan, R., 2014. Late Stone Age variability in the Main Ethiopian Rift: New data from the Bulbula River, Ziwaye Shala basin. Quaternary International 343, 53-68.

Mitik, L., 2010. Alternative Policy Strategy to ADLI for Ethiopia: A dynamic CGE Framework Analysis. PEP Network, Addis Ababa, Ethiopia.

Moeyersons, J., Nyssen, J., Poesen, J., Deckers, J., Mitiku Haile, 2006. Age and backfill/overfill stratigraphy of two tufa dams, Tigray Highlands, Ethiopia: Evidence for Late Pleistocene and Holocene wet conditions. Palaeogeography, Palaeoclimatology, Palaeoecology 230 (1–2), 165–181.

MoFED (Ministry of Finance and Economic Development), 2002. Ethiopia: sustainable development and poverty reduction program. Ministry of Finance and Economic Development, Federal Democratic Republic of Ethiopia, Addis Ababa, Ethiopia.

Munro-Hay, S., 1991. Aksum, An African Civilisation of Late Antiquity. Edinburgh University Press, Edinburgh, UK, 288 p.

Mwendera, E., Mohamed Saleem, M., Dibabe A., 1997. The effect of livestock grazing on surface runoff and soil erosion from sloping pasture lands in the Ethiopian highlands. Australian Journal of Experimental Agriculture 37(4), 421-430.

Nyssen, J., Poesen, J., Moeyersons, J., Deckers, J., Mitiku Haile, Lang, A., 2004. Human impact on the environment in the Ethiopian and Eritrean highlands - a state of the art. Earth-Science Reviews 64 (3-4), 273-320.

Nyssen, J., Descheemaeker, K., Amanuel Zenebe, Poesen, J., Deckers, J., Mitiku Haile, 2009. Transhumance in the Tigray Highlands (Ethiopia). Mountain Research and Development 29 (3), 255-264.

Nyssen, J., Frankl, A., Mitiku Haile, Hurni, H., Descheemaeker, K., Crummey, D., Ritler, A., Portner, B., Nievergelt, B., Moeyersons, J., Munro, R.N., Deckers, J., Billi, P., Poesen, J., 2014. Environmental

conditions and human drivers for changes to north Ethiopian mountain landscapes over 145 years. Science of the Total Environment 485–486, 164–179.

Nyssen, J., Frankl, A., Amanuel Zenebe, Deckers, J., Poesen, J., 2015. Land management in the Northern Ethiopian Highlands: local and global perspectives; past, present and future. Land Degradation and Development 26 (7), 759–764.

Ogbaghebriel, B., Brancaccio, L., Calderoni, G., Coltorti, M., Dramis, F., Umer, M., 1997. The Mai Maikden sedimentary sequence: a reference point for the environmental evolution of the Highlands of Northern Ethiopia. Geomorphology 23 (2–4), 127–138.

Pagani, L., Kivisil, T., Ayele, T., 2012. Ethiopian Genetic Diversity Reveals Linguistic Stratification and Complex Influences on the Ethiopian Gene Pool. Am J Hum Genet. 91(1), 83-96.

Pankhurst, R., 1990. A Social History of Ethiopia: The Northern and Central Highlands from Early Medieval Times to the Rise of Emperor Tewodros II. Addis Ababa University, Addis Ababa, Ethiopia, 371 p.

Payne, W., Hodges, J., 1997. Tropical cattle: origins, breeds and breeding policies. Blackwell Science, Oxford, UK, 318 p.

Pender, J., Gebremedhin, B., 2008. Determinants of Agricultural and Land Management Practices and Impacts on Crop Production and Household Income in the Highlands of Tigray, Ethiopia. J Afr Econ 17 (3), 395-450.

Phillipson, D., 2012. The First Millennium BC in the Highlands of Northern Ethiopia and South–Central Eritrea: A Reassessment of Cultural and Political Development. African Archaeological Review 26, 257–274.

Ratzel, F., 1896. The history of mankind. Macmillan, London, UK.

Ritler, A., 2003. Forest, land use and landscape in the Central and Northern Ethiopian Highlands, 1865-1930. PhD dissertation, Institute of Geography, Universität Bern, Bern, Switzerland.

Roberts, N., 2006. The Holocene: An environmental history. Wiley-Blackwell, Hoboken, USA, 376 p.

Semmel, A., 1971. Zur jungquartären Klima und Reliefentwicklung in der Danakilwüste und ihren westlichen Randgebieten. Erdkunde 25, 199-209.

Ståhl, M., 1974. Ethiopia: political contradictions in agricultural development. Rabén & Sjögren, Stockholm, Sweden, 186 p.

Tesfaalem A, Frankl A, Mitiku Haile, Nyssen J., 2015. Catchment rehabilitation and hydro-geomorphic characteristics of mountain streams in the western Rift Valley escarpment of Northern Ethiopia. Land Degradation and Development, online early view. DOI: 10.1002/ldr.2267.

Tesfay, A., Nyssen, J., Govaerts, B., Baudron, F., Carpentier, L., Bauer, H., Lanckriet, S., Deckers, J., Cornelis, W., 2015. Restoring cropland productivity and profitability in northern Ethiopian drylands after nine years of resource-conserving agriculture. Experimental Agriculture, online early view. DOI: 10.1017/S001447971400060X.

Tewodaj, M., Ayele Gezahegn, Paulos Zelekawork, 2008. The bang for the birr: Public expenditures and rural welfare in Ethiopia. International Food Policy Research Institute (IFPRI) Series 160, Washington DC, USA.

Tierney, J., Abram, N., Anchukaitis, K., Evans, M., Giry, C., Kilbourne, K., Saenger, C., Wu, H., Zinke, J., 2015. Tropical sea surface temperatures for the past four centuries reconstructed from coral archives. Paleoceanography, online early view. DOI: DOI: 10.1002/2014PA002717.

Umer, M., Lamb, H., Bonnefille, R., Lezine, A., 2007. Late pleistocene and holocene vegetation history of the Bale mountains, Ethiopia. Quaternary Science Reviews 26 (17-18), 2229-2246.

Umer, M., Negash, A., 2012. Historical review of pastoralism and climate change in the Horn of Africa, with special emphasis on Ethiopia. In: Mulugeta Gebrehiwot and Jean-Bosco Butera (eds.). Climate Change, Pastoral Traditional Coping Mechanisms and Conflict in the Horn of Africa. Program of the UN Affiliated University for Peace (UPEACE), Addis Ababa, Ethiopia, 11-33 p.

Vaughan, S., Mesfin, G., 2011. Rethinking business and politics in Ethiopia: The role of EFFORT, the Endowment Fund for the Rehabilitation of Tigray. Africa Power and Politics, Research Report 2, London, UK.

Verheye, W., 1978. Soils and soil evolution on the Holocene lacustrine terraces of Lake Zway, Rift valley, Ethiopia. Pédologie 28 (1), 21-45.

Verhoeven, H., 2013. The politics of African energy development: Ethiopia's hydro-agricultural state-building strategy and clashing paradigms of water security. The Philosophical Transactions of the Royal Society A 371, DOI: 10.1098/rsta.2012.0411.

World Bank, 2008. Ethiopia - A country study on the economic impacts of climate change. World Bank Group, Washington DC, USA, 81 p.

World Bank, 2015. World Bank World Bank Open Data. http://data.worldbank.org/ (accessed on 26/06/2015).

Zewdu, G., Malek, M., 2010. Implications of Land Policies for Rural-urban Linkages and Rural Transformation in Ethiopia. International Food Policy Research Institute – Ethiopia Strategy Support Program (ESSP). ESSP II Working Paper 15, 32 p.

Zielhofer, C., Faust, D., 2008. Mid- and Late Holocene fluvial chronology of Tunisia. Quaternary Science Reviews 27 (5–6), 580–588.

Chapter 10 General conclusions

Overview

Using the case of the Ethiopian Highlands, this study sought to answer the following research questions:

(i) RQ1: Did land degradation occur in a 'nonlinear-cyclic', instead of a 'gradually-accelerating' pattern over time?
(ii) RQ2a: Are phases of land degradation largely synchronous with – or slightly preceded by – climate changes?
(iii) RQ2b: Could there be an additional amplifying effect from human responses to climate change?
(iv) RQ2c: What are the implications?

Did land degradation occur in a 'nonlinear-cyclic' pattern over time?

In order to answer our first research question (RQ1), we gathered different (hydro)geomorphic records on distinct temporal scales. To assess hydrogeomorphic dynamics on a Late Holocene timescale, we dated floodplain deposits using optically stimulated luminescence (Chapter 5). Floodplain sediments can provide interesting geochronological information on the evolution of land degradation over time. A mineralogical survey allowed locating a suitable floodplain site to the northeast of Lake Ashenge (in the May Tsimble catchment), as sediments in that area contain sufficient quartz for luminescence analysis (Table 5.2). Dose rates were based on massaspectrometric determination of uranium, thorium and potassium concentrations, corrected for cosmic rays (Table A1-1). Equivalent doses were obtained from single-aliquot regenerative dose measurements with post-infrared blue OSL (Table A1-2). We corrected all deposition ages for the residual dose from two modern samples and we calculated aggradation rates over time. Our results indicate increased sediment supply after 1550 BCE up to 650 BCE, and after 400 CE (Figure 5.4). At least one incision phase occurred before the 20th century CE (possibly 18th century CE) and one later incision phase took place during the late 20th century CE. Overall, our chronology corresponds well with other radiocarbon-dated geomorphic records in the Highlands (Figure 5.6).

Further, in order to assess hydrogeomorphic dynamics over the past four centuries, we performed an integrated land cover/degradation investigation around Lake Ashenge (Chapter 8). We analyzed a deep lake core that was retrieved from the lake using thermogravimetry, X-ray sedigraphy, palynology and radiocarbon dating. Additionally, we used repeat photography and investigated historical landscape descriptions to assess land cover changes over the last four centuries. Overall, the proxy records indicate a phase of forest decline and grassland expansion during the early-18th century (see section 8.5.1.2), after a period with increased woody vegetation cover (see section 8.5.1.1). We inferred more gradual land cover changes during the early-feudal period (1850s – 1950) (see section 8.5.1.3) and identified strongly decreased vegetation cover during the period 1950-1990, with a minimum of woody vegetation at the end of the 1960s (see section 8.5.1.4). Yet, after the regime change (1990s – 2000s), increased woody vegetation cover could be inferred (see section 8.5.1.5).

To investigate hydrogeomorphic changes over the past two centuries, we performed a case-study of nine representative gully catchments in the Highlands and included sedistratigraphic analysis of gully infill sediments in some of the catchments (Chapter 4). Based on gully width proxy data derived from repeated terrestrial photographs (Frankl et al., 2011), we could reconstruct gully peak discharges since the 19th century (Table 4.4). Based on warped historical photographs from Meire et al. (2013), we performed Monte Carlo simulation of curve numbers to estimate broad hydrogeomorphic changes since the 19th century (Figure 4.5). The results show a significant increase in peak discharges over the investigated period, which cannot be attributed to large-scale land cover changes alone.

To assess land degradation dynamics on a decadal timescale, we investigated a sequence of alluvial debris fans near Lake Ashenge (Chapter 6). In order to understand the processes of alluvial debris fan built-up, we monitored daily rainfall, peak discharges, bedload transport, suspended sediment load and sediment deposition rates (see Figure 6.2). Further, we dated subrecent deposition rates from one subaquatic alluvial fan using short-lived lead isotopes as counted with a high-purity Germanium detector (Table 6.2), analyzed remote sensing imagery (Figure 6.9) and performed semi-structured interviews with farmers near the sedimentary sequence. Additionally, texture of the subaquatic alluvial fan was determined using X-ray sedigraphy. Based on the significant relation between magnitude of downstream sediment transfer and the rainfall/bedload ratio, we could reconstruct the evolution of the alluvial debris fan sequence since the 1940s (see section 6.3.7). Overall, we infer a

phase of increased (coarse) sediment supply, debris-fan built-up and land degradation during the 1970s-1980s, positioned in-between more stable geomorphic periods.

By combining all above evidence, we can clearly conclude that land degradation occurred in a 'nonlinear-cyclic', instead of a 'gradually-accelerating' pattern over time. We could identify robust phases of increased hydrogeomorphic activity in our study area on different temporal scales: around ~1500 – 500 BCE, from ~500 – 1425 CE, from ~1700 – 1800 CE and from ~1960 – 1990 CE.

Are phases of land degradation synchronous with climate changes?

In order to answer our next research question (RQ2a), we could compare these phases of land degradation with independent records of climatic shifts and long-term drought, as derived from a number of lakes across Ethiopia (Chapter 7). Our synthesis of climatic records indicates region-wide dry periods that include the Heinrich 1 and Younger Dryas events, and phases of aridity between 6650 and 5850 BCE; between 4900 and 4800 BCE; between 3700 and 1300 BCE; between 1100 to 650 BCE; between 450 CE and 1200 CE; and between 1750 and 1900 CE.

By comparing the phases of land degradation with the climatic dry periods, we can conclude that the phases of land degradation were clearly synchronous with the climate changes. We found a significant and very strong temporal association between the climatic dry periods and the phases of land degradation (see Appendix A2). Moreover, when considering the conductivity record of Lake Ashenge as a proxy for regional aridity, we can infer that climatic shifts to greater aridity systematically precede the phases of land degradation, by approximately one or more centuries (Figure 5.6). As effects cannot precede causes, this synchronicity (including the time lag) suggests that climate changes were effectively causing regional environmental changes.

Could there be an amplifying effect from human responses to climate change?

In order to answer our following research question (RQ2b), we compared the phases of land degradation and climate changes with pollen and phytolith studies, historical evidence and data on past pastoral migrations. This comparison shows that there are remarkable temporal links between climatic shifts, grassland expansions, cattle populations and hydrogeomorphic activity (Figure 9.1).

The ‘onset of degradation’, which we dated at 1550 BCE in our study area (Chapter 5), follows after the 2200 BCE event that marked the termination of the ‘African Humid Period’. This represents a large hydroclimatic shift in Northern Africa after which herder groups expanded southwards towards the Ethiopian Highlands. Radiocarbon-dated evidence for the earliest introduction of *Bos taurus* in the Highlands slightly precedes the luminescence dates for the ‘onset of degradation’ (see section 9.2.1). Furthermore, phases of hydrogeomorphic reactivation around 650 BCE, after 400 CE and 1700 CE coincided with climatic shifts to dryer conditions and overlapped with periods of decreased arboreal pollen and increased estimated cattle densities. The degradation phase that was dated to the second half of the 20th century matched with a period of harsh droughts in the region (Chapter 2), but also with the civil war in the country (Chapter 3).

Overall, the synchronicity between the climatic shifts and the lagged grassland expansions, increases in cattle populations or political instability and land degradation activity suggests that human responses to climate change were amplifying the effects of these climate changes in a positive climate-human-ecosystem feedback. The human impact can then be considered as the ‘proximal cause’ for increased land degradation, while the climatic shift can be thought of as the ‘ultimate or distal cause’. This is in line with recent studies from other regions of the world, showing how climate change can impact (pastoral) migration patterns (Kniveton et al., 2012) and political (in)stability (Zhang et al., 2011).

Nevertheless, it will be crucial to gather more high-resolution hydrogeomorphic records from the region. Such records with high dating control could be used to validate our postulation of synchronicity with Late Holocene climatic shifts, and to calculate time lags between different events. Additionally, new studies should be designed to separate the different effects of drought in an experimental setting. For instance, one could study (i) the direct or proximal hydrogeomorphic effects of dry versus wet years, (ii) the responses of pastoralists to the occurrence of dry years, as well as (iii) the hydrogeomorphic impact of increased cattle pressure. The effects of human responses to climate changes might be more significant than the effects of climate changes *in se*.

Implications for drought simulation

What are the implications of these findings (RQ2c)? When we compared the Ethiopian paleoclimatic records with independent records of ocean sea surface temperatures, we discerned a close relation

between the occurrence of long-term drought in the Ethiopian Highlands and cooler equatorial Atlantic and western Indian Ocean surface temperatures (Figure 7.2). Based on these findings, it appeared promising to investigate the impact of different remote atmospheric-oceanic pressure systems on the occurrence of dry years in North Ethiopia. We employed empirical orthogonal teleconnection analysis of meteorological re-analysis data, *in casu* assimilated mean sea level pressure (Chapter 2). While there is no evidence for a decrease of *kiremt* rainfall (June-September) in the study area, the datasets did unveil significant links with atmospheric-oceanic patterns in the Atlantic, Pacific and Indian Oceans. These include the El Niño/La Niña Southern Oscillation, the Indian Ocean Dipole and the South West Monsoons. By means of a diagnostic model we were able to model North Ethiopian *kiremt* rainfall from these three oscillations (R^2 = 64 %), representing 89% of all dry years (Table 2.3). The three atmospheric-oceanic systems contributed largely to the 1983–85 droughts (Figure 2.6). Incorporating oceanic (pressure or surface temperature) data in atmospheric prediction models opens important opportunities for more accurate medium-term drought forecasting and famine early warning in the region.

Implications for climate-resilient land management and future simulations

Our findings have also implications for future dryland management, as our paleoenvironmental synthesis shows that climatic shifts to dryer conditions are associated with significantly increased risks of land degradation and desertification, which is in line with climate model projections. At the same time, however, there is some hope for the future. For one thing, desertification is not irreversible as we showed that localized land resilience happened before – for instance during the Axumite era, after the Oromo movements or in recent decades. This suggests that dryland ecosystems can be robust and elastic for fast recovery, under appropriate management.

To understand how humans are adapting to, and causing, land degradation and drought, we performed semi-qualitative interviews with farmers and key persons from eight villages across the region (Chapter 3). Based on the interview results, we identified three broad political ecology periods: (i) the late feudal era, (ii) the wartime era, and (iii) the post-revolution era (Figure 3.2). The interview results revealed that the feudal land tenure system had a significant impact on hydrogeomorphic processes. The unequal character of land rights (*rist*) played a crucial role for increasing runoff vulnerability during the second half of the 20th century. Poor farmers 'without

land' were forced to farm at steeper slopes or in marshy areas while noblemen, rich farmers or the Church cultivated the large, flat and fertile lands. Later, during the dry 1980s, the civil war hampered further investment in soil and water conservation activities. To date, the greening of the Ethiopian Highlands shows that, despite increased population pressure, equal land rights and large conservation investments under recovered average rainfall amounts have improved economic and environmental conditions (see section 3.3.3).

Finally, to assess whether low-cost smallholder farming techniques could mitigate the effects of future degradation processes and climate change, we developed a number of land management scenarios under conditions of projected climate change (section 9.3.2). Multi-model ensembles project increased hydroclimatic variability and higher rainfall intensities by the second half of this century across the region, which can be expected under warming tropical ocean temperatures. Our simulations show that simple but water-efficient agricultural practices, such as reduced tillage and standing stubble, would lead to greater green water availability and agricultural productivity, even under projected climate change (Table 9.1). In line with the strategy for a 'climate-resilient green economy', such cost-efficient technologies can be implemented on a large scale to strengthen land resilience in regions vulnerable to the effects of future climate change.

Broader implications

We do hope that this study contributes to the debate on climate-human interactions, which is evidently central to the field of geography. One cannot understand climate-human interactions from a 20th century perspective alone, without looking into the deeper environmental dynamics that precede this last century. Therefore, from a methodological perspective, we explicitly sought to employ a long term approach, which required the use of multiple empirical proxies.

Our first (temporal) aim was to understand the 'temporal nature' of environmental changes, which appeared to evolve in rather cyclical or nonlinear ways. Our second (causal) aim sought to associate climatic, environmental and socio-political changes. The remarkable synchronicity between environmental and socio-political changes suggests that there are positive feedbacks between climatic changes and how humans respond. Clearly, neither simplified 'Ratzelian' theories of environmental determinism (Ratzel, 1896) nor 'Malthusian' theories of human resource exploitation (Malthus, 1798) are applicable.

Instead, ideas from the sub-field of political ecology can provide interesting new insights. Hydroclimatic stress has the greatest impact on the marginalized and politically vulnerable people, whether these are pastoralists or poor farmers without access to croplands. Simultaneously, marginalization can lead to political instability and, eventually, land degradation. As climate models show significantly increased aridity at the southern fringes of the Sahel zone, this should concern us all.

References

Kniveton, D., Smith, C., Black, R., 2012. Emerging migration flows in a changing climate in dryland Africa. Nature Climate Change 2, 444–447.

Zhang, D., Lee, H., Cong W., Baosheng, L., Qing, P., Zhang, J., Ylun, A., 2011. The causality analysis of climate change and large-scale human crisis. PNAS 108 (42), 17296–17301.

Nederlandse samenvatting

Overzicht

Meer dan 40 % van het aardoppervlak bestaat uit droogland, en ongeveer 38 % van de wereldbevolking woont in drooglanden. De grote problemen van land degradatie in deze gebieden ('verwoestijning') worden dikwijls geweten aan het toedoen van de lokale bevolking (snelle bevolkingsgroei, mismanagement van de gronden). Bewijsmateriaal voor een associatie tussen verwoestijning en klimaatsverandering is echter uiterst beperkt. Redenen voor deze inconsistentie zijn: (i) de problematische integratie van hydrologische en klimatologische modellen; (ii) een algemeen gebrek aan klimatologische datasets (stationmetingen, ijskernen, boomringen) in droge tropische gebieden; en (iii) een algemeen tekort aan aardwetenschappelijke databases in deze regio's op langere termijn (eeuwen – millennia).

Dit onderzoeksproject levert datasets van verwoestijningsdynamiek bij de limiet van de Afrikaanse moesson. Deze zijn gebaseerd op analyses van onstabiele isotopen, radionucliden, pollen en geaccumuleerde energie binnenin mineraaldefecten in sedimenten bij het Lake Ashenge bekken (Ethiopië), een uniek 'natuurlijk laboratorium' dat uiterst gevoelig is voor klimaatsveranderingen. De sedimentanalyses werden aangevuld met klimaatsmodeldata en hydrologische simulaties, en vormen een *benchmark* voor het vergelijken van klimaatsveranderingen, menselijke activiteit en hydrogeomorfologische respons in de Hoorn van Afrika.

De sedimentsequenties tonen aan (i) dat het moessonklimaat uiterst gevoelig blijkt voor veranderende globale oceaantemperaturen, en (ii) dat fases van versnelde verwoestijning en expansies van graslanden wel degelijk sterk geassocieerd zijn met klimaatsveranderingen. Deze zeldzame empirische vergelijkingsgrond valideert projecties van klimaatsmodellen. We berekenden echter verschillende managementsscenario's om aan te tonen dat het met vrij simpele ingrepen toch mogelijk is om deze kwestie op een efficiënte manier aan te pakken. Als toepassing stellen we een procedure voor om het voorkomen van droogtes te simuleren.

Hoe evolueerde de 'verwoestijning' in de tijd?

Om verwoestijningsdynamiek nabij Lake Ashenge op verschillende tijdschalen (millennia, eeuwen, decennia) te analyseren, onderzochten we alluviale en lacustriene sedimenten. We verzamelden verschillende datasets, op basis van vier types indicatoren.

Ten eerste kunnen sedimenten afgezet in ravijn- of riviervlaktes interessante chronologische informatie bevatten over de evolutie van verwoestijning (Hoofdstuk 5). Om deze evolutie op lange termijn in te schatten, gebruikten we een dateringstechniek genaamd optisch gestimuleerde luminescentie (OSL). Door middel van mineralogisch vooronderzoek identificeerden we gebieden waar sedimenten voldoende kwartsmineralen bevatten. Een geschikte sedimentsequentie werd gelokaliseerd ten noordoosten van het Ashenge meer. Radioactieve dosissnelheden werden verkregen uit analyse van uranium, thorium en kalium concentraties zoals bepaald met inductief gekoppelde plasma massaspectrometrie en atoomemissiespectroscopie. Metingen werden gecorrigeerd voor vochtgehalte en kosmische straling. Equivalente dosissen werden bepaald met behulp van enkele-aliquot regeneratieve dosismetingen met post-infrarood blauw OSL. Na correctie voor de residuele dosissen konden de aggradatiesnelheden in de vlakte berekend worden. De resultaten leveren een dataset met verschillende fases van hydro(geomorfo)logische activiteit over de voorbije vierduizend jaar. De resultaten liggen in de lijn van andere onafhankelijke dateringen in de Hooglanden.

Ten tweede werd een diepe meerboring uitgevoerd in Lake Ashenge. De boorstalen werden chemisch voorbehandeld om non-palynomorfen te verwijderen (Hoofdstuk 8). Stalen werden thermogravimetrisch geanalyseerd en vervolgens onderworpen aan pollenanalyse en stabiele-isotopen-ratio massaspectrometrie. De pollenstratigrafie werd statistisch geanalyseerd met stratigrafische clusteranalyse en de boorkern werd massaspectrometrisch gedateerd met radiokoolstof. De dataset reflecteert de ecohydrologische dynamiek van het endorheïsche bekken over de voorbije vier eeuwen.

Ten derde werd herhaalfotografie en sedistratigrafische analyse van een aantal drainagegeulen gebruikt om de verwoestijningsdynamiek bij en ten noorden van Lake Ashenge over de voorbije twee eeuwen te achterhalen (Hoofdstuk 4). De evolutie van piekdebieten kon worden berekend op basis van data van geulbreedtes. Herhaalfoto's, eerder met spline transformatie gedeformeerd naar het

horizontale vlak, werden gebruikt als input voor een empirisch maar gekalibreerd hydrologisch model. Confrontatie met Monte Carlo simulaties toont de hydrologische evolutie van piekdebieten en afstroming in de bekkens over de voorbije twee eeuwen.

Ten vierde monitorden we gedurende een regenseizoen waterstroming en sedimentlading bij een sequentie van puinwaaiers in een drainagesysteem nabij Lake Ashenge, om de dynamiek van land degradatie in het Ashenge bekken tijdens de laatste decennia te begrijpen (Hoofdstuk 6). In een subaquatische puinwaaier werd een boorkern genomen waardoor subrecente depositiesnelheden berekend konden worden na analyse van kortlevende isotopen met een hoge-zuiverheid germaniumdetector. Sedimenttextuur werd geanalyseerd met X-straal sedigrafie. De monitoring en dateringen werden aangevuld met interpretatie van luchtfoto's en satellietbeelden. We identificeerden een significante relatie tussen sedimentdepositie en de verhouding tussen piekdebieten en beschikbaar sediment. De resultaten leveren zodoende een dataset over de verwoestijningsgeschiedenis in het studiegebied sedert de jaren '40.

Is er een relatie met klimaatsveranderingen?

Door alle datasets samen te voegen, verkregen we een temporeel totaalbeeld van hydrogeomorfologische evolutie rond Lake Ashenge. Verwoestijning vertoont 'cyclisch' gedrag, met verschillende fases van verhoogde activiteit op verschillende tijdsschalen (rond 1500 BCE – 500 BCE, 500 CE – 1400 CE, 1700 CE – 1800 CE en 1960 CE – 1990 CE). We konden deze dynamiek vervolgens gaan vergelijken met paleoklimatologische datasets. We synthetiseerden paleoklimatologische data uit tien meren in de Hoorn van Afrika (waaronder Lake Ashenge), veelal gebaseerd op analyses van diatomeeën, stabiele zuurstofisotopenratio's en geochemische/geomagnetische karakteristieken (Hoofdstuk 7). De vele datasets laten een vergelijking toe tussen klimaat, menselijke activiteit en hydrogeomorfologische respons in deze droogtegevoelige regio. De vergelijking duidt op een significante en sterke associatie tussen het voorkomen van klimaatsveranderingen en verwoestijning ($p < 0.05$). Fases van verwoestijning en periodes van expansie van graslanden komen overeen met fases van klimaatsverandering, zowel op lange, middellange en korte termijn. Deze bevindingen liggen ook in lijn met de projecties van klimaatsmodellen. Deze projecteren significant versterkte droogtepatronen tegen de tweede helft van de 21ste eeuw; vooral in Zuid-Europa, rond de Caraïben, het Midden-Oosten en de zuidelijke delen van de Sahel zone.

Wat zijn de implicaties en toepassingen van deze bevindingen?

Mitigatie van en adaptatie aan klimaatsverandering krijgen een centrale plaats in de *Climate-Resilient Green Economy Strategy* van de Ethiopische federale regering. Om de cruciale rol van land management hierbij te evalueren, voerden we semi-kwalitatieve interviews uit met een honderdtal sleutelpersonen uit acht verschillende studiegebieden verspreid over de regio (Hoofdstuk 3). Op basis van de interviews werden drie verschillende land managementsstrategiën geïdentificeerd: (i) de feodale land managementsstrategie voor 1974, (ii) de communistisch land managementsstrategie tijdens de burgeroorlog tussen 1974 en 1991, en (iii) de post-revolutionaire land managementsstrategie na 1991. Een tijdelijke maar significante trend naar drogere condities en het feodale systeem van grondrechten liggen mee aan de basis van de meest recente fase van verwoestijning (1960-1990). Het ongelijke karakter van grondrechten heeft een belangrijke rol gespeeld bij verwoestijningsprocessen. De armste boeren 'zonder grondrechten' werden gedwongen om de steilste beboste hellingen of moerasgebieden te bewerken. Hierdoor verloren deze hellingen hun waterbufferend vermogen en werd de afstroming van regenwater versneld. De 'grote droogte' en agro-economische stagnatie onder het communistische regime en tijdens de burgeroorlog heeft geleid tot sterk verminderde investering in agro-management. Na de revolutie werd het falende beleid van industrialisatie door importsubstitutie vervangen door een politiek van 'voorrang aan landbouw' (ADLI of Agricultural Development Led Industrialization). Alle gronden werden herverdeeld en er volgden massieve publieke investeringen in de landbouwsector, alsook in bodem- en waterconservering. Durfkapitaal werd verstrekt door grote regionale agro-conglomeraten gelinkt aan het nieuwe regime. Tegenwoordig toont de sterke vergroening van de Hooglanden aan dat deze strategie, ondanks de toegenomen bevolkingsdruk, geleid heeft tot een snel herstel van het gedegradeerde land. Onder invloed van het ADLI-beleid steeg de landbouwproductiviteit in Ethiopië sneller dan het Afrikaanse gemiddelde. Het is met andere woorden zeker mogelijk om verwoestijning effectief tegen te gaan, indien voldoende geïnvesteerd wordt in aangepast land management.

Daarom voorziet de nieuwe *Climate-Resilient Green Economy Strategy* nu voor ongeveer 150 miljard US dollar aan investeringen in water- en landmanagement. We berekenden een reeks water- en landmanagement scenario's onder toekomstige klimaatsverandering. We simuleerden toekomstige klimaatsverandering tegen 2040-2050 met klimaatsmodel GISS II. De gekalibreerde scenariosimulaties tonen aan dat verdere klimaatsverandering *ceteris paribus* zal leiden tot scherper

verhoogde afstroming en erosiesnelheden. Agro-ecologische technieken, zoals verminderd ploegen of ploegen in vaste voren, hebben echter het grootste potentieel om de waterbeschikbaarheid voor gewassen omhoog te brengen, zelfs in de scenario's van klimaatsverandering. Het toekomstig potentieel op vlak van kleinschalige landbouwproductie is aanzienlijk.

Tot slot detecteerden we een sterke correlatie tussen de patronen van klimatologische droogtes in de meersedimenten en reconstructies van oceanische oppervlaktetemperaturen op basis van foraminiferen uit de equatoriaal Atlantische en westelijk Indische Oceaan. Periodes van droogte komen overeen met periodes van kouder oppervlaktewater in beide oceanen, die herhaaldelijk veroorzaakt werden door influx van Noord-Atlantisch smeltwater. De sedimentaire relatie tussen oceaantemperaturen en droge periodes in de Hoorn van Afrika, inspireerde ons om de impact van globale oceanisch-atmosferische systemen op het voorkomen van periodieke droogte in de regio te simuleren. Dit gebeurde met behulp van een empirisch orthogonale teleconnectie-analyse van meteorologische reanalysedata – *in casu* geassimileerde luchtdruk op zeeniveau. Droogte in de regio blijkt geconnecteerd met patronen in de Stille Oceaan, de Indische Oceaan en de Atlantische Oceaan. Deze omvatten respectievelijk de El Niño/La Niña Zuidelijke Oscillatie, de Indische Oceaan Dipool en de Zuidwestelijke Moesson. Een diagnostisch model kan de regenval in Noord-Ethiopië nu accuraat voorspellen (R^2 = 64 %), correct voor 89 % van alle droge jaren. Bovendien vonden we dat de drie voorgenoemde patronen een dominante invloed hebben uitgeoefend op het voorkomen van de 'grote droogte' tijdens 1983-1985. Met degelijke droogtesimulatiemodellen kunnen landbouwers beter het risico op droogte voorzien en kan men de macro-economische impact van droogtes tijdig opvolgen. Inrekenen van oceanische temperatuurspatronen, met name deze tijdens de lente in de equatoriaal Atlantische en westelijk Indische Oceaan, opent belangrijke mogelijkheden voor accurate voorspelling van droogte voor de komende moesson.

Appendices

APPENDIX A1: Mass spectroscopy and luminescence data

Table A1-1. K, Th and U concentrations, as determined by Induced Coupled Plasma Mass Spectroscopy / Atomic Emission Spectroscopy using a fusion sample preparation technique.

	Unit	X6431	X6432	X6433	X6434	X6435	X6436	X6437
Grain sizes								
Min. grain size	(mm)	180	180	180	180	180	180	180
Max . grain size	(mm)	255	255	255	255	255	255	255
Measured concentrations								
Standard fractional error	(%)	5	5	5	5	5	5	5
% K	(%)	0.697	0.905	0.672	0.706	0.755	0.64	0.43
Error (% K)	(%)	0.035	0.045	0.034	0.035	0.038	0.032	0.022
Th	(ppm)	3	4.3	3.5	3.1	3.4	2.9	2.3
Error (Th)	(ppm)	0.15	0.215	0.175	0.155	0.17	0.145	0.115
U	(ppm)	1.1	1.3	1.3	1.1	1.1	1	1.2
Error (U)	(ppm)	0.055	0.065	0.065	0.055	0.055	0.05	0.06

Table A1-2. Equivalent doses, cosmic doses, moisture content, total dose rate and age estimates.

	Unit	X6431	X6432	X6433	X6434	X6435	X6436	X6437
De	(Gy)	(0.48)	(0.27)	0.62	3.63	2.34	27.27	3.21
uncertainty		0.19	0.24	0.35	0.27	0.21	5.01	0.77
Cosmic dose calculations								
Depth	(m)	0.34	1.5	0.99	1.32	0.28	1.2	3.7
error	(m)	0.05	0.05	0.05	0.05	0.05	0.05	0.05
Average overburden density	($g.cm^3$)	1.9	1.9	1.9	1.9	1.9	1.9	1.9
error	($g.cm^3$)	0.1	0.1	0.1	0.1	0.1	0.1	0.1
Latitude		13	13	13	13	13	13	13
Longditude		40	40	40	40	40	40	40
Altitude	(m a.s.l.)	2052	2023	2023	2020	2020	2019	2019
Geomagnetic	latitude	9	9	9	9	9	9	9
Dc	(Gy/ka), 55N G.lat, 0 km Alt.	0.201	0.172	0.184	0.176	0.202	0.179	0.131
error		0.033	0.014	0.016	0.014	0.039	0.015	0.01
Cosmic dose rate	(Gy/ka)	0.249	0.213	0.228	0.218	0.25	0.222	0.162
error	0.041	0.017	0.02	0.018		0.048	0.019	0.012
Moisture content								
Measured water	(% of wet sediment)	13.27	13.64	15.38	11	17.78	14.54	19.36
Moisture	(water/wet sediment)	0.13	0.14	0.15	0.11	0.18	0.15	0.19
error	0.03	0.03	0.03	0.03		0.03	0.03	0.03
Total dose rate	(Gy/ka)	1.216	1.449	1.216	1.224	1.218	1.091	0.831
error		0.07	0.075	0.06	0.062	0.075	0.054	0.039
OSL age estimate	(yr before 2014)	(<400)	(<200)	510	2970	1920	24990	3860
error				290	270	210	4760	950

APPENDIX A2: Association between datasets

In order to assess the correspondence between paleoclimatic and paleoenvironmental changes during the Late Holocene (i.e. after 2200 BCE), we calculated the temporal correlations between different records. Independence versus association between dry phases (phases based on the analysis of Chapter 7, delineated in Table 7.3) and phases of land degradation (phases based on the analysis of section 9.1, delineated in Table A2-1) could be tested by a chi^2-test (Beguin, 1979). We therefore sampled 41 points in time, every 100 years after 2200 BCE, and recorded occurrences of drought/land degradation for every sampling point. The null hypothesis corresponds to the situation where the phases are independent while the alternative hypothesis corresponds to the situation where the phases have an association. The test can be corrected for the sample size (n = 41), and can be expressed in terms of the strength of the association, by using the Cramér's V:

$$\varphi_v = \sqrt{\frac{\chi^2}{n(k-1)}}$$

With φ_v the Cramér's V, χ^2 derived from Pearson's chi-squared test, n the total of observations and k the number of rows or the number of columns, whichever is less. The p-value for the significance of φ_v is the same one that is calculated using the Pearson's chi-squared test. The association is strong if $\varphi_v > 0.5$, moderate if $0.3 > \varphi_v > 0.5$, low if $0.1 > \varphi_v > 0.3$ and little if any association is present if $\varphi_v > 0.1$.

Note: Beguin H. 1979. Méthodes d'analyse géographique quantitative. Librairies Techniques: Paris; 283.

Table A2-1. Subsequent Late-Holocene phases of landscape (in)stability, including dates and references (see Chapter 9 for references).

Period	Dates	Description
Mid-Holocene stability	Pre 1500 BCE	Vertisol development, pedogenesis and travertine development (Semmel, 1971; Verheye, 1978; Hurni, 1982; Brancaccio et al., 1997; Nyssen et al., 2004; Moeyersons et al., 2006; Ogbaghebriel et al., 1997)
(Re)activation phase 1	~1500 BCE – 500 BCE	Sharp increase of fluvial aggradation around ~1500 BCE (Machado et al., 1998; Chapter 5) and colluvial activity around 1430-1260 BCE (Moeyersons et al., 2006); allochthonous material input in Lake Ashenge from 950-750 BCE (Marshall et al., 2009); dates for fluvial aggradation around ~650 BCE (Machado et al., 1998; Chapter 5) up to 300 BCE (Machado et al., 1998)
Axumite stability	~500 BCE – 500 CE	Geomorphic evidence for landscape stability (French et al., 2009), decreased fluvial aggradation rates (Machado et al., 1998; Chapter 5) and decreased erosion rates (Ciampalini et al., 2008)
Reactivation phase 2	500 – 1425 CE	Increased fluvial aggradation rates after 400 CE (Machado et al., 1998; Chapter 5) and greatly accelerated allochthonous input in Lake Ashenge (Marshall et al., 2009); dates for fluvial aggradation around ~1100 CE (Machado et al., 1998)
15th century stability	15th century	Phase of soil formation in the Northern Highlands with minimum age 1425-1445 CE, lasting till 1481-1660 CE (Machado et al., 1998)
Reactivation phase 3	Before and around 1714 CE	Dates for fluvial aggradation after ~1500 CE till ~1800 CE (Machado et al., 1998); evidence for strong colluvial activity resulting from erosion at steep slopes, dated to around 1714 CE (Machado et al., 1998). Oversized gully morphology is visible on early 19th century photographs, indicative of a prior activation phase (Frankl et al., 2011)
19th century stability	19th – early 20th century	Machado et al. (1998) infer 19th century landscape stability; Frankl et al. (2011) identify stable gully morphologies from ~1865-1960 CE

APPENDIX A3

Following the clues buried in the ocean sediments (Chapter 7), it may be possible to develop simple and empirical drought prediction tools. For instance, based on the dataset of chapter 2, we discerned very dry (< (μ - 1σ)) from medium ([μ - 1σ, μ]), wet ([μ, μ + 1σ]) and very wet (> (μ + 1σ)) *kiremt* seasons (June-September) in North Ethiopia (derived from the rainfall record of Mekelle-Quiha Airport, 1982-2009; μ mean and σ standard deviation) (Figure A3-1). These data can be plotted against the March WTIO index, representing the Western Tropical Indian Ocean sea surface temperature anomaly index (box 50°E - 70°E, 10°S - 10°N) (1982-2005; NOAA, 2015); and the March sea surface temperature index in the Southern Atlantic (averaged in 30-40°S, 20-30°W) (NOAA, 2015). In line with the longer-term relations discussed above, this reveals that very dry summer seasons in North Ethiopia occur below two empirical ocean temperature threshold values in boreal spring (March) (March SST Atlantic < 21.2°C; March WTIO index < -0.1) (Figure A3-1).

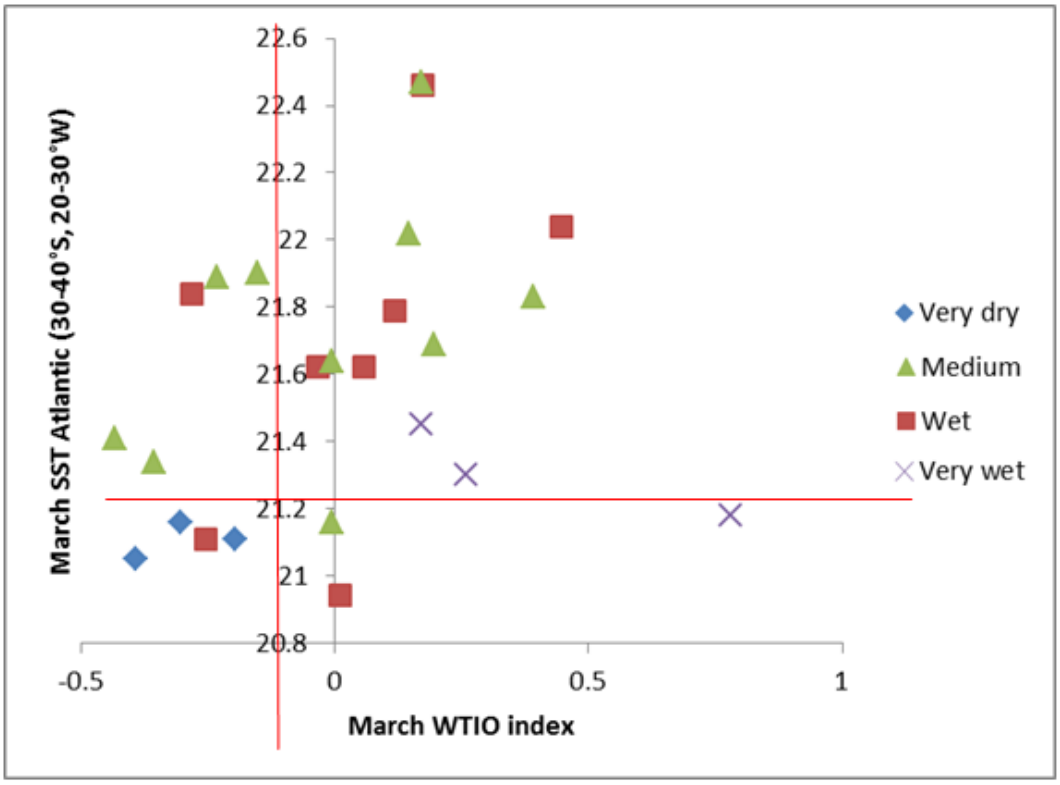

Figure A3-1. March SST Atlantic (30-40°S, 20-30°W) plotted against March Western Tropical Indian Ocean temperature index (WTIO) for very dry (< 345 mm), medium (345 to 483 mm), wet (483 to 621 mm) and very wet (> 621 mm) *kiremt* rainy seasons in North Ethiopia. Red lines indicate threshold values below which very dry seasons can occur (March SST Atlantic < 21.2°C; March WTIO index < -0.1). See chapter 2 for a full description of the rainfall data.

APPENDIX A4

Appendix A4 contains 32 historical photographs in Lake Ashenge basin and their recent repeats. All copyright holders of the photographs are indicated; the copyright holder of one photograph could not be identified, and S. Salgado's press photographs (1984) have been resampled at lower resolution. Metadata and statistics of the interpretation are presented in Supplementary Tables A4-1 and A4-2.
The repeated photographs are subsets of the photographic material used in wider studies (Frankl et al., 2011; Munro et al. 2008; Nyssen et al., 2009, 2014). The archives from where the photographs have been retrieved are detailed by Nyssen et al. (2010).

References

Frankl, A., Nyssen, J., De Dapper, M., Mitiku Haile, Billi, P., Munro, R.N., Deckers, J. Poesen, J. 2011. Linking long-term gully and river channel dynamics to environmental change using repeat photography (North Ethiopia). Geomorphology, 129 (3-4): 238-251.

Munro, R.N., Deckers, J., Mitiku Haile, Grove, A.T., Poesen, J., Nyssen, J., 2008. Soil landscapes, land cover change and erosion features of the Central Plateau region of Tigrai, Ethiopia: Photo-monitoring with an interval of 30 years. Catena, 75: 55-64.

Nyssen, J., Mitiku Haile, Naudts, J., Munro, R.N., Poesen, J., Moeyersons, J., Frankl, A., Deckers, J., Pankhurst, R., 2009. Desertification? Northern Ethiopia re-photographed after 140 years. Science of the Total Environment, 407: 2749 – 2755.

Nyssen, J., Frankl, A., Munro, R.N., Billi, P. Mitiku Haile, 2010. Digital photographic archives for environmental and historical studies: an example from Ethiopia. Scottish Geographical Journal, 126 (3): 185-207.

Nyssen, J., Frankl, A., Mitiku Haile, Hurni, H., Descheemaeker, K., Crummey, D., Ritler, A., Portner, B., Nievergelt, B., Moeyersons, J., Munro, R.N., Deckers, J., Billi, P., Poesen, J., 2014. Environmental conditions and human drivers for changes to north Ethiopian mountain landscapes over 145 years. Science of the Total Environment, 485–486 (164-179).

Supplementary Figures of Appendix A4. All repeat photographs used to assess changes in vegetation cover since 1868. Metadata of all figures in Supplementary Table A4-1. Recent photographs were presented in black and white for interpretation.

KO-1868-RE-422a

1868 © Kings Own Regiment Museum, Lancaster (U.K.)	2011 © Jan Nyssen
	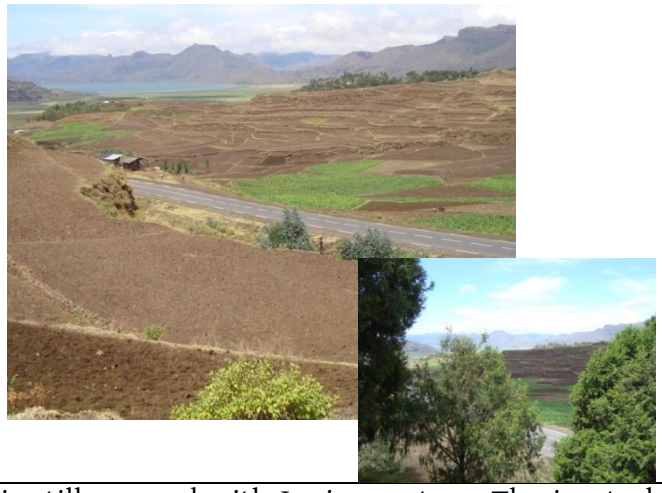

Note: The viewpoint is a hill that was and is still covered with Juniperus trees.The inset photo at right is taken from the same viewpoint as the original photograph, but trees hinder the view and only a small part of the landscape is visible. The larger recent photograph covers the same landscape from a slightly different viewpoint.

KO-1868-RE-28

1868 © Kings Own Regiment Museum, Lancaster (U.K.) 2008 © Jan Nyssen

This view over the alluvial plains around Lake Ashenge was taken from the foot of the hills surrounding the lake. Though many features appear across the landscape in 2008, especially fenced land-holding boundaries, the traditional ‘daget’ structures with abundant vegetation on the risers in 1868 offer a much better protection from soil erosion (and thus a better land management practice) than the narrow grass strips in 2008. In the field, it appeared impossible to avoid the two tall trees while taking the repeat photograph, which indicates that they have grown after 1868.

KO-1868-RE-29

1868 © Kings Own Regiment Museum, Lancaster (U.K.) 2008 © Jan Nyssen

The village on the hill has grown, and so has the vegetation around it. Also the slopes at the back bear much more trees nowadays, and are better protected from erosion. When shown the 1868 photograph, villagers mentioned that a couple of decades ago, *before development*, their village and its environment looked like that. On the other hand, scarcity of land has pushed the farmers to plough the foot of the terrace riser, which has retreated and is less stable nowadays due to absence of vegetation and existence of a subvertical slope.

KO-1936-AN-I19

1936 © Istituto agronomico per l'Oltremare (IAO), Firenze (I.)	2009 © Jan Nyssen
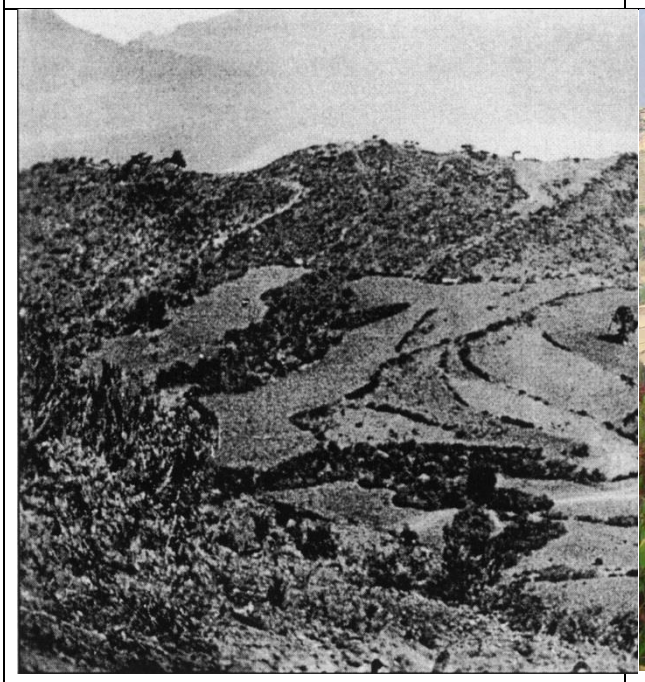	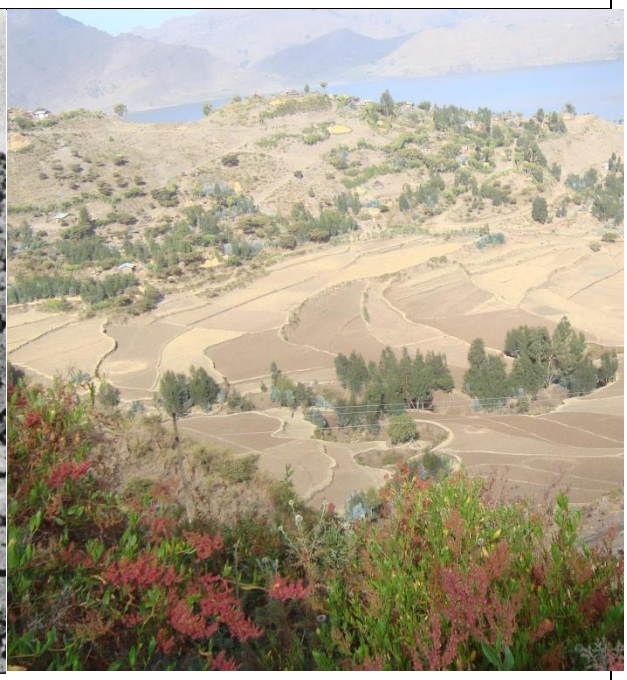

KO-1936-LU-9733

1936 © Foto Luce	2009 © Jan Nyssen
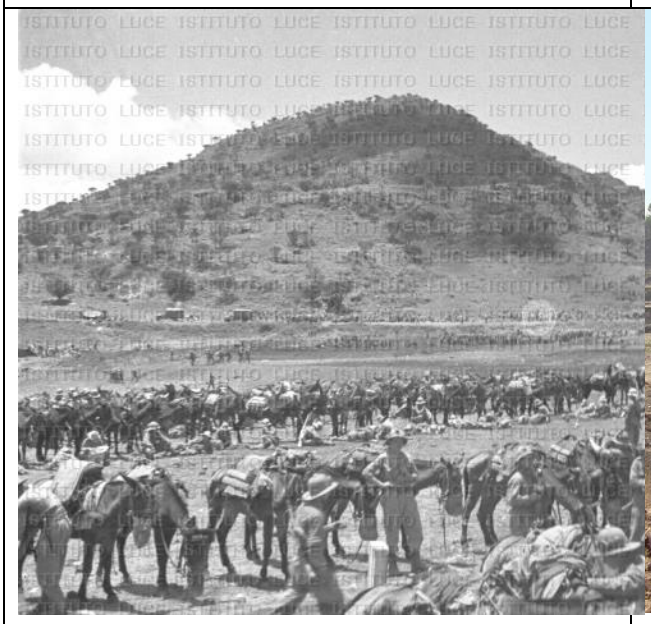	

KO-1936-ME-F1

1936 © Giovanni Merla	2009 © Jan Nyssen
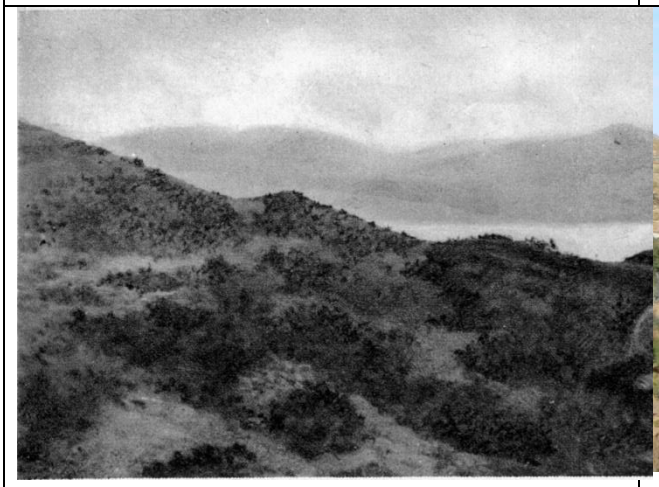	

KO-1936-ME-F2

1936 © Giovanni Merla	2009 © Jan Nyssen
	

KO-1936-ME-53

1936 © Giovanni Merla	2009 © Jan Nyssen
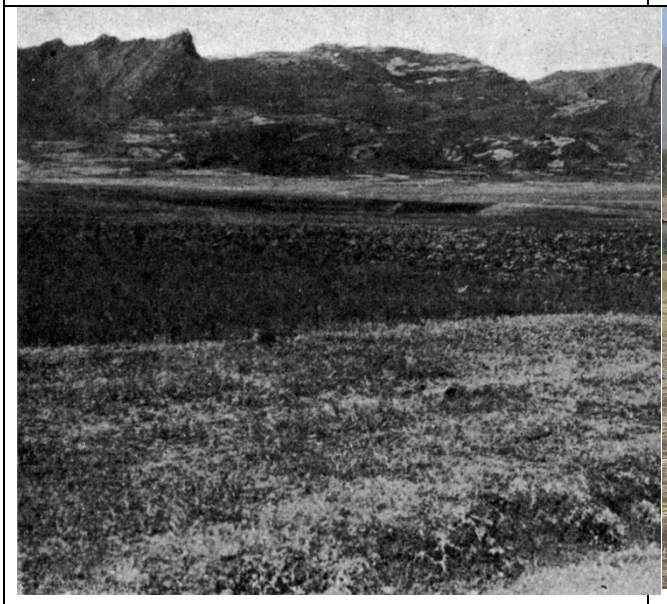	

The repeat photograph was taken from a viewpoint that is 300 m closer, since the foreground of the old photograph (roadside) is now built-up area

KO-1936-CA-I18

1936 © ImaGo	2009 © Jan Nyssen
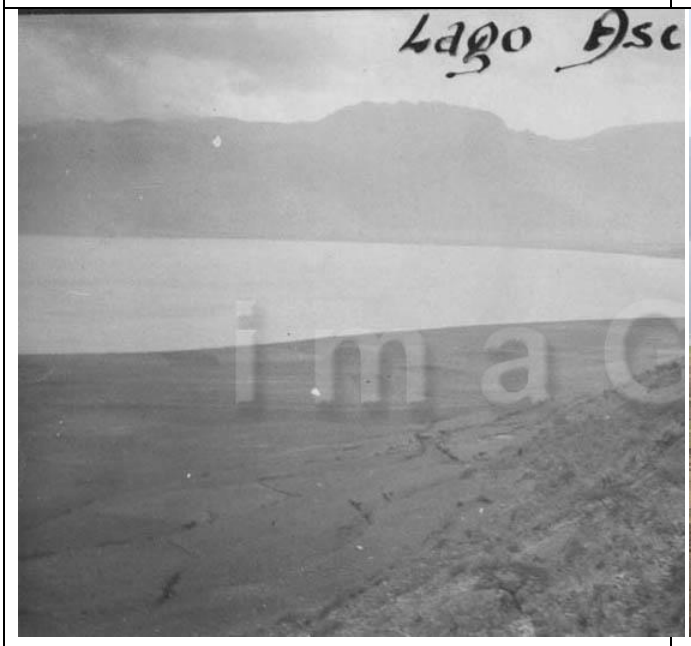	

KO-1937-MA-16-503

1937 © Istituto agronomico per l'Oltremare (IAO), Firenze (I.)	2009 © Amaury Frankl
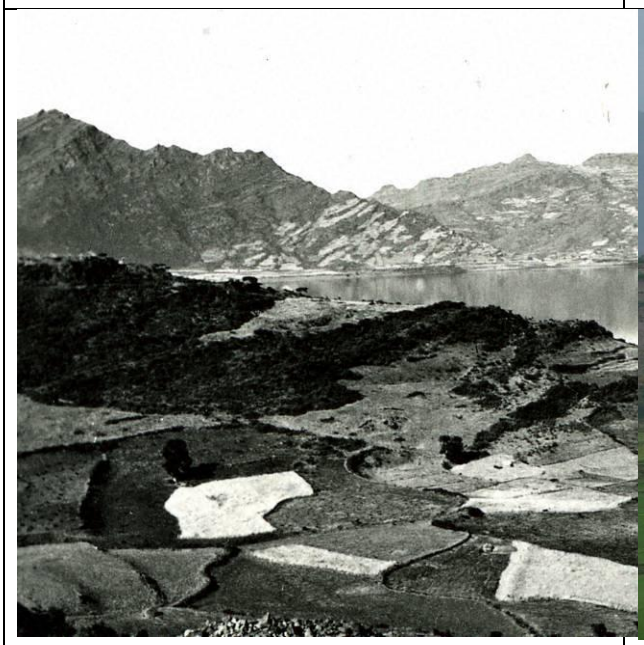	

Only the landscape in the foreground was interpreted. Note however that in 1937, the very steep slopes on the opposite side of the lake were cultivated; something that does not occur anymore nowadays

KO-1937-MA-16-505

1937 © Istituto agronomico per l'Oltremare (IAO), Firenze (I.)	2009 © Amaury Frankl
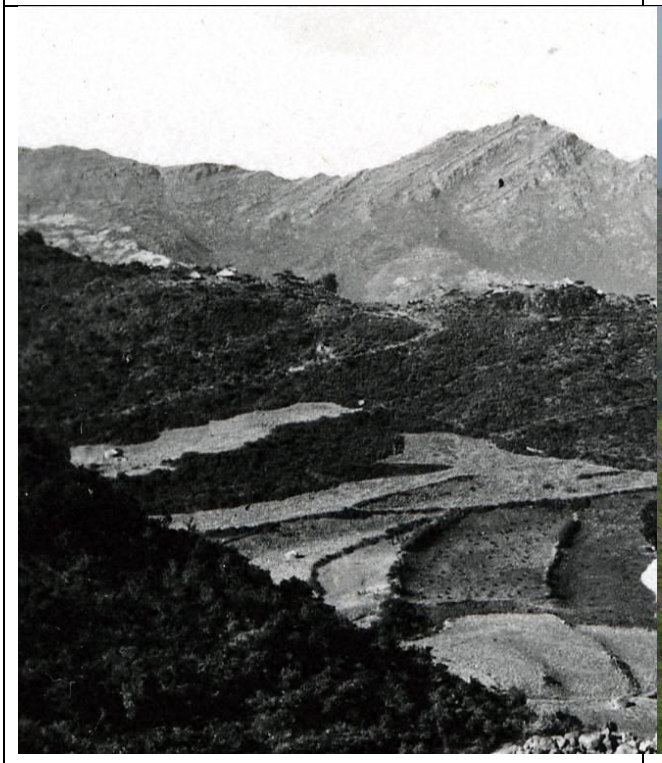	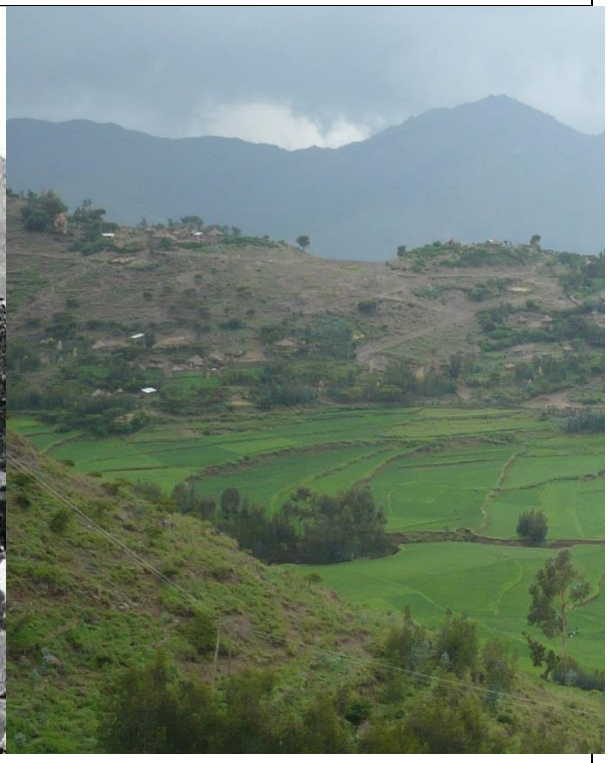

KO-1937-MA-66-21

1937 © Istituto agronomico per l'Oltremare (IAO), Firenze (I.)	2009 © Amaury Frankl
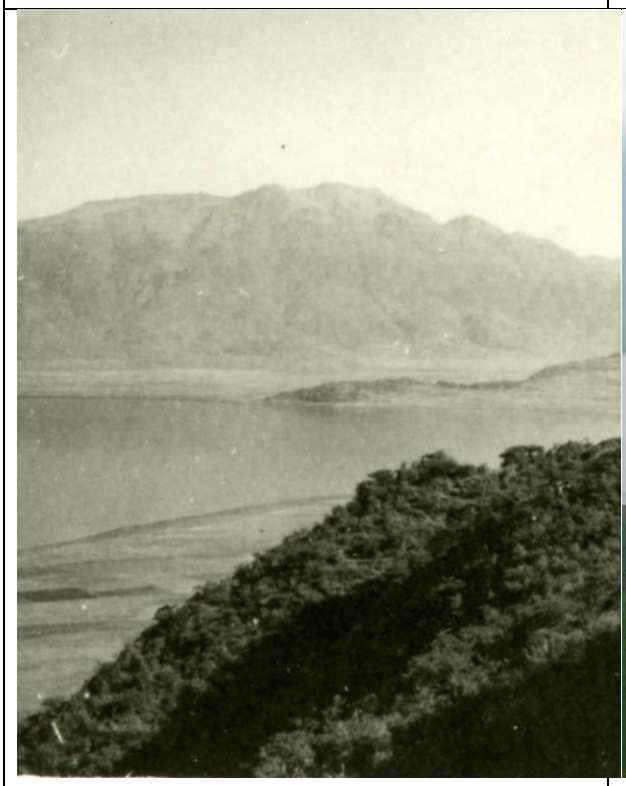	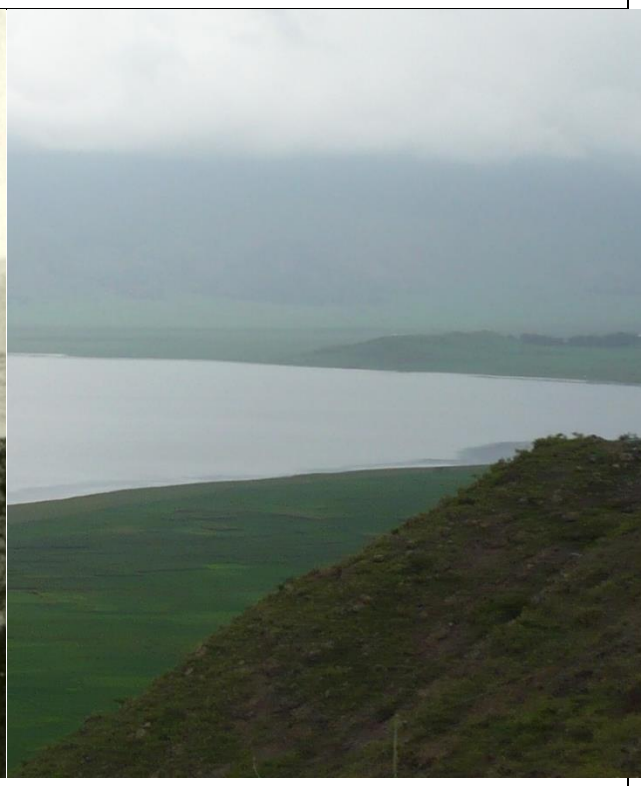

KO-1937-MA-66AOI_7a

1937 © Istituto agronomico per l'Oltremare (IAO), Firenze (I.)	2011© Jan Nyssen
	

KO-1937-MA-66AOI_7b

1937 © Istituto agronomico per l'Oltremare (IAO), Firenze (I.)	2011 © Jan Nyssen
	

KO-1937-MA-66AOI_7c

1937 © Istituto agronomico per l'Oltremare (IAO), Firenze (I.)	2011 © Jan Nyssen
	

KO-1937-MA-66AOI_7d

1937 © Istituto agronomico per l'Oltremare (IAO), Firenze (I.)	2011 © Jan Nyssen
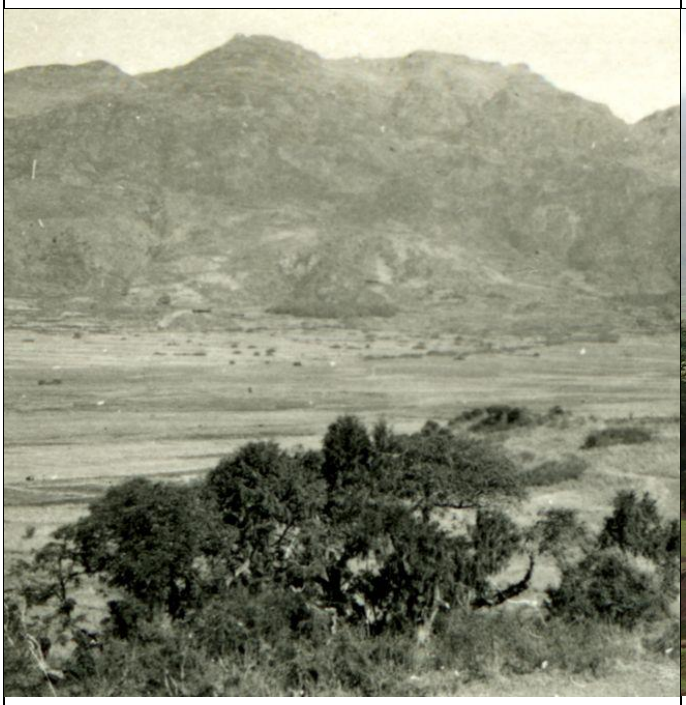	

The historical photograph was taken from a bit higher position – most probably because the road was in a higher position in the 1930s

KO-1937-MA-66AOI_7e

1973 © Istituto agronomico per l'Oltremare (IAO), Firenze (I.)	2011 © Jan Nyssen
	

KO-1939-MA-45-61a

1939 © Istituto agronomico per l'Oltremare (IAO), Firenze (I.)	2009 © Amaury Frankl
	

KO-1939-MA-45-62a

1939 © Istituto agronomico per l'Oltremare (IAO), Firenze (I.)	2009 © Amaury Frankl
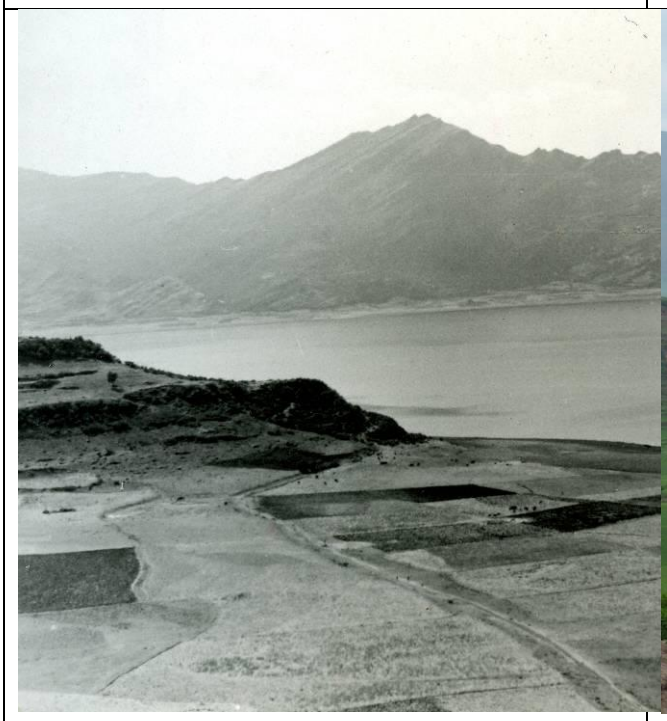	

KO-1939-MA-I1

1939 © Istituto agronomico per l'Oltremare (IAO), Firenze (I.)	2007 © Jan Nyssen
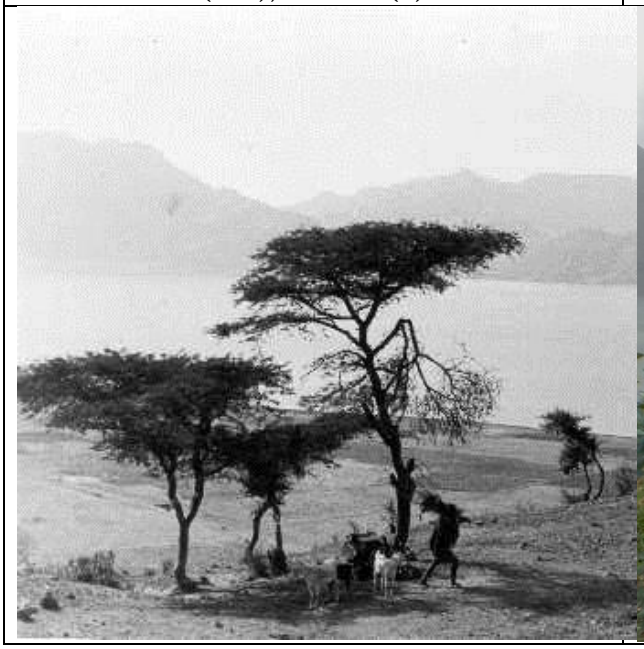	

KO-1961-GR-528

1961 © A.T. (Dick) Grove	2007 © Jan Nyssen
	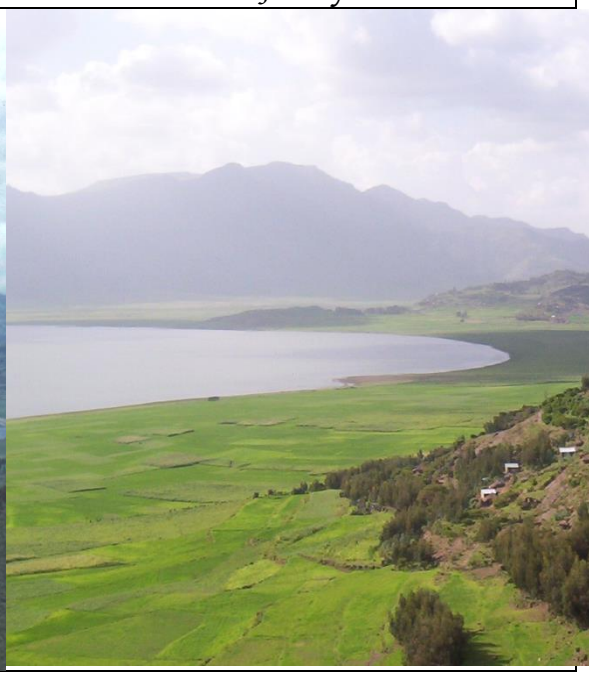

KO-1961-GR-531

1961 © A.T. (Dick) Grove	2007 © Jan Nyssen
	

KO-1970-AB-802

1970 © Ernesto Abbate	2009 © Jan Nyssen
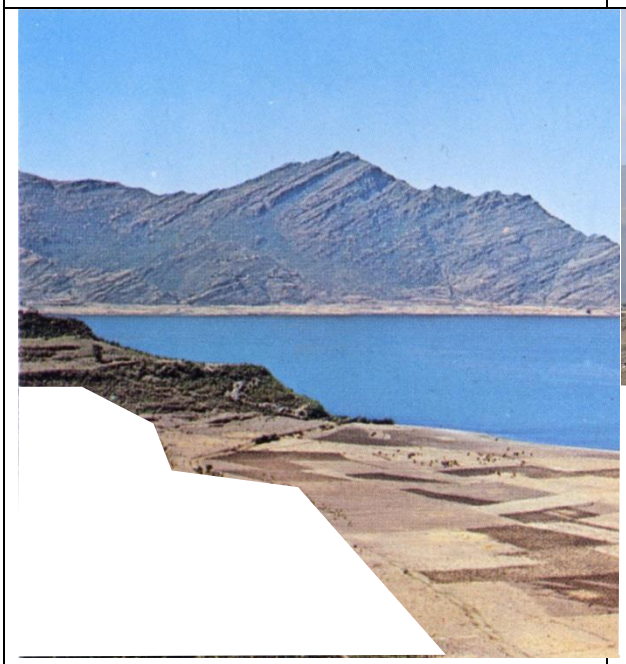	

Foreground could not be repeated exactly, hence it was hidden for interpretation.

KO-1974-75-VE-613

1974 © Vernon Robertson, R. Neil Munro	2007 © Jan Nyssen
	

KO-1975-MU-186

1975 © R. Neil Munro

2007 © Amaury Frankl

KO-1975-MU-187

1975 © R. Neil Munro

2007 © Jan Nyssen

KO-1975-MU-188

1975 © R. Neil Munro	2007 © Amaury Frankl
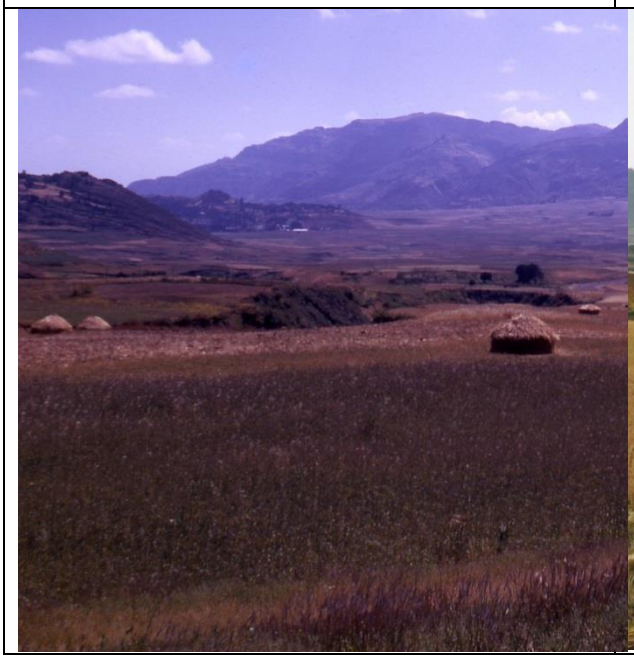	

KO-1975-MU-190

1975 © R. Neil Munro	2007 © Jan Nyssen
	

KO-1984-AN-1

1984 © Sebastiaõ Salgado	2009 © Jan Nyssen
	

The left photo has been darkened in order to better represent the back slope (at the expense of the person pictured by famous press photographer Sebastiaõ Salgado during the 1984 famine).

KO-1984-AN-2

1984 © Sebastiaõ Salgado	2009 © Jan Nyssen
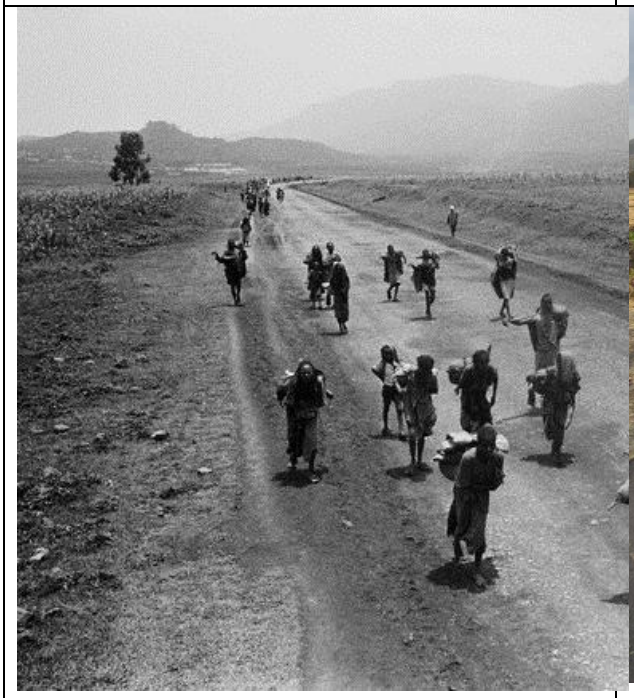	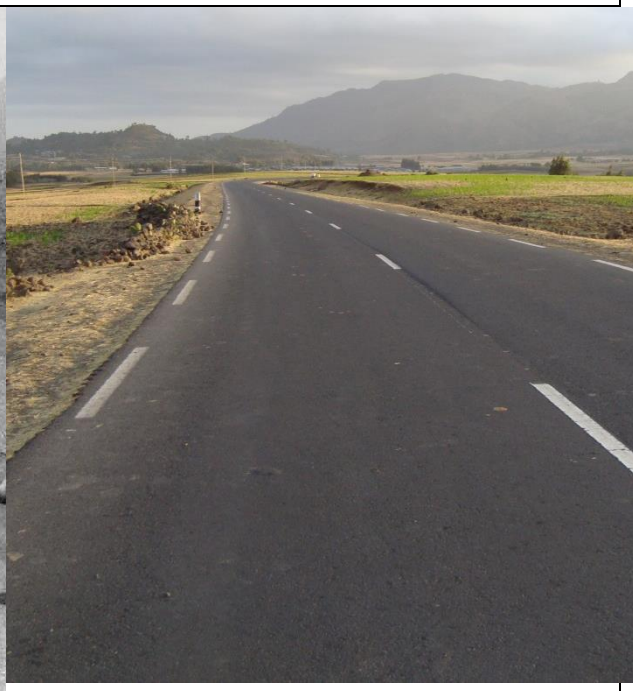

Another photo by Sebastiaõ Salgado in 1984

KO-1994-CR-5

1994 © André Crismer	2010 © Amaury Frankl
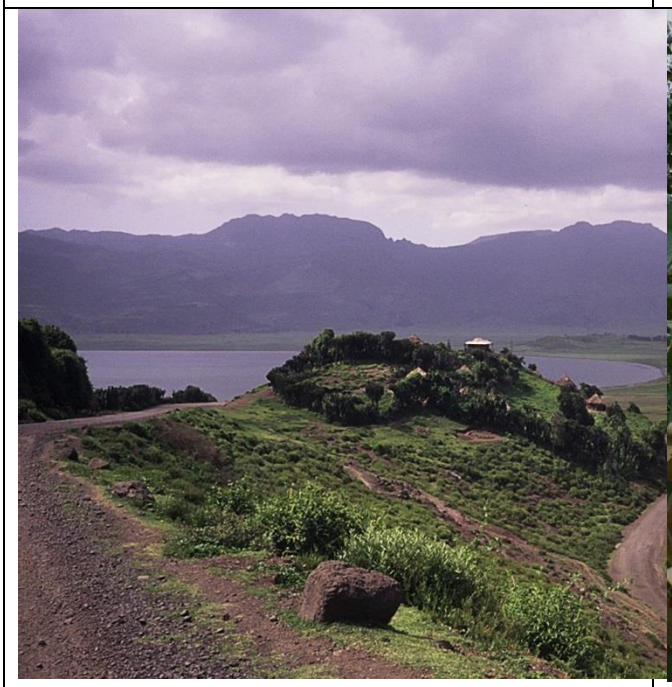	

KO-1994-CR-6

1994 © André Crismer	2010 © Amaury Frankl
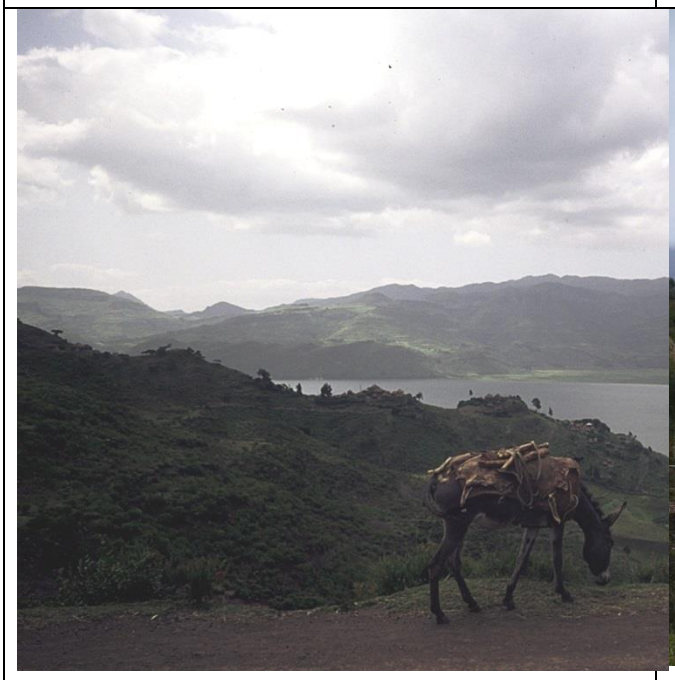	

Supplementary tables of Appendix A4

Table A4-1. Overview of historical photographs of Lake Ashenge basin, interpreted and compared to the current situation

Historical photograph	Author	Year	Repeat year	Score [a]	Coordinates of photo midground (°N, °E)
KO-1868-RE-422a	Royal Engineers	1868	2011	2	12.644850, 39.528504
KO-1868-RE-28	Royal Engineers	1868	2007	1.5	12.643700, 39.517331
KO-1868-RE-29	Royal Engineers	1868	2007	-2	12.635766, 39.503127
KO-1936-AN-I19	Anonymous	1936	2009	-1	12.566456, 39.517121
KO-1936-LU-9733	Anonymous	1936	2009	-1	12.591835, 39.535984
KO-1936-ME-F1	G. Merla	1937	2009	-1	12.563918, 39.518188
KO-1936-ME-F2	G. Merla	1937	2009	-1	12.563380, 39.522117
KO-1936-ME-53	G. Merla	1937	2009	-2	12.519599, 39.507369
KO-1936-CA-I18	Anonymous	1937	2009	-2	12.570110, 39.520020
KO-1937-MA-16-503	A. Maugini	1937	2009	-1	12.563380, 39.522117
KO-1937-MA-16-505	A. Maugini	1937	2009	0.5	12.563418, 39.519378
KO-1937-MA-66-21	A. Maugini	1937	2009	1	12.564530, 39.521308
KO-1937-MA-66AOI_7a	A. Maugini	1937	2011	0	12.617205, 39.522615
KO-1937-MA-66AOI_7b	A. Maugini	1937	2011	1	12.619519, 39.524661
KO-1937-MA-66AOI_7c	A. Maugini	1937	2011	0	12.620222, 39.526188
KO-1937-MA-66AOI_7d	A. Maugini	1937	2011	-1	12.621834, 39.526362
KO-1937-MA-66AOI_7e	A. Maugini	1937	2011	-1	12.623563, 39.527254
KO-1939-MA-45-61a	A. Maugini	1939	2009	-0.25	12.567133, 39.519500
KO-1939-MA-45-62a	A. Maugini	1939	2009	-0.5	12.569181, 39.518740
KO-1939-MA-I1	A. Maugini	1940	2007	1	12.567403, 39.523705
KO-1961-GR-528	A.T. (Dick) Grove	1961	2007	-1	12.570886, 39.521230
KO-1961-GR-531	A.T. (Dick) Grove	1961	2007	-1	12.568406, 39.522882
KO-1970-AB-802	E. Abbate	1970	2009	-1	12.567998, 39.515916
KO-1974-75-VE-613	V. Robertson	1975	2007	1	12.644850, 39.528504
KO-1975-MU-186	R.N. Munro	1975	2007	ND [b]	12.564663, 39.517985
KO-1975-MU-187	R.N. Munro	1975	2007	ND [b]	12.570221, 39.521429
KO-1975-MU-188	R.N. Munro	1975	2007	-1	12.548950, 39.517880
KO-1975-MU-190	R.N. Munro	1975	2007	0	12.548950, 39.517880
KO-1984-AN-1	S. Salgado	1984	2009	-1	12.551673, 39.512026
KO-1984-AN-2	S. Salgado	1984	2009	-1	12.551673, 39.512026
KO-1994-CR-5	A. Crismer	1994	2010	-1	12.569544, 39.523475
KO-1994-CR-6	A. Crismer	1994	2010	-1	12.569544, 39.523475

[a] Median of scores given by 5-12 geographers (Jan Nyssen, Alfons Ritler, Amaury Frankl, Mitiku Haile, Hans Hurni, Katrien Descheemaeker, Donald Crummey, Brigitte Portner, Bernhard Nievergelt, Jan Moeyersons, Neil Munro, Jozef Deckers, Paolo Billi and Jean Poesen) for woody vegetation cover depicted on the historical photographs (-2 much less than on the recent photograph; 0 similar; +2 much more). [b] Repeat photograph under different angle was not used in the quantitative interpretation.

Table A4-2. Summary statistics of scores given to historical photographs (Supplementary Table A4-1), that were used to prepare Figure 8.9. All photographs of 2007-2011 received a score of 0 as it was the standard against which the historical scenery was interpreted.

Period	Average score	St. dev.	n
1868	0.50	2.18	3
1936-1939	-0.49	0.95	17
1961-1976	-0.50	0.84	6
1985-1994	-1.00	0	4
2007-2011	0	0	30

APPENDIX A5: Additional information on the interview methods used for Chapter 3

We followed Blaikie (1985) in his basic assertion that soil erosion can be driven by marginalization of peasant farmers, land tenure, ways of agricultural production and use of surpluses, and prices of market inputs and outputs. Additionally, we followed the assertion by Massey (1984) that the structure of local economies can be seen as a product of the combination of 'layers' of the successive deposition of new waves of investment. The physical landscape can thus be read as a historical product of the combination of successive layers of economic activity and conservation policies.

We interviewed 40 local farmers in seven villages. During random walks in these villages, we asked random farmers if they could remember the period before the civil war – and if so, if we could interview them. Consequently, only local farmers of relatively higher ages were considered for the interviews. All interviews were recorded independently and individually, in the presence of the first author together with a local and experienced translator (native speaker of Tigrinya). We did not use maps or aerial images, but encouraged all respondents to show everything on the terrain and fields.

The interviews lasted for approximately 30 minutes and were broadly structured as follows:

(i) The land distribution during feudal times—and the evolution towards today;
Where were the croplands located?
Where were the forests and grazing lands located?
Where were the larger parcels located?
Where were the smaller parcels located?
What were the differences between the feudal times and today?
Can you show all of this in the landscape?
Was there more forest; and grazing lands?
Was there more cropland?
Were the parcels larger or smaller than today?
Where were the lands of the Church?
(repetition of these questions for the civil war period)

(ii) The land tenure system during feudal times—and the evolution towards today;
Who owned the croplands?
Who rented cropland parcels?
Were there farmers without land ownership?

Could everybody rent parcels?
How much was the cost to rent a parcel?
Were there more poor people as compared to today?
Were there more rich people as compared to today?
Who were the noblemen?
Can you give some names of *dejazmach* in the village?
Did the Church own or rent lands?
Who cultivated the Church lands?
(repetition of these questions for the civil war period)

(iii) The land degradation during feudal times—and the evolution towards today;
Were the gullies more active than today?
Where were the gullies located?
Were the gullies deeper or less deep?
Were there landslides?
Were there conservation measures on the fields?
Were there conservation measures in the gullies?
Can you explain the conservation measures and show them here in the field?
Were there more or less conservation measures?
(repetition of these questions for the civil war period)

The questionnaire of Naudts (2002) was different from our questionnaire, as it also focussed more on the agronomic aspects. Nevertheless, we could use the interpretations of the interviews of Naudts (2002), as these contained valuable additional information on the feudal land tenure. Overall, our methodology bears some similarities with the AGERTIM method (Assessment of Gully Erosion Rates Through Interviews and Measurements) that was developed in the study area (Nyssen et al., 2006). Nevertheless, our study did not comprise measurements and monitoring of gully volumes, and was based on individual interviews instead of group interviews.

Finally, all interview answers were digitized, and answers and quotes were grouped per village; and villages were coded with one or two letters. To ensure that no statements of farmers who were 'exagerating' or 'lying' could be incorporated in the study, care was taken to ensure that if one or more of the interviewed farmers were giving statements that were inconsistent with statements by other farmers in the village, no answers and insights of the farmers in this village were used. Then, the subset of 'trustable' answers and quotes was structured per theme (land distribution, land tenure and land

degradation) and per time period (feudal era, civil war, era of the TPLF) for interpretation.

References

Blaikie, P., 1985. The Political Economy of Soil Erosion in Developing Countries. Longman, London, UK.

Massey D. 1984. Spatial divisions of labour: social structures and the structure of production. MacMillan, London, UK.

Naudts, J., 2002. Les Hautes Terres de Tembien, Tigré, Ethiopie; Résistance et limites d'une ancienne civilisation agraire; Conséquences sur la dégradation des terres. Mémoire présenté en vue de l'obtention du Diplôme d'Agronomie Tropicale CNEARC, Montpellier.

Nyssen, J., Poesen, J., Veyret-Picot, M., Moeyersons, J., Mitiku Haile, Deckers, J., Dewit, J., Naudts, J., Kassa Teka, Govers, G., 2006. Assessment of gully erosion rates through interviews and measurements: a case study from northern Ethiopia. Earth Surface Processes and Landforms 31 (2), 167–185.

APPENDIX A6: Global drylands under future climate change

As stated in Chapter 1, drylands are defined as 'areas where the ratio of annual precipitation to annual potential evapotranspiration is smaller than 0.65'. To evaluate the potential extent of future climate change impact on dryland ecosystems, we retrieved multi-model projections of the ratio of annual precipitation to annual potential evapotranspiration under the A2 emission scenario (CCKP, 2015). We then computed the ensemble average of the 9 used circulation models. The evaluated circulation models include GFDL-CM2.1, IPSL-CM4, MIROC3.2 (medres), ECHO-G, ECHAM5/MPI-OM, MRI-CGCM2.3.2, CGCM3.1 (T47), CNRM-CM3 and GFDL-CM2.0. Finally, we calculated the change in the ratio of annual precipitation to annual potential evapotranspiration between a historical baseline (1961-1990) (Figure A6-1) and the end of this century (2081-2100) (Figure A6-2). The multi-model projection suggests significant global changes in conditions of aridity, most notably in southern Europe, southeast North America, northeast South America, the southern coasts of Australia and the southern fringes of the Sahel zone (Figure A6-2).

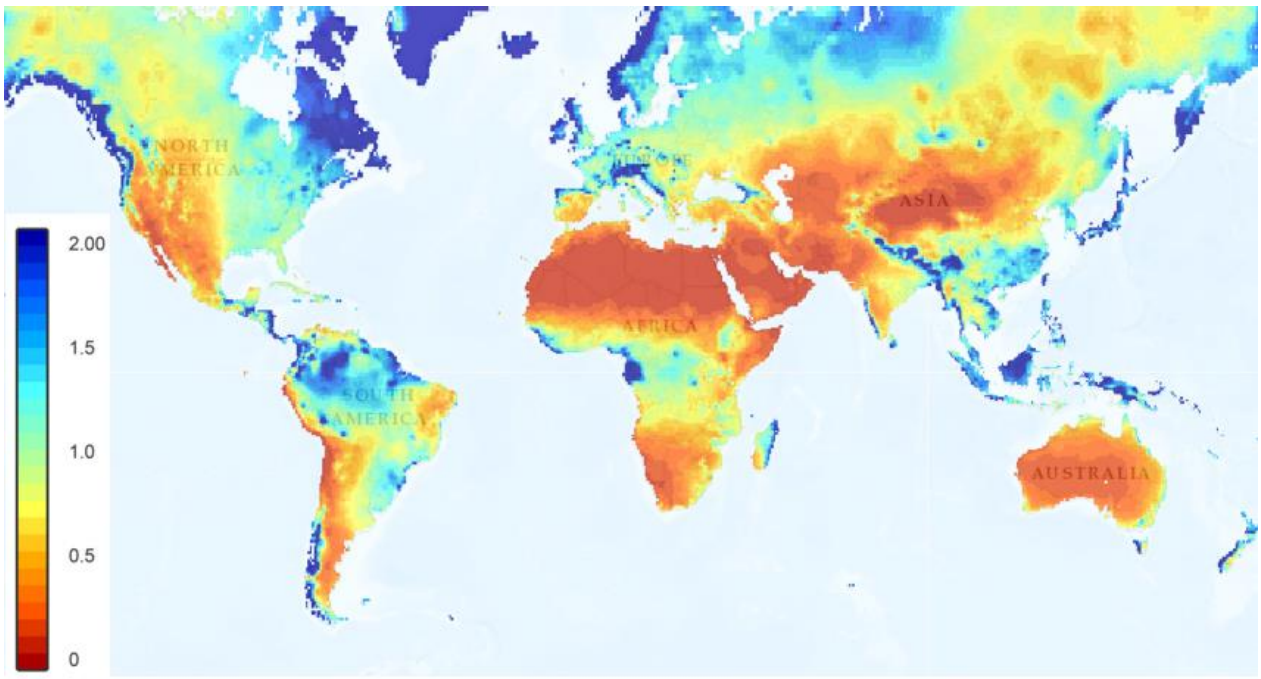

Figure A6-1. Multi-model baseline map of the ratio of annual precipitation to annual potential evapotranspiration for the period 1961 to 1990.

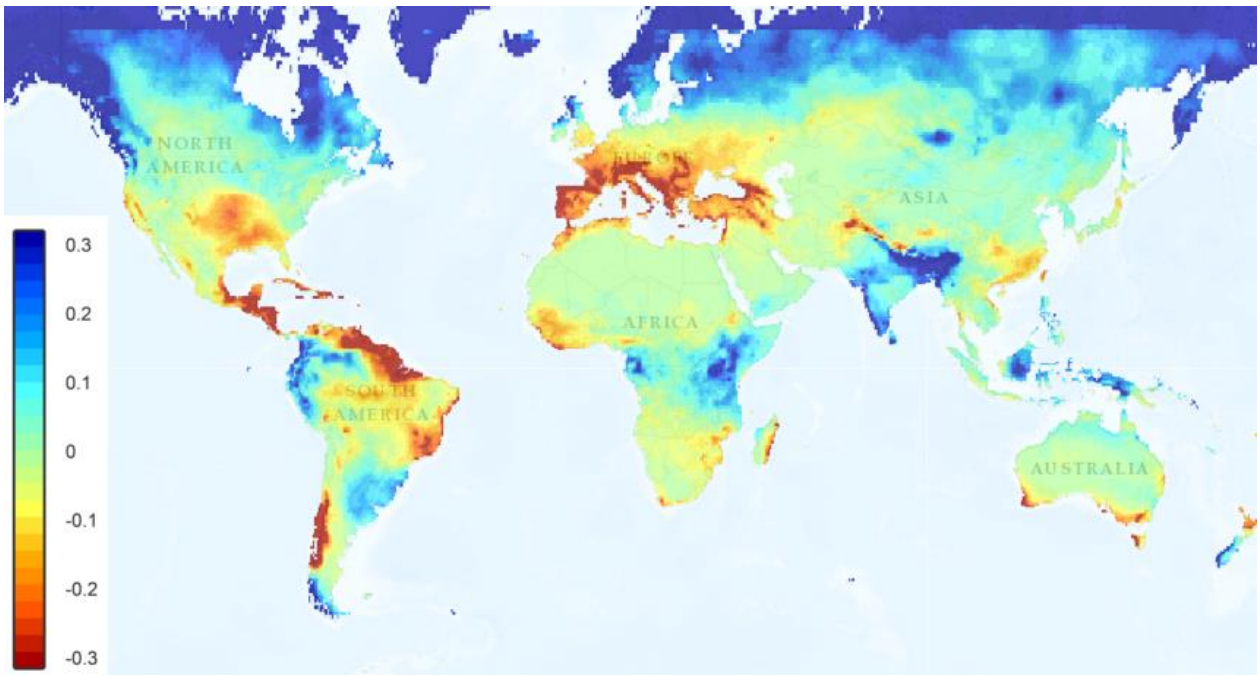

Figure A6-2. Projected multi-model change in the ratio of annual precipitation to annual potential evapotranspiration between the baseline period and the end of this century (2081-2100).

Reference: CCKP, 2015. Climate Change Knowledge Portal, Climate Analysis Tool. Available from: http://climatewizard.ciat.cgiar.org/index1.html (accessed on 14/11/2015).